

University of Alberta Library



0 1620 3069304 6






EX LIBRIS  
UNIVERSITATIS  
ALBERTÆNSIS

---





Digitized by the Internet Archive  
in 2025 with funding from  
University of Alberta Library

<https://archive.org/details/0162030693046>











**University of Alberta**

**Library Release Form**

Name of Author: **Zhanping Xu**

Title of Thesis: **Removal of Acetic Acid from Water by Catalytic Distillation**

Degree: **Doctor of Philosophy**

Year this Degree Granted: **1997**

Permission is hereby granted to the University of Alberta Library to reproduce single copies of this thesis and to lend or sell such copies for private, scholarly, or scientific research purposes only.

The author reserves all other publication and other rights in association with the copyright in the thesis, and except as hereinbefore provided, neither the thesis nor any substantial portion thereof may be printed or otherwise reproduced in any material form whatever without the author's prior written permission.







University of Alberta

**REMOVAL OF ACETIC ACID FROM WATER BY CATALYTIC DISTILLATION**

by

**ZHANPING XU**



A thesis submitted to the Faculty of Graduate Studies and Research in partial fulfillment of  
the requirements for the degree of **Doctor of Philosophy**

in

**Chemical Engineering**

Department of Chemical and Materials Engineering

Edmonton, Alberta

Fall 1997





**University of Alberta**

**Faculty of Graduate Studies and Research**

The undersigned certify that they have read, and recommend to the Faculty of Graduate Studies and Research for acceptance, a thesis entitled **Removal of Acetic Acid from Water by Catalytic Distillation** submitted by **Zhanping Xu** in partial fulfillment of the requirements for the degree of **Doctor of Philosophy** in Chemical Engineering.





## ABSTRACT

Dilute acetic acid is produced in many chemical and petrochemical industrial applications. One of the current technologies for removing the acetic acid from water is by azeotropic distillation. It is very energy-consuming and the costs involved in the manufacture and maintenance of the equipment is very high because of the very corrosive nature of concentrated acetic acid.

Preliminary computer simulation showed that catalytic distillation could be an alternative and more competitive process. In the catalytic distillation column, methanol is introduced to react with acetic acid. The reaction product, methyl acetate, is removed from the column top and water is discharged from the bottom. In this way, a relatively small amount of product is withdrawn from the column top and the acetic acid concentration in the column is kept lower than that in the feed. Therefore, both energy consumption and investment costs can be reduced.

In this thesis research, catalytic distillation experiments for the removal of acetic acid from water were conducted in a 100 mm diameter column installed with proprietary column internals composed of catalyst units and separation trays. An ion exchange catalyst (Amberlyst 15) was used to accelerate the reaction. The effects of feed rate, reflux ratio, product rate and feed location on the operation performance were investigated. For the feed containing 2.5 to 9.9 wt% of acetic acid in water, more than 50 wt% of the acid was removed in the 1.5 m high test column.

Detailed studies were conducted on the reaction kinetics, vapor-liquid equilibrium and separation efficiencies for the modeling and simulation of the catalytic distillation process. A simulation program was established by incorporating the basic models into a





commercial simulation package. The models and the simulation program were verified by a variety of experimental data.

From the simulation results, it is estimated that catalytic distillation consumes only 14.8% of the energy that simple distillation does for the separation of dilute acetic acid from water. The investment is reduced because of the smaller column size and the avoidance of the corrosion problem.





## **Acknowledgments**

I am very grateful to many people who helped me in the thesis research.

First of all, I wish to express my deep gratitude to my supervisor, Dr. K.T. Chuang, for his guidance and encouragement throughout this program.

I would also like to thank the Killam Trusts and the University of Alberta for the awarding of an Izaak Walton Killam Memorial Scholarship and an Andrew Stewart Graduate Prize.

My thanks are also due to Dr. A.E. Mather and Dr. S.E. Wanke for their helpful discussions, Mr. A. Afacan for his suggestions and assistance in the experimental work, Ms. A. Koenig for her assistance in GC analysis, and the Department Machine Shop and Instrument Shop for building the test column.

Above all, I would like to thank my wife, Yuehua, for supporting me in every possible way during the entire program.



## Table of Contents

### 1. INTRODUCTION

1.1	Introduction To Catalytic Distillation	1
1.2	Applications Of Catalytic Distillation	2
1.3	Column Configurations	5
1.4	Problem Statement And Research Strategy	6
1.5	Literature Cited	13

### 2. REACTION KINETICS 16

2.1	Introduction	16
2.2	Kinetic Model	17
2.3	Experimental	21
2.4	Results And Discussion	24
2.4.1	Selection of Catalyst	24
2.4.2	Effect of Stirrer Speed	26
2.4.3	Internal Resistance	26
2.4.4	Apparent Equilibrium Constant	27
2.4.5	Reaction Constant	28
2.4.6	Effect of Temperature	28
2.4.7	Effect of Catalyst Loading	29
2.4.8	Kinetic Equation	29
2.4.9	Catalyst Reusability	30
2.5	Conclusions	30
2.6	Nomenclature	32
2.7	Literature Cited	43





<b>3.</b>	<b>EFFECT OF INTERNAL DIFFUSION ON HETEROGENEOUS CATALYTIC ESTERIFICATION OF ACETIC ACID</b>	<b>45</b>
3.1	Introduction	45
3.2	Theoretical	47
3.3	Results And Discussion	50
3.3.1	Solution of Equation (3.18)	50
3.3.2	Effective Diffusivity	51
3.3.3	Concentration of Acid Sites in Amberlyst 15	53
3.3.4	Internal Diffusion in Amberlyst 15	53
3.4	Conclusions	57
3.5	Nomenclature	58
3.6	Literature Cited	66
<b>4.</b>	<b>CORRELATION OF VAPOR-LIQUID EQUILIBRIUM DATA FOR METHYL ACETATE-METHANOL-WATER-ACETIC ACID MIXTURES</b>	<b>68</b>
4.1	Introduction	68
4.2	Vapor-Liquid Equilibria In Mixtures Containing Acetic Acid	70
4.3	Activity Coefficients	72
4.4	Results And Discussion	73
4.5	Conclusions	76
4.6	Nomenclature	77
4.7	Literature Cited	89
<b>5.</b>	<b>DESIGN OF CATALYTIC DISTILLATION COLUMN</b>	<b>91</b>
5.1	Introduction	91
5.2	Computer Simulation	91
5.3	Column Sizing And Configuration	93



5.4	Internals For Reaction/Separation Section	95
5.5	Hydraulic Tests	99
5.6	Pressure Drop Of Liquid Flow Through Catalyst Bed	101
5.7	Nomenclature	103
5.8	Literature Cited	111
<b>6.</b>	<b>SEPARATION EFFICIENCY OF DUALFLOW TRAYS</b>	<b>113</b>
6.1	Introduction	113
6.2	Experimental	117
6.3	Results And Discussion	118
6.3.1	Froth Height and Froth Structure	119
6.3.2	Effect of Sampling Position and Catalyst Units	123
6.3.3	Effect of Physical Properties	124
6.3.4	Component Tray Efficiencies	126
6.4	Conclusions	131
6.5	Nomenclature	132
6.6	Literature Cited	156
<b>7.</b>	<b>CATALYTIC DISTILLATION – EXPERIMENTAL RESULTS</b>	<b>159</b>
7.1	Introduction	159
7.2	Experimental	161
7.3	Results And Discussion	163
7.3.1	Effect of the Catalyst	165
7.3.2	Effect of the Catalyst Zone	167
7.3.3	Effect of the Boil-up Rate	168
7.3.4	Effect of the Top Product Rate	169
7.3.5	Effect of the Feed Ratio of Methanol to Acetic Acid	171
7.3.6	Effect of the Feed Location	171





7.4	Conclusions	173
7.5	Literature Cited	183
<b>8.</b>	<b>CATALYTIC DISTILLATION – MODELING AND SIMULATION</b>	<b>184</b>
8.1	Introduction	184
8.2	Basic Models	184
8.2.1	Reaction Kinetics	185
8.2.2	Vapor-Liquid Equilibrium	186
8.2.3	Mass Transfer	186
8.2.4	Column Internals	191
8.3	Model Equations And Solution Methods	192
8.3.1	Model Equations	192
8.3.2	Solution Methods	193
8.4	Results And Discussion	198
8.4.1	Effective Liquid Hold-up in Catalyst Units	198
8.4.2	Simulation of the Experimental Results	199
8.4.3	Other Simulation Case Studies	201
8.4.4	Simulation for an Industrial Column	204
8.5	Conclusions	205
8.6	Nomenclature	207
8.7	Literature Cited	237
<b>9.</b>	<b>CONCLUSIONS AND RECOMMENDATIONS</b>	<b>242</b>
9.1	Literature Cited	248
<b>APPENDIX</b>	<b>Input And Output Files For The Simulation Of Catalytic Distillation Using Aspen Plus</b>	<b>250</b>



## **List of Tables**

Table 1-1	Catalytic Distillation Processes	10
Table 2-1	Physical and Chemical Properties of Catalysts	33
Table 3-1	Concentration of Acid Sites in Amberlyst 15	61
Table 3-2	Effectiveness Factors for Various Sizes of Amberlyst 15	62
Table 4-1	Binary Model Parameters	79
Table 4-2	Constants in Equations (4.12) and (4.13)	80
Table 4-3	Statistical Errors for the Margules, Wilson and NRTL Models	81
Table 4-4	Mean Deviations between Measured and Predicted Vapor Compositions	82
Table 6-1	Column and Tray Dimensions	134
Table 6-2	Physical Properties of Test Components	135
Table 6-3	Mixture Compositions on Each Tray for Run #8, 11, 14	136
Table 7-1	Summary of Catalytic Distillation Data	174
Table 8-1	Component Tray Efficiencies	210
Table 8-2	Rigorous Methods for Simulation of Catalytic Distillation	211
Table 8-3	Simulation Results for Removal of Acetic Acid from Water by Catalytic Distillation and Simple Distillation	212





## List of Figures

Figure 1-1	Production of MTBE by Catalytic Distillation	11
Figure 1-2	Connections between Chapters	12
Figure 2-1	Experimental Set-up for Kinetic Tests	34
Figure 2-2	Reaction Activity of Catalysts	35
Figure 2-3	Effect of Stirrer Speed on Reaction Rate	36
Figure 2-4	Dependence of Equilibrium Constant on Temperature	37
Figure 2-5	Plot of Left Term in Eq. (2-9) vs. Time	38
Figure 2-6	Effect of Temperature on Reaction Rate	39
Figure 2-7	Activation Energy	40
Figure 2-8	Effect of Catalyst Loading on Reaction Rate	41
Figure 2-9	Catalyst Reusability	42
Figure 3-1	Effectiveness Factor for Amberlyst 15 in Acetic Acid Esterification	63
Figure 3-2	Predicted Effectiveness Factor for Various Sizes of Catalyst Particles	64
Figure 3-3	Effect of Particle Size on Reaction Rate	65
Figure 4-1	Measured and Predicted Vapor Compositions for the Methyl Acetate-Methanol System	83
Figure 4-2	Measured and Predicted Vapor Compositions for the Methyl Acetate-Water System	84
Figure 4-3	Measured and Predicted Vapor Compositions for the Methyl Acetate-Acetic Acid System	85



Figure 4-4	Measured and Predicted Vapor Compositions for the Methanol-Water System	86
Figure 4-5	Measured and Predicted Vapor Compositions for the Methanol-Acetic Acid System	87
Figure 4-6	Measured and Predicted Vapor Compositions for the Water-Acetic Acid System	88
Figure 5-1	Column Configuration for Removal of Acetic Acid from Water by Catalytic Distillation	104
Figure 5-2	Catalytic Distillation Module	105
Figure 5-3	Dualflow Tray Structure	106
Figure 5-4	Catalyst Unit (cylindrical)	107
Figure 5-5	Catalyst Unit (rectangular)	108
Figure 5-6	Hydraulic Test Flow Sheet Using Air-Water System	109
Figure 5-7	Support for Catalyst Units	110
Figure 6-1	Distillation Test Flowsheet	137
Figure 6-2	Liquid Sampling Structure	138
Figure 6-3	Variation of Froth Height with Tray Location and Liquid Composition	139
Figure 6-4	Variation of Froth Height with Tray Location and Liquid Composition	140
Figure 6-5	Effect of Liquid Composition on Froth Height	141
Figure 6-6	Variation of M-index with Tray Location	142
Figure 6-7	Enlarged Photograph for Figure 6-6c	143
Figure 6-8	Measured Tray Efficiencies with Different Sampling Locations	144





Figure 6-9	Measured Tray Efficiencies with and without Catalyst Units	145
Figure 6-10	Measured Component Composition Profiles	146
Figure 6-11	Measured Component Composition Profiles	147
Figure 6-12	Measured Component Composition Profiles	148
Figure 6-13	Measured Component Tray Efficiencies	149
Figure 6-14	Measured Component Tray Efficiencies	150
Figure 6-15	Measured Component Tray Efficiencies	151
Figure 6-16	Measured Tray Efficiencies for Methyl Acetate	152
Figure 6-17	Measured Tray Efficiencies for Methanol	153
Figure 6-18	Measured Tray Efficiencies for Water	154
Figure 6-19	Measured Tray Efficiencies for Acetic Acid	155
Figure 7-1	Effect of Catalyst on Column Performance	175
Figure 7-2	Effect of Boil-up Rate on Column Performance	176
Figure 7-3	Effect of Boil-up Rate on Acid Removal	177
Figure 7-4	Effect of Top Product Rate on Column Performance	178
Figure 7-5	Effect of Top Product Rate on Column Performance	179
Figure 7-6	Effect of Feed Ratio of Methanol to Acetic Acid on Column Performance	180
Figure 7-7	Effect of Feed Ratio of Methanol to Acetic Acid on Column Performance	181
Figure 7-8	Effect of Feed Location on Column Performance	182
Figure 8-1	Equilibrium Stage Model	213



Figure 8-2	Non-Equilibrium Stage Model	214
Figure 8-3	Column Model	215
Figure 8-4	Simulation of Run #4 with Top Product Rate of 50.1 g/min	216
Figure 8-5	Simulation of Run #8 with Top Product Rate of 27.6 g/min	217
Figure 8-6	Simulation of Run #9 with Top Product Rate of 23.3 g/min	218
Figure 8-7	Simulation of Run #19 with Top Product Rate of 16.7 g/min	219
Figure 8-8	Simulation of Run #11 with Reflux Ratio of 10.2	220
Figure 8-9	Simulation of Run #12 with Reflux Ratio of 14.8	221
Figure 8-10	Simulation of Run #14 with Methanol to Acetic Acid Ratio of 3.7	222
Figure 8-11	Simulation of Run #20 with Methanol to Acetic Acid Ratio of 6.1	223
Figure 8-12	Simulation of Run #16 with Acetic Acid-Water Feed Rate of 180 g/min	224
Figure 8-13	Simulation of Run #17 with Acetic Acid-Water Feed Rate of 220 g/min	225
Figure 8-14	Simulation of Run #22 with Acetic Acid-Water Feed Moved Down	226
Figure 8-15	Simulation of Run #23 with Acetic Acid-Water Feed Moved Down	227
Figure 8-16	Simulation of Run #24 with Methanol Feed Moved up	228
Figure 8-17	Simulation of Run #25 with Methanol Feed Moved up	229
Figure 8-18	Simulation of Run #30 with Acetic Acid Feed Containing 9.9 wt% of Acetic Acid	230
Figure 8-19	Simulation of Run #31 with Acetic Acid Feed Containing 2.55 wt% of Acetic Acid	231
Figure 8-20	Simulation for the Effect of Tray Efficiency	232
Figure 8-21	Simulation for the Effect of Liquid Hold-up	233





Figure 8-22	Simulation for the Effect of Catalyst Bed Height on Acid Removal	234
Figure 8-23	Simulation for Optimum Height of Catalyst Bed	235
Figure 8-24	Simulation for the Effect of Catalyst Zone on Column Performance	236



## CHAPTER 1. INTRODUCTION

### 1.1 Introduction To Catalytic Distillation

A solid catalyzed chemical reaction and a multistage distillation can be carried out simultaneously. This combined unit operation is called catalytic distillation. By continuously separating products from reactants while the reaction is in progress, the reaction can proceed to a much higher level of conversion than otherwise possible. It especially suits those chemical reactions where the reaction equilibrium limits the conversion in a fixed-bed reactor to a low-to-moderate level.

The concept of combining reaction and distillation is not new. The technique was first applied in the 1920s to esterification processes using homogeneous liquid catalysts (Backhaus, 1921). Employing catalytic distillation that relies on a heterogeneous solid catalyst is a more recent development (Smith et al., 1987). The advantages of using solid catalysts in catalytic distillation over homogeneous catalysts are obvious: they are easy to separate from reaction mixtures, easy to handle, and there is less waste. Solid catalysts also offer the potential for superior effectiveness and environmental integrity. However, the column internals are more complicated when using solid catalysts.

The most important benefit of catalytic distillation is a reduction in capital investment. By carrying out the catalytic reaction and distillation in the same vessel, one process step is eliminated, along with the associated pumps, piping, and instrumentation. Other benefits depend on the specific chemical reaction. Chemical reactions that are characterized by unfavorable reaction equilibrium, high heat of reaction, and significant





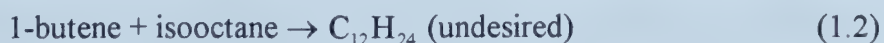
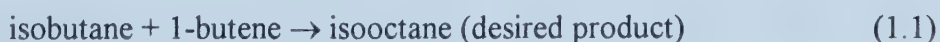
rate of reaction at distillation temperatures are particularly good candidates for catalytic distillation (DeGarmo et al., 1992).

Combining reaction with distillation is not always advantageous (Doherty and Buzad, 1992). At the very least, it must be possible to achieve reasonable reaction rates at the relatively low temperatures and pressures normally encountered in distillation. Clearly, all high temperature and/or high pressure gas-phase reactions such as hydrogenation and hydrodealkylation are not candidates for catalytic distillation. Moreover, the catalyst life must be long in order to avoid frequent start-up and shut-down.

## 1.2 Applications Of Catalytic Distillation

Catalytic distillation is potentially attractive whenever a liquid phase reaction must be carried out with a large excess of one reactant. Under such circumstances, conventional processes incur large recycling costs for the excess reactant. It may also be used for the separation of difficult systems. Some examples are given as follows:

(1) To Suppress Side Reaction. In the case of butane alkylation, the following two reactions occur simultaneously (Doherty and Buzad, 1992):



Excess butane is normally employed to keep the concentrations of 1-butene and isooctane at a low level, thereby reducing the rate of reaction (1.2). In catalytic distillation, however, the natural separation between isooctane and 1-butene reduces the second



reaction from taking place and greatly reduces the formation of unwanted by-products. Because of this, the feeds to the column can be much closer to a stoichiometric ratio.

(2) To Overcome Limitations Imposed by Chemical Equilibrium. Methyl *tert*-butyl ether (MTBE) is a gasoline octane booster and is made from methanol and isobutene in an equilibrium-limited liquid-phase reaction catalyzed by a strong acid ion-exchange resin (Doherty and Buzad, 1992):



Typically, the isobutene is mixed with other C<sub>4</sub> species (mostly n-butane, isobutane and n-butenes) that are inert under the process conditions.

The conventional process is carried out in a liquid-phase catalytic reactor with a slight excess of methanol to prevent isobutene reacting with itself to form a dimer. Isobutene conversion is in the order of 90 to 95%. The inerts and reaction products are then separated by distillation. This step is complicated by the presence of minimum boiling azeotropes between MTBE and methanol and isobutene and methanol. In addition, unreacted isobutene is difficult to separate from n-butane and the n-butenes because of their low relative volatilities.

A catalytic distillation process was invented by Smith (1981) in which catalyst bales are packed in the middle of a distillation column, as shown in Figure 1-1. Since the reaction is exothermic it is desirable, for good energy management, to carry out most of the reaction in the primary reactor(s) before the catalytic distillation column. A near-equilibrium mixture is fed to the column where the remaining isobutene is reacted to extinction. This is achieved by placing the reactive section between a non-reactive



stripping section and a non-reactive rectifying section. The stripping section separates MTBE (bottom product) from the reactants, which are continually forced up into the reaction zone. The rectifying section separates the inerts (plus any excess methanol) from the reacting components which are forced down into the reaction zone. The net effect is a very economical process for making MTBE. Almost all new MTBE plants use this technology.

Another gasoline octane booster, tertiary amyl methyl ether (TAME), can be manufactured by a method similar to MTBE (Marker, 1993) by changing C4 olefins in the feed to C5 olefins.

Some other catalytic distillation processes with equilibrium limited reactions are shown in Table 1-1.

(3) To Separate Close-Boiling Components. Catalytic distillation technology has also been suggested as a way of separating isomers. Mixtures of m- and p-xylene can barely be separated by an ordinary distillation technique even if extractive distillation is used. Saito et al. (1971) adopted the catalytic distillation technique to enrich p-xylene based on the fact that only m-xylene reacts with tert-butylbenzene. The reaction product is much heavier than p-xylene and therefore is easy to separate from p-xylene. Terrill et al. (1985) and Cleary and Doherty (1985) have also explored the possibility of using fast, reversible, selective reactions combined with distillation to enhance the separation of m- and p-xylene.





### 1.3 Column Configurations

In the presence of a solid catalyst, the catalytic distillation can be carried out in several different configurations in a column.

In one configuration, the solid-catalyzed chemical reaction and the multistage distillation occur simultaneously in a continuum – that is, there is spatial continuity along the length of the column. Both reaction and distillation take place in every thin horizontal slice of the catalytic reaction-distillation section of the column.

In another configuration, the reaction and distillation proceed in alternating steps. Here, the catalytic reaction-distillation section of a column contains both the catalyst contact device and the distillation device. Reaction occurs in the catalyst contact device and then the reacting phase passes to the distillation device for vapor/liquid contact and separation. These two steps occurs alternatively. By making the steps of infinitely small size, this configuration becomes equivalent to the first one.

In both of these configurations, a rectification section may be located above the catalytic reaction-distillation section of the column and a stripping section may be located below it, depending upon the purity requirement.

Feed locations where reactants are injected into a catalytic distillation column are dependent on the relative volatility between the reactants as well as between the reactants and reaction products. They should be chosen to make the reactants effectively contact with each other in the reaction zone of the column.



## 1.4 Problem Statement And Research Strategy

In the chemical/petrochemical plants that deal with acetic acid (e.g., manufacture of terephthalic acid, dimethyl terephthalate, acetic acid, esters involving the use of acetic anhydride, cellulose acetate and acetate rayon) dilute acetic acid is produced. The most common problem of acetic acid recovery from these streams involves the separation of the acid from relatively large amounts of water. The past practice of further dilution and biodegradation or discarding may in the future overload local disposal systems as both industry and population increase in density.

Five acetic acid recovery processes are generally considered: (1) azeotropic distillation, (2) simple distillation, (3) liquid-liquid extraction, (4) chemical treatment, and (5) adsorption. Among these, simple or azeotropic distillation facilities are most competitive (Mcketta, 1976). In an acetic acid/water system, acetic acid has a higher boiling point. Therefore, the consumption of energy is very high in conventional distillation because a large amount of water has to be vaporized. Also, with the increase in acetic acid concentration as the solution moves down the column, it becomes increasingly corrosive. Therefore, costs of manufacturing and maintaining the column are very high.

The objective of this thesis research is to investigate a novel approach for the removal of dilute acetic acid from water, catalytic distillation (CD).

To carry out catalytic distillation, a stream of methanol is introduced into the column together with the wastewater containing acetic acid. In the column, acetic acid reacts with methanol to form methyl acetate and at the same time methyl acetate is separated from water. It is expected that by using the new method energy consumption



can be dramatically reduced and the corrosion problem avoided compared with conventional distillation processes.

The acetic acid esterification with methanol in a reactive distillation column using homogeneous liquid catalysts (e.g. sulfuric acid) has been studied by Backhaus (1921), Corrigan and Ferris (1969), Agreda et al. (1984, 1990), and Sawistowski and Pilavakis (1979, 1988). Most of them used concentrated acetic acid for the manufacture of methyl acetate. Eastman Chemical Co. (Agreda et al., 1984, 1990) developed a unique process for the manufacture of high-purity methyl acetate through reactive distillation using sulfuric acid as a catalyst. A homogeneous catalyst was used because of the simple column structure involved (a tray column with high liquid hold-up). Sawistowski and Pilavakis (1979, 1988) studied the same process in a packed column. The main drawback of the packed column is the low liquid hold-up and therefore, low conversion rate.

For the removal of dilute acetic acid from water, homogeneous catalysts cannot be used because they will contaminate the water. Because of the low reactant concentrations, the reaction rate is low so a large liquid hold-up or a long liquid residence time in the reaction zone of the CD column are desirable. Therefore, special column internals are needed for the process.

To study the catalytic distillation process, the research program consists of the following tasks:

(1) Reaction Kinetics. To design the CD column and simulate the CD process, information for the reaction kinetics is needed. The kinetics was measured in a batch reactor since it is not available from the literature. The research includes: screening solid





acid catalysts; studying the effect of internal and external diffusion, temperature, catalyst loading, and reactant concentration on reaction rate; and deriving a kinetic equation. This part will be discussed in Chapters 2 and 3.

(2) Vapor-Liquid Equilibrium. An accurate vapor-liquid equilibrium model is vital in the design and simulation of the catalytic distillation processes. Experimental data for the system of interest are available from the literature but the only model developed in the literature (third-order Margules equation) is difficult to use in conjunction with the existing commercial process simulation packages. A new model based on the NRTL model was developed. This part will be discussed in Chapter 4.

(3) Design of Catalytic Distillation Column and Column Internals. Based on the preliminary simulation results by incorporating the reaction kinetics and vapor-liquid equilibrium model into a commercial simulation package – Aspen Plus (Aspen Technology, Inc., 1996), the test column was sized and column configuration was determined. A novel column internal was designed for the process. This part will be discussed in Chapter 5.

(4) Measurement of Mass Transfer Efficiency. In this research, dualflow trays were chosen for the mass transfer device. The multicomponent tray efficiencies were measured with a similar column configuration and operating conditions as in the catalytic distillation experiments. The efficiency data were then applied in the modeling and simulation of the catalytic distillation process. This part will be discussed in Chapter 6.

(5) Catalytic Distillation Experiments. These experiments were conducted to study the effect of feed location, reaction zone, feed composition, reflux ratio, and column



throughput on the conversion of acetic acid and product compositions. The measured data (concentration profiles) were used to verify the simulation results. This part will be discussed in Chapter 7.

(6) Modeling and Simulation of Catalytic Distillation. Simulation of the catalytic distillation process was conducted by incorporating basic models for vapor-liquid flow in the column, reaction kinetics, vapor-liquid equilibrium and mass transfer into the Aspen Plus process simulation package (Aspen Technology, Inc., 1996). The simulation results were compared with the catalytic distillation experimental results. The verified simulation program was then used in the design simulation of an industrial catalytic distillation column for the removal of acetic acid from water. This part will be discussed in Chapter 8.

The flow chart in Figure 1-2 shows the logical connections between chapters.

The research program involves various chemical engineering disciplines. The low reactant (acetic acid) concentration caused unique experimental problems such as slow reaction rate, and relatively small methanol feed and top product rates. A novel column internal was needed to contain as much catalyst as possible for the slow reaction. The small flow rates of methanol feed and top product required accurate delivery and measurement systems. The continuous operation required that the whole system be controlled automatically. Different analysis methods were needed to detect the very different mixture compositions in the column.



Table 1-1. Catalytic Distillation Processes

Catalytic Reaction	Reference
isobutene+ethanol $\rightleftharpoons$ ETBE	Bakshi et al. (1991)
benzene+ethylene $\rightleftharpoons$ ethyl benzene	Smith et al. (1991)
propylene+benzene $\rightleftharpoons$ isopropylbenzene (cumene)	Shoemaker and Jones (1987)
methyl acetate+water $\rightleftharpoons$ methanol+acetic acid	Fuchigami (1990)
acetic acid+ethanol $\rightleftharpoons$ ethyl acetate+water	Savkovic-stevanovic (1992)
formic acid+cyclohexene $\rightleftharpoons$ cyclohexyl formate acrylic acid+cyclohexene $\rightleftharpoons$ cyclohexyl acrylate methacrylic acid+cyclohexene $\rightleftharpoons$ cyclohexyl methacrylate	Saha and Sharma (1996)





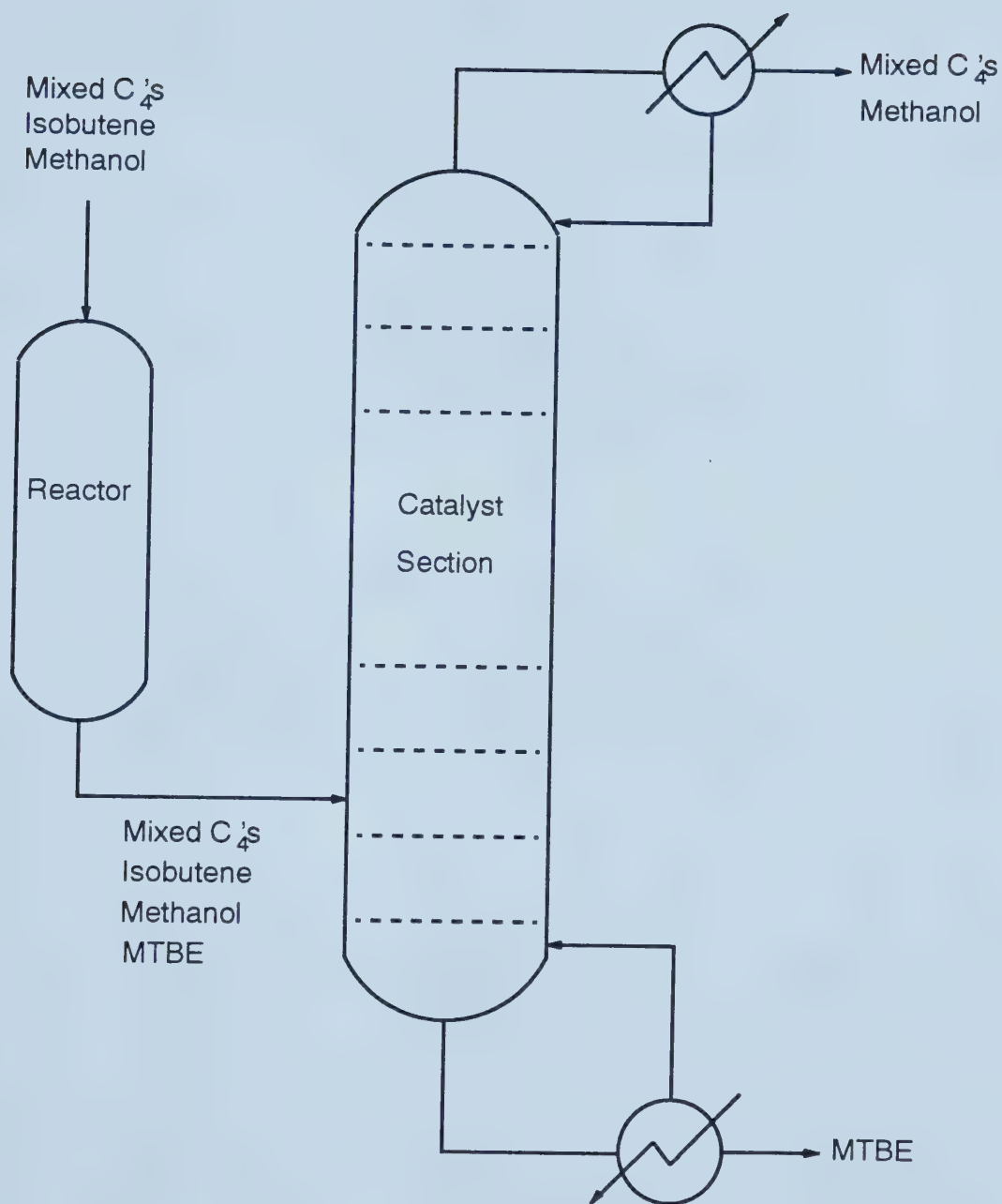


Figure 1-1 Production of MTBE by Catalytic distillation



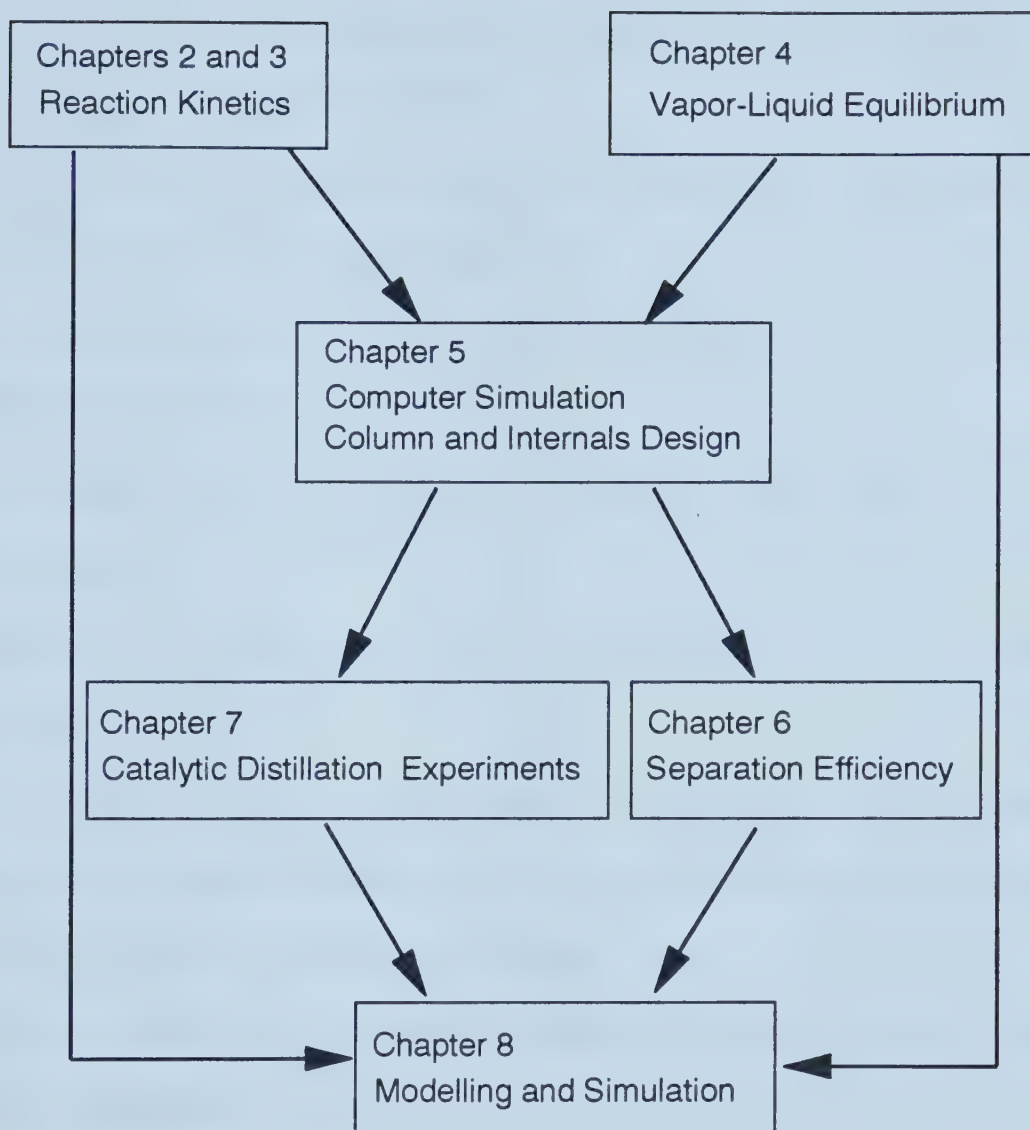


Figure 1-2 Connections between Chapters



## 1.5 Literature Cited

- Agreda, V.H. and Partin, L.R. (1984) Reactive Distillation Process for the Production of Methyl Acetate. *US Patent* No. **4,435,595**.
- Agreda, V.H., Partin, L.R. and Heise, W.H. (1990) High-Purity Methyl Acetate via Reactive Distillation. *Chem. Eng. Prog.* **86**, 40-46.
- Agreda, V.H., Pond, D.M. and Zoeller, J.R. (1992) From Coal to Acetic Anhydride. *CHEMTECH* **22**, 172-181.
- Aspen Technology, Inc. (1996) *Aspen Plus*, version **9.3**, Aspen Technology, Inc., Massachusetts.
- Backhaus, A.A. (1921) Continuous Process for the Manufacture of Esters. *US Patent* No. **1,400,849**.
- Bakshi, A., Smith, L., Jones, E. and Hickey, T.P. (1991) Low Cost of Octane Enhancement. Catalytic Distillation Route. paper presented at *EFCE Meeting, Distillation Perspectives*, Amsterdam, Netherlands.
- Chakrabarti, A. and Sharma, M.M. (1993) Cationic Ion Exchange Resins as Catalyst. *Reactive Polymers* **20**, 1-45.
- Cleary W. and Doherty, M.F. (1985) Separation of Closely Boiling Mixtures by Reactive Distillation. 2. Experiments. *Ind. Eng. Chem. Process Des. Dev.* **24**, 1071-1073.
- Corrigan, T.E. and Ferris, W.R. (1969) A Development Study of Methanol Acetic Acid Esterification. *Can. J. Chem. Eng.* **47**, 334-335.





- DeGarmo, J.L., Parulekar, V.N. and Pinjala, V. (1992) Considering Reactive Distillation. *Chem. Eng. Prog.* **88**(3), 43-50.
- Doherty, M.F., and Buzad, G. (1992) Reactive Distillation by Design. *Trans. IChemE* **70**, part A, 448-458.
- Flato, J. and Hoffmann, U. (1992) Development and Start-up of a Fixed Bed Reaction Column for Manufacturing Antiknock Enhancer MTBE, *Chem. Eng. Technol.* **15**, 193-201.
- Fuchigami Y. (1990) Hydrolysis of Methyl Acetate in Distillation Column Packed with Reactive Packing of Ion Exchange Resin, *J Chem. Eng. Jpn.* **23**, 354-358.
- Marker, T.L. (1993) Etherification of C<sub>5</sub>-Plus Olefins by Catalytic Distillation. *US Patent* No. **5,258,560**.
- Mcketta, J.J. (1976) *Encyclopedia of Chemical Processing and Design*, vol. 1, Marcel Dekker, Inc., New York.
- Saha, B. and Sharma, M.M. (1996) Esterification of Formic Acid, Acrylic Acid and Methacrylic Acid with Cyclohexene in Batch and Distillation Column Reactors: Ion Exchange Resins as Catalysts. *Reactive & Functional Polymers* **28**, 263-278.
- Saito, S., Michishita, T. and Maeda, S. (1971) Separation of Meta- and Para-xylene Mixture by Distillation Accompanied by Chemical Reactions. *J. Chem. Eng. Jpn.* **4**, 37-43.
- Savkovic-Stevanovic, J, Misic-Vukovic, M., Boncic-Caricic, G., Trisovic, B. and Jezdic, S. (1992) Reaction Distillation with Ion Exchangers. *Separation Science and Technology* **27**, 613-630.



- Sawistowski, H. and Pilavakis, P.A. (1988) Performance of Esterification in a Reaction-Distillation Column. *Chem. Eng. Sci.* **43**, 355-360.
- Sawistowski, H. and Pilavakis, P.A. (1979) Distillation with Chemical Reaction in a Packed Column. *I. Chem. E. Symposium Series* No. 56, 4.2/49-63.
- Shoemaker, J.D. and Jones, E.M., Jr (1987) Cumene by Catalytic Distillation. *Hydrocarbon Processing* **66**(6), 57-58.
- Smith, L.A., Jones, E.M. and Hearn, D. (1987) Working with Catalytic Distillation. paper presented at *AIChE Summer National Meeting*, August 16-19.
- Smith, L.A. (1981) Catalytic Distillation Process. *US Patent* No. **4,307,254**.
- Smith, L.A., Jones, E.M. and Hearn, D. (1991) Catalytic Distillation-a New Chapter in Unit Operations. paper presented at *Spring Meeting of AIChE*, Houston
- Terrill, D.L., Sylvestre, L.F. and Doherty, M.F. (1985) Separation of Closely Boiling Mixtures by Reactive Distillation 1. Theory. *Ind. Eng. Chem. Process Des. Dev.* **24**, 1062-1071
- Thomas, S.J.M. (1992) Solid Acid Catalysts. *Scientific American* **266** (4), 112-118



## CHAPTER 2. REACTION KINETICS\*

### 2.1 Introduction

In the catalytic distillation column, the methanol reacts with the acetic acid to form methyl acetate and water:



Because methanol and methyl acetate have lower boiling points than water, the reaction product, methyl acetate, and excess methanol (if necessary) can be removed at the top of the column while the cleaned water is discharged at the bottom.

To accelerate the reaction of Equation (2.1), use of acid catalysts is proposed. Although mineral acids such as sulfuric acid have been used as catalysts in such a reaction (Sawistowski and Pilavakis, 1979, 1988; Agreda et al., 1990; Backhaus, 1921; Agreda and Partin, 1984), they cannot be used in this process because they will contaminate the water leaving the bottom of the catalytic distillation column.

There exist many solid acid catalysts (Thomas, 1992; Chakrabarti and Sharma, 1993; Tanabe et al., 1989). Among them, cation ion exchange resins are the most commonly used solid acid catalysts in organic reactions (Chakrabarti and Sharma, 1993). Ion exchange resins have also been used in esterification (Savkovic-Stevanovic et al., 1992) and hydrolysis of methyl acetate in a catalytic distillation column (Fuchigami, 1990).

Assuming the same reaction rate with the same amount of catalytically active ions, 1 g of sulfuric acid (a typical mineral acid catalyst) is equivalent to 4.2 g of dry Amberlyst

---

\* A version of this chapter has been published: Z.P. Xu and K.T. Chuang (1996) *Can. J. Chem. Eng.* **74**, 493-500.





15 (a typical solid acid catalyst). In the industrial applications, the amount of mineral acids used as a catalyst is limited because a high acid concentration will give rise to an increased corrosion rate and separation problems. If solid acid catalysts are used, corrosion and separation problems are avoided and the catalytic capacity can be increased dramatically by increasing the amount of catalyst.

To the best of our knowledge, no report has been released regarding kinetics of the reaction of Equation (2.1) catalyzed by a cation ion exchange resin. In this study, various ion exchange catalysts for this reaction were compared. A kinetic equation for the most active catalyst was developed for use in the design of a catalytic distillation column.

## **2.2 Kinetic Model**

Catalysis systems can be distinguished as homogeneous or heterogeneous. In homogeneous catalysis, a small catalyst molecule or ion is consumed in an early reaction step and is restored in a later step. In heterogeneous catalysis, the forces active at a solid surface distort or even dissociate an adsorbed reactant molecule to increase the rate of reaction. In the case of catalysis by ion exchange resins this classification is not as clearly defined (Helfferich and Hwang, 1988). Homogeneous catalysis can be carried out using an ion exchange resin containing the catalyst ion as its counterion. The reaction mechanism and kinetic orders remain those of homogeneous catalysis.

Chakrabarti and Sharma (1993) pointed out that most resin-catalyzed reaction can be classified either as quasi-homogeneous or as quasi-heterogeneous. The idealized homogeneous state requires complete swelling of the resin and total dissociation of the



polymer-bound  $-\text{SO}_3\text{H}$  group. They concluded that in all cases which have so far been studied, and in which limitations due to slow diffusion process can be ruled out, the kinetic order of the chemical reaction in the particles was found to be the same as in homogeneous catalysis by a dissolved electrolyte. This is a strong evidence in support of the view that the reaction mechanism is essentially the same in both cases.

Kumbhar and Yadav (1989) proposed a model for solid-catalyzed liquid reactions. A power law model was used to describe the surface reaction. Later, Yadav and Mehta (1994) applied this model to heterogeneous catalytic esterification. Patwardhan and Sharma (1990) also used the power law model to fit their experimental data for the esterification of carboxylic acids with olefins using cation ion exchange resins. They found that Amberlyst 15 had the highest activity among various catalysts.

In fact, the familiar power law model usually used for homogeneous reaction can be deduced from the Langmuir-Hinshelwood model for heterogeneous reaction by assuming that the adsorption is weak for all components. Assuming that the surface reaction is controlling, the Langmuir-Hinshelwood rate function for the reaction shown by Equation (2.1) can be expressed as

$$\frac{dC_{MeAc}}{dt} = k_1 \bar{C}_{MeOH} \bar{C}_{HAc} - k_{-1} \bar{C}_{MeAc} \bar{C}_{H_2O} \quad (2.2)$$

where  $\bar{C}_j$  is the concentration of adsorbed component  $j$ . If  $L$  is defined as the molal concentration of total sites and  $\bar{\theta}_j = \bar{C}_j/L$ , i.e., fraction of active sites occupied by  $j$ , Equation (2.2) can be rewritten as:



$$\frac{dC_{MeAc}}{dt} = L^2 \left( k_1 \theta_{MeOH} \theta_{HAc} - k_{-1} \theta_{MeAc} \theta_{H_2O} \right) \quad (2.3)$$

For competitive equilibrium adsorption,

$$\theta_i = \frac{b_i C_i}{1 + \sum_j b_j C_j} \quad (2.4)$$

where i, j = methanol, acetic acid, methyl acetate and water;  $b_i$  = adsorption constants.

Substituting Equation (2.4) into Equation (2.3),

$$\frac{dC_{MeAc}}{dt} = L^2 \left[ \frac{k_1 b_{MeOH} b_{HAc} C_{MeOH} C_{HAc} - k_{-1} b_{MeAc} b_{H_2O} C_{MeAc} C_{H_2O}}{\left( 1 + b_{MeOH} C_{MeOH} + b_{HAc} C_{HAc} + b_{MeAc} C_{MeAc} + b_{H_2O} C_{H_2O} \right)^2} \right] \quad (2.5)$$

When adsorption is weak for all components, i.e. values of  $b_i$  are small, the denominator of Equation (2.5) on the right side approaches unity, and Equation (2.5) becomes

$$\frac{dC_{MeAc}}{dt} = L^2 \left( k_1 b_{MeOH} b_{HAc} C_{MeOH} C_{HAc} - k_{-1} b_{MeAc} b_{H_2O} C_{MeAc} C_{H_2O} \right) \quad (2.6)$$

By combining the constants in Equation (2.6), it becomes

$$\frac{dC_{MeAc}}{dt} = k_2 \left( C_{MeOH} C_{HAc} - C_{MeAc} C_{H_2O} / K \right) \quad (2.7)$$

where

$$\begin{aligned} k_2 &= L^2 k_1 b_{MeOH} b_{HAc} \\ k_{-2} &= L^2 k_{-1} b_{MeAc} b_{H_2O} \\ K &= k_2 / k_{-2} \end{aligned} \quad (2.8)$$

Equation (2.7) is the familiar power law model for a homogeneous reaction.





From the above derivation, it can be seen that, even though the active group in the catalysts is not ideally dissociated from the carrier, the reaction can be quasi-homogeneous as long as the adsorption is weak for all components. In the absence of both external and internal diffusion resistance to mass transfer, it is possible to determine the intrinsic kinetics from the experimental data.

In this study, the reaction catalyzed by cation ion exchange resins was assumed to be quasi-homogeneous and Equation (2.7) was used to describe the reaction rate.

The equilibrium constant  $K$  in Equation (2.7) can be found from the equilibrium composition of the reaction mixture and is independent of reactant concentration. After  $K$  is obtained, the only parameter needed to be found in Equation (2.7) is the forward reaction constant  $k_2$ . Integrating Equation (2.7) yields,

$$\frac{1}{\sqrt{B^2 - 4AC}} \ln \left[ \frac{(B + \sqrt{B^2 - 4AC})C_{MeAc} + 2C}{(B - \sqrt{B^2 - 4AC})C_{MeAc} + 2C} \right] \equiv Y = k_2 t \quad (2.9)$$

where

$$\begin{aligned} A &= 1 - 1/K \\ B &= -a - b - d/K \\ C &= ab \end{aligned} \quad (2.10)$$

a, b and d = initial concentrations of methanol, acetic acid and water, respectively.

In this study, Equation (2.7) was used to model the kinetics of the reaction of Equation (2.1). If the kinetic model is valid, plotting the left term “Y” in Equation (2.9) vs. time “t” should yield a straight line. The forward reaction constant  $k_2$  can be found



from the slope of the line. The value of  $k_2$  is a function of temperature and catalyst loading, and can be expressed as

$$k_2 = k_0 W \exp\left(-\frac{E}{RT}\right) \quad (2.11)$$

where  $W$  is the catalyst loading,  $k_0$  is preexponential constant and  $E$  is activation energy.

### 2.3 Experimental

**CHEMICALS.** Methanol was obtained from Anachemia (Montreal, Quebec) and acetic acid from BDH Chemicals (Toronto, ON), both in analytical reagent grade. They were used as received.

**CATALYSTS.** Three catalysts (Amberlyst 15, Amberlyst 35 and Amberlite IR-120 Plus, supplied by Rohm and Haas, Philadelphia, PA) were chosen for preliminary tests. The preliminary tests showed that Amberlyst 15 had the best activity and was chosen for detailed studies. The typical physical and chemical properties of the catalysts are listed in Table 2-1.

**ANALYSIS.** The liquid samples were analyzed using a gas chromatograph (HP 5890 Series II, supplied by Hewlett-Packard (Canada) Ltd., Mississauga, ON) equipped with two detectors, TCD and FID, installed in series, for the determination of water, methanol, methyl acetate and acetic acid concentrations. Usually, only the data from TCD were used in the data processing while those from FID were for reference only. Helium was used as the column carrier gas and hydrogen plus air for the FID.

Because of the presence of large amounts of water, it was found to be quite difficult to find an adequate GC column and running conditions to separate the reaction



mixture in a reasonable period of time. After trying many columns (Porapak Q, Porapak R, Porapak QS, Supel-Q, SPB-5, etc., supplied by Supelco, Inc., Bellefonte, PA), it was found that a Supel-Q plot column (Fused Silica capillary column 30m  $\times$  0.32 mm ID) was satisfactory. The operating conditions for the gas chromatograph are:

Temperature ( $^{\circ}$ C):	Injector:	230
	Detector:	250
	Oven:	35, 2 min $\rightarrow$ 15/min $\rightarrow$ 130, 1 min
Flow rate (mL/min):	Column:	2.1
	Split flow:	74
	TCD aux:	2.5
	TCD ref:	16.5
	FID aux:	28.7
	FID hydrogen:	32.8
	FID air:	352

The injection size of samples was 1  $\mu$ L. The approximate retention time for the four components under the above operating conditions was:

water:	2.7 min
methanol:	3.3 min
methyl acetate:	8.1 min
acetic acid:	8.6 min

**EQUIPMENT AND OPERATING PROCEDURE.** A slurry reactor as shown in Figure 2-1 was used for the experiments. The reactor was made of glass with a capacity of



1000 mL. The reaction mixture was stirred and auxiliary heated by a hot plate/stirrer (PC-520, Corning, Inc., New York). The mixture was mainly heated by a heating tape wound around the reactor. A temperature controller (Series SR24, SHIMADEN Co., Ltd, Tokyo, Japan) was connected to the heating tape to control the reaction temperature, which was measured by a thermo-couple and a calibrated glass thermometer with a division of  $0.1^{\circ}\text{C}$ . During the reaction, the reactor temperature was controlled to  $\pm 0.1^{\circ}\text{C}$ .

In all experiments, water was first mixed with methanol in the reactor. A given amount of catalyst was added. Then, the heater, the stirrer and the cooling water valve were simultaneously turned on. After the mixture was heated to the set temperature, a given amount of heated acetic acid was added through the funnel into the reactor. The moment of addition of acetic acid was taken as the starting time of the reaction and the reaction temperature was recorded. Samples with a size of about 0.5 mL were withdrawn from the reactor using a syringe at regular intervals, quenched, and analyzed by a gas chromatograph. The total volume withdrawn from the reactor during a run was negligible compared with the total volume of the system.

Although the amount of acetic acid was only about 3 mass% of the reaction mixture, the addition of it could cause the reactor temperature to fluctuate by more than  $0.3^{\circ}\text{C}$  if the acetic acid was not heated to the appropriate temperature. This was especially true at higher reaction temperatures. Experience showed that the acetic acid should be heated to a temperature  $20^{\circ}\text{C}$  higher than the set reaction temperature because the acetic acid would lose some heat during the addition through the funnel.





## 2.4 Results And Discussion

### 2.4.1 Selection of Catalyst

In this study, three types of ion exchange resin (Amberlyst 15, Amberlyst 35 and Amberlite IR-120 Plus) were used in the preliminary tests for the catalytic activity. The tests were conducted under the following conditions:

Initial composition of reactants (mole fraction):

methanol:	0.00925
acetic acid:	0.00863
Reaction temperature:	$94 \pm 0.1^{\circ}\text{C}$
Catalyst (wet) loading:	1.5 mass%
Stirrer speed:	550 rpm

Figure 2-2 shows the production rate of methyl acetate vs. time. From this figure, it can be seen that Amberlyst 15 and Amberlyst 35 give much higher yields of methyl acetate than Amberlite IR-120 Plus. Amberlite IR-120 Plus is a gel-type cation resin of the sulfonated polystyrene type. It has a microporous structure so that the internal resistance to reactants could be very high. Amberlyst 15 and Amberlyst 35 are alike in their similar physical and chemical properties. They are spherical, macroporous beads consisting essentially of micro-beads fused together in the last stages of polymerization. The macroporous structure allows the reactants to move easily into the interior of the beads so that their reaction activity is much higher than that of Amberlite IR-120 Plus. Tanabe et al. (1989) summarized the results obtained by using macroporous and gel-type of catalysts. Kunin et al. (Tanabe et al., 1989) compared the catalytic activities of Amberlyst 15 and



Amberlite-120 for the decomposition of *t*-butyl acetate at 25°C. After one hour the conversion with the former catalyst was 80% of equilibrium, whereas the latter catalyst showed less than 1% conversion. Similar results were also obtained for the synthesis of *t*-butyl methacrylate from isobutene and methacrylic acid at 0°C. These results were obtained in the absence of strongly polar compounds such as water. From this study, it can be seen that, even though the reaction mixture is mostly water which is supposed to swell the resin network and allow the access of reactant molecules to the particle interior, the catalytic activity for gel-type resins is still much lower than that of macroporous resins.

Although Amberlyst 35 may be a superior catalyst for the production of MTBE, as reported by Rohm and Haas (1992), it showed no advantage in catalytic activity over Amberlyst 15 for this application. From Table 1 it can be seen that Amberlyst 35 has a higher concentration of acid sites and larger average pore size but lower surface area and larger particle size. It is difficult to draw a conclusion on catalytic activity from these data.

Yadav and Mehta (1994) used several solid acid catalysts (Filtrol-24, Amberlyst 15, Sulfated Zirconia and heteropoly acids) in the preparation of phenethyl acetate and cyclohexyl acetate. They found that Amberlyst 15 had the highest activity among those catalysts. Patwardhan and Sharma (1990) reported that Amberlyst 15 showed higher catalytic efficiency than Amberlyst XN1010 and Monodisperse K2661 in the esterification of carboxylic acids with olefins. In view of the results in the literature and those obtained in this study, Amberlyst 15 appears to be the best available catalyst and was chosen for the kinetic study.



### ***2.4.2 Effect of Stirrer Speed***

The external mass transfer resistance to the reaction process can be affected by stirrer speed. The effect of external mass transfer on the catalytic efficiency was investigated under the similar conditions as those reported in Section 2.4.1 except that the stirrer speed was varied from 160 to 760 rpm.

Figure 2-3 shows that the production rate of methyl acetate is independent of stirrer speed. This indicates that the external mass transfer resistance is negligible. Chakrabarti and Sharma (1993) pointed out that the external diffusion doesn't generally control the overall rate in ion exchange resin catalyzed process unless the viscosity of the reactant mixture is very high or the speed of agitation is very low. In the subsequent tests, the stirrer speed of 550 rpm was used to ensure that the measured reaction rate is free from external diffusion influences.

### ***2.4.3 Internal Resistance***

For the macroporous ion exchange catalyst without external mass transfer resistance, the rate-controlling steps can be the reaction at the micro-particle surface or diffusion within the macropores. In the preparation of phenethyl acetate and cyclohexyl acetate, Yadav and Mehta (1994) concluded that the internal diffusional resistance was absent for all the catalysts including Amberlyst 15. However, their simple analysis was based on the consideration of only the forward reaction, and no experimental data are available. The validity of the analysis is questionable.





To investigate the internal diffusion effects on the reaction of Equation (2.1), commercial Amberlyst 15 was screened into several different particle sizes. It was found that the reaction rate was higher when using smaller particles. A theoretical study on the internal mass transfer resistance effects will be discussed in detail in Chapter 3. It can be seen that internal resistance exists for particle sizes larger than 0.6 mm. The average effectiveness factor for the commercial Amberlyst 15 was found to be about 0.9. This indicates that the effect of internal diffusion on reaction rate is not significant.

#### 2.4.4 Apparent Equilibrium Constant

From Equation (2.7), the apparent equilibrium constant can be found from the equilibrium composition of the mixture:

$$K = \frac{C_{MeAc,e} C_{H_2O,e}}{C_{MeOH,e} C_{HAc,e}} \quad (2.12)$$

The equilibrium constants at reaction temperatures, 40, 65, 80 and 94°C were measured. The reaction equilibrium was reached in 5 to 26 hours depending on the reaction temperature and catalyst loading.

Figure 2-4 shows that K increases slightly with a decrease in reaction temperature. The values of K varied from 5.27 to 5.93 in the test range of reaction temperature. Agreda et al. (1990) reported that the equilibrium constant for the reaction of Equation (2.1) is 5.2 and reasonably independent of temperature. Because the reaction is exothermic, the trend that K increases with the decrease in reaction temperature is reasonable.



### 2.4.5 Reaction Constant

As discussed in Section 2.2, Equation (2.9) can be used to find superficial reaction constants from the measured concentration of methyl acetate with time. Figures 2-5 shows the plot of  $Y$  (see Equation (2.9)) vs. time for one typical run. From the figure, it can be seen that the data of  $Y$  vs. time can be described by a straight line through the point of origin. The superficial reaction rate constant can be found from the slope of the line. In this study, 35 runs were conducted for various stirrer speeds, reaction temperatures, catalyst loadings and reactant concentrations. Most of the runs lasted about two hours.

The fact that the plot of  $Y$  vs. time yields a straight line through the origin point shows that the reaction of Equation (2.1) catalyzed by Amberlyst 15 is quasi-homogeneous and Equation (2.7) can be used to describe the kinetics of the reaction.

### 2.4.6 Effect of Temperature

The effect of temperature on the reaction rate constant was investigated by setting the reaction temperature at 40, 65, 80 and 94°C under otherwise the similar conditions, as reported in Section 2.4.1.

From Figure 2-6 it can be seen that the effect of temperature on the rate of methyl acetate production is very significant. The reaction rate increased sharply with increasing temperature.

Figure 2-7 shows that the plot of  $\ln(k_2)$  vs.  $1/T$  can be represented by a straight line. From the slope of the line, the activation energy for reaction (2.1) was found to be



58.5 kJ/mol. The straight line shown in Figure 2-7 with a high activation energy indicates that the surface reaction is the rate-controlling step.

#### 2.4.7 Effect of Catalyst Loading

The effect of catalyst loading on reaction rates at temperatures of 80 and 94°C was investigated with catalyst loadings from 1.5 to 6.0%. Figure 2-8 shows that the reaction constant increases proportionally with the increase in catalyst loading. Acetic acid itself is a weak acid and has some catalytic activity. Therefore, slow reaction would occur even in the absence of added catalyst. But the values of  $k$  for blank runs (no catalyst added) were found to be 0.0081 and 0.0171 min<sup>-1</sup> at temperatures of 80 and 94°C, respectively. These two points are perfectly located on the two straight lines. With the increase in catalyst loading, the surface area and the total number of active sites increase linearly, and so do the reaction rate constants.

#### 2.4.8 Kinetic Equation

By combining Equations (2.7) and (2.11), the final kinetic equation for the reaction Equation (2.1) catalyzed by Amberlyst 15 is expressed as:

$$\frac{dC_{MeAc}}{dt} = k_0 W \exp(-E / RT) (C_{MeOH} C_{HAc} - C_{MeAc} C_{H_2O} / K) \quad (2.13)$$

where each component concentration is given as the mole fraction. By using the measured kinetic data under various reaction temperatures, catalyst loadings and reactant concentrations,  $k_0$  was found to be close to a constant:

$$k_0 = 1.76 \times 10^6 \quad (2.14)$$



Combining the information for activation energy in Section 2.4.6 and the equilibrium constant determined in Section 2.4.4, a complete kinetic equation was obtained.

#### **2.4.9 Catalyst Reusability**

Amberlyst 15 resin can be used at temperatures up to approximately 120°C. Gradual desulfonation resulting in loss of capacity may be evident at higher temperatures. In order to avoid fouling, poisoning or degradation, it is necessary to remove turbidity, colloidal particles, inorganic salts and organic peroxides from the stream prior to its contact with the catalyst.

In this study, precaution was taken to prevent the decrease in the catalyst effectiveness. The reusability test was conducted by using the same catalyst in four runs with the similar operating conditions as in Section 2.4.1. Figure 2-9 shows the results from the four runs. No sign of deactivation was observed for the reused catalyst. The difference between the production rate of methyl acetate using the fresh and reused catalyst is within the experimental error.

### **2.5 Conclusions**

Amberlyst 15 was found to be effective as a catalyst for the reaction in water between acetic acid and methanol at low reactant concentrations. The effects of stirrer speed, reaction temperature, reactant concentration and catalyst loading on the reaction rate were investigated. It was found that external resistance to the reaction process was





easily eliminated. The internal mass transfer resistance is not significant. A kinetic equation has been developed. This equation can be used in the design of the catalytic distillation column to remove low concentration of acetic acid from wastewater.



## 2.6 Nomenclature

$a$	initial concentration of methanol, mol/mol of mixture
$b$	initial concentration of acetic acid, mol/mol of mixture
$b_i$	adsorption constant of component i
$C_i$	concentration of component i in mixture, mol/mol of mixture
$C_{i,e}$	equilibrium concentration of component i in mixture, mol/mol of mixture
$d$	initial concentration of water, mol/mol of mixture
$dC_{MeAc} / dt$	reaction rate, mol/s·L <sub>liq</sub>
DVB	divinylbenzene
$E$	activation energy, kJ/mol
$K$	reaction equilibrium constant
$k_1, k_{-1}$	surface reaction constants, 1/min
$k_2, k_{-2}$	reaction constants, 1/min
$k_0$	preexponential constant
$L$	total number of catalytically active sites
$t$	time, min.
$T$	temperature, K
$W$	catalyst loading, (g. cat)/L <sub>liq</sub>
$Y$	defined in Equation (2-9)
$\theta_i$	ratio of catalytically active sites occupied by component i



Table 2-1

## Typical Physical and Chemical Properties of Catalysts

(Rohm and Haas, 1978,1992a, 1992b; Tanabe, et al., 1989)

Properties	Amberlite-IR120	Amberlyst 15	Amberlyst 35
Physical Form	light yellow, spherical beads	opaque, spherical beads	opaque, dark spherical beads
Ionic Form	H <sup>+</sup>	H <sup>+</sup>	H <sup>+</sup>
Concentration of Acid Sites, meg/(g.cat)	4.3	4.9	5.4
Moisture Content, mass%	-	53	56
Particle Size, mm	0.30 - 1.00	0.35 - 1.20	0.4 - 1.25
Porosity, mL/g	0.018	0.30	0.35
Average Pore Diameter, nm	-	25.0	30.0
Surface Area, m <sup>2</sup> /g	< 0.1	45	44
Maximum Temperature, °C	-	120	140
Crosslinking Density, (% DVB)	-	20	20





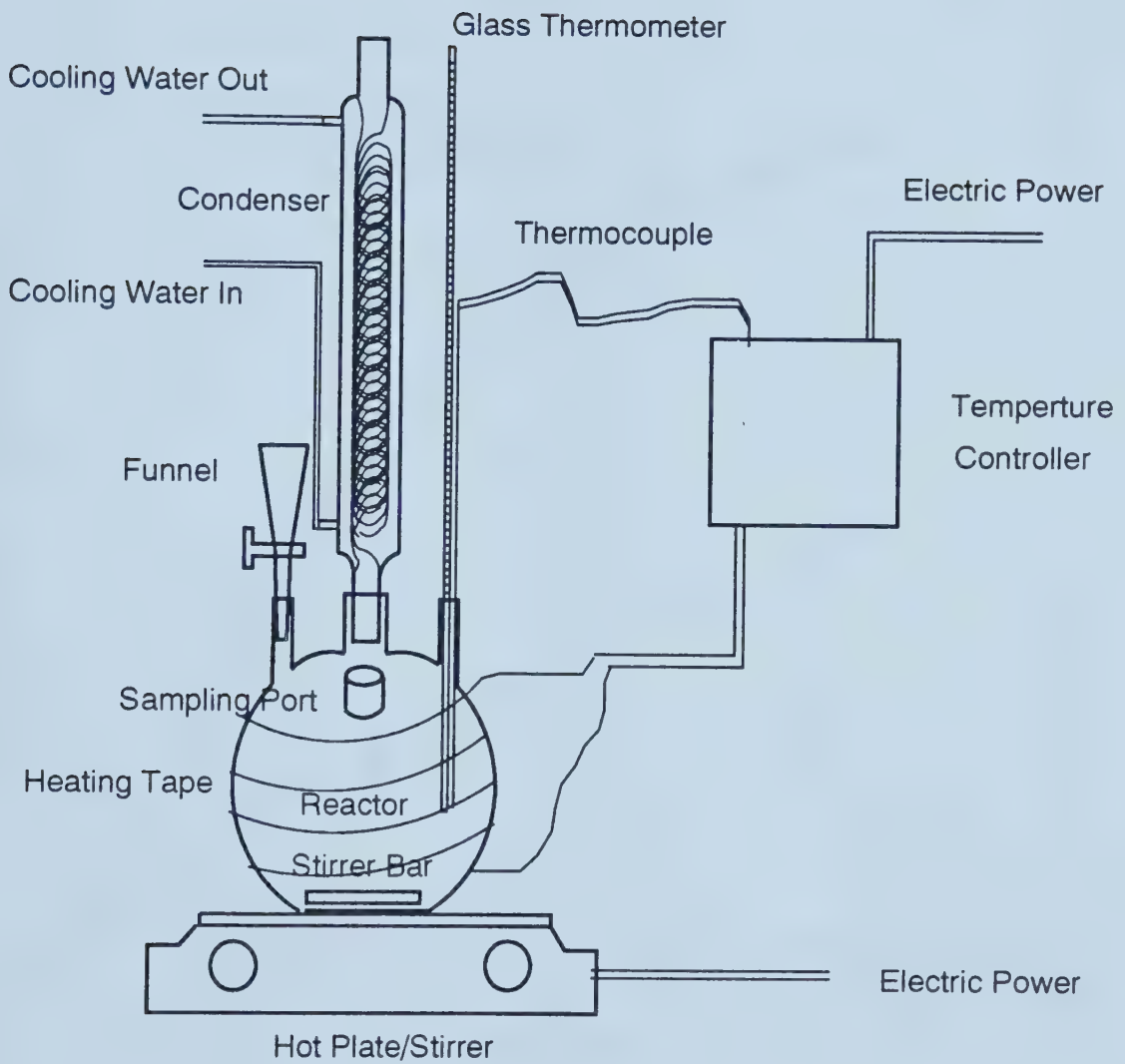


Figure 2-1 Experimental Set-up for Kinetic Tests



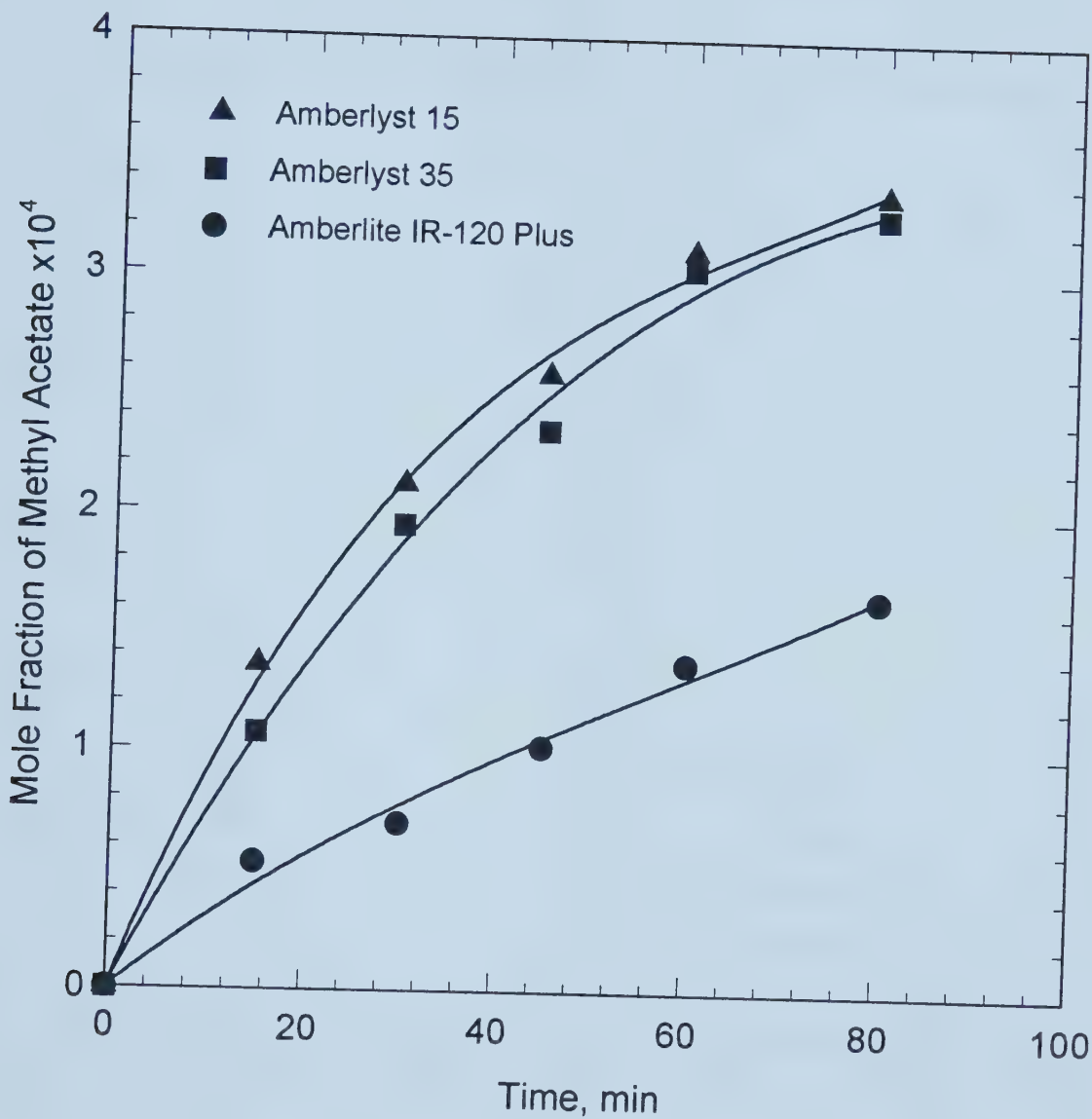


Figure 2-2. Reaction Activity of Catalysts. Initial reactant concentration (mole fraction): MeOH=0.00925, HAc=0.00863; Reaction temperature: 94°C; Catalyst loading: 1.5 mass%; Stirrer speed: 550 rpm



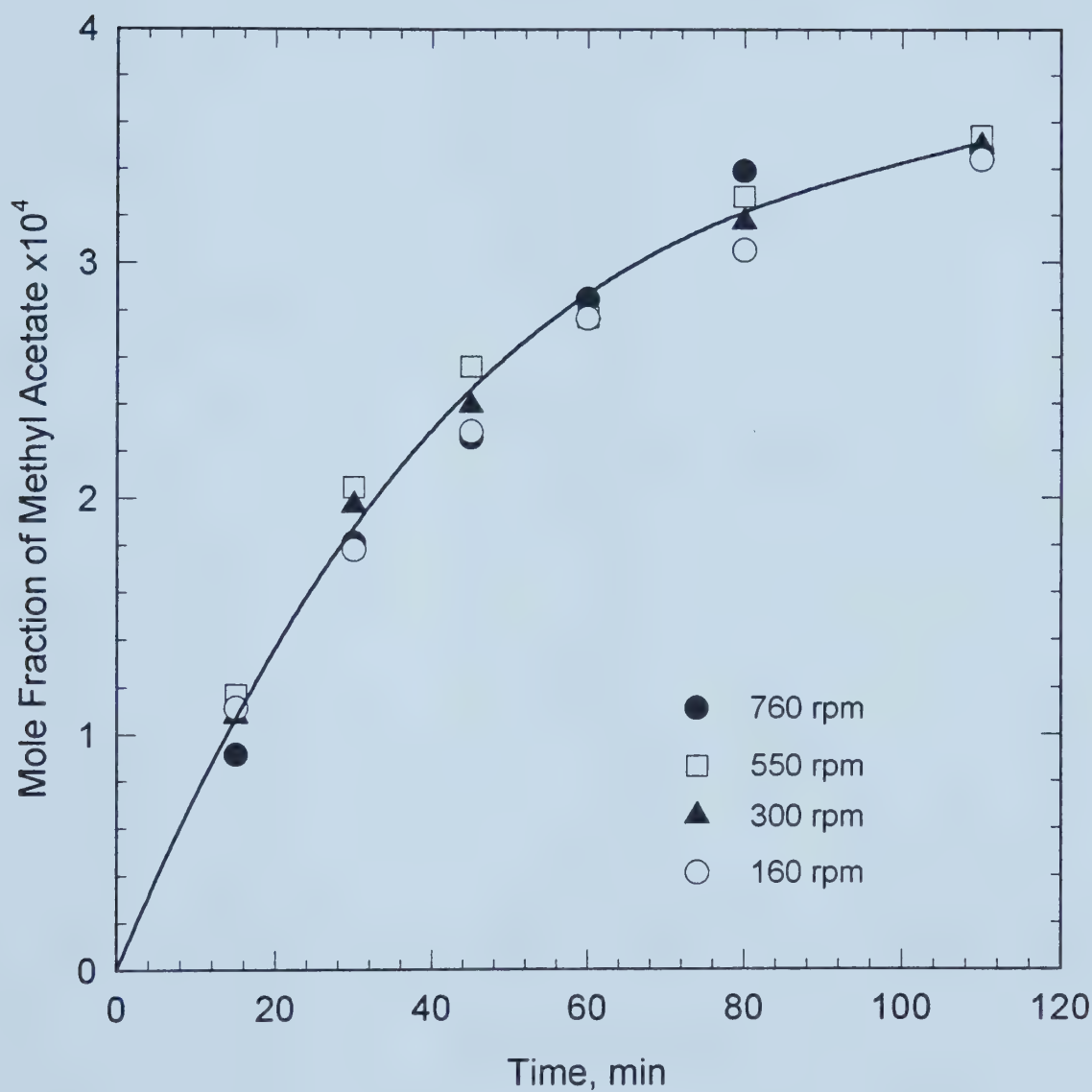


Figure 2-3. Effect of Stirrer Speed on Reaction Rate. Initial reactant concentration (mole fraction): MeOH=0.00925, HAc=0.00863; Reaction temperature: 94°C; Catalyst loading: 1.5 mass%



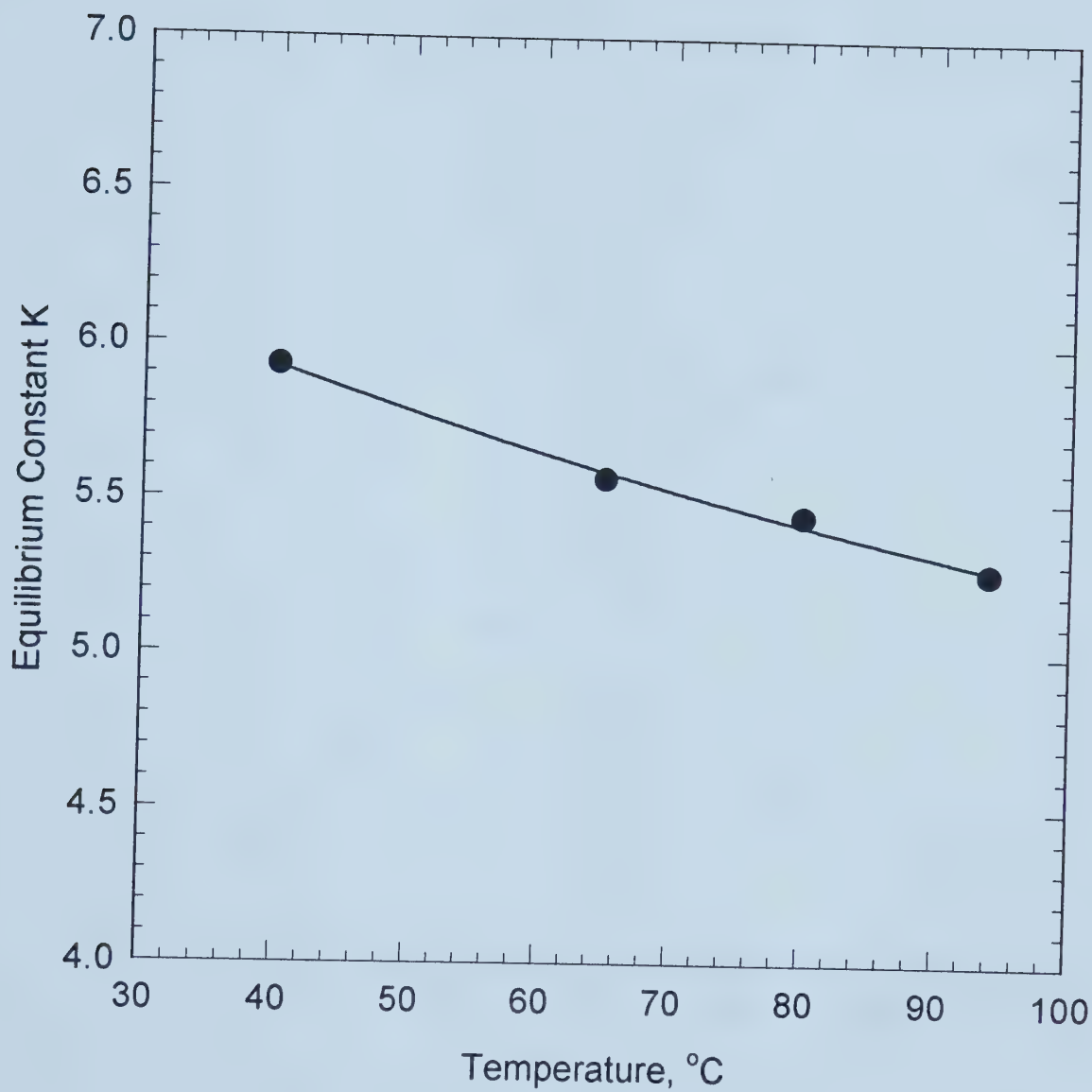


Figure 2-4. Dependence of Equilibrium Constant on Temperature





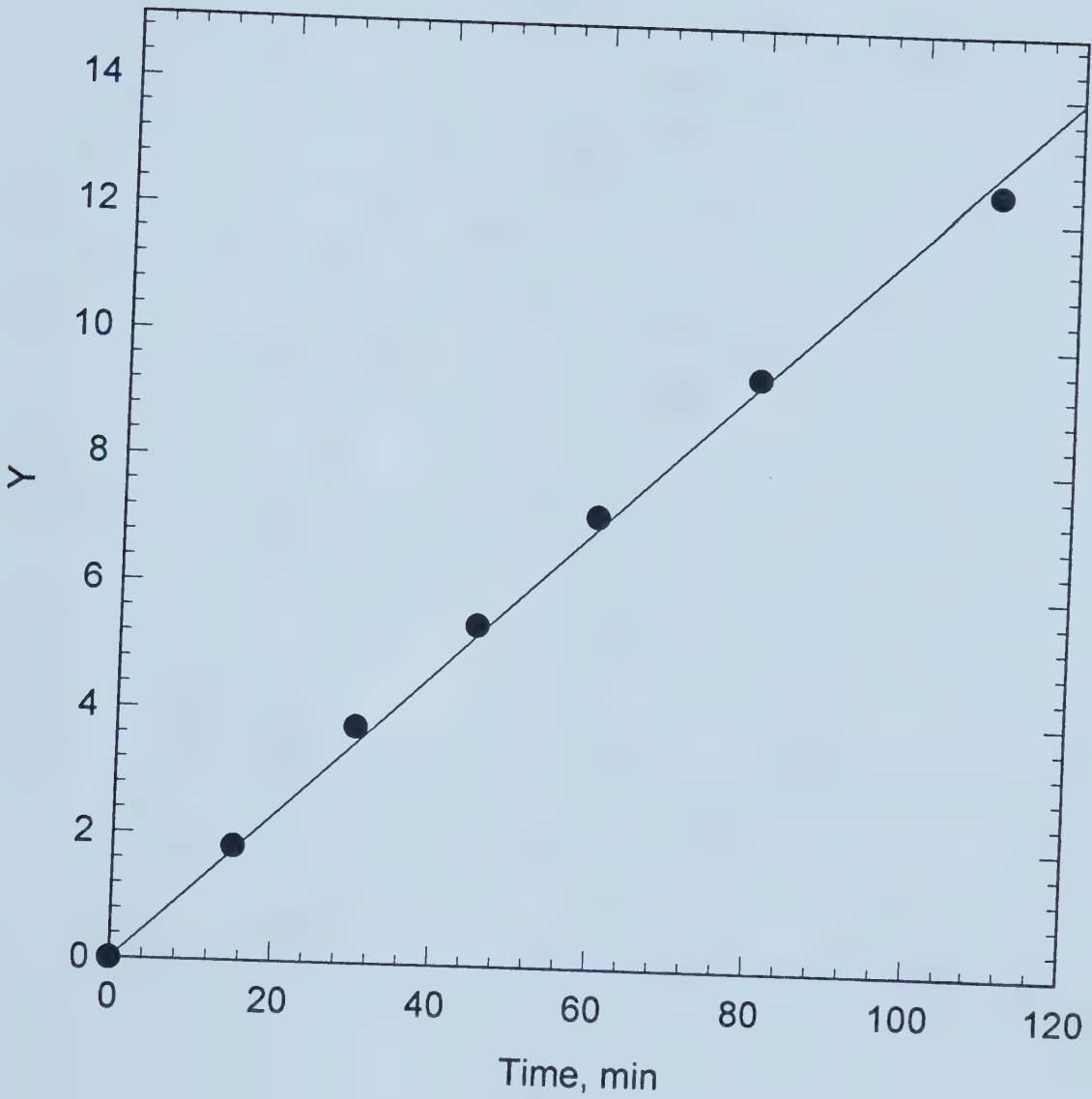


Figure 2-5. Plot of Left Term in Eq. (2-9) vs. Time. Initial reactant concentration (mole fraction): MeOH=0.00925, HAc=0.00863; Reaction temperature: 94°C; Catalyst loading: 1.5 mass%; Stirrer speed: 550 rpm;  $k_2=0.114$  1/min



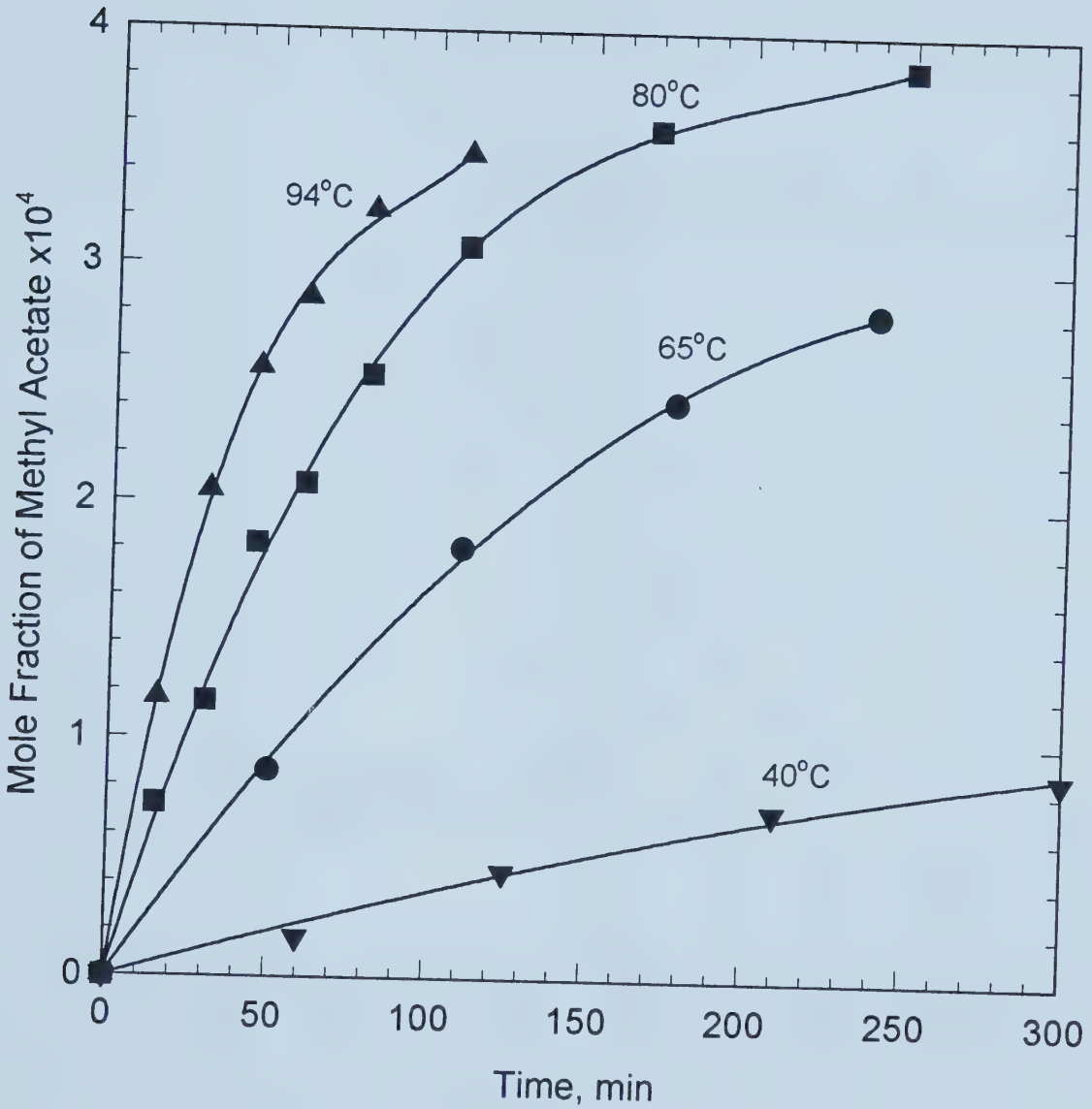


Figure 2-6. Effect of Temperature on Reaction Rate. Initial reactant concentration (mole fraction): MeOH=0.00925, HAc=0.00863; Catalyst loading: 1.5 mass%; Stirrer speed: 550 rpm



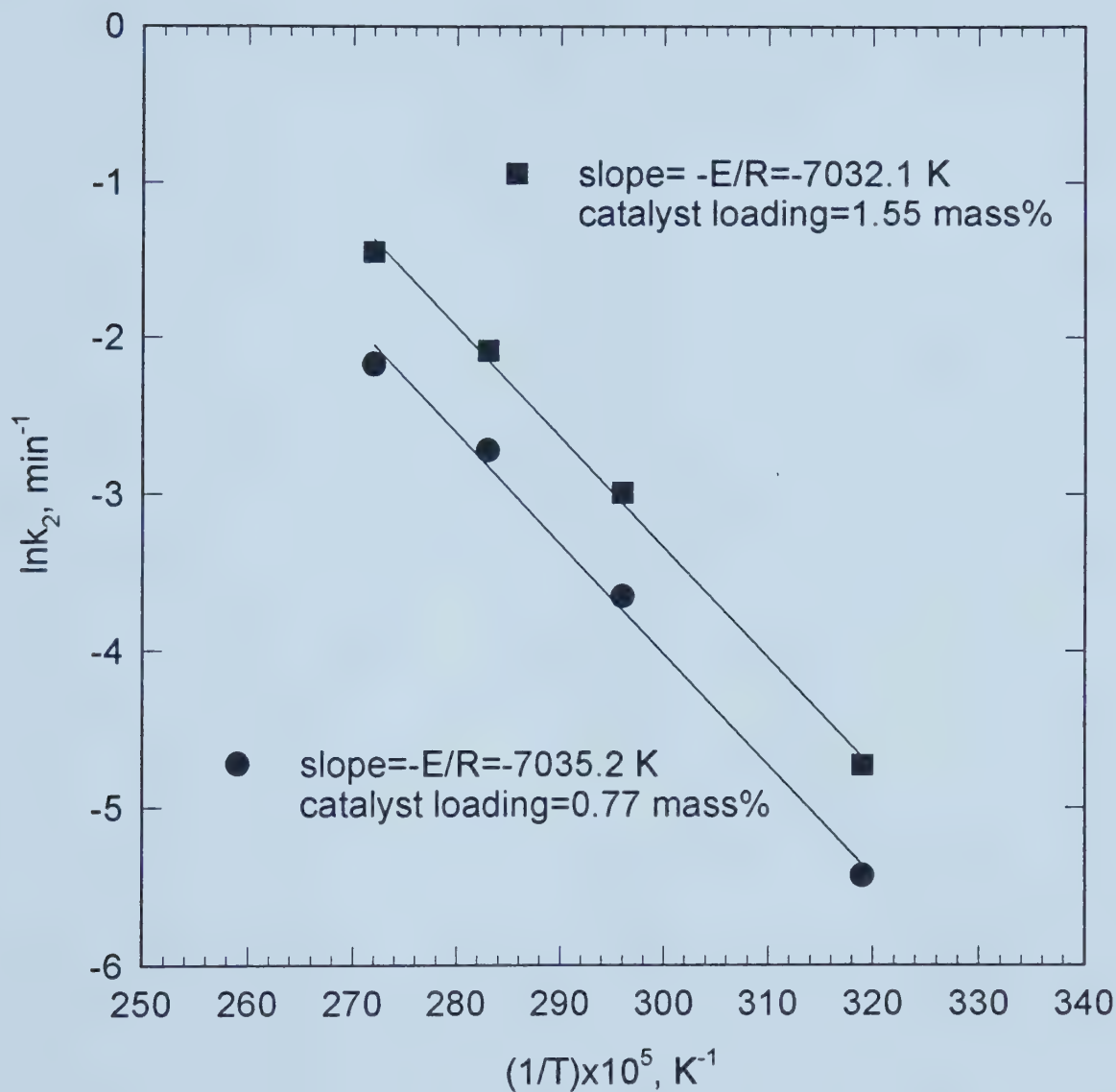


Figure 2-7. Activation Energy. Initial reactant concentration (mole fraction): MeOH=0.00925, HAc=0.00863; Stirrer speed: 550 rpm



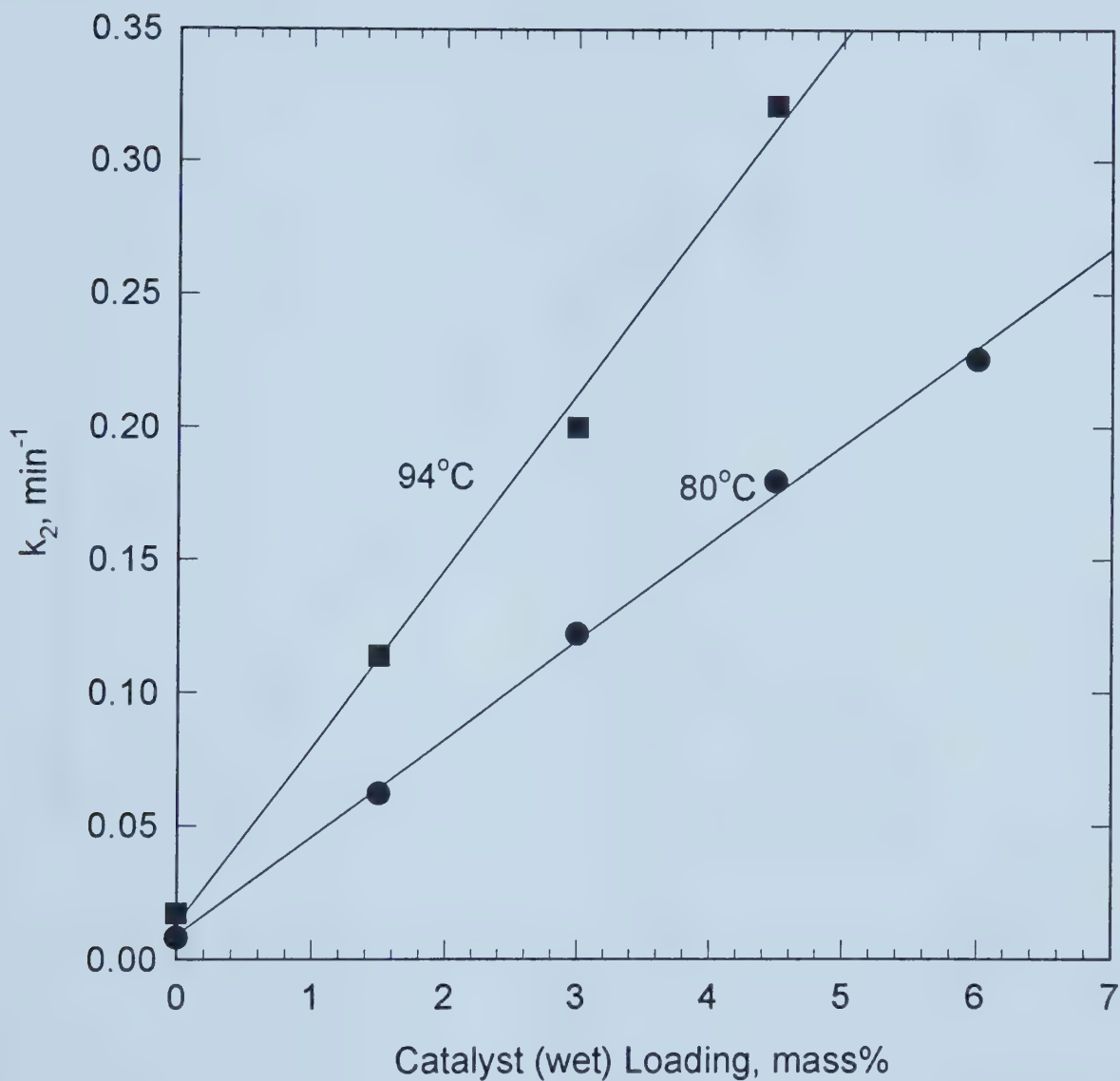


Figure 2-8. Effect of Catalyst Loading on Reaction Rate. Initial reactant concentration (mole fraction): MeOH=0.00925, HAc=0.00863; Stirrer speed: 550 rpm





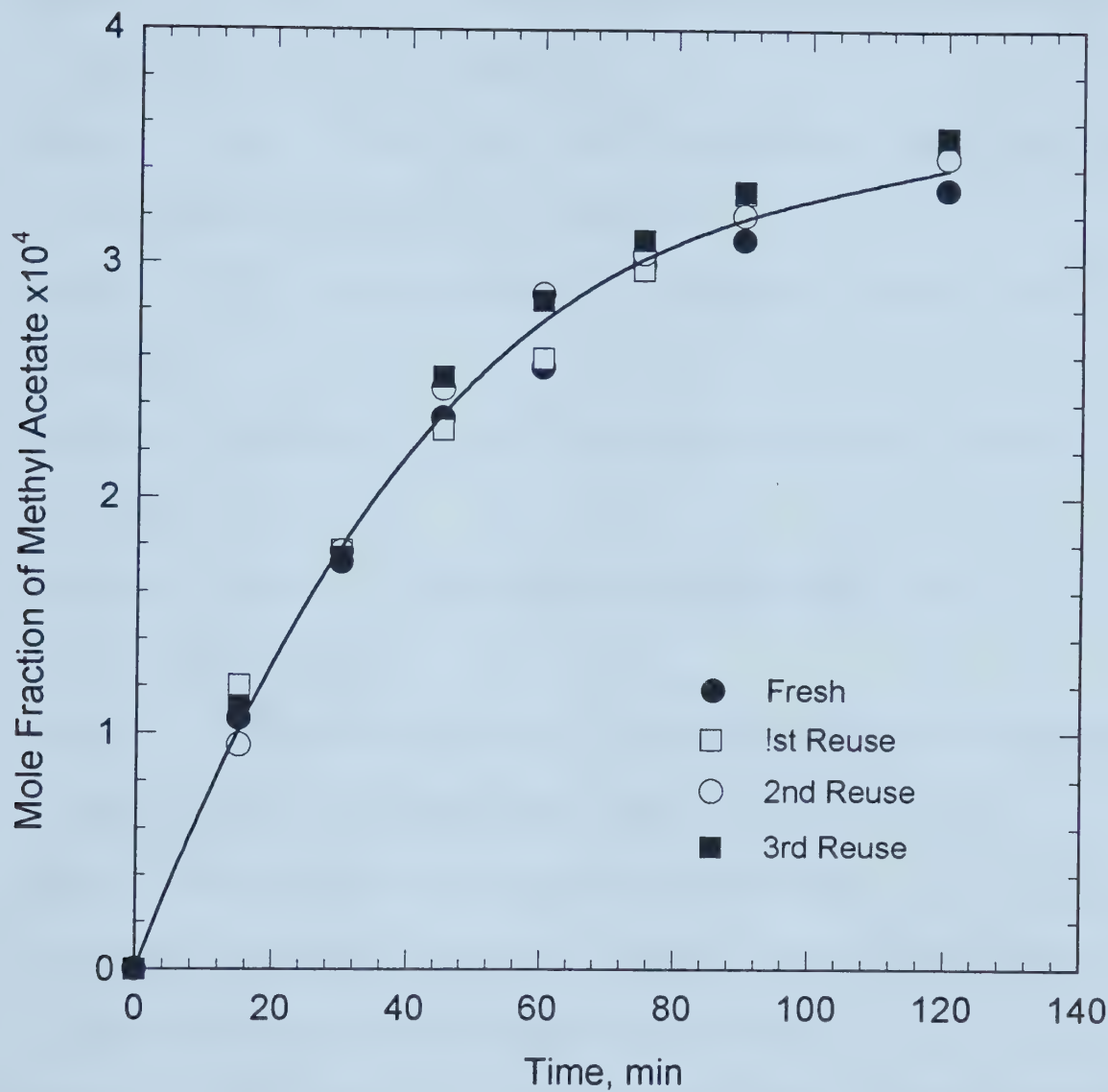


Figure 2-9. Catalyst Reusability. Initial reactant concentration (mole fraction):

MeOH=0.00925, HAc=0.00863; Reaction temperature: 94°C; Catalyst

loading: 1.5 mass%; Stirrer speed: 550 rpm



## 2.7 Literature Cited

- Agreda, V.H. and Partin, L.R. (1984) Reactive Distillation Process for the Production of Methyl Acetate. *US Patent* No. **4,435,595**.
- Agreda, V.H., Partin, L.R. and William, H.H. (1990) High-Purity Methyl Acetate via Reactive Distillation. *Chem. Eng. Prog.* **86**(2), 40-46.
- Backhaus, A.A. (1921) Continuous Process for the Manufacture of Esters. *US Patent* No. **1,400,849**.
- Chakrabarti, A. and Sharma, M.M. (1993) Cation Ion Exchange Resin as Catalyst. *React. Polym.* **20**, 1-45.
- Doherty, M.F. and Buzad, G. (1992) Reactive Distillation by Design. *Trans. Inst. Chem. Eng.* **70**, Part A, 448-458.
- Fuchigami, Y., (1990) Hydrolysis of Methyl Acetate in Distillation Column Packed with Reactive Packing of Ion Exchange Resin. *J. Chem. Eng. Jpn* **23**, 354-358.
- Hefferich, F.(1962) *Ion Exchange*, p.548, McGraw-Hill, New York.
- Helfferich, F.G. and Hwang, Y. (1988) Ion Exchangers as Catalysts. In *Ion Exchange for Industry*, M. Streat, Ed., Ellis Horwood Publisher, New York.
- Kumbhar, P.S. and Yadav, G.D. (1989) Catalysis by Sulfur-promoted Superacidic Zirconia: Condensation reactions of Hydroquinone with Aniline and Substituted Anilines. *Chem. Eng. Sci.* **44**, 2535-2544.
- McKetta, J.J. (1976) *Encyclopedia of Chemical Processing and Design*, vol.1, Marcel Dekker, Inc., New York.



- Patwardhan, A.A. and Sharma, M.M. (1990) Esterification of Carboxylic Acids with Olefins Using Cation Exchange Resins as Catalysts. *React. Polym.* **13**, 161-176.
- Rohm and Haas (1992) *Ion Exchange Resin Data Sheet-Amberlyst 35 Wet Polymeric Catalyst*, Rohm and Haas Company, Philadelphia, PA.
- Rohm and Haas (1978) *Ion Exchange Resin Data Sheet- Amberlite IR-120 Plus*, Rohm and Haas Company, Philadelphia, PA.
- Rohm and Haas (1992) *Ion Exchange Resin Data Sheet- Amberlyst 15 Wet Polymeric Catalyst*, Rohm and Haas Company, Philadelphia, PA.
- Savkovic-Stevanovic, J., Mistic-Vukovic, M., Boncic-Caricic, G., Trisovic, B and Jezdic, S. (1992) Reactive Distillation with Ion Exchangers. *Sep. Sci. Technol.* **27**, 613-630.
- Sawistowski, H. and Pilavakis, P.A. (1979) Distillation with Chemical Reaction in a Packed Column. *I. Chem. Eng. Symp. Ser.* **56**, 4.2/49-63.
- Sawistowski, H. and Pilavakis, P.A. (1988) Performance of Esterification in a Reaction-Distillation Column. *Chem. Eng. Sci.* **43**, 355-360.
- Tanabe, K., Misono, M., Ono, Y. and Hattori, H. (1989) *New Solid Acids and Bases*, Kodansha Ltd., Tokyo and Elsevier Science Publishers B.V., Amsterdam.
- Thomas, Sir John Meurig, (1992) Solid Acid Catalysts. *Sci. Am.* **266**(4), 112-118.
- Yadav, G.D. and Mehta, P.H. (1994) Heterogeneous Catalysis in Esterification Reactions: Preparation of Phenethyl Acetate and Cyclohexyl Acetate by Using a Variety of Solid Acidic Catalysts. *Ind. Eng. Chem. Res.* **33**, 2198-2208.



## CHAPTER 3. EFFECT OF INTERNAL DIFFUSION ON HETEROGENEOUS CATALYTIC ESTERIFICATION OF ACETIC ACID\*

### 3.1 Introduction

Kinetics for the esterification of acetic acid with methanol have been studied in Chapter 2. The reaction was catalyzed by Amberlyst 15 (Rohm and Haas, USA), a solid bead form, strongly acidic resin with a size distribution from 0.35 mm to 1.2 mm. The kinetic tests with two batches of beads ( $d_p=0.42$  to 0.60 and 0.85 to 1.0 mm) showed that the reaction rate for the smaller beads was higher than that for the larger beads at a reaction temperature of 94°C. The observed difference in catalyst activity under otherwise similar conditions can only be attributed to internal diffusion resistance if the concentration of the acid sites are independent of the particle size.

Physically, the bead-form particles are agglomerates of gel-type microparticles estimated to be about 0.1  $\mu\text{m}$  diameter. About 5% of the active acid sites,  $-\text{SO}_3\text{H}$  groups, are on the outer surface of the microparticles and the remainder are inside these small particles (Leung et al., 1986). The reaction can proceed on these external active sites without being preceded by permeation into the microparticles. However, the molecules from the external phase must penetrate through the polymer matrix in order to gain access to the inner active functional groups. Because of the small size of the microparticles, Leung et al. (1986) estimated that the effectiveness factor for the microparticles should be

---

\* A version of this chapter has been published: Z.P. Xu and K.T. Chuang (1997) *Chem. Eng. Sci.* **52**, 3011-3017.





close to unity. This implies that the internal diffusion resistance can only be due to the macropores.

The effect of internal diffusion on reactions catalyzed using ion exchange resin has been reported to be dependent on many factors such as catalyst composition, reaction medium, reaction temperature, particle size. Beasley and Jakovac (1984) used Amberlyst 15 in the conversion of isobutylene to MTBE. They found that there was no particle size effect on the reaction rate, but they did not disclose the particles size and reaction conditions. Leung et al. (1986) measured the rates of hydration of isobutene with Amberlyst 15 in liquid-full as well as trickle-bed reactors. They found that internal diffusion resistance was significant, as indicated by effectiveness factors from 0.26 for the large size catalyst particles ( $d_p=1.04$  mm) at  $60^\circ\text{C}$  to 0.84 for the smaller particles ( $d_p=0.45$  mm) at  $30^\circ\text{C}$ . They pointed out that the internal diffusion resistance is due to the macropores surrounding the very small gel-type microparticles of which the particles were composed. Kaiser et al. (1962) measured conversions in an integral reactor of Amberlyst 15 particles for the hydration of propylene. The overall activation energy was found to decline with increasing temperature. This suggests that internal diffusion resistance is significant. Patwardhan and Sharma (1990) studied the esterification of acetic acid with olefins and isobutylene in the presence of Amberlyst 15 in the temperature range of 10 to  $100^\circ\text{C}$ . They found no effect on the rate of reaction for the variation in the particle size from 0.3 to 0.6 mm. In the preparation of phenethyl acetate, Yadav and Mehta (1994) concluded that internal diffusion resistance was absent for all the catalysts used in the study, including Amberlyst 15.



As discussed in the previous paper by Xu and Chuang (1996), acetic acid esterification with methanol catalyzed by Amberlyst 15 is a reversible second-order reaction. To the best of our knowledge, the effect of internal diffusion on this catalytic reaction has not been reported. In this work, the internal diffusion effect on the acetic acid esterification catalyzed by Amberlyst 15 was analyzed theoretically. Kinetic measurements have also been conducted and compared with the predictions of the theoretical analysis.

### 3.2 Theoretical

The effect of internal diffusion on catalytic reactions has been widely reported. Most of the publications dealt with simple reactions. Schneider and Mitschka published a series of papers (1965, 1966a, 1966b) on the effect of internal diffusion on several types of reactions. One of them (1966a) is a reversible, second-order reaction with Langmuir-Hinshelwood type rate equation. The analysis was based on gas-solid catalytic reactions. Their analysis can be extended to determine the effect of internal diffusion on the second-order reversible esterification in liquid phase catalyzed by Amberlyst 15.

It is known from Chapter 2 that the rate of reaction (2.1) can be expressed by

$$R_i = k_i(C_1C_2 - C_3C_4 / K) \quad (3.1)$$

where the subscripts represent the components of the system: 1, 2 - acetic acid and methanol, 3, 4 - methyl acetate and water.

The effect of internal diffusion on the catalytic reaction can be accounted for by an effectiveness factor  $\eta$  which is defined as:

$$\eta = \frac{\text{actual rate for the whole pellet}}{\text{rate evaluated at outer surface conditions}} \quad (3.2)$$



To determine  $\eta$ , the concentration profile within the pellet must be found. For a spherical particle at steady-state conditions, Equation (3.3) can be deduced from the mass balance:

$$\frac{1}{r^2} \frac{d}{dr} \left( r^2 D_{e1} \frac{dC_1}{dr} \right) = R_i \quad (3.3)$$

Under isothermal conditions Equation (3.3) can be rewritten as Equation (3.4):

$$\frac{d^2 C_1}{dr^2} + \frac{2}{r} \frac{dC_1}{dr} = \frac{R_i}{D_{e1}} \quad (3.4)$$

To solve Equation (3.4),  $R_i$  needs to be expressed as a function of  $C_1$ . The relationships between  $C_j$  and  $C_1$  can be expressed as (Schneider and Mitschka, 1966a):

$$C_j = C_{js} - \delta_j C_{1s} + \delta_j C_1 \quad (3.5)$$

where

$$\delta_j = \frac{a_j D_{e1}}{a_1 D_{ej}} \quad (3.6)$$

$a_j$  - stoichiometric coefficient of component  $j$  for reaction (2.1),  $a_1=a_2=-1$ ,  $a_3=a_4=1$

Substituting Equation(3.5) into Equation (3.1) and rearranging it,

$$R_i = (K_{24} C_1^2 + K_{14} C_1 - K_{04}) \quad (3.7)$$

where

$$K_{24} = k_i (\delta_2 - \delta_3 \delta_4 / K) \quad (3.8)$$

$$K_{14} = k_i \left( C_{2s} - \delta_2 C_{1s} - \frac{\delta_3 C_{4s}}{K} + \frac{2\delta_3 \delta_4 C_{1s}}{K} - \frac{\delta_4 C_{3s}}{K} \right) \quad (3.9)$$

$$K_{04} = \frac{k_i}{K} \left[ C_{1s} (\delta_3 \delta_4 C_{1s} - \delta_4 C_{3s} - \delta_3 C_{4s}) + C_{3s} C_{4s} \right] \quad (3.10)$$



The concentration  $C_1$  in the porous structure of the catalyst can be normalized by

$$y = (C_1 - C_1^*) / (C_{1s} - C_1^*) \quad (3.11)$$

where  $C_1^*$  is the equilibrium concentration of component 1 and can be found by setting

$C_1 = C_1^*$  and  $R_i = 0$  in Equation (3.7) so that

$$K_{24}C_1^{*2} + K_{14}C_1^* - K_{04} = 0 \quad (3.12)$$

$$C_1^* = \left( -K_{14} \pm \sqrt{K_{14}^2 + 4K_{24}K_{04}} \right) / (2K_{24}) \quad (3.13)$$

Substituting Equation (3.11) into Equation (3.7) and rearranging it,

$$R_i(y) = A[y(y+C) / (1+C)] \quad (3.14)$$

where

$$C = \left[ 2C_1^* + (K_{14} / K_{24}) \right] / (C_{1s} - C_1^*) \quad (3.15)$$

$$A = K_{24}(1+C)(C_{1s} - C_1^*)^2 = R_i(y=1) \quad (3.16)$$

The dimension of a spherical pellet can be normalized as

$$x = (R-r) / R \quad (3.17)$$

Substituting Equations (3.11), (3.14) and (3.17) into Equation (3.4), the final differential equation with dimensionless variables and parameters is obtained:

$$\frac{d^2 y}{dx^2} - \frac{2}{1-x} \frac{dy}{dx} = M_R^2 \frac{y(y+C)}{(1+C)} \quad (3.18)$$

where the catalyst modules  $M_R$  are defined as

$$M_R = R \sqrt{A / [D_{e1}(C_{1s} - C_1^*)]} \quad (3.19)$$

Equation (3.18) can be solved numerically with the following boundary conditions:





$$\begin{aligned} x = 0 & \quad y = 1 \\ x = 1 & \quad dy/dx = 0 \end{aligned} \quad (3.20)$$

The effectiveness factor  $\eta$  can be determined from the concentration profile shown in Equation (3.18) and the definition of effectiveness factor shown in Equation (3.2):

$$\eta = \frac{4\pi R^2 D_{e1} (dC_1 / dr) \big|_{r=R}}{(4/3)\pi R^3 R_i (y=1)} = - \frac{(dy / dx) \big|_{x=0}}{M_R^2 / 3} \quad (3.21)$$

It should be noted that reactant 1 can be either acetic acid or methanol. However, the concentration of reactant 2 in the catalyst pores should always be non-negative even when the concentration of reactant 1 is zero. From Equation (3.5), the criterion for choosing reactant 1 is

$$C_{2s} - \delta_2 C_{1s} \geq 0 \quad (3.22)$$

In this study, methanol is always in excess and effective diffusivity of acetic acid is lower than methanol. To satisfy the above criterion, the choice for reactant 1 is acetic acid.

### 3.3 Results and Discussion

#### 3.3.1 Solution of Equation (3.18)

The nonlinear ordinary differential equation (3.18) with boundary conditions (3.20) can be solved by finite difference formulation using quasilinearization algorithm. The method replaces the single nonlinear equation by a sequence of linear equations. The successive solutions of this sequence are pre-supposed to converge in the limit to the solution of the nonlinear equation. Three iterations may be needed to obtain the convergent results with the following criterion:



$$error = \sum_{j=1}^4 |y_{i,j} - y_{i-1,j}| < 1.0 \times 10^{-5} \quad (3.23)$$

The convergence behavior is very good for any feasible values of parameter  $C$  in Equation (3.18). Values of  $C$  should be in the range of  $-1 > C \geq 0$  to guarantee the positive reaction rate, as shown in Equation (3.14).

From the solution of Equation (3.18), effectiveness factors can be determined using Equation (3.21) for various values of  $M_R$ . Some of the numerical results are plotted in Figure 3-1. From this figure, it can be seen that  $\eta$  decreases with increasing value of the catalyst modules  $M_R$  for all values of  $C$ . For a given  $M_R$ , higher values of  $\eta$  were obtained with negative values of  $C$ , and with increasing  $C$  for both negative and positive values of  $C$ . The effect of  $C$  on  $\eta$  can be neglected when  $|C| > 10.0$ . From Equation (3.14), it can be seen that the reaction is close to first order for  $|C| > 10.0$ .

### 3.3.2 Effective Diffusivity

To predict the rate of internal diffusion in a catalyst, the effective diffusivity of the solute molecule in the pore filled with liquid needs to be evaluated first. Usually, the effective diffusivity is obtained by applying a series of correction factors to the diffusivity of the solute molecule in a bulk liquid phase (Ternan, 1987; Satterfield et al., 1973).

Data and models on the solute molecule diffusion in macropores of catalysts are scarce. Ternan (1987, 1996) proposed the following model to calculate the effective diffusivity of liquid in macropores and mesopores:

$$D_{ej}' / D_{mj} = (1 - \lambda_j)^2 / (1 + P_j \lambda_j) \quad (3.24)$$



where  $\lambda_j = d_{mj} / d_p$  and  $P_j$  is a adjusted model parameter.  $D_{ej}'$  is evaluated based on the available space for solute to diffuse within catalyst particles. The values of  $P_j$  so obtained are in the range of 2 to 20, depending on the mixture and temperature. The higher the temperature and the larger the pore size, the lower are the values of  $P_j$ .

In the present case, the reaction temperature is higher, pore size is larger and molecule size is smaller. The values of  $P_j$  are expected to be in the order of 1. Since the average pore size for the catalyst is  $250 \text{ \AA}$  and molecular diameters are in the range of  $3.1 - 4.9 \text{ \AA}$ ,  $\lambda_j$  is expected to be in the order of 0.01. Therefore,  $D_{ej}'/D_{mj}$  is close to 1.0. From the effective diffusivity of isobutene in water obtained by Leung et al. (1986) with Amberlyst 15, it can also be concluded that  $D_{ej}'/D_{mj}$  is close to 1.0. Hence, the values of  $D_{mj}$  were used for  $D_{ej}'$ .

In the evaluation of the effectiveness factor, the effective diffusivity based on the entire catalyst particles,  $D_{ej}$ , is needed. The relationship between  $D_{ej}$  and  $D_{ej}'$  can be expressed as  $D_{ej} = \varepsilon D_{ej}'$ .

Because of the low concentrations of methanol, acetic acid and methyl acetate, the bulk liquid diffusivity can be estimated using the correlation developed by Wilke and Chang (1955):

$$D_{mj} = 7.4 \times 10^{-8} \frac{(\phi_j M_j)^{1/2} T}{\mu_j V_j^{0.6}} \quad (3.25)$$



### 3.3.3 Concentration of Acid Sites in Amberlyst 15

In addition to the internal diffusion resistance, the difference in the concentration of acid sites between the different sizes of catalysts can also cause a difference in the reaction rates. Therefore, the concentration of acid sites for the catalysts with diameters of 0.42 to 0.60 and 0.85 to 1.00 mm were each determined by titration method. 1 g of catalyst samples was added to about 50 mL of NaCl solution (200 g/L) and stirred. The ion exchange between  $H^+$  and  $Na^+$  was allowed to proceed for 24 hours. The mixture was then titrated with 0.1 N NaOH solution. The test results are listed in Table 3-1. It can be seen that the concentration of acid sites is essentially independent of the particle size, and that the values are very close to the value (4.7 meq/g dry) reported by Rohm and Haas (1990). Therefore, any difference in the reaction rates between the two sizes of catalyst can only be attributed to the internal diffusion resistance.

### 3.3.4 Internal Diffusion in Amberlyst 15

A sample calculation of effectiveness factor is shown as follows:

Reaction Conditions:

Reaction temperature:  $94^{\circ}C$

Catalyst particle size  $d_p$ : 0.8 mm

Reaction constant  $k_i$ :  $0.124 \text{ min}^{-1}$

Equilibrium constant  $K$ : 5.28

Reaction composition and diffusivity:





j	$C_{js}$ (mol/mol)	$D_{ej} \times 10^9$ (m <sup>2</sup> /s)
acetic acid	0.00863	1.93
methanol	0.00925	2.47
methyl acetate	0.00025	1.63
water	0.982	4.03

Calculation Results:

$$K_{24}=0.123 \quad K_{14}=2.199 \quad K_{04}=1.033 \quad C_1^*=0.458 \quad C=2457.5$$

$$A=0.0177 \quad M_R/3=0.596 \quad \eta=0.835$$

The two most important factors which affect internal diffusion are particle size and reaction temperature. Figure 3-2 shows the predicted values of the effectiveness factor for various particle sizes and temperatures. As expected, the effectiveness factor decreases with the increase in either temperature or particle size.

To evaluate the predictions of the theoretical analysis, kinetic measurements using two sizes of Amberlyst 15 were conducted in a one litre batch reactor similar to that described by Xu and Chuang (1996). Two batches of beads with sizes of 0.42 to 0.6 and 0.85 to 1.00 mm were obtained from the screening of the commercial catalyst Amberlyst 15. The tests were conducted under the following conditions:

Initial composition of mixture (mole fraction):

methanol: 0.00925

acetic acid: 0.00863

water: 0.982

Reaction temperature:  $94 \pm 0.1^\circ\text{C}$



Catalyst (dry) loading: 0.77 wt%

Stirrer speed: 550 rpm

The reaction temperature was maintained slightly below that of the mixture bubbling point to reduce any loss of volatile components. The inlet concentrations of acetic acid and methanol were chosen to be close to those to be used in catalytic distillation. It has been shown that external diffusion is not a rate-controlling step within the stirrer speeds of 160 to 760 rpm (Xu and Chuang, 1996). A speed of 550 rpm was chosen to ensure that the measured reaction rate is free from external diffusion influences.

As shown by Xu and Chuang (1996), the global reaction constants can be found by measuring the change of mixture composition with time. Figure 3-3 shows the change of methyl acetate concentration with reaction time for the two sizes of catalyst particles. It is clear that under similar reaction conditions, other than catalyst sizes, the reaction rate is higher with small particles than that with large particles. The global reaction constants were found to be:

$$k_s = 0.123 \quad \text{for} \quad d_{ps} = 0.42 \text{ to } 0.60 \text{ mm}$$

$$\text{and} \quad k_L = 0.105 \quad \text{for} \quad d_{pL} = 0.85 \text{ to } 1.00 \text{ mm}$$

The global reaction rate for the two sizes of catalyst can be expressed as

$$R_s = (\eta R_i)_s = k_s (C_1 C_2 - C_3 C_4 / K) \quad (3.26)$$

$$R_L = (\eta R_i)_L = k_L (C_1 C_2 - C_3 C_4 / K) \quad (3.27)$$

Without internal diffusion resistance,

$$(R_i)_s = (R_i)_L \quad (3.28)$$



Under similar reaction conditions, other than particle sizes, the following relationship can be combined by combining Equations (3.26) to (3.28)

$$\eta_s/\eta_L = k_s/k_L \quad (3.29)$$

The ratio of global rate constants  $k_s:k_L$  can be found from experimental results and ratio of effectiveness factors  $\eta_s:\eta_L$  can be found from theoretical analysis.

From the experimental results,

$$k_s/k_L = 0.123/0.105 = 1.17 \quad (3.30)$$

The ratio of  $\eta_s$  to  $\eta_L$  at a temperature of 94°C and average particle radii of 0.25 and 0.46 mm can be found from Figure 3-2:

$$\eta_s/\eta_L = 0.922/0.795 = 1.16 \quad (3.31)$$

The agreement between these values indicates that the difference between the reaction rates of the two sizes of catalysts is due to the internal diffusion resistance, and therefore the theoretical predictions agree well with the experimental results.

The intrinsic reaction rate constant  $k_i$  under the above reaction conditions can be found by either  $k_s/\eta_s$  or  $k_L/\eta_L$ . Both of these ratios yield a value of 0.133 min<sup>-1</sup>. If the catalyst size distribution is known, the average effectiveness factor for the commercial Amberlyst 15 can be predicted by:

$$\bar{\eta} = \sum_j v_j \eta_j \quad (3.32)$$

Then the overall global reaction constant for Amberlyst 15 can be predicted by:

$$\bar{k} = \bar{\eta} k_i \quad (3.33)$$



The catalyst size distribution and corresponding effectiveness factor are listed in Table 3-2. From the data, the average effectiveness factor was found to be 0.87. The overall global reaction constant for Amberlyst 15 was predicted to be  $0.116 \text{ min}^{-1}$  using Equation (3.33). The measured value of overall global reaction constant is  $0.114 \text{ min}^{-1}$  (Xu and Chuang, 1996). It can be seen that the measured value of reaction rate constant is in excellent agreement with that estimated from Equation (3.33).

### 3.4 Conclusions

The effect of internal diffusion on the catalytic esterification of acetic acid has been analyzed theoretically. The predicted values for the effectiveness factors are in excellent agreement with those obtained from experiments. Overall, the internal diffusion resistance within the commercial catalyst Amberlyst 15 has been shown to be insignificant for the second-order reversible esterification of acetic acid with methanol, because of the relatively small size of the catalyst particles and the high activation energy for the reaction.





### 3.5 Nomenclature

$A$	constant defined in Equation (3-16)
$a_j$	stoichiometric coefficient of component $j$
$C$	constant defined in Equation (3-15)
$C_j$	concentration of component $j$ in mixture, mol/mol solution or mol/L
$C_j^*$	reaction equilibrium concentration in the catalyst beads, mol/L
$C_{js}$	concentration of component $j$ at the outer surface of catalyst beads, mol/L
$D_{mj}$	molecular diffusivity of component $j$ in mixture, $m^2/s$
$D_{ej}$	effective diffusivity of component $j$ in pores based on whole particle volume, $m^2/s$
$D_{ej}'$	effective diffusivity of component $j$ in pores based on available space for diffusion, $m^2/s$
$d_p$	particle diameter, mm
$d_{mj}$	molecule size of component $j$ , mm
$k$	global reaction constant, $L_{sol}^2/(L_{cat} \text{ min. mol})$ or $\text{min}^{-1}$
$\bar{k}$	average global reaction constant, $L_{sol}^2/(L_{cat} \text{ min. mol})$ or $\text{min}^{-1}$
$K$	reaction equilibrium constant
$K_{24}, K_{14}, K_{04}$	constants defined in Equations (3-8)-(3-10)
$k_i$	intrinsic reaction constant, $L_{sol}^2/(L_{cat} \text{ min. mol})$ or $\text{min}^{-1}$
$M_j$	molecular weight of component $j$ , g/mol
$M_R$	dimensionless catalyst modules



$P_j$	parameter in equation (3-24)
$r$	dimension of catalyst beads, mm
$R$	radius of catalyst beads, mm
$R_i$	intrinsic reaction rate, mol/(l <sub>cat</sub> min)
$R_L$	global reaction rate with large particles, mol/(l <sub>cat</sub> min)
$R_S$	global reaction rate with small particles, mol/(l <sub>cat</sub> min)
$t$	time, min
$T$	reaction temperature, K
$V_j$	molar volume of solute j (cm <sup>3</sup> /mol)
$x$	dimensionless size of catalyst beads
$y$	dimensionless concentration of acetic acid
$\phi_j$	association factor of component j
$\delta_j$	defined in Equation (3-6)
$\eta$	effectiveness factor
$\bar{\eta}$	average effectiveness factor
$\mu_j$	liquid viscosity of component j, cp
$v_j$	weight fraction of catalyst particles with a certain size
$\rho_j$	liquid density, kg/m <sup>3</sup>
$\varepsilon$	porosity of catalyst particle, m <sup>3</sup> /m <sup>3</sup>
$\lambda_j$	= $d_{mj}/d_p$
subscript	
1	acetic acid



2	methanol
3	methyl acetate
4	water
L	particle size of 0.85-1.0 mm
S	particle size of 0.42-0.60 mm



Table 3-1. Concentration of Acid Sites in Amberlyst 15

Catalyst Size $\times 10^3$ (m)	Sample Weight (g)	NaCl Solution Added (mL)	NaOH (0.1 N) Consumed (mL)	Concentration of Acid Sites (meq/g dry)
0.42-0.60	1.0178	50	48.18	4.734
0.85-1.0	0.9990	50	46.98	4.703





Table 3-2. Effectiveness Factors for Various Sizes of Amberlyst 15 (94 °C)

$d_{pj} \times 10^3 \text{ (m)}$	0.35-0.42	0.42-0.60	0.60-0.85	0.85-1.0	1.0-1.2
$\nu_j$	0.0301	0.283	0.533	0.147	0.0067
$\eta_j$	0.95	0.92	0.86	0.80	0.76



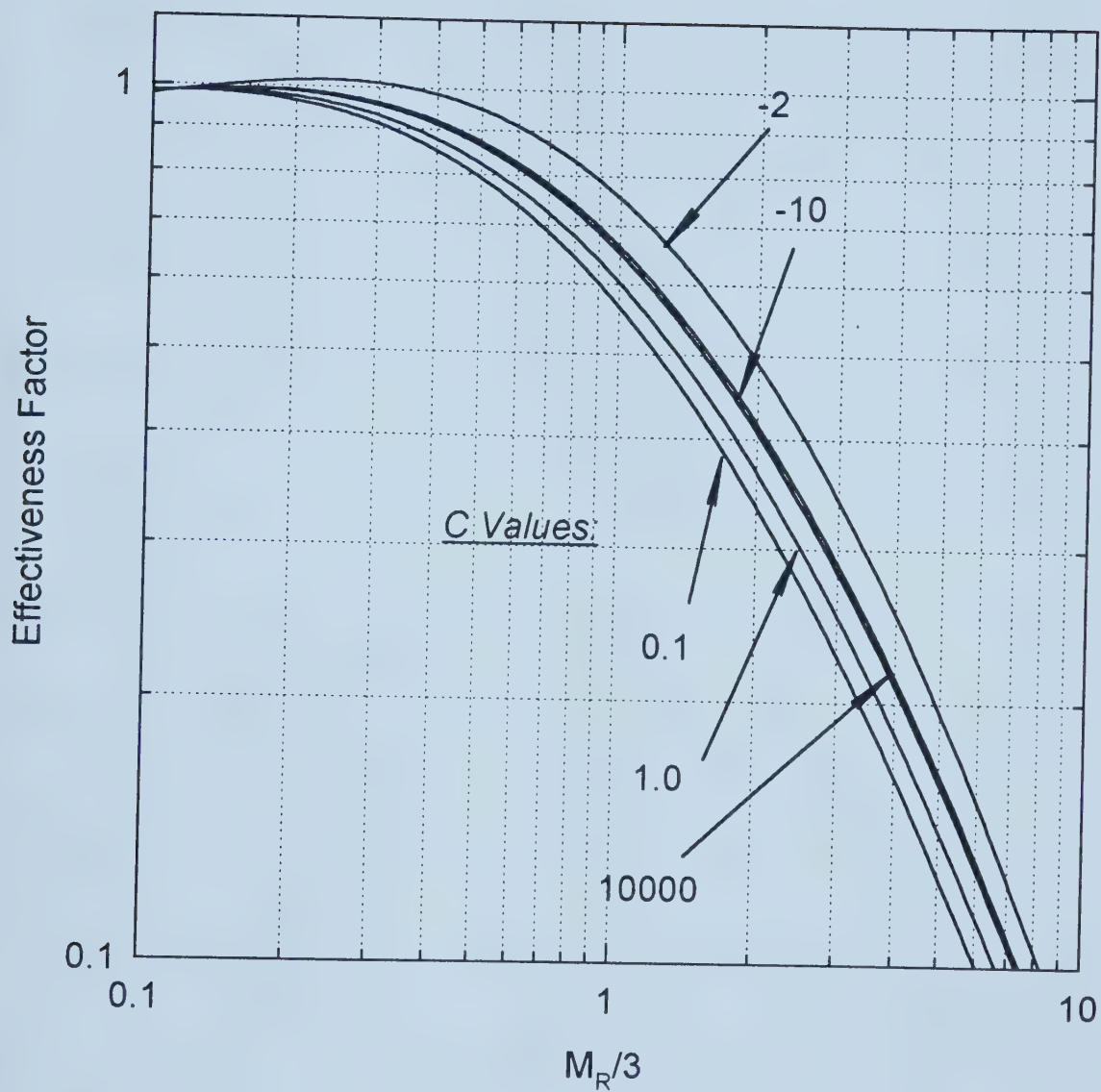


Figure 3-1. Effectiveness Factor for Amberlyst 15 in Acetic Acid Esterification.



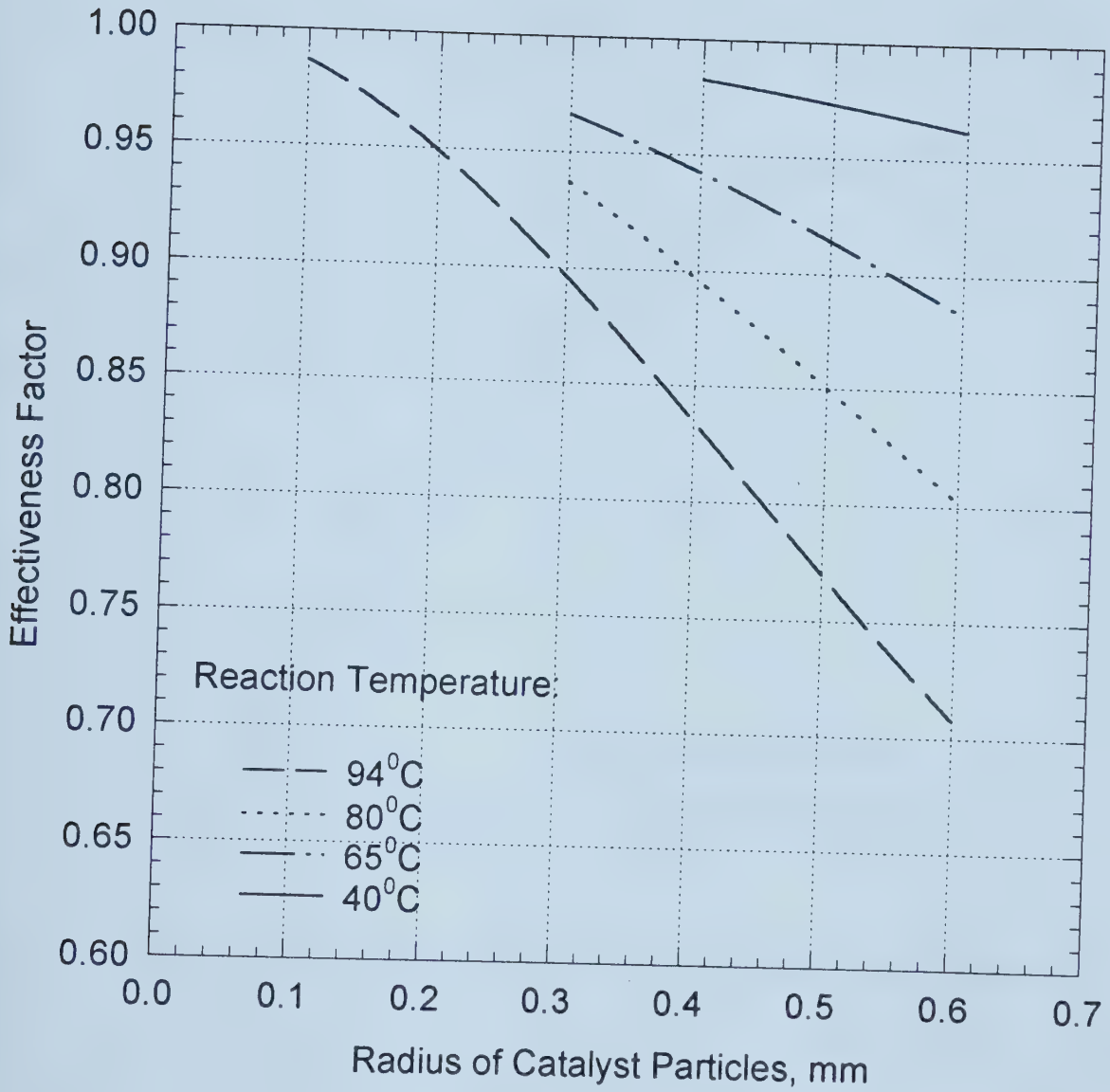


Figure 3-2. Predicted Effectiveness Factor for Various Sizes of Catalyst Particles.



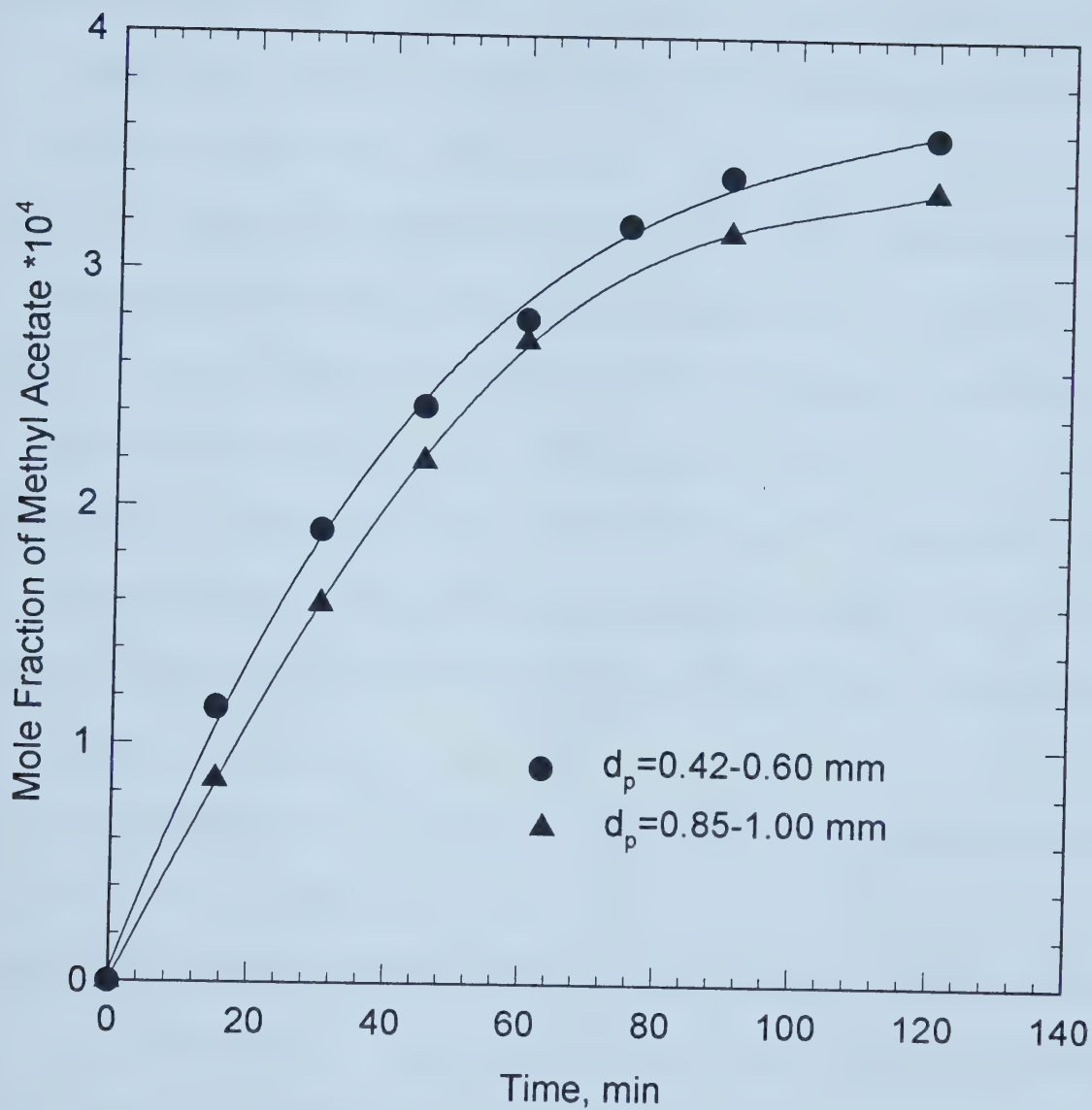


Figure 3-3. Effect of Particle Size on Reaction Rate.





### 3.6 Literature Cited

- Beasley, G.B. and Jakovac, I.J. (1984) Ion Exchange Resin Catalysts Having Improved Catalytic Activity and Enhanced Thermal Stability, In *Ion Exchange Technology*, pp. 441-449, Ellis Horwood Ltd., Chichester, U.K.
- Kaiser, J.R., Beuther, H., Moore, L.D. and Odioso, R.C. (1962) Direct Hydration of Propylene over Ion-exchange Resins. *Ind. Eng. Chem. Prod. Res. Dev.* **1**, 296-302.
- Leung, P., Zorrilla, C., Recasens, F. and Smith, J.M. (1986) Hydration of Isobutene in Liquid-full and Trickle-bed Reactors. *AIChE J.* **32**, 1839-1847.
- Patwardhan, A.A. and Sharma, M.M. (1990) Esterification of Carboxylic Acids with Olefins Using Cation Exchange Resins as Catalysts. *Reactive Polymer* **13**, 161-176.
- Rohm and Haas (1990) *Amberlyst 15 - Ion Exchange Resin for Catalyst*, Rohm and Haas Company, Philadelphia.
- Satterfield, C.N., Colton, C.K. and Pitcher, W.H. (1973) Restricted Diffusion with Fine Pores. *AIChE J.* **19**, 628-635.
- Schneider, P. and Mitschka, P. (1965) Effect of Internal Diffusion on Catalytic Reactions. I. Irreversible Reaction without a Change in the Number of Moles. *Collection Czechoslov. Chem. Commun.* **30**, 146-157.
- Schneider, P. and Mitschka, P. (1966a) Effect of Internal Diffusion on Catalytic Reactions. IV. Reversible Second-Order Reaction with Langmuir-Hinshelwood Type of Rate Equation. *Collection Czechoslov. Chem. Commun.* **31**, 3677-3701.



- Schneider, P. and Mitschka, P. (1966b) Effect of Internal Diffusion on Catalytic Reactions. *Chem. Eng. Sci.* **21**, 455-463.
- Smith, J.M. (1981) *Chemical Engineering Kinetics*, third edition, McGraw-Hill Book Company.
- Ternan, M. (1987) The Diffusion of Liquids in Pores. *Can. J. Chem. Eng.* **65**, 244-249.
- Ternan, M. (1996) Pore Diffusion of Vacuum Residue Molecules and Hydrogen Dissociation on Reaction Sites: Essential Steps in Hydrocracking Catalysis. *Preprints*, 14th Canadian Symposium on Catalysis, Whistler, B.C.
- Wilke, C.R. and Chang, P. (1955) Correlation of Diffusion Coefficients in Dilute Solutions. *AIChE J* **1**, 264-270.
- Xu, Z.P. and Chuang, K.T. (1996) Kinetics of Acetic Acid Esterification Over Ion Exchange Catalysts. *Can. J. Chem. Eng.* **74**, 493-500.
- Yadav, G.D. and Mehta, P.H. (1994) Heterogeneous Catalysis in Esterification Reactions: Preparation of Phenethyl Acetate and Cyclohexyl Acetate by Using a Variety of Solid Acidic Catalysts. *Ind. Eng. Chem. Res.* **33**, 2198-2208.



## CHAPTER 4. CORRELATION OF VAPOR-LIQUID EQUILIBRIUM DATA FOR METHYL ACETATE-METHANOL-WATER-ACETIC ACID MIXTURES\*

### 4.1 Introduction

In the catalytic distillation column for acetic acid esterification catalyzed by Amberlyst 15, four components, methyl acetate, methanol, water and acetic acid, are present. Accurate prediction of the vapor-liquid equilibrium of the system is vital to the simulation and design of the process.

To correlate the vapor-liquid equilibrium in mixtures containing an associating substance like acetic acid, Marek's method (Marek and Standart, 1954; Marek, 1955) in combination with liquid activity coefficient models is usually used.

At present, there are more than six different types of correlations for the prediction of activity coefficients in chemical systems. Since the superiority of one method over the others is not always obvious, practice must rely on experience and analogy. The most comprehensive comparison of five of the methods (van Laar, Margules, Wilson, NRTL, and UNIQUAC) was made in the DECHEMA Vapor Liquid Equilibrium Data Collection (Gmehling et al., 1977a,b, 1982, 1988). From this statistical analysis, the Wilson equation was found to be the best, and the van Laar and UNIQUAC methods tied for last. However, there are also marked differences for a given class of substances. For example, the NRTL was found to be the best model for aqueous systems (Walas, 1985).

---

\* A version of this chapter has been published: Z.P. Xu and K.T. Chuang (1997) *Ind. Eng. Chem. Res.* **36**, 2866-2870.



Sawistowski and Pilavakis (1982) experimentally studied the vapor-liquid equilibrium behavior of the quaternary system, methyl acetate-methanol-water-acetic acid.

To correlate their experimental data, they tried third-order Margules (Marek, 1954), Wilson, and NRTL models for liquid activity coefficients and concluded that the Wilson and NRTL models could not correlate the quaternary system as well as the third-order Margules equation. Therefore, they finally chose the third order Margules equation.

Suzuki et al. (1970) tried to formulate relations between the liquid and vapor compositions of the same quaternary system. They failed to obtain good correlation results with the Margules equation modified by Marek (1954). Sawistowski and Pilavakis (1982) explained that the failure may be due to the fact that they used only quaternary experimental data to fit their constants. Suzuki et al. (1970) then rearranged the Margules equation, which contains 64 constants for the quaternary system. They claimed that the calculated values were in good agreement with experimental data in practical use. However, Sawistowski and Pilavakis (1982) later tested their equation with binary, ternary, and quaternary vapor-liquid equilibrium data, and the results were found to be unsatisfactory.

Compared with the Margules equation, the Wilson and NRTL models have two major advantages: (1) only binary parameters are required for the multicomponent system; (2) they can predict the effect of temperature, which is especially useful for distillation. Therefore, the Wilson and NRTL models are preferred for most chemical systems.

In fact, Sawistowski and Pilavakis' work was conducted before 1974 (Pilavakis, 1974). With more reliable vapor-liquid equilibrium data available now, we were able to





review their conclusion by recorrelating the quaternary experimental data using new Wilson and NRTL model parameters (Gmehling et al., 1977a,b, 1982, 1988).

In this study, both the Wilson and NRTL models were used in combination with Marek's method (Marek and Standart, 1954; Marek, 1955) for predicting the vapor-liquid equilibrium of the quaternary system containing the associating component acetic acid. The calculated results are then compared with the third order Margules equation suggested by Sawistowski and Pilavakis' (1982).

#### 4.2 Vapor-Liquid Equilibria In Mixtures Containing Acetic Acid

For a mixture that contains an associating component (e.g., acetic acid), a model was developed by Marek and Standart (1954) and Marek (1955) to correlate the vapor-liquid equilibrium data. For the associating component A,

$$Py_A Z_A = p_{AC} x_A \gamma_A \quad (4.1)$$

where

$$Z_A = \frac{[1 + 4KPy_A(2 - y_A)]^{1/2} - 1}{2KPy_A(2 - y_A)} \quad (4.2)$$

$$p_{AC} = \frac{\sqrt{1 + 4k_A p_A^s} - 1}{2k_A} \quad (4.3)$$

For the nonassociating component B,

$$Py_B Z_B z_B = p_B^s x_B \gamma_B \quad (4.4)$$

where



$$Z_B = \frac{2(1 - y_A + \sqrt{1 + 4KPy_A(2 - y_A)})}{(2 - y_A)(1 + \sqrt{1 + 4KPy_A(2 - y_A)})} \quad (4.5)$$

The factors  $Z_A$  and  $Z_B$ , which express the influence of the vapor-phase association of A, may be evaluated from a knowledge of its association constant K. The association constant of acetic acid at 760 mmHg was obtained by Marek (1955). The dependence of K on temperature was expressed as

$$-\log K = 9.7535 + 0.00425t - \frac{3166}{t + 273.2} \quad (4.6)$$

where t is the temperature in °C.

The equation for the factor  $z_B$  is a correlation for the nonideality in the vapor phase and may be evaluated from various generalized relationships. At atmospheric pressure,  $z_B \rightarrow 1.0$ . For the associating substance A, the nonideality of the vapor phase is usually included in the correlation of the association constant.

The corrected vapor pressure of the association component,  $p_{AC}$ , may be determined from the association constant of pure acetic acid,  $k_A$ , at its vapor pressure,  $p_A^s$ . The correlations between  $k_A$  and  $p_A^s$  as well as  $p_A^s$  and temperature have been given by Marek (1955). With these correlations and Equation (4.3),  $p_{AC}$  can finally be expressed as a function of temperature (Marek, 1955):

$$\log p_{AC} = 15.6699 - \frac{10821.1}{t + 698.09} \quad (4.7)$$

The vapor pressure of the nonassociating component  $p_B^s$  may be determined using the Antoine equation.



The liquid-phase nonideality is influenced by a number of factors. It is impossible to evaluate rigorously the liquid-phase association constant from the equilibrium data alone. It is a common practice to include the liquid-phase association constants in the empirical constants for the correlation of the activity coefficients.

### 4.3 Activity Coefficients

For multicomponent systems, the dependence of the activity coefficients on the liquid-phase composition for the Wilson and NRTL models was expressed respectively by Equations (4.8) and (4.10):

Wilson:

$$\ln \gamma_i = -\ln \left( \sum_{j=1}^m x_j \Lambda_{ij} \right) + 1 - \sum_{k=1}^m \frac{x_k \Lambda_{ki}}{\sum_{j=1}^m x_j \Lambda_{kj}} \quad (4.8)$$

where

$$\Lambda_{ij} = \frac{V_j^L}{V_i^L} \exp \left( -\frac{\lambda_{ij} - \lambda_{ii}}{RT} \right) \quad (4.9)$$

$$\Lambda_{ii} = \Lambda_{jj} = 1$$

NRTL:

$$\ln \gamma_i = \frac{\sum_{j=1}^m \tau_{ji} G_{ji} x_j}{\sum_{l=1}^m G_{li} x_l} + \sum_{j=1}^m \frac{x_j G_{ij}}{\sum_{l=1}^m G_{lj} x_l} \left( \tau_{ij} - \frac{\sum_{n=1}^m x_n \tau_{nj} G_{nj}}{\sum_{l=1}^m G_{lj} x_l} \right) \quad (4.10)$$

where



$$\begin{aligned}
\tau_{ji} &= \frac{g_{ji} - g_{ii}}{RT} \\
G_{ji} &= \exp(-\alpha_{ji} \tau_{ji}) \\
\tau_{ii} &= \tau_{jj} = 0 \\
G_{ii} &= G_{jj} = 1
\end{aligned} \tag{4.11}$$

The binary model parameters in the above equations were obtained from the DECHEMA Vapor Liquid Equilibrium Data Collection (Gmehling et al., 1977a,b, 1982, 1988) and are listed in Table 4-1. The original experimental data can be found from the references listed in Table 4-1.

#### 4.4 Results And Discussion

The saturation pressure of pure components was calculated by the Antoine equation:

$$\log p_i^s = A_i - \frac{B_i}{C_i + t} \tag{4.12}$$

The Antoine constants recommended by DECHEMA (Gmehling et al., 1977a,b, 1982, 1988) were used, and their values are listed in Table 4-2. The molar volume of the pure liquid was obtained from Holmes and van Winkle (1970). The molar volume dependence on temperature was correlated by

$$V_i^L = D_i + E_i T + F_i T^2 \tag{4.13}$$

The values of the constants in Equation (4.13) are also listed in Table 4-2.

With Equations (4.1) to (4.13) and the data listed in Tables 4-1 and 4-2, we are able to predict the vapor composition by both the Wilson and NRTL models in





combination with Marek's method. A total of 113 sets of experimental data were obtained for the quaternary system by Sawistowski and Pilavakis (1982). The deviation between these measured data and the correlated values was expressed by the root mean square deviation (r.m.s.d.) as used by Sawistowski and Pilavakis (1982):

$$r.m.s.d. = \sqrt{\frac{\sum_{i=1}^m \sum_{j=1}^n (\Delta y_{ij})^2}{m \times n}} \quad (4.14)$$

The value of r.m.s.d. was found to be 0.023 by using the third order Margules equation (Sawistowski and Pilavakis, 1982). The computational results from this study show that r.m.s.d is 0.025 for the Wilson model and 0.023 for the NRTL model. It can be seen that the NRTL model is comparable with the third order Margules equation while the Wilson model is slightly poorer than the other two.

The number of model parameters required by the third order Margules, Wilson, and NRTL equations is 16, 12, and 18, respectively. It can be seen that the Wilson model needs fewer model parameters than the others. For the NRTL model, Walas (1985) pointed out that the activity coefficients were relatively insensitive to the third model parameter,  $\alpha_{12}$ , in the range 0.1 to 0.5. From Table 4-1, it can be seen that most of the values of  $\alpha_{12}$  are in this range. Walas (1985) also concluded that if an estimation of  $\alpha_{12}$  has to be made, it should be about 0.3 for nonaqueous mixtures and about 0.4 for aqueous organic mixtures. This information indicates that we may use one value of  $\alpha_{12}$  for the six binary mixtures instead of six separate values. In this way, the number of NRTL model parameters for the quaternary system can be reduced from 18 to 13. By first trial of  $\alpha_{12}=0.35$ , we obtained the same value of r.m.s.d. (0.023) as that for the 18 parameters. In



fact, the value of r.m.s.d. was found to be insensitive to the value of  $\alpha_{12}$  in the range 0.3 to 0.4. The optimum value of  $\alpha_{12}$  is 0.37, and the corresponding value of r.m.s.d. is 0.022.

In addition to the r.m.s.d., the accuracy of prediction can be more directly described by the mean deviation (m.d.) and mean relative deviation (m.r.d.), which are defined by

$$m.d. = \frac{1}{m \cdot n} \sum_i \sum_j |\Delta y_{ij}| \quad (4.15)$$

$$m.r.d. = \frac{1}{m \cdot n} \sum_i \sum_j \frac{|\Delta y_{ij}|}{y_{ij}} \quad (4.16)$$

Table 4-3 lists the statistical values of r.m.s.d., m.d., and m.r.d. between the experimental data (Sawistowski and Pilavakis, 1982) and the values predicted by using the Margules equation (Sawistowski and Pilavakis, 1982) and the Wilson and NRTL models. From the table it can be seen that the NRTL model gives the best results for the correlation of the quaternary system.

The above models for the quaternary system can be used for predicting the vapor-liquid equilibrium of the six binary systems (methyl acetate-methanol, methyl acetate-water, methyl acetate-acetic acid, methanol-water, methanol-acetic acid, and water-acetic acid) by assigning the concentrations of the two components not present in the system to zero.

Figures 4-1 to 4-6 show the comparison of the predicted vapor compositions with the experimental values. The NRTL model is used for all the predictions. From these figures, it can be seen that the model can well predict vapor-liquid equilibrium of the six



binary systems, including the azeotropic behavior in methyl acetate-methanol and methyl acetate-water systems.

Table 4-4 shows the mean deviations between the measured and the predicted vapor compositions. The mean deviations obtained by Gmehling et al. (1977a,b, 1982, 1988) are also shown in the table for comparison. It can be seen that these two sets of deviation values are comparable.

#### 4.5 Conclusions

The vapor-liquid equilibrium data of the methyl acetate-methanol-water-acetic acid system can be correlated by using the Wilson and NRTL models instead of the third order Margules equation, as suggested by Sawistowski and Pilavakis (1982). Compared with the third order Margules equation, the NRTL model has fewer model parameters, includes the effect of temperature, is easier to be incorporated into computer simulation programs and can better predict the vapor-liquid equilibria of the methyl acetate-methanol-water-acetic acid system. The best correlation was the NRTL model with the third model parameter  $\alpha_{12}=0.37$  for all six binary mixtures.

The models can also be used for the prediction of vapor-liquid equilibrium of the binary systems. The predictions of vapor compositions by the NRTL model for the six binary systems agree well with the measured values.



## 4.6 Nomenclature

$A_i, B_i, C_i$	Antoine constants in Equation (4.12)
$D_i, E_i, F_i$	constants in Equation (4.13)
$\Delta g_{ji}$	NRTL model parameters ( $=g_{ji}-g_{ii}$ ), cal/mol
$K$	association constant in the vapor phase, 1/mmHg
$k_A$	equilibrium constant in the pure gaseous associating substance, 1/mmHg
$m$	number of components
$n$	number of data sets
$P$	total pressure, mmHg
$p_i^s$	saturated vapor pressure, mmHg
$p_{AC}$	corrected vapor pressure of acetic acid, mmHg
$R$	gas constant, =1.987 cal/mol·K
$t, T$	temperature in °C, K respectively
$V_i^L$	liquid molar volume of component $i$
$x_i$	mole fraction of component in the liquid phase
$y_i$	mole fraction of component in the vapor phase
$Z_A$	factor for the influence of the vapor phase association of A
$Z_B$	factor for the influence of the vapor phase association of B
$z_B$	factor for the correction of nonideality in the vapor phase
$\alpha_{12}$	NRTL third parameter
$\gamma_i$	activity coefficient of component $i$





$\Delta\lambda_{ij}$       Wilson model parameter ( $=\lambda_{ij}-\lambda_{ji}$ )



Table 4-1. Binary Model Parameters (P=760 mmHg)

System (1-2)	$\Delta\lambda_{12}$	$\Delta\lambda_{21}$	$\Delta g_{12}$	$\Delta g_{21}$	$\alpha_{12}$	References
methyl acetate-methanol	-125.69	891.14	566.15	456.94	1.0293	Gmehling and Onken (1977b)
methyl acetate-water	887.37	1966.71	879.14	1709.49	0.3830	Gmehling and Onken (1977a)
methyl acetate-acetic acid	-696.50	1123.14	1218.87	-635.89	0.3600	Gmehling et al. (1982)
methanol-water	216.85	468.60	-245.90	921.33	0.2989	Gmehling and Onken (1977a)
methanol-acetic acid	1.7144	2.1503	-39.582	0.5767	0.3055	Gmehling et al. (1988)
water-acetic acid	870.21	-65.80	981.10	-187.72	0.2960	Gmehling and Onken (1977a)



Table 4-2. Constants in Equations (4.12) and (4.13)

Components	A <sub>i</sub>	B <sub>i</sub>	C <sub>i</sub>	D <sub>i</sub>	E <sub>i</sub>	F <sub>i</sub>
methyl acetate	7.06524	1157.630	219.726	135.998	-0.46705	9.221×10 <sup>-4</sup>
methanol	8.08097	1582.271	239.726	64.5109	-0.19716	3.874×10 <sup>-4</sup>
water	8.07131	1730.630	233.426	23.0130	-0.03710	6.960×10 <sup>-5</sup>
acetic acid	7.5596	1644.048	233.524	34.0350	0.08220	-9.375×10 <sup>-6</sup>



Table 4-3. Statistical Errors for the Margules, Wilson and NRTL Models

Model Parameters	Margules Sawistowski and Pilavakis, 1982	Wilson Table 1	NRTL Table 1	NRTL Table 1 with $\alpha_{12}=0.37$
r.m.s.d.	0.0229	0.0252	0.0232	0.0217
m.d.	0.0171	0.0182	0.0164	0.0145
m.r.d.	0.126	0.121	0.109	0.099





Table 4-4. Mean Deviations between Measured and Predicted Vapor Compositions

System	Gmehling et al. (1977a,b, 1982, 1988)	This work
methyl acetate-methanol	0.0071	0.0072
methyl acetate-water	0.0157	0.0182
methyl acetate-acetic acid	0.0124*	0.0259
methanol-water	0.0057	0.0056
methanol-acetic acid	0.0243	0.0076
water-acetic acid	0.0123	0.0100

\* Two liquid compositions are different from the original data (Sawistowski and Pilavakis, 1982)



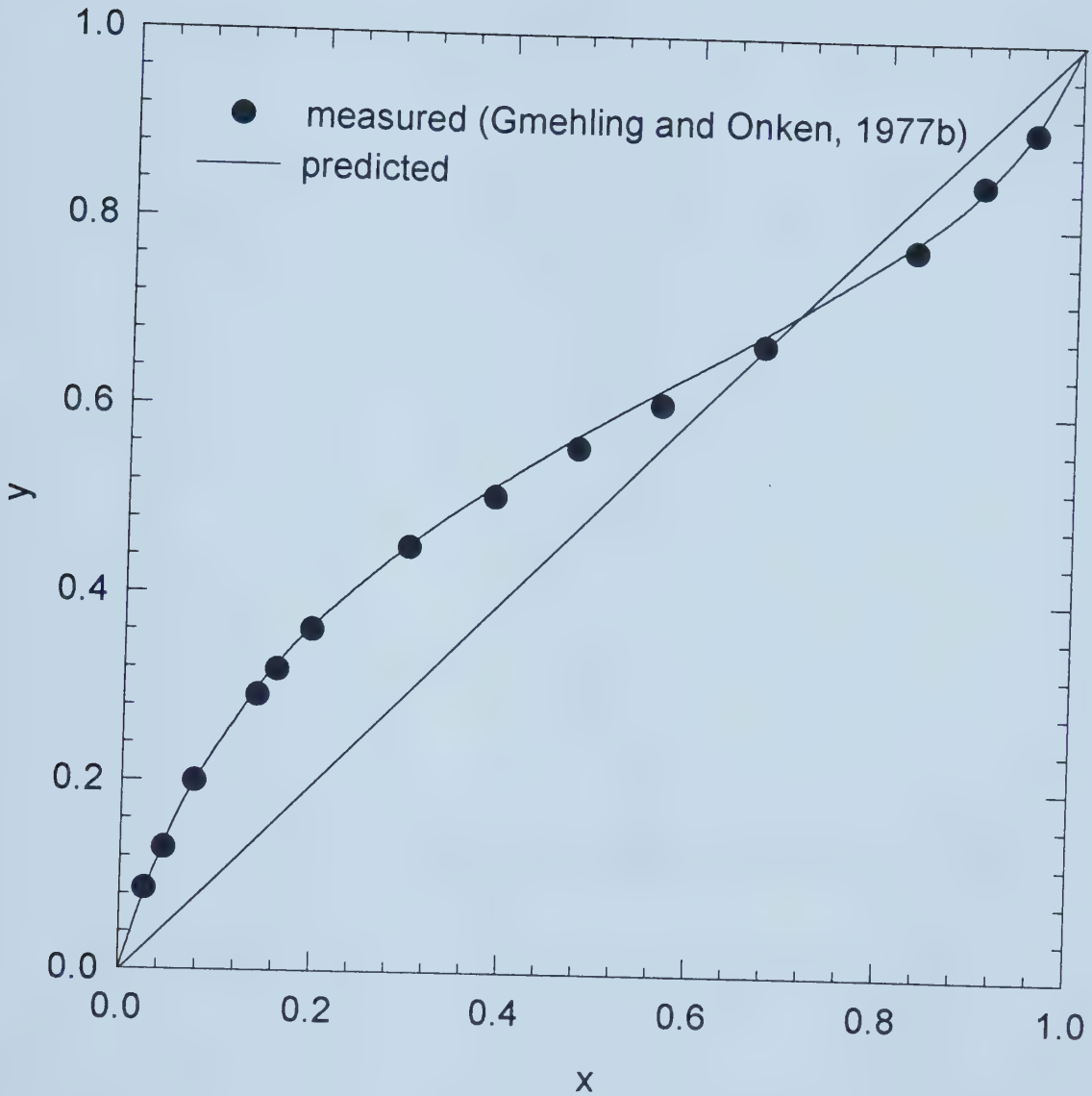


Figure 4-1. Measured and predicted vapor compositions for the methyl acetate-methanol system.



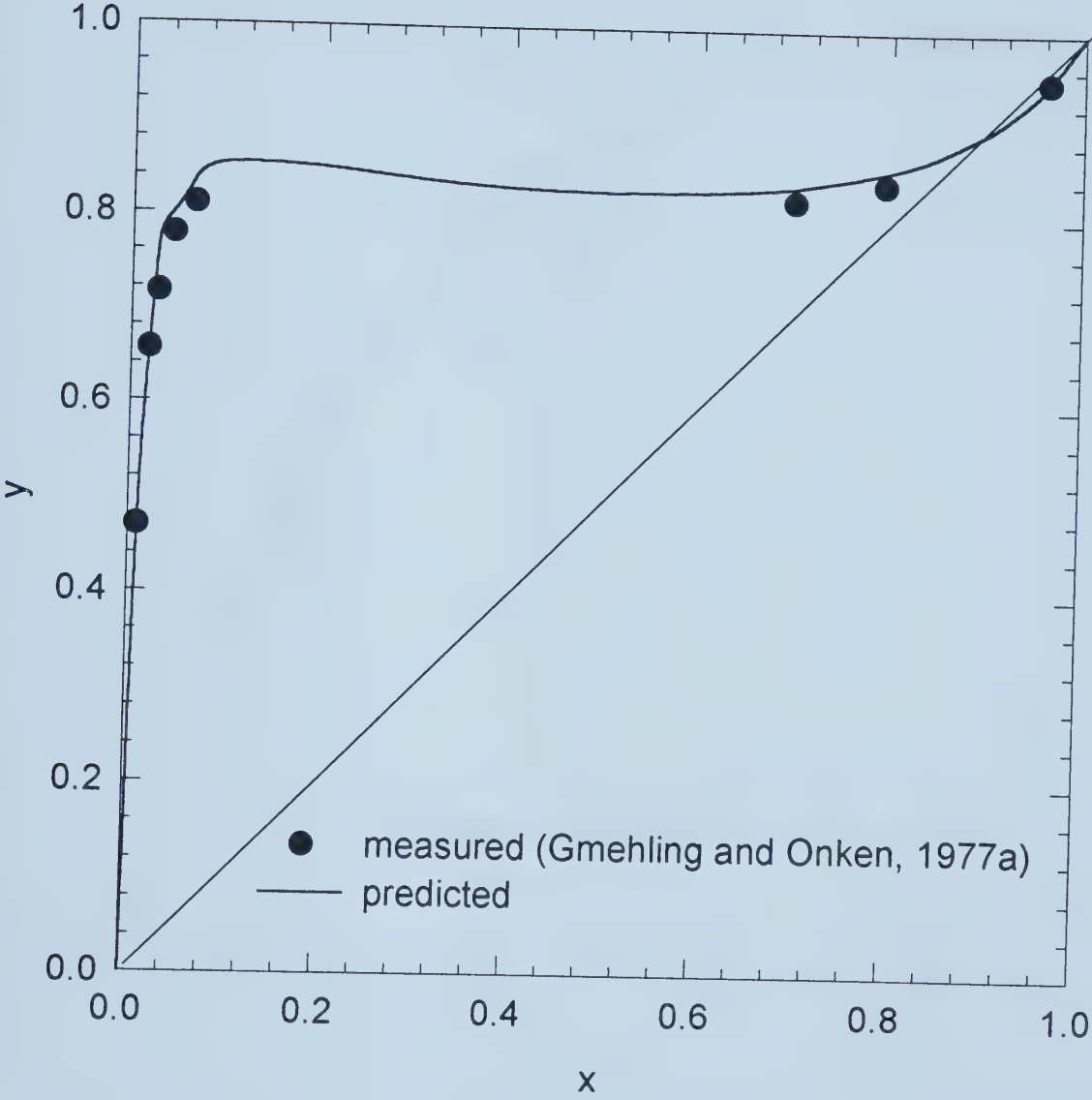


Figure 4-2. Measured and predicted vapor compositions for the methyl acetate-water system.



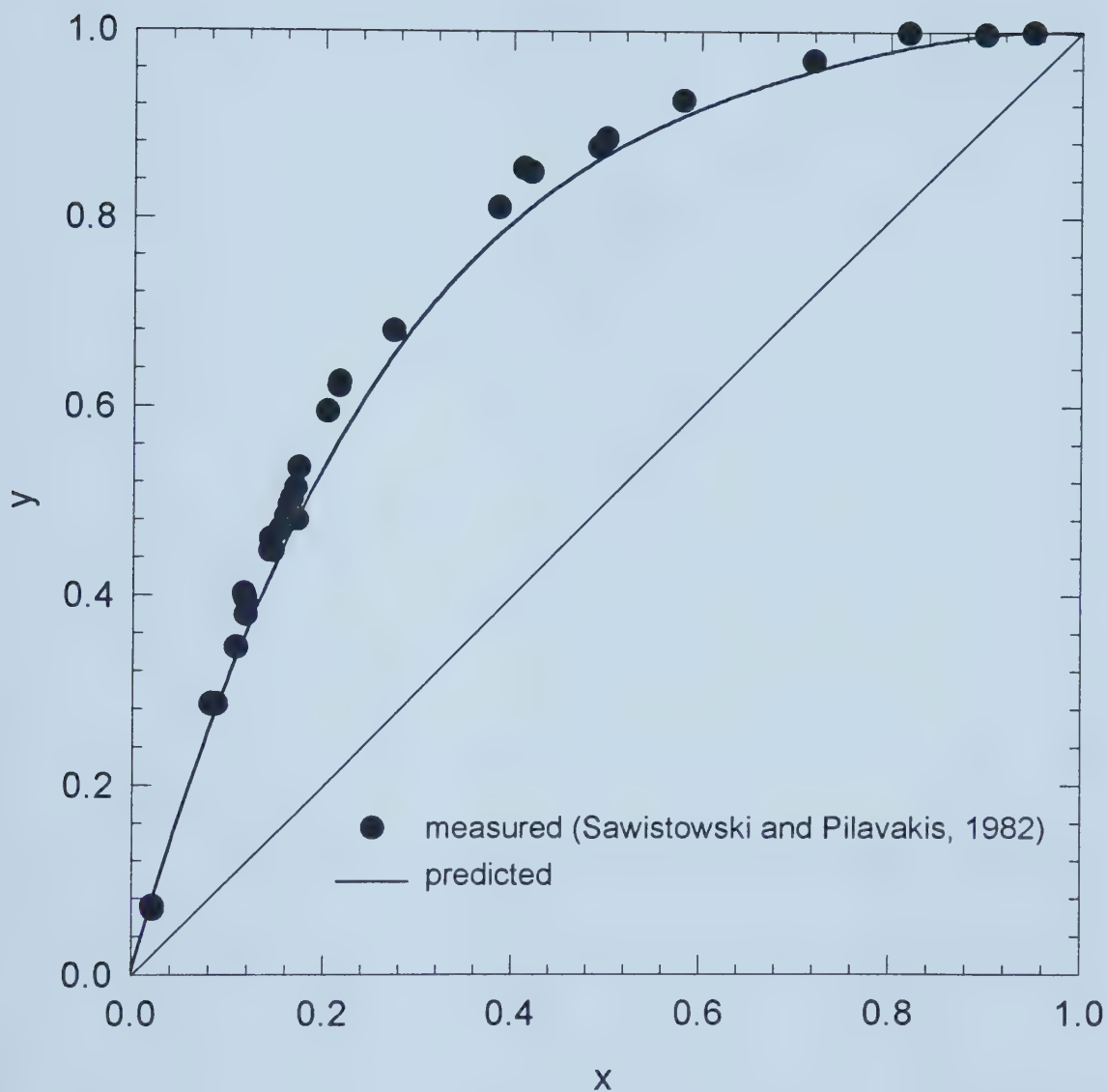


Figure 4-3. Measured and predicted vapor compositions for the methyl acetate-acetic acid system.





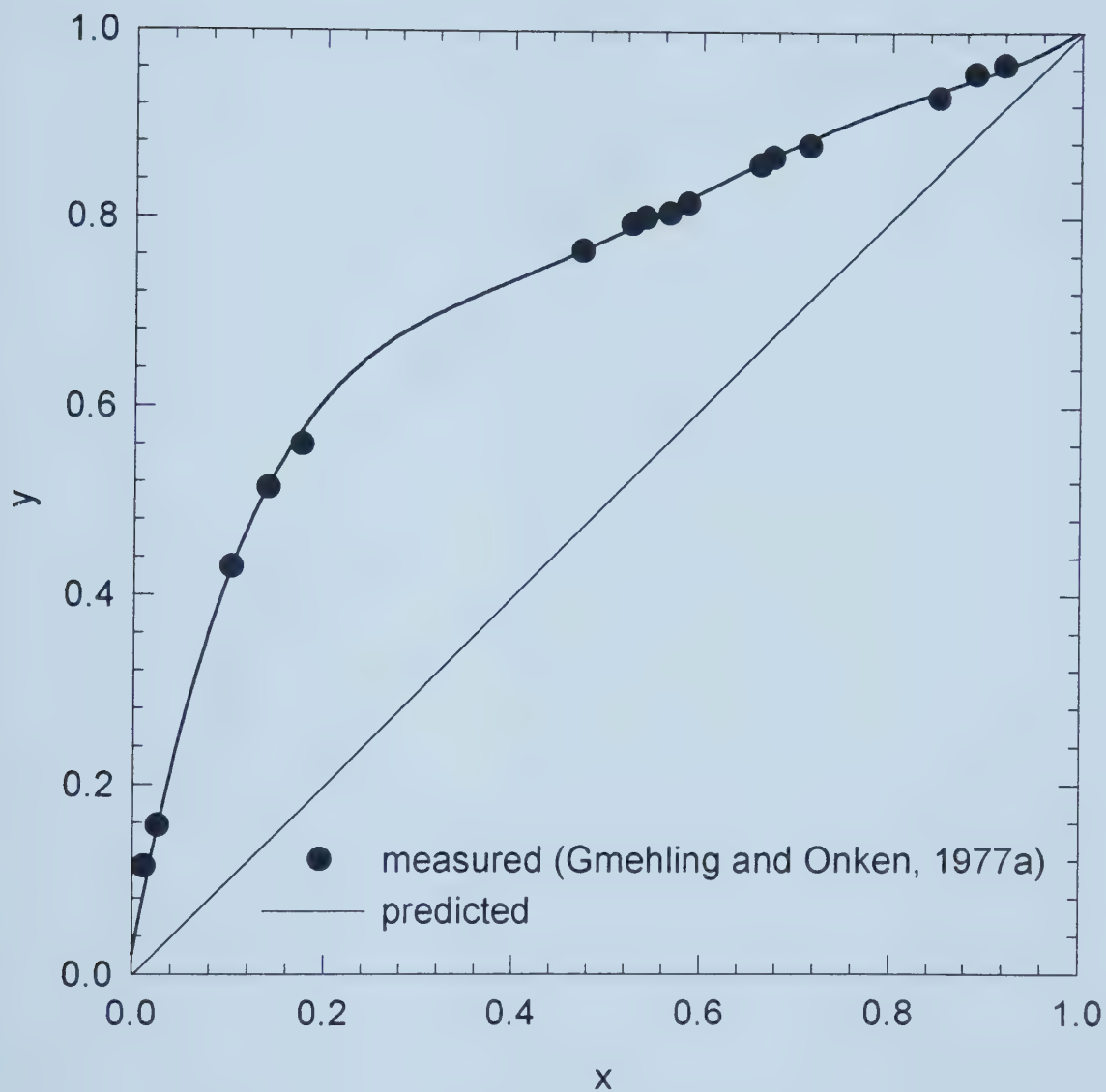


Figure 4-4. Measured and predicted vapor compositions for the methanol-water system.



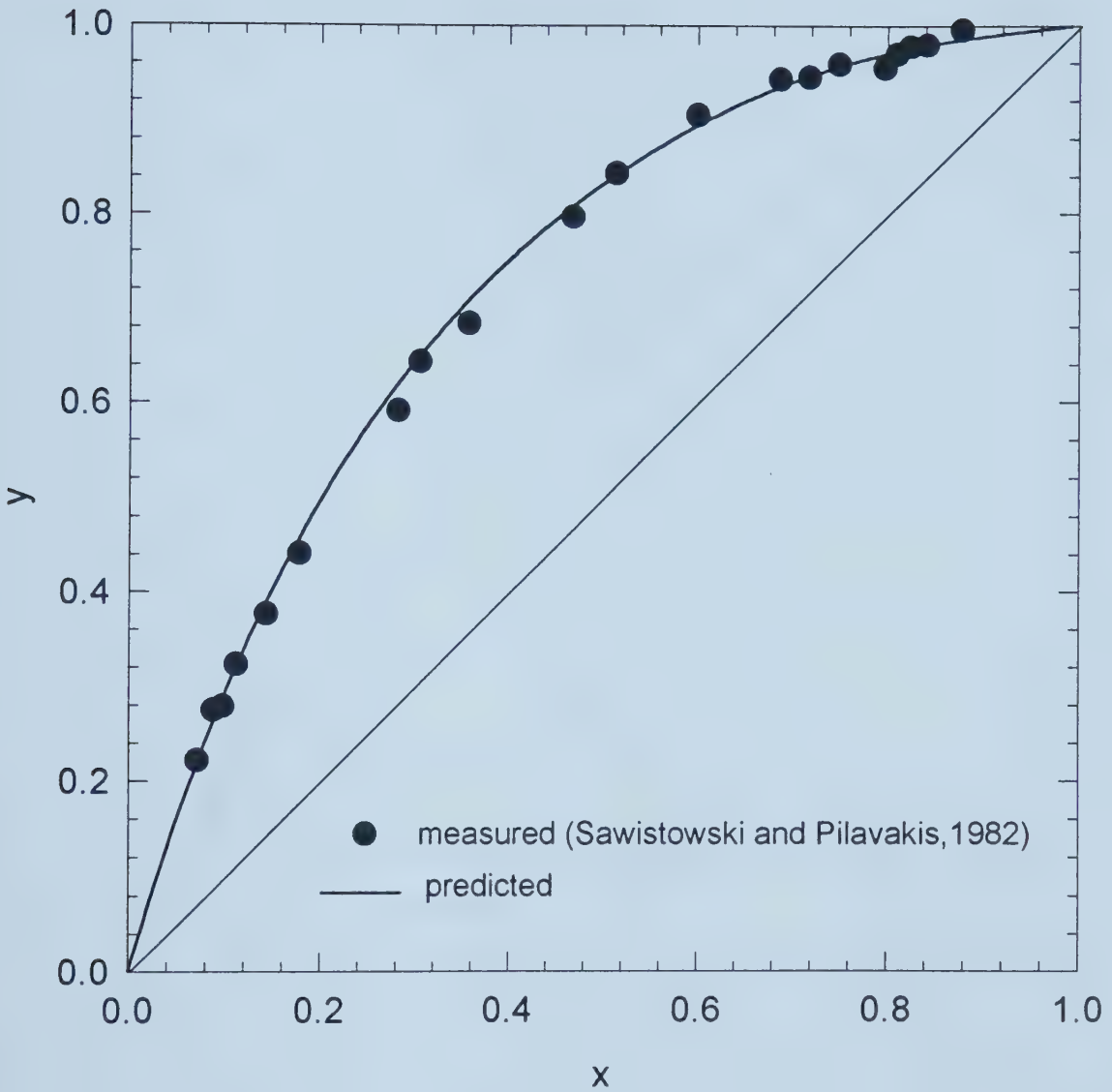


Figure 4-5. Measured and predicted vapor compositions for the methanol-acetic acid system.



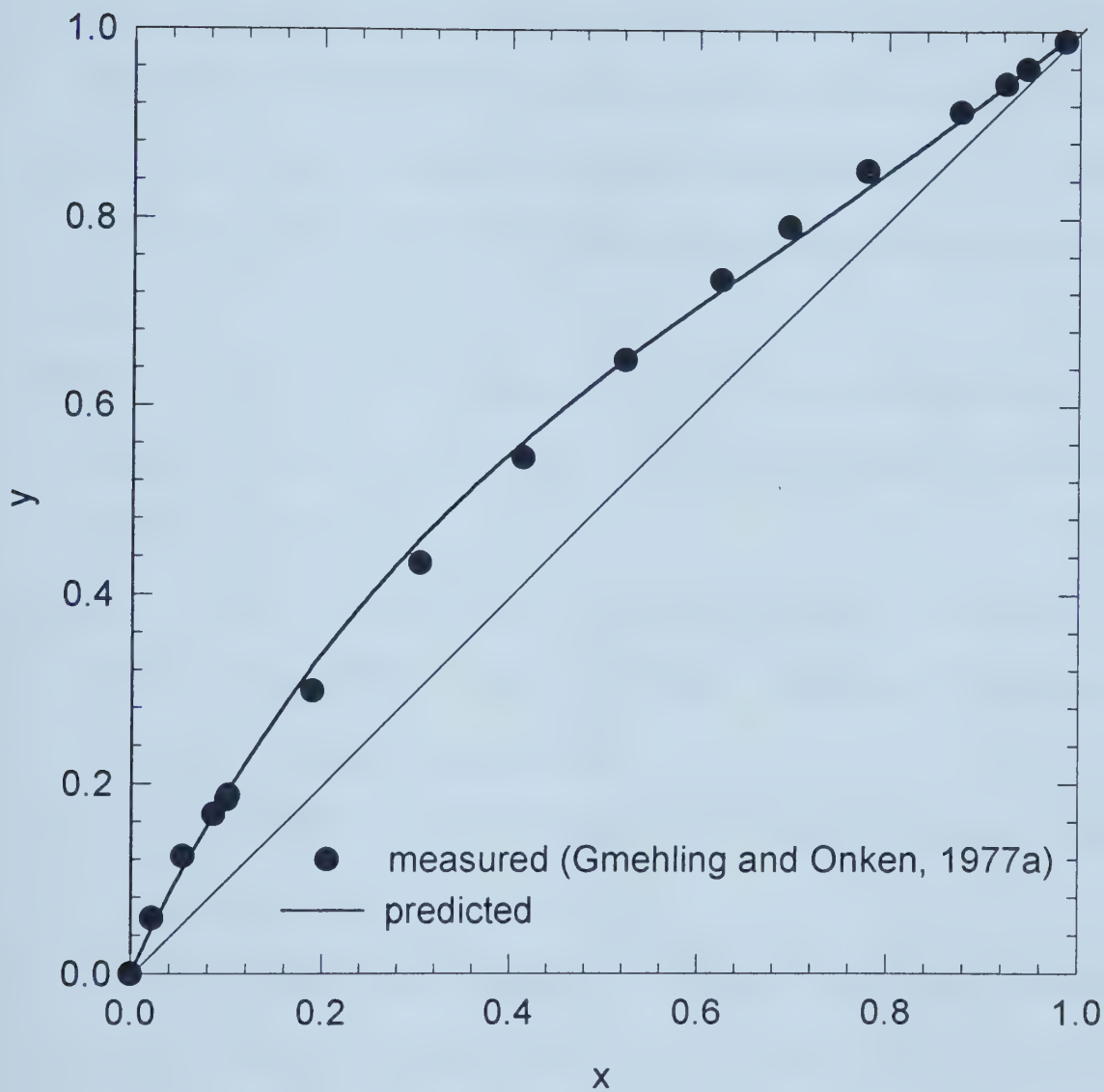


Figure 4-6. Measured and predicted vapor compositions for the water-acetic acid system.



## 4.7 Literature Cited

- Gmehling, J. and Onken, U. (1977a) *Vapor-Liquid Equilibrium Data Collection-Aqueous Organic Systems*; DECHEMA Chemistry Data Series, vol.1, part 1, pp.54, 116, 264.
- Gmehling, J. and Onken, U. (1977b) *Vapor-Liquid Equilibrium Data Collection-Organic Hydroxy Compounds: Alcohols*; DECHEMA Chemistry Data Series, vol.1, part 2a, pp.105.
- Gmehling, J., Onken, U. and Grenzheuser, P. (1982) *Vapor-Liquid Equilibrium Data Collection-Carboxylic Acids, Anhydrides, Esters*; DECHEMA Chemistry Data Series, vol.1, part 5, pp.83.
- Gmehling, J., Onken, U. and Rarey-Nies, J.R. (1988) *Vapor-Liquid Equilibrium Data Collection-Organic Hydroxy Compounds: Alcohols (Supplement 3)*; DECHEMA Chemistry Data Series, vol.1, part 2e, pp.38.
- Holmes, M.J. and Winkle, M.V. (1970) Prediction of Ternary Vapor-Liquid Equilibria from Binary Data. *Ind. Eng. Chem.* **62**, 21-31.
- Marek, J. (1955) Vapor-Liquid Equilibrium in Mixtures Containing an Associating Substance. II. Binary Mixtures of Acetic Acid at Atmospheric Pressure. *Collection Czechoslov. Chem. Commun.* **20**, 1490-1502.
- Marek, J. (1954) Quaternary Four-Suffix Margules Equation. *Collection Czechoslov. Chem. Commun.* **19**, 1-3.





- Marek, J. and Standart, G. (1954) Vapor-Liquid Equilibrium in Mixtures Containing an Associating Substance. I. Equilibrium Relationships for Systems with an Associating Component. *Collection Czechoslov. Chem. Commun.* **19**, 1074-1084.
- Pilavakis, P.A. (1974) *Distillation with Chemical Reaction: Esterification in a Packed Column*, Ph.D. Dissertation, Imperial College of Science and Technology, England.
- Sawistowski, H. and Pilavakis, P.A. (1982) Vapor-Liquid Equilibrium with Association in Both Phases. Multicomponent Systems Containing Acetic Acid. *J. Chem. Eng. Data* **27**, 64-71.
- Suzuki, I., Komatsu, H. and Hirata, M. (1970) Formulation and Prediction of Quaternary Vapor-Liquid Equilibria Accompanied by Esterification. *J. Chem. Eng. Jpn* **3**, 152-157.
- Walas, S.M. (1985) *Phase Equilibria in Chemical Engineering*, Butterworth Publishers



## CHAPTER 5. DESIGN OF THE CATALYTIC DISTILLATION COLUMN

### 5.1 Introduction

Using the developed kinetics and vapor-liquid equilibrium models, the catalytic distillation process for acetic acid esterification with methanol was simulated by incorporating these models into a commercial simulation package. Based on the simulation results, a catalytic distillation column was designed and a novel column internal was developed for the tests of the catalytic distillation process. The detailed procedure is given in the following sections.

### 5.2 Computer Simulation

Commercial simulation packages, such as Aspen Plus (Aspen Technology, Inc., 1996) and PRO/II (Simulation Sciences, Inc., 1994), were used in combination with our kinetics and vapor-liquid equilibrium models to simulate the catalytic distillation process. It was found that it was much easier to obtain converged results by using Aspen Plus. Therefore, most of the simulation work was done using Aspen Plus.

The accuracy of the simulation results is dependent mainly on the selection or input of valid models for vapor-liquid equilibrium, reaction kinetics, column internals and separation efficiency. At this stage, component tray efficiencies were not measured. Therefore, the Murphree tray efficiencies were set at 100% for all components.



The effects of number of theoretical stages, feed composition (ratio of methanol to acetic acid), feed locations, reflux ratio and column pressure on column operation were studied. The results are summarized as follows:

i) Feed locations are very important to column performance. The position for the acetic acid/water feed should be above that of the methanol. A rectifying section should be located above the acetic acid/water feed and a stripping section located below the methanol feed for pure products. Between the two feed locations is the reaction/separation section.

ii) The reflux ratio will affect both mass transfer efficiency and reaction rate. A higher reflux ratio favors separation but not necessarily reaction rate. There exists a optimum reflux ratio for each set of operating conditions and column configurations.

iii) The higher the mole ratio of the methanol to the acetic acid in the feed, the lower the acetic acid concentrations are in the distillate and bottoms, but more methanol needs to be recycled. The proper mole ratios of methanol to acetic acid are between 1:1 and 8:1 depending on the number of separation plates and reaction/separation units and other operating parameters;

iv) The reaction-separation section should be located in the middle to lower portion of the column. Catalyst should not be applied in the rectifying section to prevent net reverse reaction due to the high concentration of the methyl acetate and the low concentration of the acetic acid. The most effective zone for reaction is located between the two feeds;



The above simulation results provided guidelines for the design of our pilot catalytic distillation column.

### 5.3 Column Sizing And Configuration

In the design of the test column, several factors were considered.

i) The column will be operated continuously and therefore, the column diameter should not be too large, or too much chemicals will be consumed in the operation of the column. On the other hand, the column should not be too small or the liquid delivery, flow rate measurement, operation control and the manufacture of column internals will be very difficult.

ii) The column should have several plates so that: (1) feed location can be varied to investigate its effect on column operation; (2) a wide range of temperature and concentration profiles can be obtained for the process simulation; and (3) an appreciable conversion rate of acetic acid can be obtained with the dilute aqueous solutions and low reaction rate.

iii) The design of the column internals is the key to the proper operation of the column. Because of the relatively low reaction rate, the liquid must have enough residence time in catalyst bed. The division of the column space for the reaction and mass transfer to obtain optimal operation results depends on many factors. The principle is that both the mass transfer and reaction should not reach equilibrium at any location in the column and the mass transfer process should match the reaction process.





iv) The condenser and reboiler should be designed to have the capacity to change the feed rate, feed ratio, reflux ratio, etc.

v) The column operation should be automatically controlled. It is difficult to keep the column operation in a steady state for several hours with manual control.

vi) The column should be designed to have the flexibility to change the feed location and reaction zone.

Based on the above considerations and the information from computer simulation, the column was sized and stream flow rates were estimated:

Column diameter: 100 mm

Column height: 1.5 m

Feed rates: acid (2 to 10 wt% of acetic acid in water), 100 to 300 g/min

methanol (pure methanol), 5 to 50 g/min

Top product rate: 5 to 50 g/min

Bottom product rate: 100 to 300 g/min

Reflux ratio: 5 to 25

Typical column throughputs: vapor, 16 m<sup>3</sup>/h ; liquid, 25.8 L/h

The column configuration is shown in Figure 5-1. For the rectifying and stripping sections, conventional distillation trays and packings can be used for separation. In this study, conventional dualflow trays are used because of the small diameter column and the simple construction of the trays.



## 5.4 Internals For Reaction/Separation Section.

The function of the column internals for the reaction/separation section is to carry out both catalytic reaction and mass transfer simultaneously. In the past two decades, numerous patents have been awarded for new designs of the internals. They can be classified as follows:

i) Cloth Belt (Smith, 1980). The catalyst is sealed in a cloth belt. The belt is then wrapped in open mesh knitted stainless steel wire. Liquid can penetrate into and flow out from the catalyst through the cloth. The wetted surface of the cloth belt provides the vapor-liquid interfacial area for mass transfer. The mass transfer efficiency for this kind of catalyst unit is low because of the low interfacial area. The effectiveness of the catalyst inside the belt may change from location to location because of the different liquid residence times. This reduces the overall efficiency.

ii) Catalyst Container Held on a Tray (Jones, 1984, 1985). One version of this catalytic distillation unit consists of a normal distillation tray and a parallel array of rectangular tubes (troughs) filled with catalyst. The tubes (troughs) are constructed from metal screen and closed at the ends. The parallel tubes (troughs) may be supported above a distillation tray but should be in the froth zone when the column is in operation. The liquid flow across the tray is either parallel or at right angles to the tubes (troughs).

Another version of this unit consists of a normal distillation tray and closed porous containers containing catalyst. The containers are located above or on the distillation trays.



The structure of these units is usually quite complex. The catalyst quantity that can be loaded is limited. It is not suitable if the catalytic reaction rate is very slow because the reaction process may not match the mass transfer process.

iii) Packings. Random packings, e.g. Raschig rings, can be made from a polymer catalyst such as ion exchange resins (Flato and Hoffmann, 1992). The random packing in the column acts as both a catalyst and a mass transfer device. The random packing can also be made by rigid containers having a volume substantially smaller than the volume of the catalytic distillation column (Adams, 1991). The catalyst is loaded into the containers. Openings in the containers are provided to allow vapor and liquid passage into and out of the containers. The surfaces of the containers provide the necessary vapor-liquid contact surfaces for the distillation. The rigidity of the containers provides for spacing the structures and the necessary free space for the distillation.

Another version of this unit consists of a catalyst component and a resilient component closely associated with it (Smith, 1984). The resilient component has at least 70 volume% open space and is present with the catalyst component in an amount such that the catalyst distillation structure consists of at least 10 volume% open space.

Koch Engineering Co. developed a Katamax structured packing for catalytic distillation (DeGarmo et al., 1992). The packing structure is similar to corrugated metal sheet packing. The catalyst is held in a screen envelope. Each envelope consists of two parallel layers of crimped screen, roughly one foot square, which are sealed at the edges. The envelopes are stacked and bound to make a “brick”, a number of which are stacked to fill the column.



The other version of this unit consists of rigid, cellular monoliths coated with a catalytically active material (Palmer and Hagen, 1993).

Liquid holdup in the columns containing these internals is low. Therefore, it is not suitable for slow reaction applications. Like the cloth belt, the effectiveness of the catalyst may change from the surface to the inside because of the different liquid residence times. The cost of the internals can be very high.

iv) Tray Plus Fixed Bed of Catalyst (Jones, 1992; Quang et al., 1991; Nocca et al., 1991). In these catalytic distillation units, the reactive zone consists of alternating beds of catalyst and catalyst-free distillation zones. Passageways may be provided for a vapor phase in the fixed bed. Distillation zones contain conventional distillation trays and liquid distribution plates.

These units are suitable for slow reaction rates but the structure is very complex. The liquid flow pattern may be far from the plug flow which would reduce the efficiency.

v) Conventional Distillation Tray with Catalyst Placed in Downcomer (Etal, 1971; Haunschild, 1971, 1972; Gentry and Binkley, 1994; Yeoman et al., 1994). In these units, downcomers attached to the conventional trays are filled with catalyst which serves as a reaction zone and the trays act as a separation zone.

As shown in Chapter 2, the reaction rate for acetic acid esterification is very low and units i), ii), iii), and v) are not suitable for this application because of the relatively low liquid residence time in the column. Unit iv) may be the best choice for this application but its structure is quite complicated.





The catalytic distillation internals proposed in this study alternate a conventional dualflow tray and a catalyst unit. See Figure 5-2.

As shown in Figure 5-3, the dualflow trays have the simplest structure of all the distillation trays and can perform as both mass transfer device and liquid distributor for the catalyst unit underneath. They are made of metal sheets with punctured holes. The open hole area is usually 10 to 40%. The higher the open hole area, the higher the column capacity. In this study, dualflow trays with 12.5% open area are used because of the limited liquid flow through the catalyst beds in the column. The tray spacing was 216 mm.

The catalyst unit is composed of a catalyst basket filled with a solid acid catalyst, Amberlyst 15. It is placed between two dualflow trays. Passageways are provided for the vapor flow. The catalyst basket can be made in the form of concentric cylinders (shown in Figure 5-4) or parallel rectangular troughs (shown in Figure 5-5) depending on the column diameter. For the small column used in this study, the unit with concentric cylinders was adopted.

From Figure 5-4 it can be seen that the catalyst basket used in this study consists of three concentric cylinders with the bottom closed by a metal screen. The three zones formed are designated as zone A, zone B and zone C as shown in the figure. Zones A and C are filled with catalysts with the top closed by a mesh screen. Zone B is a open channel for vapor flow and occupies about 30% of the column cross-sectional area. A cap is installed above the vapor channel to prevent liquid from bypassing the zone. The catalyst baskets are made to tightly fit into the column with a height of 90 mm. A space of 100 mm between the bottom of the basket and the lower tray is used as a vapor-liquid contacting



zone for mass transfer. A space of 25 mm between the top of the basket and the upper tray is designed for vapor mixing and redistribution, and also for pressure drop measurement.

In the operation, vapor will flow up through the vapor channel to the top dualflow tray while liquid is distributed by the dualflow tray to the fixed catalyst bed beneath and then flows through the fixed bed to the lower dualflow tray.

With the proposed catalytic distillation internals, full use of the column space can be made for reaction and mass transfer and the vapor/liquid backmixing is reduced to a minimum.

## 5.5 Hydraulic Tests

The hydraulic tests were conducted with an air-water system. The objective for the hydraulic test is to observe the vapor-liquid contacting phenomena on the tray and the liquid distribution from the tray to the catalyst unit.

The test diagram is shown in Figure 5-6. The existing 150 mm diameter column was reduced to 100 mm to obtain results comparable to our 100 mm diameter distillation column. The tray spacing is 216 mm. Two dualflow trays with 21% openings were installed. Cross- or ring-type supports (see Figure 5-7) for the catalyst unit were placed on each of the dualflow trays to observe their effect on liquid distribution under the tray. The combination of tray 1 and the catalyst unit was used as a test object.

Air was introduced to the 150 mm column section and the volumetric rate was measured by a rotameter. The water was distributed to the first tray by a 4-point liquid



distributor. The water flow rate was also measured by a rotameter. For each run, air and water flow rates and froth heights on trays were measured. The vapor-liquid contacting phenomena and the liquid holdup in catalyst basket were observed and recorded.

With different supports for the catalyst unit on tray 1, different liquid distribution patterns from the tray were observed. With no objects on the dualflow tray, the liquid dripped down from random locations of the tray at the tested flow range of air and water. With ring-type support on the tray, the liquid distribution is similar to that for the dualflow tray. The reason for this is that the ring wall is very thin (less than 1 mm) and its interference with air flow is insignificant. However, with a cross-type support on the tray, more liquid dripped down from the middle point of the tray where the joint point is on the cross. It is believed that an object on the dualflow tray will more or less interfere with the vapor/gas flow. If the interference is more severe at some locations than at other locations, the liquid will drip down there because of the lower gas/vapor kinetic energy.

In the preliminary design, zone A and zone C in the catalyst unit, as shown in Figure 5-4, were separated by zone B and therefore, one of them would usually be flooded first depending on the liquid distribution; liquid distribution is related to the type of support of the catalyst unit used on the tray. With the ring-type of support, it was found that zone C usually flooded first even though the liquid distribution from tray 1 was quite uniform. The reason for this is that because of the mechanical construction of the catalyst basket about 50% of the bottom open area at zone C was blocked while only 17% was blocked at zone A. However, with the cross-type support, zone A usually flooded first because much more liquid dripped down from the middle point.



The test results suggest that zone A and zone C in the catalyst unit should be connected with each other by liquid channels so that the two zones can keep same liquid level or be flooded at the same time regardless of the liquid distribution patterns and the catalyst basket structure. In the final design, the catalyst basket was modified to have four horizontal liquid channels connecting the two zones.

## 5.6 Pressure Drop Of Liquid Flow Through The Fixed Catalyst Bed

In the operation with the internals consisting of dualflow trays and catalyst units, the catalyst units should not be flooded with liquid because the flooded liquid will not pass through the catalyst bed. Therefore, the prediction of liquid pressure drop through the catalyst bed is very important in the design of the catalyst unit.

The pressure drop of liquid flowing through a fixed porous media with a particle size distribution can be estimated from the following equation (Liu and Masliyah, 1996):

$$-\Delta p = 65.4H \frac{\mu_f (1 - \varepsilon)^2 V_f}{d_s^2 \varepsilon^{11/3}} \quad (5.1)$$

From Equation (5.1) it can be seen that the void fraction is the most important factor affecting the pressure drop. Although the void fraction for the packed bed with known particle size distribution can be predicted it is difficult to measure the particle size distribution accurately, especially for the fine particles which may reduce the void fraction of catalyst bed. In fact, the void fraction of the catalyst bed can be measured experimentally.

The measurement was conducted using a 250 mL glass graduated cylinder. The procedure is:







1. Weigh the cylinder,  $W_1 = 258.2 \text{ g}$
2. Load  $V_C = 250 \text{ mL}$  catalyst (wet, pores were filled with water) into the cylinder
3. Weigh the cylinder with catalyst,  $W_2 = 449.1 \text{ g}$
4. Slowly add water to the cylinder until the water level reaches the top of the catalyst bed
5. Weigh the cylinder with catalyst and water,  $W_3 = 529.8 \text{ g}$

The volume of water added can be found by  $V_w = W_3 - W_2 = 80.7 \text{ g} = 80.7 \text{ mL}$

The void fraction of the catalyst bed was found to be

$$\varepsilon = V_w / V_C = 0.323 \quad (5.2)$$

To check the accuracy of Equation (5.1), the pressure drop was measured using water in a catalyst bed with a diameter of 63 mm and a height of 90 mm. The water rate was slowly increased until the liquid level reached the top of the catalyst bed. It was found that the water rate was 39 L/h. The measured pressure drop was 90 mm H<sub>2</sub>O.

At a water temperature of 20 °C,  $\mu_f = 1 \times 10^{-3} \text{ Pa} \cdot \text{s}$ . The medium particle size,  $d_s$ , is estimated to be 0.8 mm. Substituting these numbers into Equation (5.1), the predicted pressure drop is 93.7 mm H<sub>2</sub>O, which is close to the measured 90 mm H<sub>2</sub>O. Therefore, Equation (5.1) together with Equation (5.2) was used to estimate the flooding point of the fixed bed with Amberlyst 15 and to choose the loading of the operating liquid.



## 5.7 Nomenclature

$d_s$	medium diameter of particles, m
$H$	height of fixed packed bed, m
$\Delta p$	pressure drop for liquid flowing through fixed porous media, Pa
$V_C$	volume of catalyst, mL
$V_f$	liquid superficial velocity in the packed bed, m/s
$V_w$	volume of water, mL
$\mu_f$	liquid viscosity, Pa·s
$\varepsilon$	void fraction of catalyst packed bed



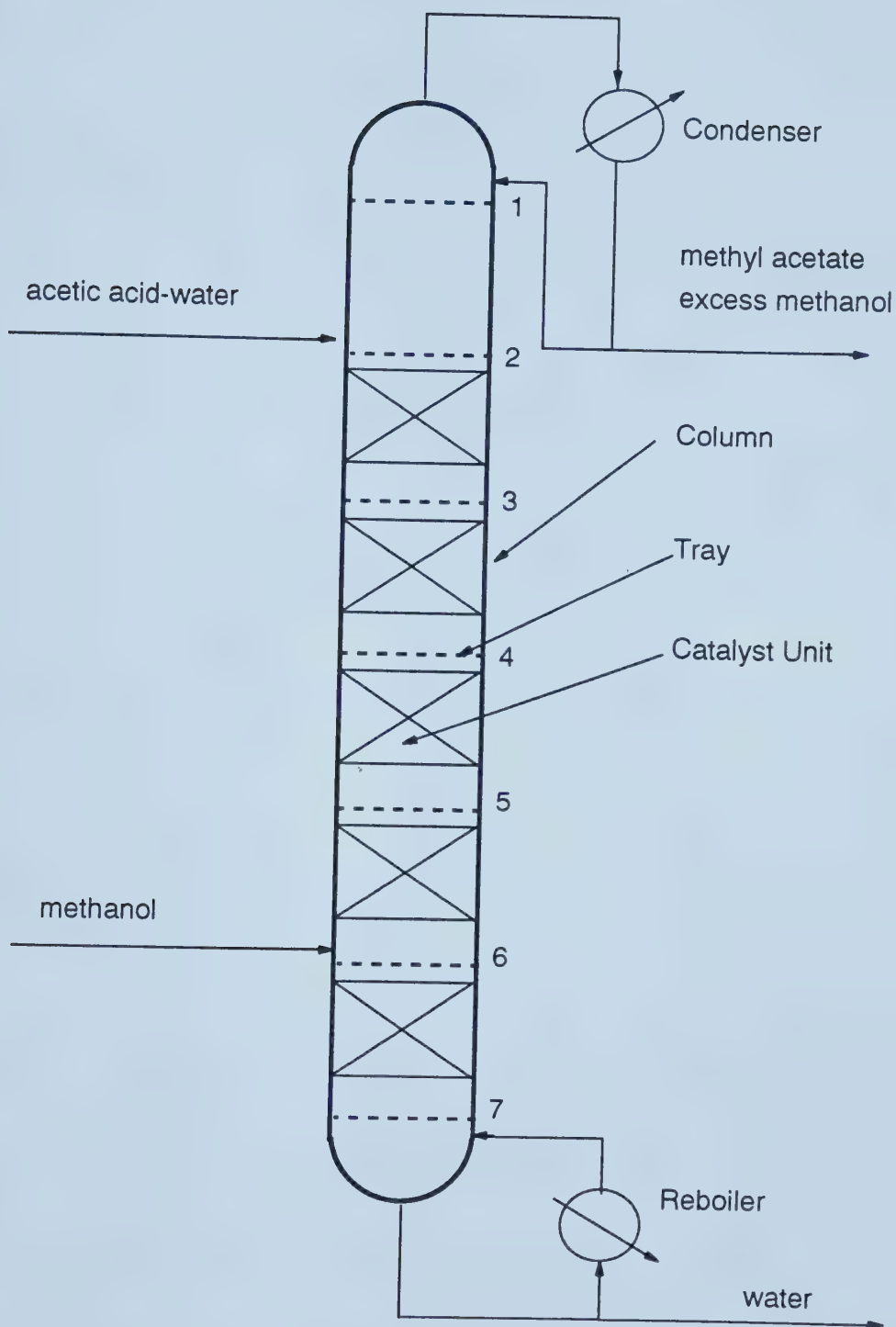


Figure 5-1 Column Configuration for Removal of Acetic Acid by Catalytic Distillation



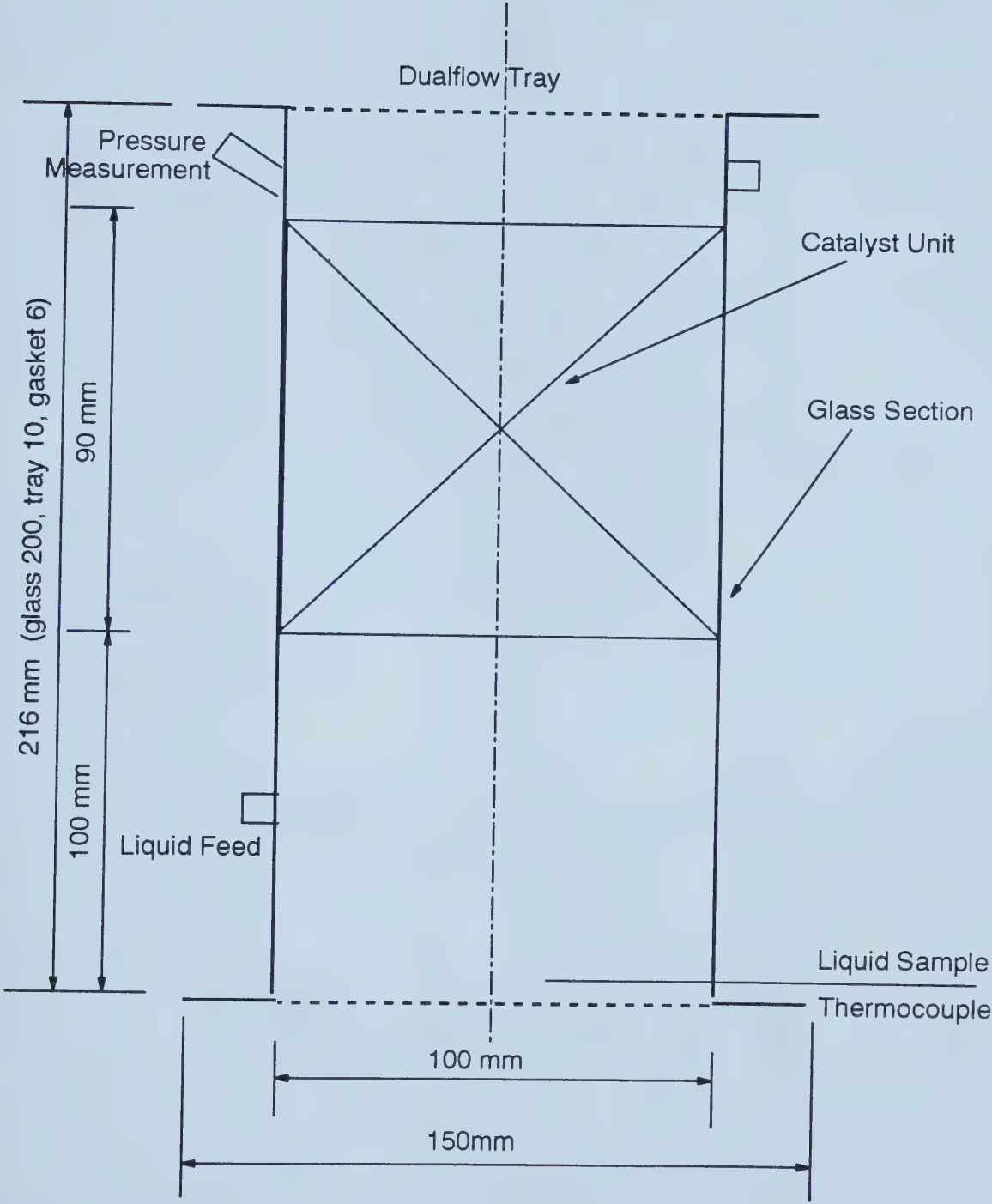


Figure 5-2 Catalytic Distillation Module





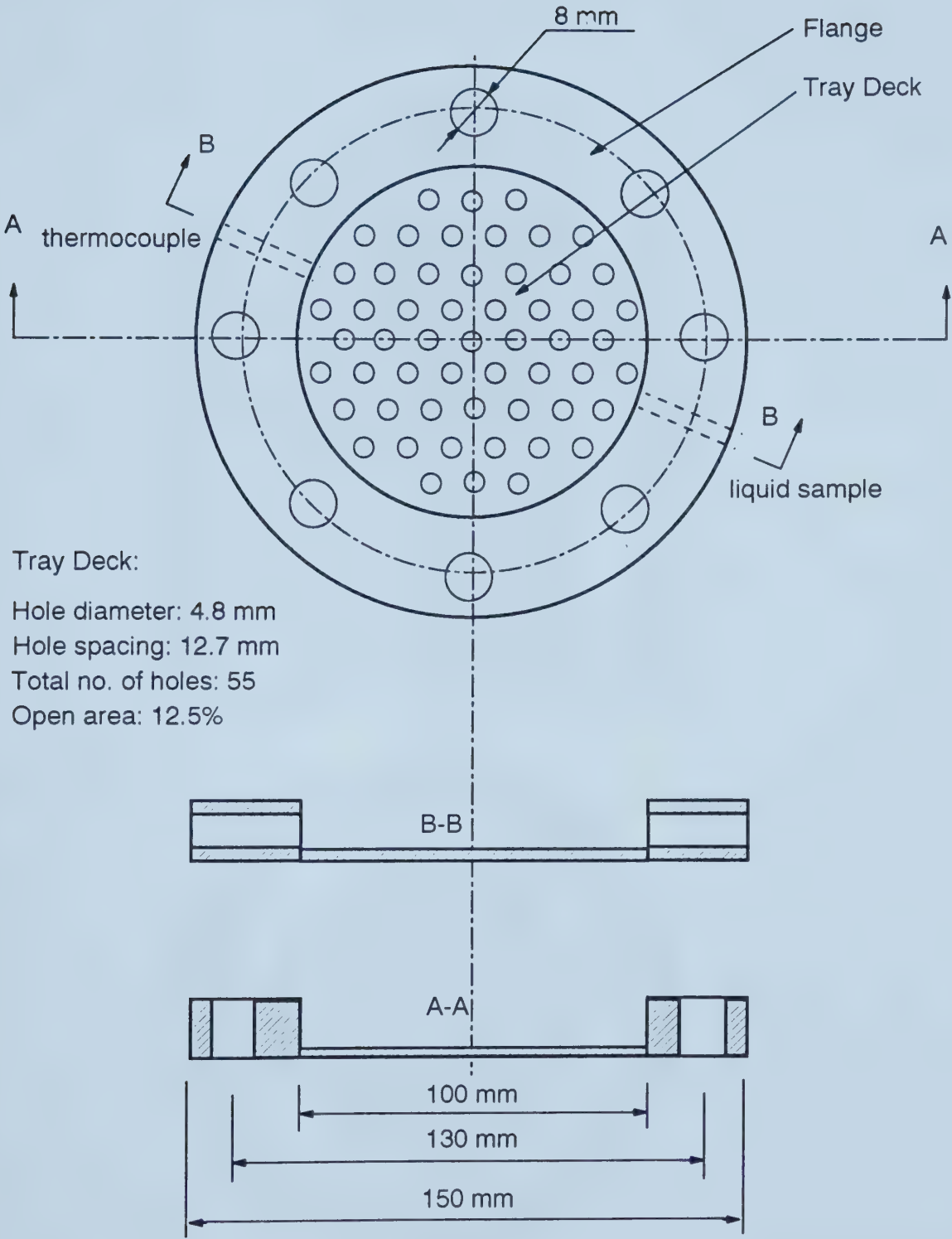


Figure 5-3 Dualflow Tray Structure



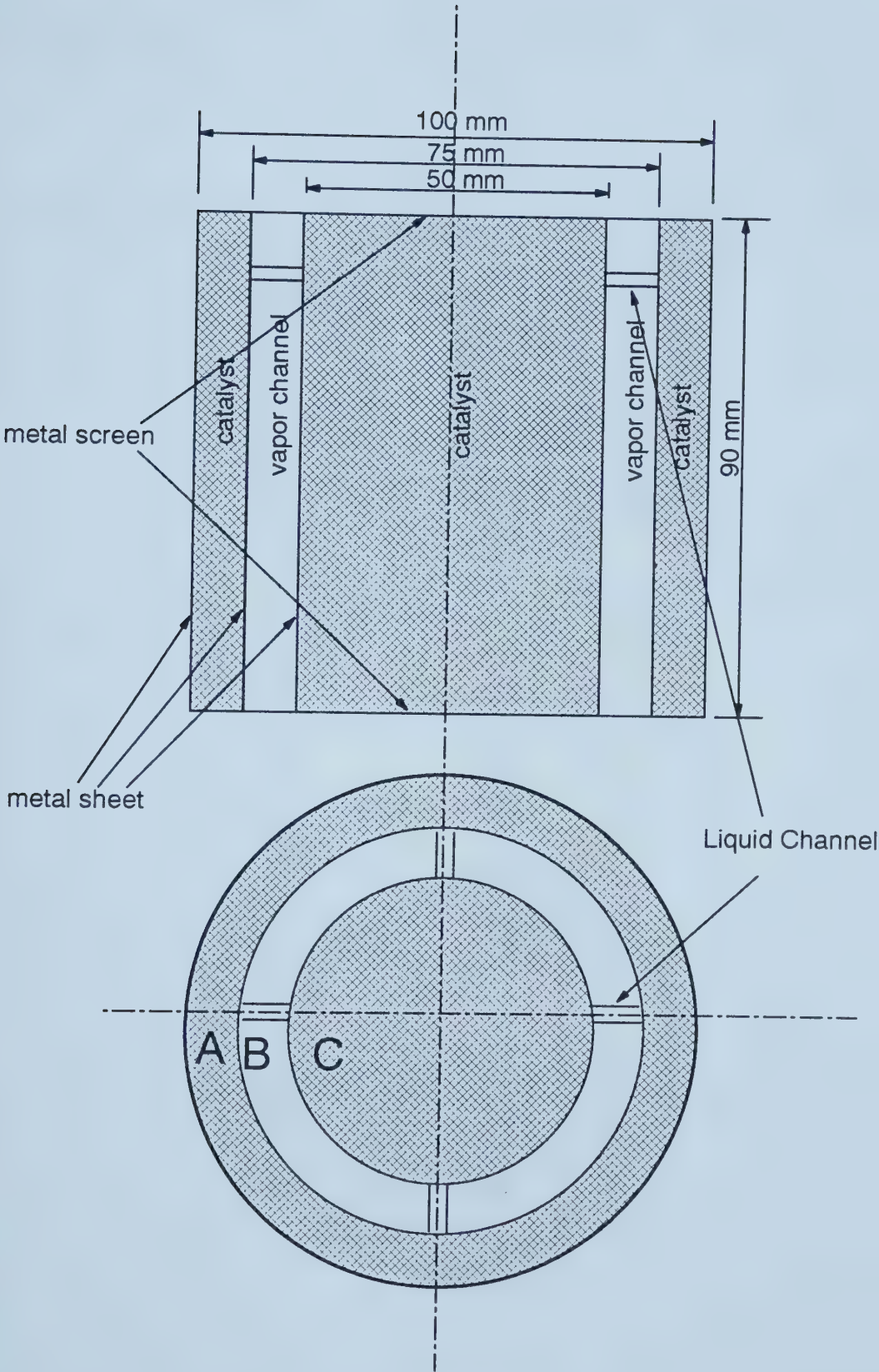


Figure 5-4 Catalyst Unit (cylindrical)



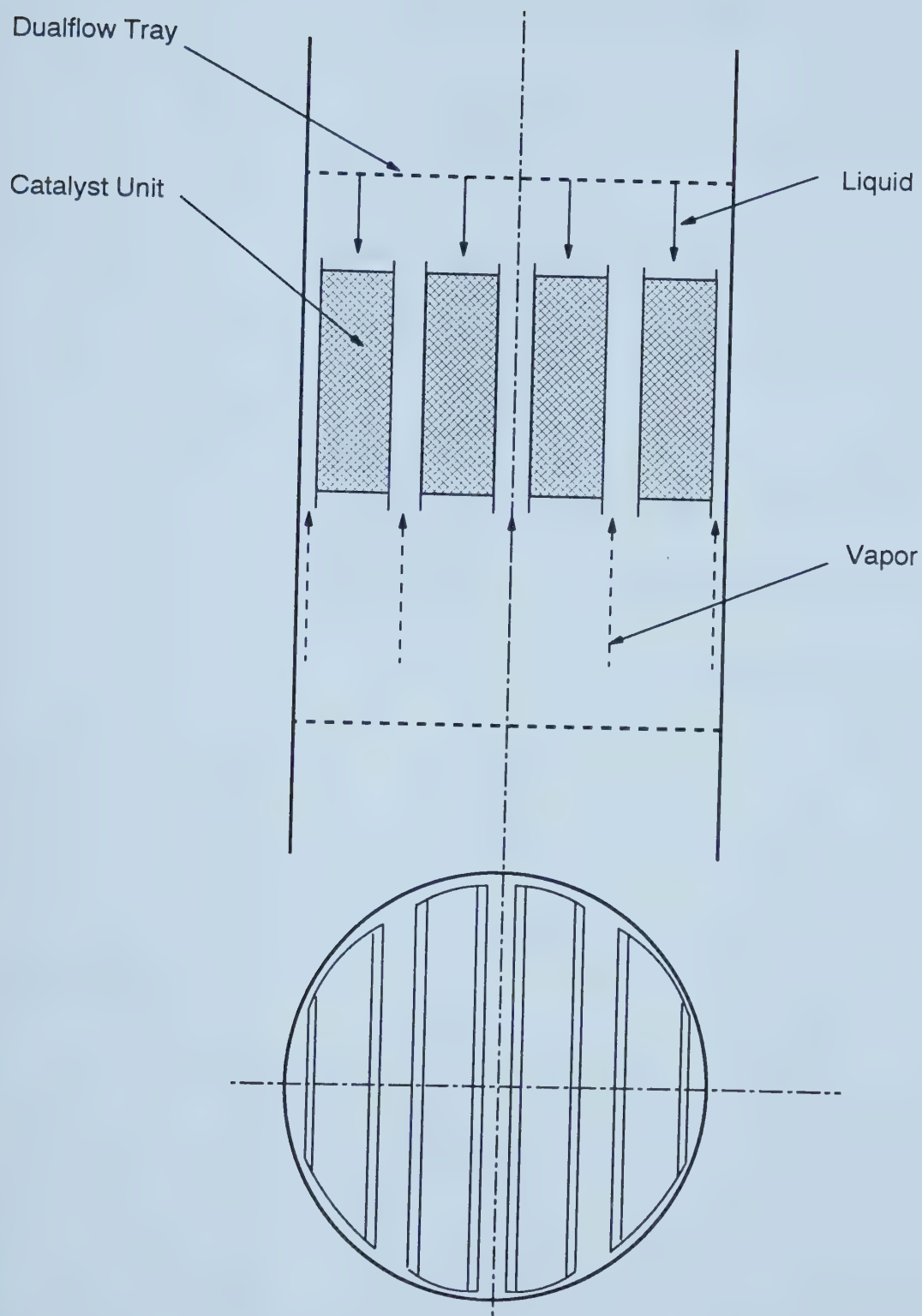


Figure 5-5 Catalyst Unit (rectangular)



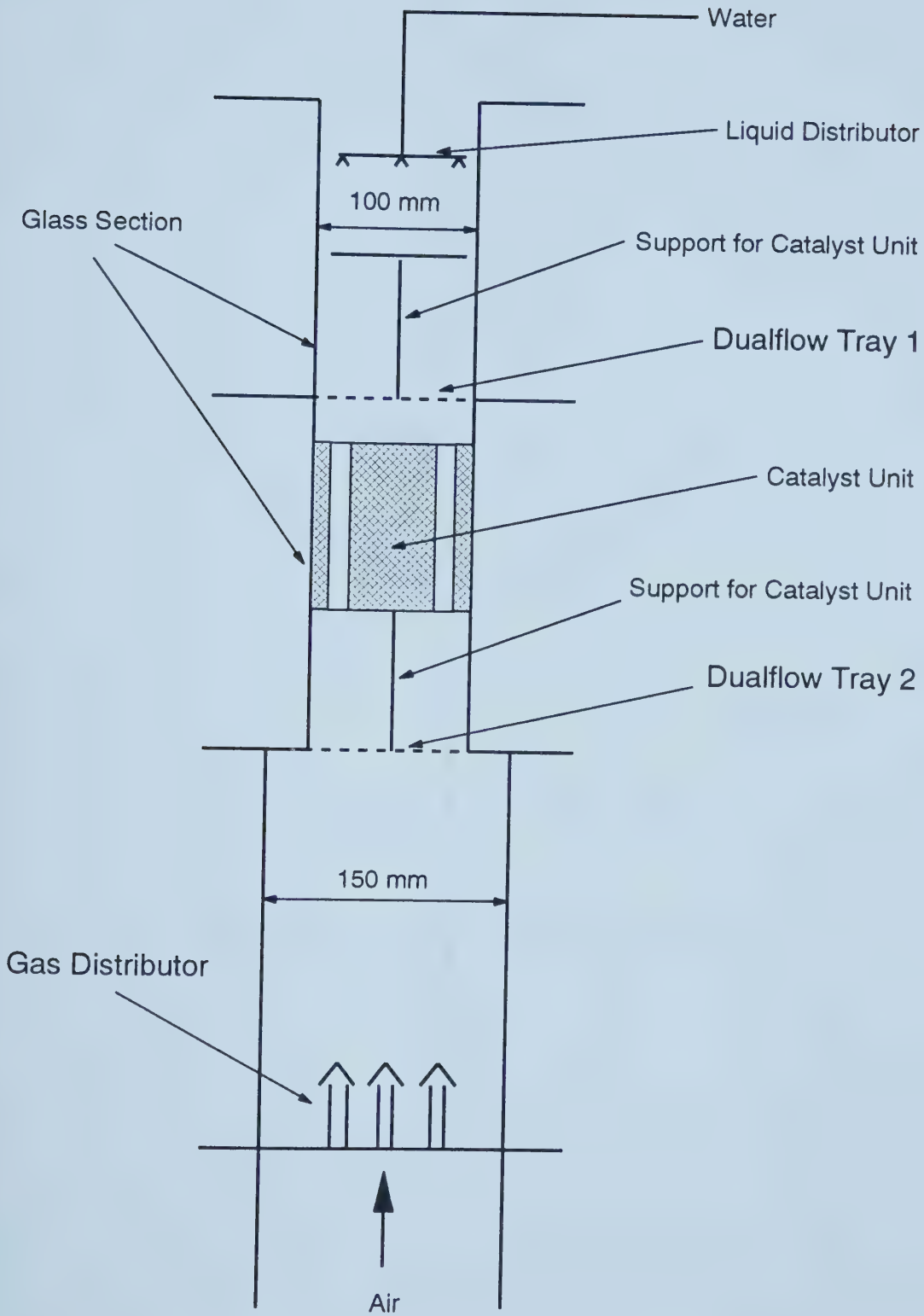


Figure 5-6 Hydraulic Test Using Air/Water System





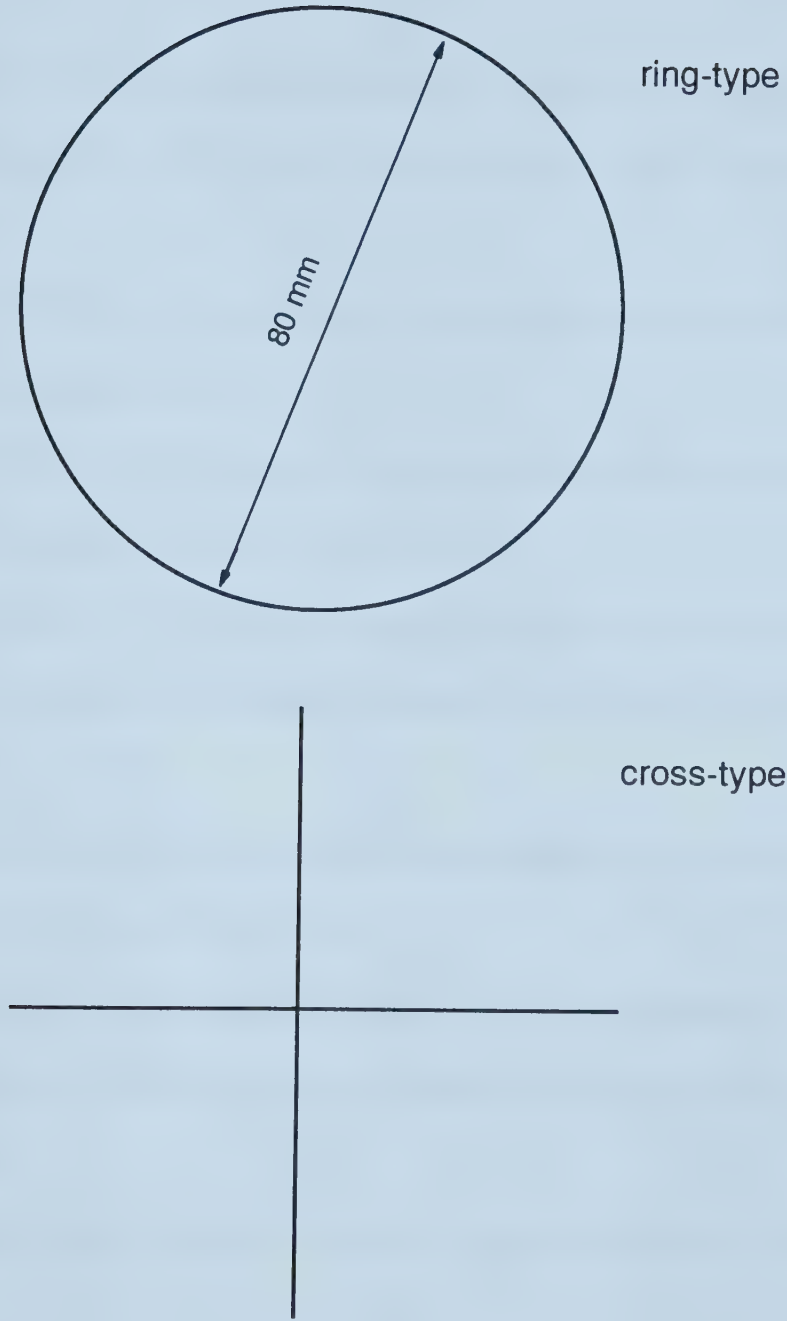


Figure 5-7 Support for Catalyst Units



## 5.8 Literature Cited

- Adams, J.R. (1991) Catalytic Distillation Structure. *US Patent* No. **5,057,468**.
- Aspen Technology, Inc. (1996) *Aspen Plus*, version **9.3**, Aspen Technology, Inc., Massachusetts.
- DeGarmo, J.L., Parulekar, V.N. and Pinjala, V. (1992) Considering Reactive Distillation. *Chem. Eng. Prog.* **88(3)**, 43-50.
- Etal, K.S. (1971) Column for Carrying Out Organic Chemical Reactions in Contact with Fine Particulate Catalysts. *US Patent* No. **3,579,309**.
- Flato, J. and Hoffmann, U. (1992) Development and Start-up of a Fixed Bed Reaction Column for Manufacturing Antiknock Enhancer MTBE, *Chem. Eng. Technol.* **15**, 193-201.
- Gentry, J.C. and Binkley, M.J. (1994) Method and Apparatus for Catalyst-Downcomer-Tray Operation. *US Patent* No. **5,277,847**.
- Haunschild, W.M. (1972) Separation and Catalysis. *US Patent* No. **3,634,535**.
- Haunschild, W.M. (1971) Separation of Linear Olefins from Tertiary Olefins. *US Patent* No. **3,629,478**.
- Jones, E.M. (1984) Contact Structure for Use in Catalytic Distillation. *US Patent* No. **4,439,350**.
- Jones, E.M. (1985) Contact Structure for Use in Catalytic Distillation. *US Patent* No. **4,536,373**.
- Jones, E.M. (1992) Catalytic Distillation Reactor. *US Patent* No. **5,130,102**.



- Liu, S. and Masliyah, J.H. (1996) Single Fluid Flow in Porous Media. *Chem. Eng. Comm.* **148-150**, 653-732.
- Nocca, J.L., Leonard, J., Gaillard, J.F. and Amigues, P. (1991) Apparatus for Reactive Distillation. *US Patent* No. **5,013,407**.
- Palmer, D.A. and Hagen, G.P. (1993) Catalytic Distillation Using Rigid Cellular Monoliths as Catalyst-Packing Material. *US Patent* No. **5,235,102**.
- Quang, D.V., Amigues, P. and Gaillard, J.F. (1991) Apparatus for Reactive Distillation. *US Patent* No. **5,026,459**.
- Simulation Sciences, Inc. (1994) *User's Guide* (PROvision 1.0 with PRO/II 4.0). Simulation Science, Inc., California.
- Smith, L.A.Jr. (1980) Catalyst System for Separating Isobutene from C<sub>4</sub> Streams. *US Patent* No. **4,215,011**.
- Smith, L.A.Jr. (1984) Catalytic Distillation Structure. *US Patent* No. **4,443,559**.
- Yeoman, N., Pinaire, R., Ulowetz, M.A., Nace, T.P. and Furse, D.A. (1994) Method and Apparatus for Concurrent Reaction with Distillation. WO 94/08679.



## CHAPTER 6. MASS TRANSFER EFFICIENCY OF DUALFLOW TRAYS

### 6.1 Introduction

To understand and simulate the catalytic distillation process with the methyl acetate-methanol-water-acetic acid quaternary system it is necessary to find the separation efficiency of the distillation trays. There are several definitions for the separation efficiency in distillation (Lockett, 1986), but the most commonly used one is Murphree tray efficiency which is defined as:

$$E_{MV,i,j} = \frac{y_{i,j} - y_{i,j+1}}{y_{i,j}^* - y_{i,j+1}}, j = 1, 2, \dots, n; i = 1, 2, \dots, m \quad (6.1)$$

where  $i$ =component number;  $j$ =tray number counted from the top of the column.

For a multicomponent system, the separation efficiencies are usually different from component to component. Therefore, component tray efficiency should be used for the accurate prediction of component concentration profiles along the distillation column.

A complication of determining multicomponent tray efficiencies is due to the fact that the mass flux of a component depends not only on its own concentration driving force, but also strongly on other component concentrations in the mixture. This is especially true for the highly nonideal systems in which molecular sizes and polarity are very different from one another. The presence of these interaction effects can lead to (Toor, 1957):

1. Diffusion barrier - no net mass transfer occurs even when there is a driving force





2. Reverse diffusion - mass transfer occurs in a direction opposite to the concentration driving force
3. Osmotic diffusion - mass transfer occurs even though no concentration driving force is present

Although the majority of distillation processes separate multicomponent mixtures, relatively few efficiency data are available compared with a simple case such as binary systems. From the published results on multicomponent tray efficiencies, some important points are highlighted as follows:

a) Most of the experimental results were obtained using ternary or quaternary systems (Biddulph et al., 1988a, 1988b; Krishna et al., 1977; Medina et al., 1979; Diener and Gerster, 1968; Vogelpohl, 1979; Chan and Fair, 1984; Ognisty and Sakata, 1987; Young and Weber, 1972).

b) For a thermodynamically nonideal system significant differences exist among the individual component point efficiencies (Biddulph et al., 1988a; Krishna et al., 1977; Diener and Gerster, 1968; Vogelpohl, 1979; Young and Weber, 1972).

c) The middle components, i.e. the components with middle volatilities, usually showed the highest point efficiency. The Murphree point efficiencies of those components were not bounded between 0 and 1.0 (Biddulph et al., 1988a, 1988b; Krishna et al., 1977; Medina et al., 1979; Diener and Gerster, 1968; Vogelpohl, 1979). Although the offset efficiencies could be caused by the particular physical situations (reverse diffusion, diffusion barriers, osmotic diffusion), they are mainly due to errors in concentration measurements for the middle components with maximum concentrations. Under these



circumstances the magnitudes of the numerator and the denominator of Equation (6-1) become comparable with the experimental errors. However, these offset efficiencies will not have a significant effect on the prediction of the composition of that component (Medina et al., 1979).

d) The component point efficiencies are composition dependent and scattered by the influence of the varying compositions of the other components. Maximum variation in individual component point efficiencies was obtained when one of the middle components reached its composition maximum (Biddulph et al., 1988a, 1988b; Biddulph, 1977a,b; Krishna et al., 1977; Medina et al., 1979; Diener and Gerster, 1968; Vogelpohl, 1979; Young and Weber, 1972).

e) The key components have similar values for tray efficiency and the designation of key components may vary with the column position depending on the component concentrations at a specific location (Biddulph, 1977a,b).

Although multicomponent mass transfer theory has been developed for decades (Toor, 1957, 1964a,b,c; Krishna and Standart, 1976; Krishna, 1977, 1981; Taylor and Smith, 1982; Smith and Taylor, 1983), the multicomponent efficiency models were rarely used for systems with more than three components. The main reasons are: 1) most models are limited to equimolar counterflow, ideal vapor phase, and no liquid phase resistance conditions; 2) few sets of reliable vapor/liquid equilibrium data are available; 3) a lack of experimental data to validate models; and 4) there are so many factors affecting tray efficiencies, including column geometry, vapor/liquid physical properties, and operating conditions, that no reliable binary efficiency models are available for predicting tray



efficiencies. It is common practice to assume that the binary efficiency based on the key components can be applied to all members of the multicomponent mixture (Chan and Fair, 1984). The assumption appears to be reasonably accurate for mixtures of similar compounds (Ognisty and Sakata, 1987).

In the catalytic distillation column, a dualflow tray was used as both a mass transfer device and a liquid distributor. In the dualflow tray liquid and vapor flow countercurrently through the same tray holes. These trays have a greater capacity and a lower pressure drop than trays with downcomers because the fluids can flow through the entire cross-section of the column. In addition, dualflow trays are the only device suitable for fouling and dirty services. In the existing column internals, dualflow trays have the simplest structure and occupy the least column space. The main shortcoming of dualflow trays is the sensitivity of the tray efficiency to tray levelness, vapor/liquid loading and physical properties (Xu et al., 1994). The dualflow trays are best used in small columns with a diameter less than one metre and where high turndown ratio is not important.

No component tray efficiencies have been reported for dualflow trays with the methyl acetate-methanol-water-acetic acid system. In this study, component tray efficiencies of the dualflow trays were measured for this quaternary system. The efficiency values were then applied to a simulation of the catalytic distillation process with the same system.



## 6.2 Experimental

The dualflow tray efficiencies were measured in the same column with the same trays used for the catalytic distillation experiments. A schematic diagram of the experimental apparatus and the detailed dimensions of the column and the tray are shown in Figure 6-1 (with feed and product lines closed for total reflux operation) and Table 6-1, respectively. The column contained seven identical trays spaced 216 mm apart. The middle five trays were used as test trays. To make the hydrodynamic conditions similar to catalytic distillation, similar boil-up rates were used and the catalyst units as shown in Chapter 5 were placed above tray 3 to 7 (counting from the top of the column) in the column. The catalyst units were composed of catalyst baskets filled with inert glass beads with a diameter of 0.7 mm instead of catalyst particles (Amberlyst 15 with an average size of 0.7 mm).

The column sections were constructed with glass so that the vapor/liquid contacting phenomena and the liquid distribution from the trays to the catalyst units could be visually observed. The trays and catalyst baskets were constructed with stainless steel (SS316). During the operation, the column was insulated with 60 mm thick fiberglass to minimize heat loss. The insulation can be removed for observing column operation and for measuring froth height.

Each tray was equipped with a thermocouple and a liquid sampler. The sampler is a 3 mm tube with a valve at the end. The tubing just rests on the tray deck horizontally and can be moved back and forth (see Figure 6-2) so that liquid samples can be taken at different locations in a radial direction. A 3 mL syringe was used to withdraw the liquid







samples through the tubing. The tray pressure drop was measured with a U-type manometer with water as an indicator.

Quaternary mixtures of methyl acetate-methanol-water-acetic acid used in catalytic distillation experiments, as well as binary mixtures of methanol-water were used to obtain component tray efficiency. The distillation was conducted at total reflux under ambient pressure. To apply the measured tray efficiencies for the analysis and simulation of catalytic distillation results, similar operating conditions and mixture compositions as used in catalytic distillation experiments were chosen for the efficiency measurements.

After steady state was reached, liquid samples were taken from each tray and analyzed by a gas chromatograph. Other hydraulic data were recorded, including tray pressure drop and visual froth heights.

Assuming total mixing of liquids, the component tray efficiencies at total reflux were calculated using Equation (6.1).

### **6.3 Results And Discussion**

Unlike trays with downcomers, cross flow of liquid does not occur on dualflow trays. The radial concentration gradient in both vapor and liquid phases can be neglected in small columns. Therefore, tray efficiency is similar to point efficiency when no serious channeling of fluids occurs on the tray.

The efficiency of dualflow trays is known to be affected by three main factors: vapor/liquid loading, physical properties and tray open hole area (Xu et al., 1994). In the present study, only 12.5% of the tray open hole area was used. The vapor/liquid loadings



were not changed significantly. F-factors were about  $0.6 \text{ (kg/m)}^{0.5}/\text{s}$  at the top of the column. The main focus was on the effect of mixture compositions and their physical properties on tray efficiencies.

Table 6-2 lists the physical properties of the four pure components, methyl acetate, methanol, water and acetic acid. From the component boiling points, it is expected that methyl acetate and methanol will ascend and acetic acid and water descend in the distillation column. Of the four components, methanol has the lowest liquid density and water has the highest surface tension.

### ***6.3.1 Froth Height and Froth Structure***

The vapor-liquid interfacial area and mass transfer efficiency of dualflow trays are dependent on froth height and froth structure. The froth height and froth structure are determined by the physical properties of the mixture.

Figure 6-3 (Figures 6-3a, 6-3b and 6-3c) shows variations of froth height and froth structure along the distillation column for three operations with the same boil-up rate but different mixture compositions. It can be seen that with the same tray dimensions, the froth height changes from tray to tray and operation to operation because of the changes in mixture composition. Table 6-3 lists the mixture compositions on each tray for the three runs. Higher froth heights were observed on trays 2 and 3 in Figure 6-3a, tray 1 in Figure 6-3b and trays 3, 4 and 5 in Figure 6-3c. The observed values of froth heights are plotted in Figure 6-4. It is interesting to note that the maximum froth heights shift from left to right (column top to bottom) with the increase in methanol and/or methyl acetate



concentrations in the column. It was observed that when a tray had a high froth, the froth was in bubble structure.

The froth height,  $h_f$ , can be related to clear liquid height,  $h_L$ , and froth porosity,  $\varepsilon$ , using Equation (6.2):

$$h_f = h_L / (1 - \varepsilon) \quad (6.2)$$

For non-foaming and low-foaming systems, the clear liquid height can be correlated as (Mahendru and Hackl, 1979; Xu et al., 1994):

$$h_L = b_1 \frac{L^{b_2} (u_s \sqrt{\rho_G})^{b_3}}{\rho_L} \quad (6.3)$$

Mahendru and Hackl (1979) proposed the following equation to predict the froth porosity:

$$\varepsilon = 1.0 - 0.0946 \left[ \frac{u_s^2 \rho_G}{g h_L \rho_L} \right]^{-0.2} \quad (6.4)$$

Combining Equations (6.2) to (6.4),

$$h_f \propto 1.0 / \rho_L \quad (6.5)$$

From the above equations, it can be seen that only liquid density is considered in the correlation of froth height. The lower the liquid density, the higher is the froth height. According to this, higher froth should be obtained for tray 2 in Figure 6-3a, tray 1 in Figure 6-3b and tray 3 in Figure 6-3c. The first two are consistent with our measured froth height but not the last one.

It is easier to test the above equations using the measured froth height for the methanol-water system. The higher the methanol concentration, the lower is the liquid



density. From the above correlations, higher froth should occur with higher methanol concentration. Figure 6-5 shows the measured froth height vs. methanol concentration for the methanol-water binary system. It can be seen that the froth height does not increase but decreases with the increase in methanol concentration at the high concentration range of methanol.

The lower froth height at the column top for the binary and the quaternary systems indicates that froth height may be affected by not only liquid density but also other physical properties such as surface tension and surface tension gradient. The low surface tension will facilitate formation of small bubbles and small bubbles are more stable than large bubbles. The positive surface tension gradient makes bubbles stable. Therefore, a froth with bubble structure can probably be created with a low surface tension and a significant positive surface tension gradient.

The effect of the surface tension gradient can be examined using M-index as a quantitative variable (Dribika and Biddulph, 1987):

$$M = (x - y^*) \frac{d\sigma}{dx} \quad (6.6)$$

where  $\sigma$  is the mixture surface tension,  $x$ =base component mole fraction in liquid phase and  $y^*$ =equilibrium composition of vapor with liquid. A significant positive value of M-index is necessary to keep the bubble structure stable.

For multicomponent systems, it may be difficult to apply Equation (6.6) because the sign and magnitude of M-index are dependent on the choice of the base component. This is especially true when the middle components have maximum concentration values in the column. One alternative is to group the components with similar surface tension. For





the methyl acetate-methanol-water-acetic acid system, methyl acetate, methanol and acetic acid have similar surface tensions and can be grouped as one pseudocomponent with water as another component. The base component can be either the pseudocomponent or water.

Figure 6-6 shows the variations of M-index along the column for the three runs shown in Figure 6-3. From Figures 6-3 and 6-6, it can be seen that all the top trays with lower froth heights (no bubble structure observed) have negative or very small positive values of M-index. This is true for all fourteen runs. It can be concluded that the surface tension gradient is one of the most important factors in determining froth height and froth structure. If the surface tension gradient is negative, froth height is low and no bubble structure is observed.

In addition to the physical properties, vapor and liquid loadings are also factors affecting froth height. The higher the vapor/liquid loadings, the higher is the froth height. Although same boil-up rates were used for the three runs in Figure 6-3, the vapor F-factor and liquid loadings changed from run to run and tray to tray due to the differences in latent heat among the components. Generally speaking, F-factor decreases down the column because water has the highest latent heat.

Figure 6-7 shows enlarged pictures of Figure 6-3c. From this figure, it can be seen clearly that in the middle of the column, the froth is high with bubble structure while at the column ends, no bubbles can be observed and froth is low because of either a negative surface tension gradient (at the column top) or a high liquid density and high surface



tension combined with low vapor/liquid rates (at the column bottom). Similar phenomena were observed for all the other runs.

### 6.3.2 *Effect of Sampling Position and Catalyst Units*

Accuracy in liquid sampling from a dualflow tray is dependent on the sampling device, column size, froth regime and froth height. To ensure that typical liquid samples were obtained from the dualflow trays using the simple sampler shown in Figure 6-2, the methanol-water binary system was used to investigate the effect of sampling position on tray efficiency. Figure 6-8 shows the tray efficiencies obtained with the sampling position in the middle or at the side of the trays. It can be seen that the effect of sampling position on tray efficiency is not significant. This indicates that the liquid on the trays is totally mixed because of the small size of the column. In the rest of the tests, all the liquid samples were taken from the middle of the trays.

One of the interesting features in Figure 6-8 is that the tray efficiencies are very high and some of them even exceed 100%. It was expected that the tray efficiencies would be high because of the relatively low vapor rates (F-factors are in the range of 0.45 to 0.64  $(\text{kg/m})^{0.5}/\text{s}$ ) and low tray openings (resulting in high froth). However, as stated before, the dualflow tray efficiency is similar to point efficiency, and therefore it should not exceed 100%. There are three explanations for the unusual high efficiency: 1) the froth on the tray was high while the vapor rate was very low so that the liquid on the tray might not be totally mixed in the vertical direction; 2) additional vaporization might have occurred because of the large relative volatility of the methanol-water system and consequently



large temperature change from tray to tray (Lockett and Ahmed, 1983); 3) the catalyst unit contributed to some extent to mass transfer on the tray. For example, it was observed that some liquid bypassed the packed bed with glass beads and dropped down through the vapor channel and the gap between the catalyst basket and the column wall. Also, at the bottom of the catalyst unit, there was a layer of liquid film and a group of liquid droplets formed. These liquids contacted the upflow vapor and therefore, increased tray efficiency because the tray efficiency was based on a combination of measurements from the tray and the catalyst unit above.

The effect of the catalyst units on tray efficiency was tested by taking the catalyst units out of the column and repeating the runs with only dualflow trays under similar operating conditions. Figure 6-9 shows that without catalyst units on the dualflow trays, the tray efficiencies are consistently lower than those with catalyst units and always below 100%. This means that the catalyst units did contribute to tray mass transfer efficiency.

### ***6.3.3 Effect of Physical Properties***

The line without catalyst baskets as shown in Figure 6-9 demonstrates the same trend as we obtained in a 300 mm diameter column with the same methanol-water system, but with much higher vapor/liquid loadings (Xu et al., 1994). At low concentrations of methanol, the tray efficiency increases with the increase in methanol concentration until the methanol mole fraction reaches 0.8. Beyond this concentration, the tray efficiency starts decreasing. From this figure it can be seen that the liquid mixture composition, because of its physical properties, has a significant effect on tray efficiency.





The physical properties that affect tray hydraulics and efficiency are mainly liquid density, surface tension and surface tension gradient. The liquid density affects the froth density and froth height, and therefore the vapor-liquid contact time and interfacial area. As shown by Xu et al. (1994), the higher the liquid density, the higher the froth density and the lower the froth height. As explained in Section 6.3.1, surface tension and surface tension gradient affect the froth structure, and therefore, the interfacial area. In the froth regime, the tray with steady bubble structure should have a high efficiency.

Figure 6-5 shows variations of the froth height with liquid composition for the methanol-water binary system. At methanol mole fractions below 0.2, no bubbles were observed in the froth. This is due to the high liquid density and high surface tension. With increasing methanol concentration, both liquid density and surface tension decrease, so froth height increases. Also, a proper positive surface tension gradient maintains the froth zone with a stable bubble structure. The high froth height and bubble structure resulted in a large interfacial area, and therefore a high mass transfer efficiency as shown in Figure 6-9. When methanol concentration increases further to above  $x=0.8$ , the froth height drops and no bubbles were observed in the froth zone. The only explanation for this phenomenon is the lack of surface tension gradient, which results in the collapse of the bubble structure. From Figure 6-9 it can be seen that tray efficiency drops in this zone.

The above results indicate that dualflow trays are more suitable where liquid density, surface tension and surface tension gradient are not a strong function of the liquid composition. Otherwise, different tray dimensions (mainly the open hole area) along the column should be considered to ensure uniform froth height on each tray. Because of the





use of catalyst units in our catalytic distillation column which also contributed to mass transfer, the tray efficiency did not change significantly with liquid concentration and the same tray dimensions were used for the rest of the tests.

#### **6.3.4 Component Tray Efficiencies**

Multicomponent tray efficiencies were measured with the methyl acetate-methanol-water-acetic acid quaternary system through the changes in mixture compositions to cover the component concentration ranges to be used in our catalytic distillation experiments. The acetic acid concentration in the catalytic distillation tests was no higher than the acetic acid-water feed concentration, that is, 10 wt%. Water concentration was in the range of 2 to 99 wt% and methanol 0 to 90 wt%. The methyl acetate was concentrated on the top two trays and the concentration was expected to be below 50 wt%. The test was focused on the effect of mixture compositions on component tray efficiency.

Figures 6-10 to 6-12 show the measured concentration profiles of the four components in the distillation column. For multicomponent systems, the concentration of the lightest component, methyl acetate in this study, always increases from column bottom to top while the heaviest one, acetic acid, shows the opposite trend. The middle components, methanol (see Figures 6-10 and 6-11) and water (see Figure 6-12), may have a maximum concentration at a specific location of the column.

Figures 6-13 and 6-14 show the component tray efficiencies corresponding to Figures 6-10 and 6-11, respectively. The component tray efficiencies vary from one



another and change significantly with column position (mixture compositions). Although the methanol concentration profiles are similar for the two runs, the component tray efficiencies are dramatically different at the maximum concentrations. Figure 6-15 also shows that component tray efficiencies fluctuate sharply when the component concentrations reach maxima. The abnormal fluctuations are due to the small difference between the sample composition and the equilibrium composition in combination of the efficiency definition described in Equation (6.1).

From Figures 6-13 to 6-15 it can be seen that the component tray efficiencies are different from one another and the maximum fluctuation in component tray efficiencies is observed when the component concentration reaches maximum. Similar results were obtained by other authors (Biddulph et al., 1988a, 1988b; Krishna et al., 1977; Medina et al., 1979; Diener and Gerster, 1968; Vogelpohl, 1979; Chan and Fair, 1984; Ognisty and Sakata, 1987; Young and Weber, 1972).

With five test trays (total of seven trays) installed in the column, five efficiency points with different compositions could be obtained for each component from each run. A total of 14 runs were conducted by changing overall mixture compositions. In this way, the effect of mixture compositions on component tray efficiencies can be thoroughly investigated.

Figure 6-16 shows that most of the component efficiencies for methyl acetate are between 0.6 to 0.8. The efficiencies below 0.6 were all obtained from tray 2. Carefully checking the froth height and froth structure for these points with efficiencies lower than 0.6, it was found that froth heights were usually below 60 mm with no bubbles in the froth



mostly because of the negative surface tension gradient. The points with efficiencies above 0.6 have froth heights from 60 to 140 mm with bubble structure due to the positive surface tension gradient. The catalyst units may have also contributed to some extent to the mass transfer for those trays below tray 2.

The component efficiencies for methanol as shown in Figure 6-17 are more scattered. Few points having very high (say above 2.5) or very low (say below 0.0) efficiencies are excluded from the figure because all those points were obtained with methanol concentrations in the peak zone and therefore, those extreme efficiencies are due to experimental errors and the efficiency definition. Figure 6-17 can be divided into three zones. For zone I with methanol concentration below 0.4, the efficiencies are mostly between 1.0 to 1.2. The large variation in efficiencies at a very low concentration (below 0.02) of methanol may be attributed to experimental error. The higher efficiencies in this zone were all obtained from tray 3 to tray 6 with catalyst units placed above the trays. As shown in the binary methanol-water system, the catalyst units may contribute to mass transfer. For zone II with methanol concentration higher than 0.4 and efficiencies between 0.9 to 1.2, the efficiencies do not change significantly and show very similar magnitudes and trends as the methanol-water binary system. All these points were obtained from tray 3 to tray 6 with catalyst units. The rest of the figure is zone III. In this zone, efficiencies are low and most of the points were obtained from tray 2. There are three reasons for the low efficiencies: 1) there was no catalyst unit on tray 2; 2) there was low froth height with no bubbles in the froth mostly because of the negative surface tension gradient; 3) some



points were obtained with methanol concentrations in the peak zone and experimental error could have been excessive.

The component efficiency points of the water as shown in Figure 6-18 have a similar distribution pattern to those of methanol. Those points with efficiencies below 0.9 were mostly obtained from tray 2. The reasons for the low efficiencies are similar to those for methanol. Those points with efficiencies higher than 0.9 were all obtained from trays 3 to 6 with catalyst units on the trays and show a trend similar to the methanol-water binary system. The efficiencies are mostly between 0.9 and 1.2. Few points having very high or very low efficiencies are excluded from the plot for the same reason as stated above for methanol.

Figure 6-19, showing the acetic acid component efficiencies, can be divided into two zones. Those points with tray efficiencies of about 0.6 were obtained from the pseudobinary system of acetic acid-water because of the low concentration of methanol and methyl acetate present. Acetic acid-water is a surface tension negative system. The visual froth height was low (25 to 35 mm) and no bubbles could be observed in the froth as expected for these points. Therefore, the vapor-liquid interfacial area, and thus the mass transfer efficiency is low. Those points with efficiencies of about 0.8 were obtained from higher froth heights (30 to 100 mm) and most have bubble structure due to the higher content of methanol and methyl acetate.

The scattered component efficiencies shown in Figures 6-16 to 6-19 are due to four factors.







- Tray structure – the middle five trays (2 to 5 counting from the top) were used as test trays. The catalyst units were placed on tray 3 to 5 but not 2. This is because in the catalytic distillation experiments, no catalyst units were put on trays 1 and 2 to prevent a possible net reverse reaction. Therefore, the efficiency for tray 2 may have been different from the others even when the mixture compositions and vapor/liquid loading were the same as the others. Therefore, in all the four figures, a different symbol is used for tray 2.
- Different mixture compositions may result in very different froth height and froth structure. For example, with the same concentration of methyl acetate (say,  $x=0.1$ ) and the rest of the methanol and water, if the methanol concentration is high (say above 0.85) or low (say below 0.3), the froth height could be very low (say 30 mm), and no bubbles may be observed because of the lack of a positive surface tension gradient and/or too high of a surface tension as discussed above. On the other hand, if the methanol concentration is about 0.75, 100 mm of froth with bubble structure may be obtained. Obviously in the latter case, the vapor-liquid interfacial area, therefore the component tray efficiency for methyl acetate would be much higher than in the first case, although the concentration of methyl acetate is the same.
- Experimental errors produced when component concentration is in extreme or reaches maximum. In either case, the difference between the component concentration and its equilibrium concentration is very small and any errors in



sampling and analysis could result in significantly different tray efficiencies.

This is one drawback of the Murphree tray efficiency defined in Equation (6.1);

- Interaction among the components due to the difference in molecular size, polarity, or diffusivity. This interaction may cause diffusion barriers, reverse diffusion and osmotic diffusion as shown by Toor (1957).

## 6.4 Conclusions

Component tray efficiencies for the quaternary system, methyl acetate-methanol-water-acetic acid, were measured in a 100 mm diameter column installed with seven dualflow trays. The mixture compositions were widely changed to investigate the effect of component composition on tray efficiencies. The component tray efficiencies were found to be different from one another. The middle two components, methanol and water, have higher but more scattered efficiencies than the other two. The component efficiencies for the trays with catalyst units on them (trays 3 to 6) are mostly between 0.6 to 0.8, 0.9 to 1.2, 0.9 to 1.2, 0.6 to 0.9 for methyl acetate, methanol, water and acetic acid, respectively. The efficiencies on tray 2 without a catalyst unit are usually lower because of the lower froth height (negative surface tension gradient at the column top) and the absence of a catalyst unit on it.



## 6.5 Nomenclature

$b_1, b_2, b_3$	constants in Equation (6.3)
$E_{MV}$	Murphree tray efficiency
F-factor	$=u_s\rho_G^{0.5}$ , (kg/m) <sup>0.5</sup> /s
$g$	gravity, (=9.81 m/s <sup>2</sup> )
$h_f$	froth height, m
$h_L$	clear liquid height, m
$\Delta H_v$	vaporization heat at normal boiling point, kcal/kmol
$L$	liquid flow rate, m <sup>3</sup> /s
$m$	total component number
$M$	M-index as defined in Equation (6.6), dyn/cm
MW	molecular weight, g/mol
$n$	total tray number
$t_b$	normal boiling point, °C
$u_s$	vapor superficial velocity, m/s
$x$	component mole fraction in liquid phase
$y$	component mole fraction in vapor phase
$y^*$	equilibrium component mole fraction in vapor with liquid
$\rho$	fluid density, kg/m <sup>3</sup>
$\varepsilon$	froth porosity
$\sigma$	surface tension, dyn/cm



$\mu$  fluid viscosity, cp

#### Subscript

i component number

j tray number

G vapor

L liquid





Table 6-1. Column and Tray Dimensions

Column diameter (mm)	100
Tray thickness (mm)	2
Hole diameter (mm)	4.76
Open hole area (%)	12.5
Tray spacing (mm)	216



Table 6-2. Physical Properties of Pure Components (20 °C)

	Methyl Acetate	Methanol	Water	Acetic Acid
$t_b$ (°C)	57.1	64.7	100.0	118.1
MW	74.08	32.04	18.02	60.05
$\rho_G$ (kg/m <sup>3</sup> )	3.08	1.33	0.75	2.50
$\rho_L$ (kg/m <sup>3</sup> )	924	792	998	1049
$\mu_G$ ( $\times 10^4$ , cp)	81	94	120 (100°C)	83
$\mu_L$ (cp)	0.38	0.62	1.01	1.2
$\sigma$ (dyn/cm)	24.2	22.5	74.1	27.8
$\Delta H_V$ (kcal/kmol)	7430	8430	9729	5810



Table 6-3. Mixture Compositions (Mole Fraction) on Each Tray for Run #8, 11, 14

	Methyl Acetate	Methanol	Water	Acetic Acid
Run#8 (Fig.3a)				
Tray 1	0.565	0.376	0.059	0.0
Tray 2	0.419	0.434	0.144	0.003
Tray 3	0.097	0.393	0.479	0.031
Tray 4	0.004	0.107	0.821	0.068
Tray 5	0.001	0.025	0.875	0.099
Tray 6	0.001	0.003	0.872	0.125
Run#11 (Fig.3b)				
Tray 1	0.299	0.429	0.269	0.004
Tray 2	0.088	0.345	0.557	0.010
Tray 3	0.001	0.071	0.905	0.023
Tray 4	0.0	0.008	0.961	0.031
Tray 5	0.0	0.001	0.959	0.039
Tray 6	0.0	0.0	0.951	0.048
Run#14 (Fig.3c)				
Tray 1	0.273	0.700	0.027	0.0
Tray 2	0.103	0.836	0.061	0.0
Tray 3	0.029	0.893	0.077	0.0
Tray 4	0.007	0.845	0.146	0.002
Tray 5	0.001	0.696	0.297	0.006
Tray 6	0.0	0.350	0.630	0.020



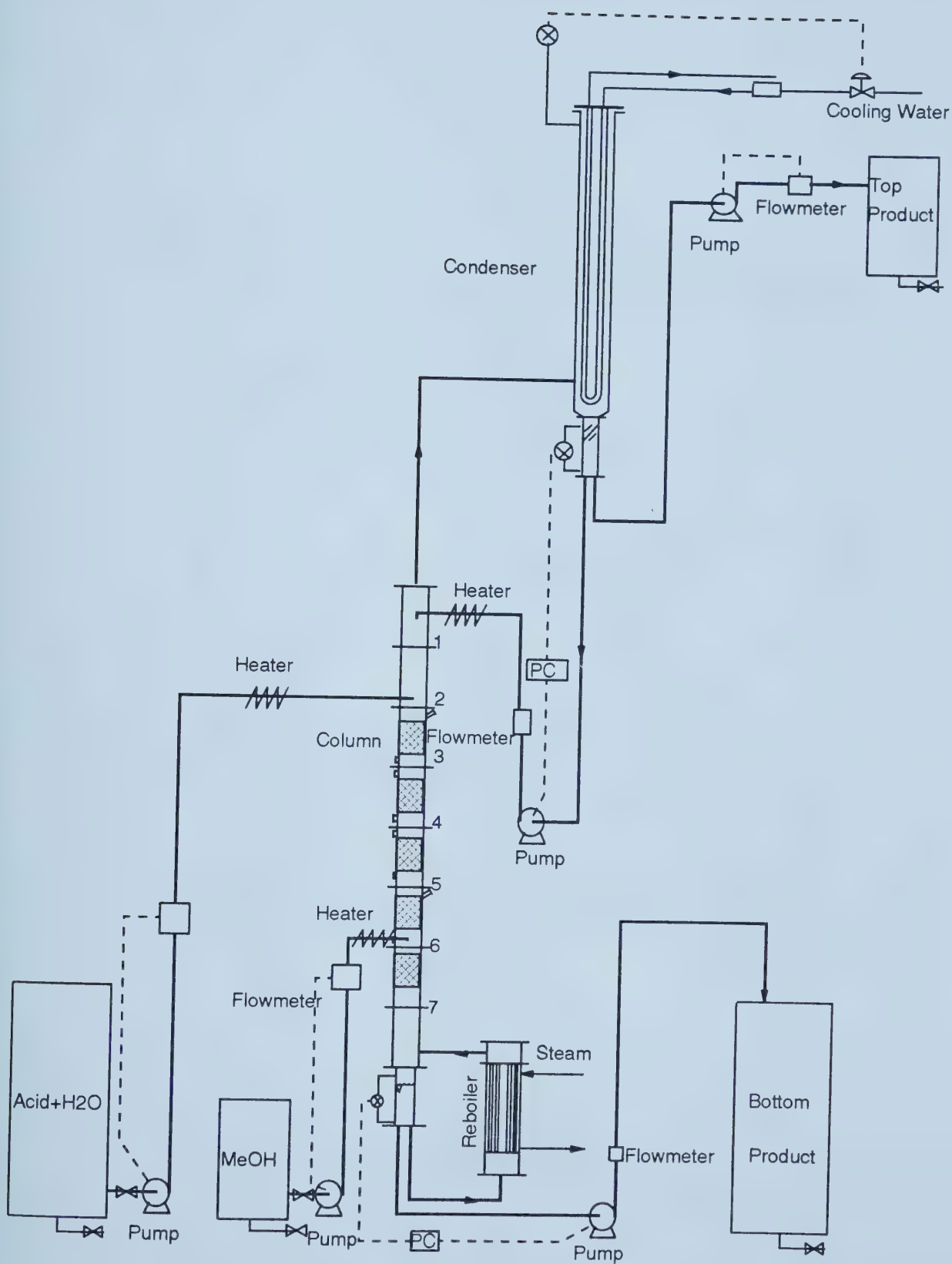


Figure 6-1 Distillation Test Flow Sheet





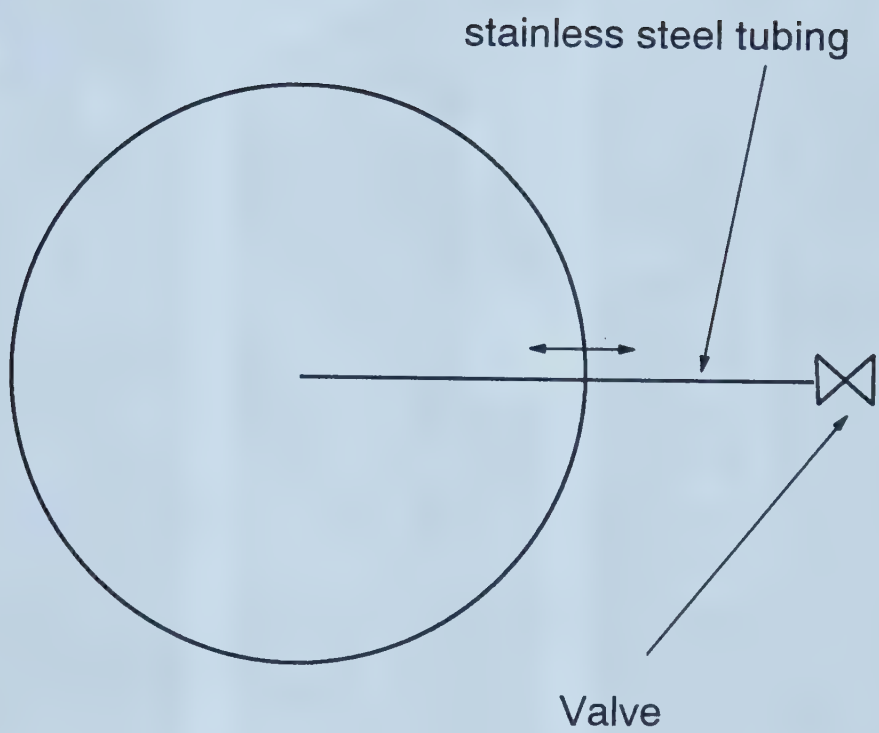


Figure 6-2 Liquid Sampling Structure



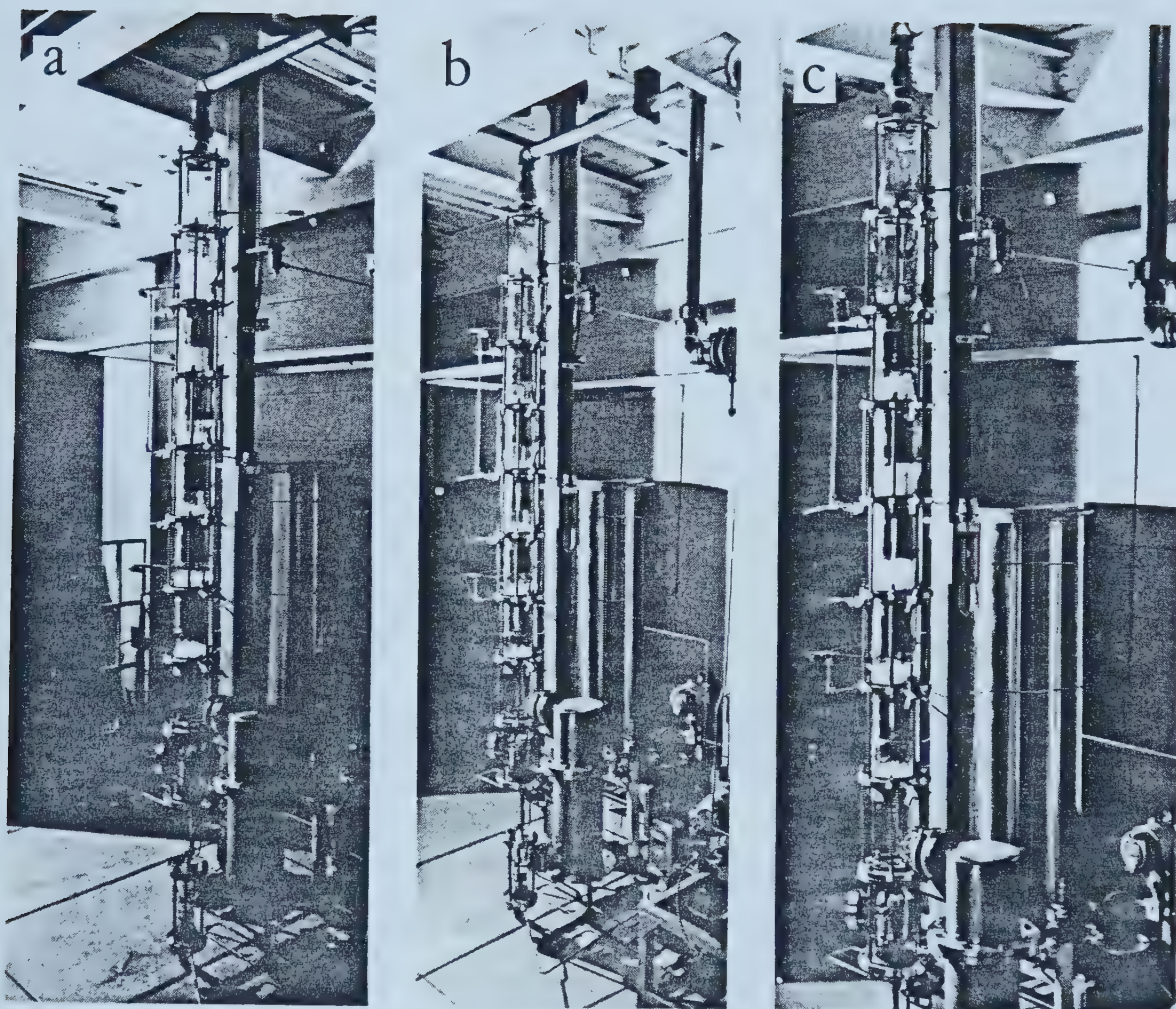


Figure 6-3. Variation of Froth Height with Tray Location and Liquid Composition  
(photograph, methyl acetate-methanol-water-acetic acid system).



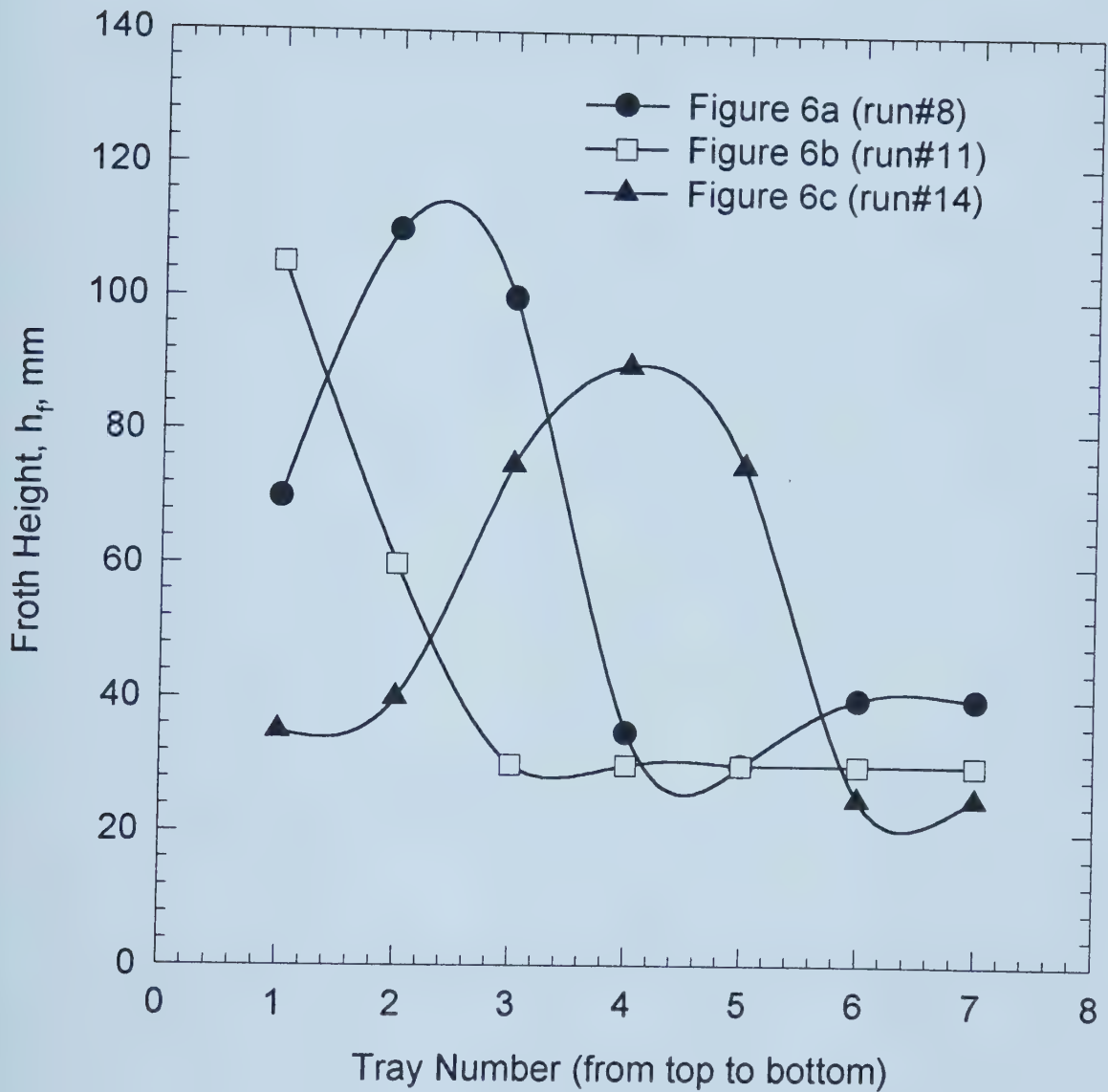


Figure 6-4. Variation of Froth Height with Tray Location and Liquid Composition (methyl acetate-methanol-water-acetic acid system).



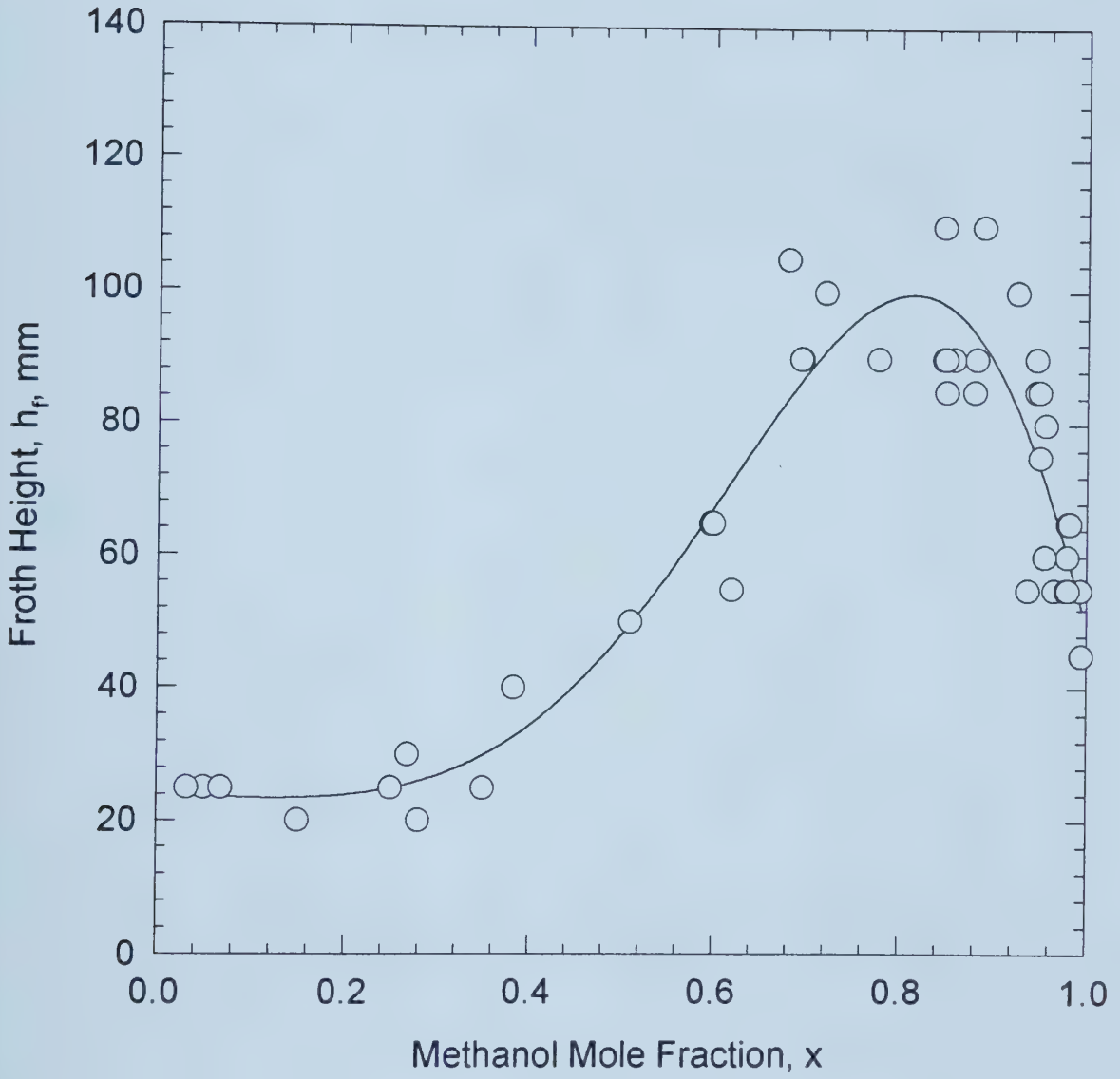


Figure 6-5. Effect of Liquid Composition on Froth Height (methanol-water system).





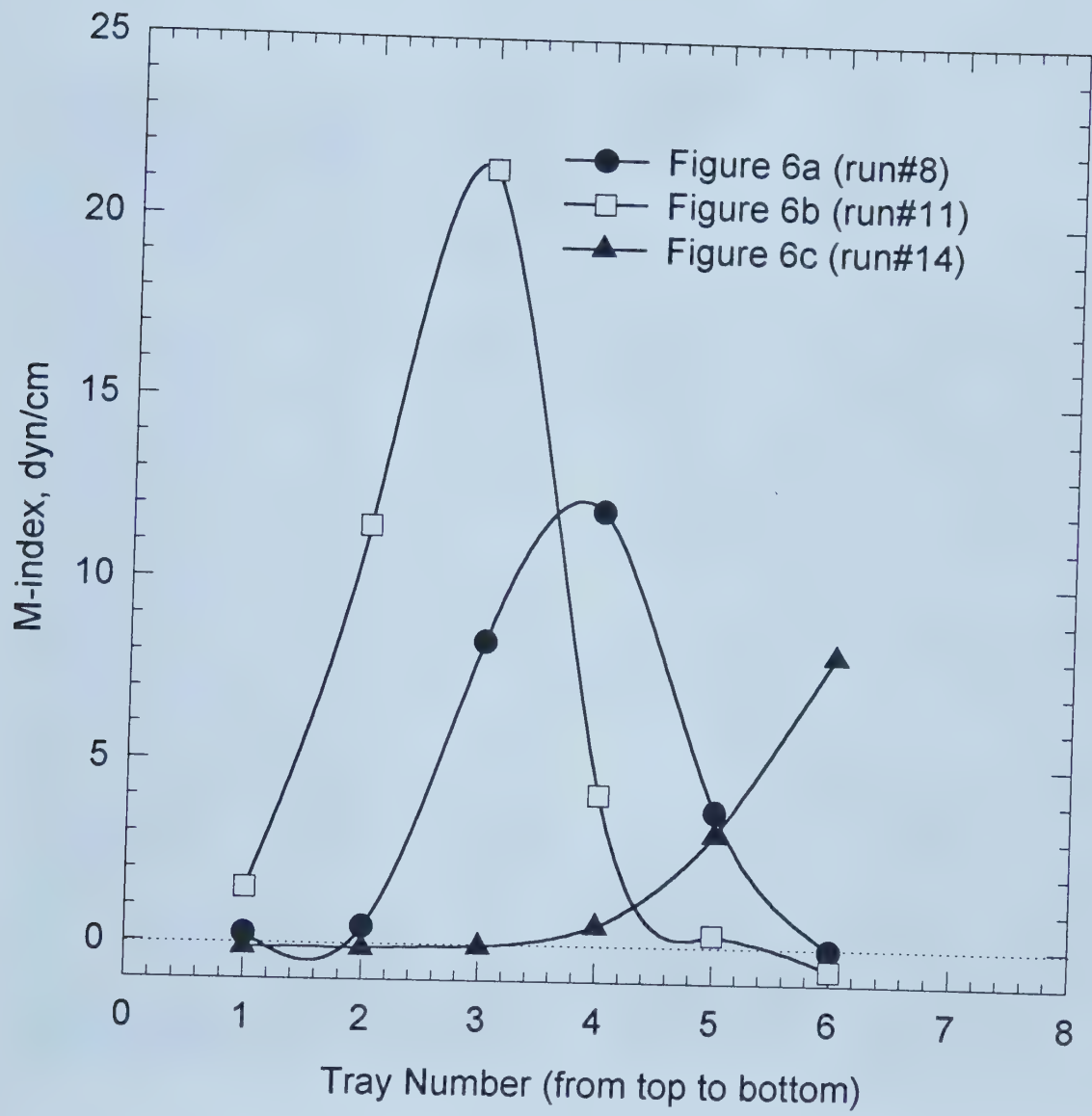


Figure 6-6. Variation of M-index with Tray Location.



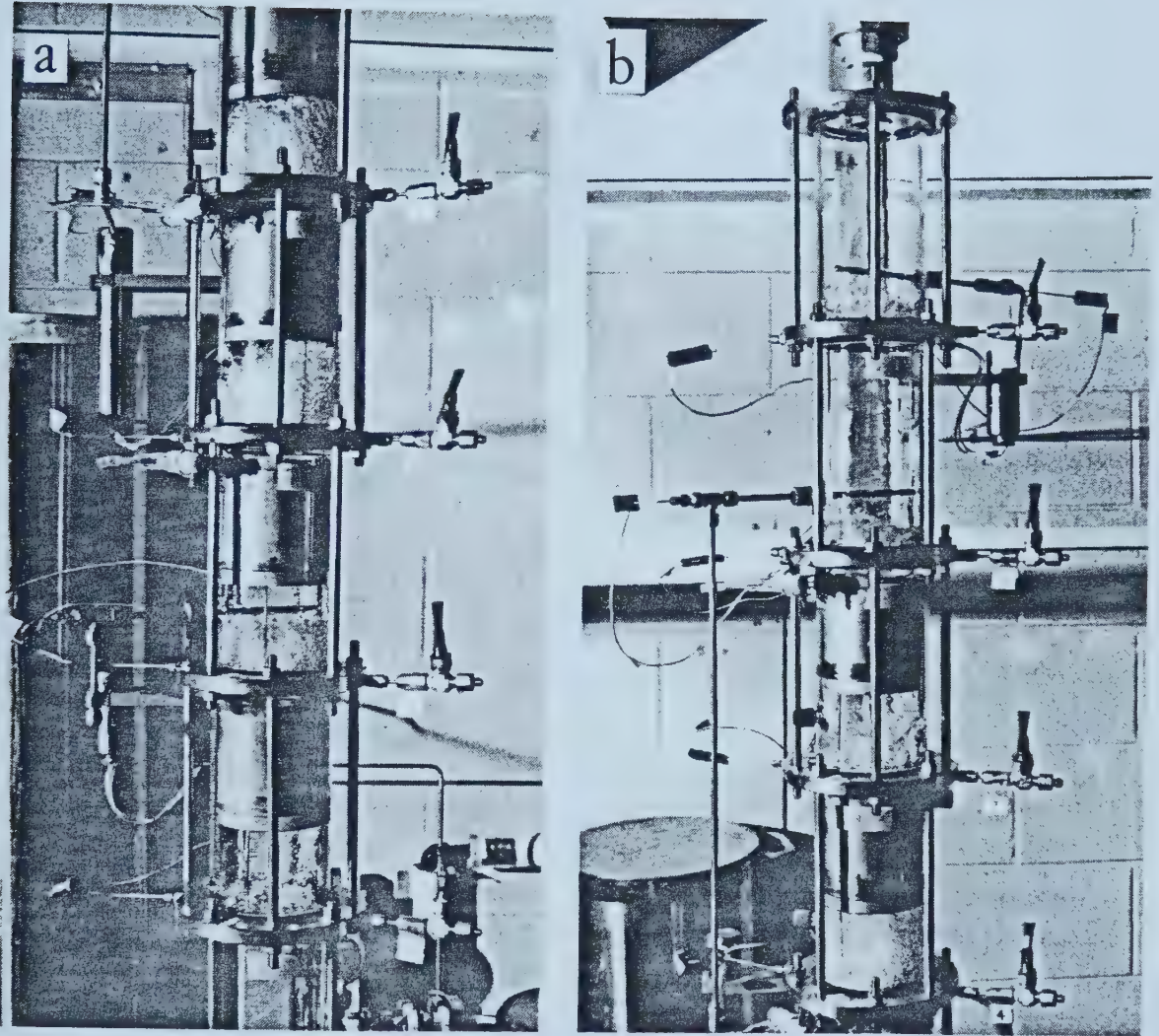


Figure 6-7. Enlarged Photograph for Figure 6-3c.



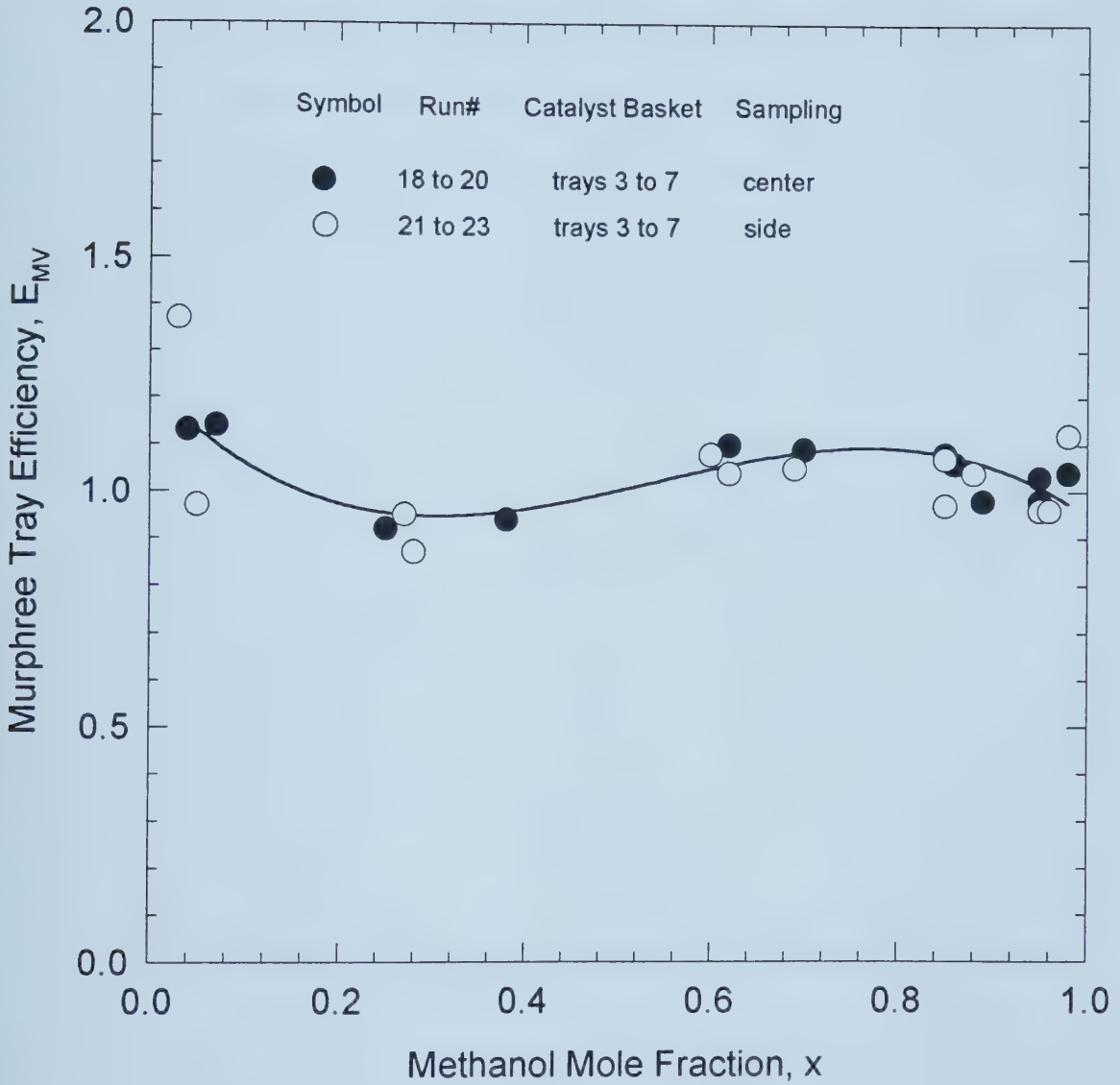


Figure 6-8. Measured Tray Efficiencies with Different Sampling Locations (methanol-water system).



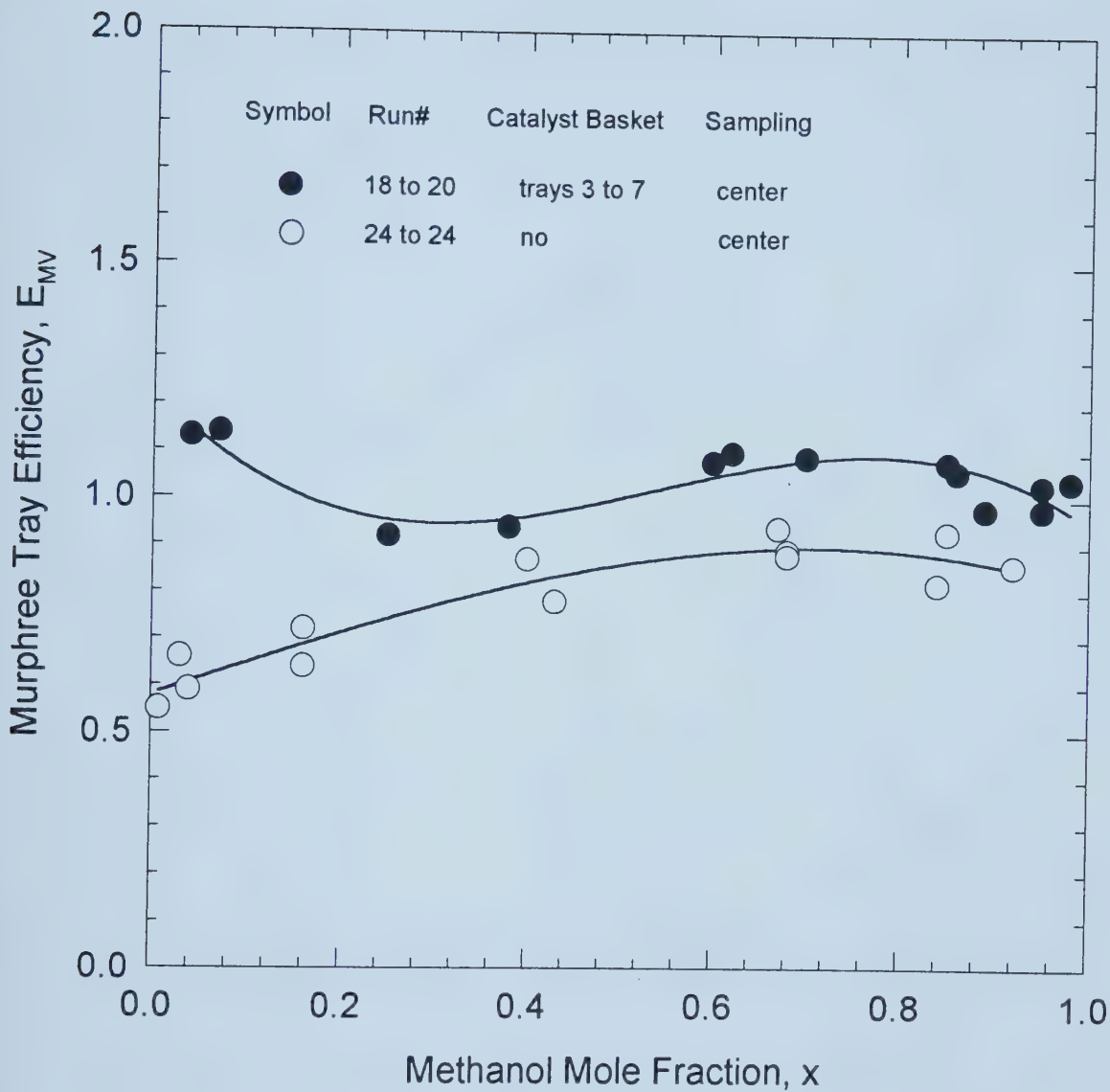


Figure 6-9. Measured Tray Efficiencies with and without Catalyst Units (methanol-water system).





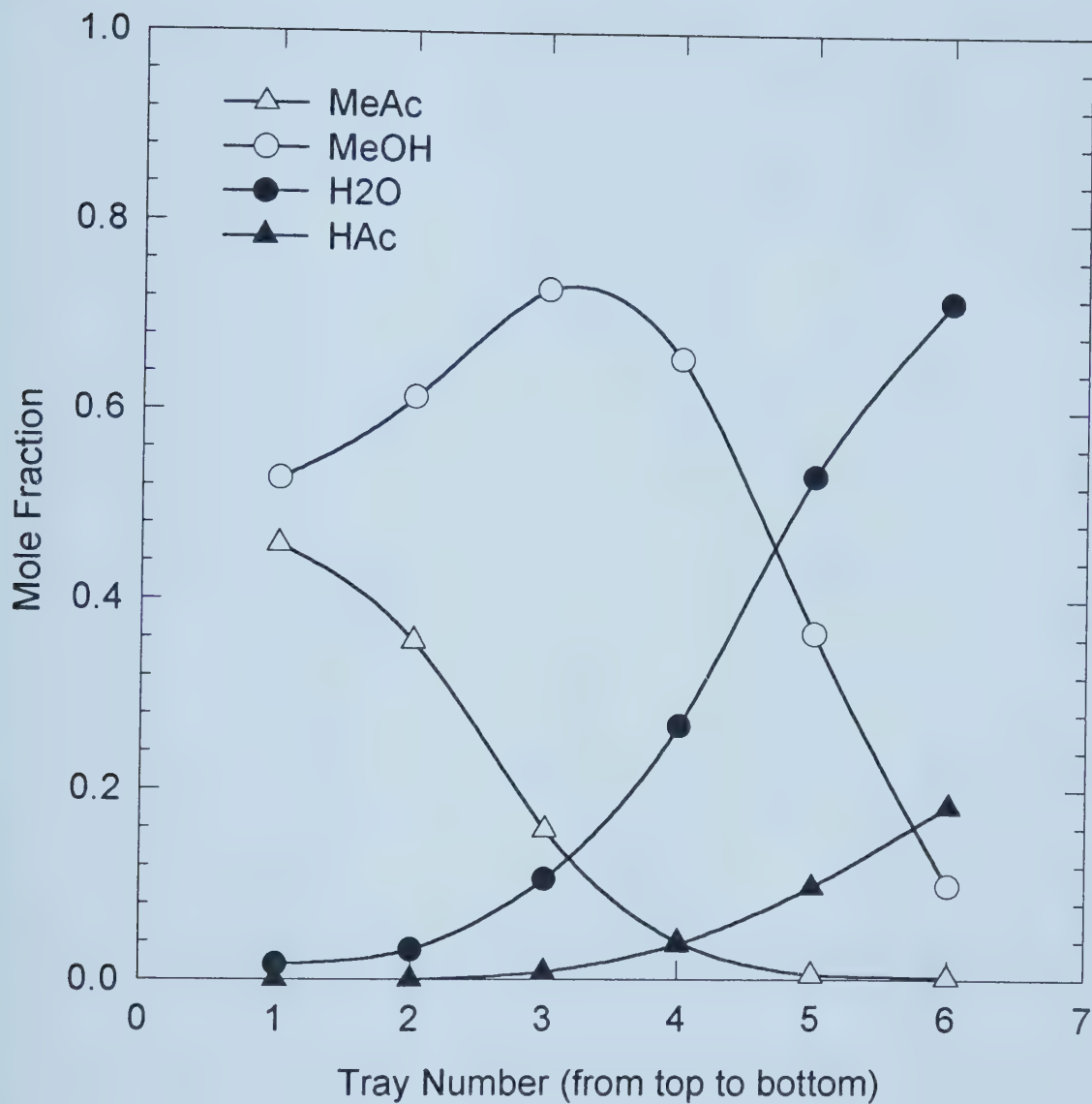


Figure 6-10. Measured Component Composition Profiles.



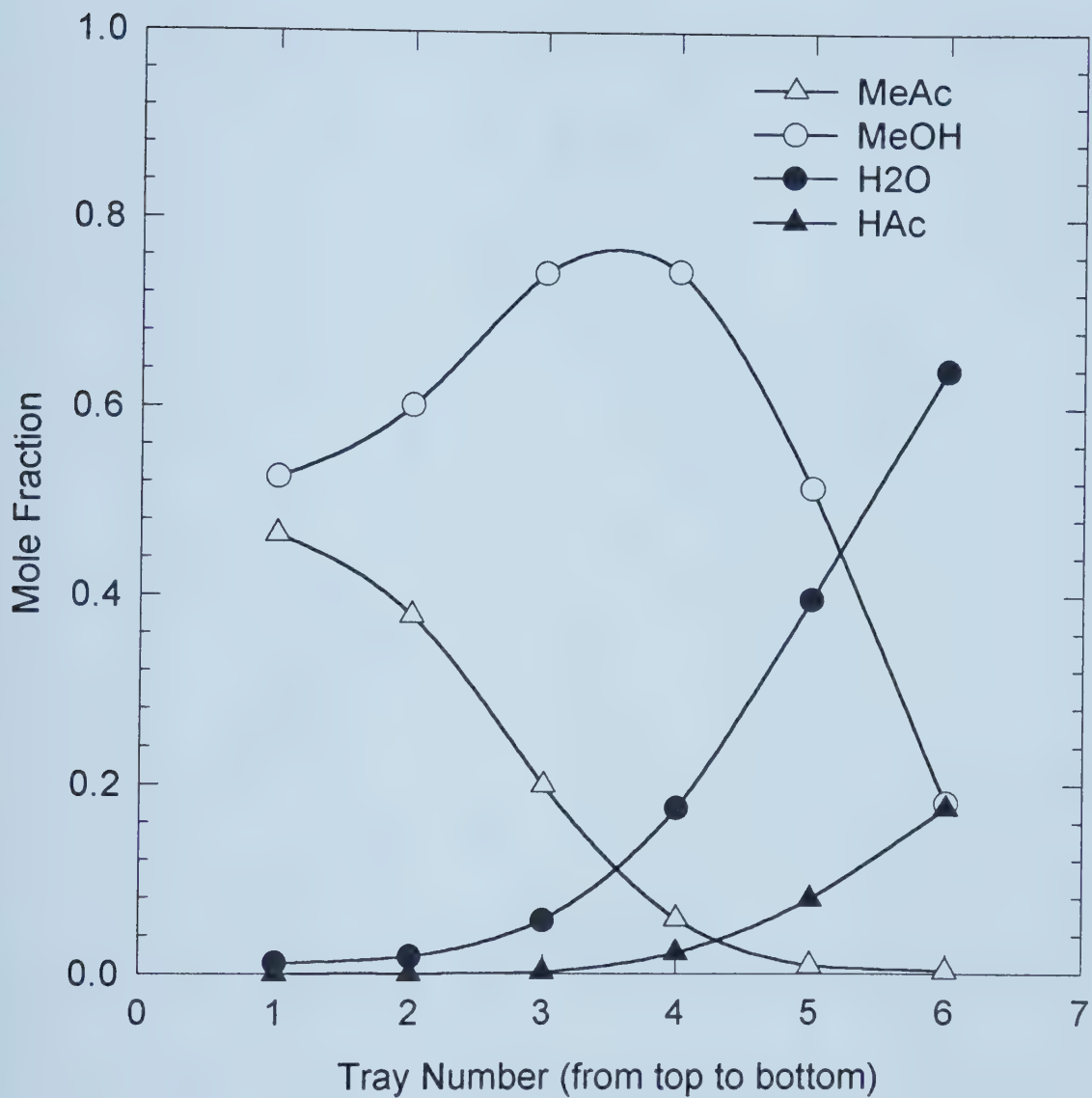


Figure 6-11. Measured Component Composition Profiles.



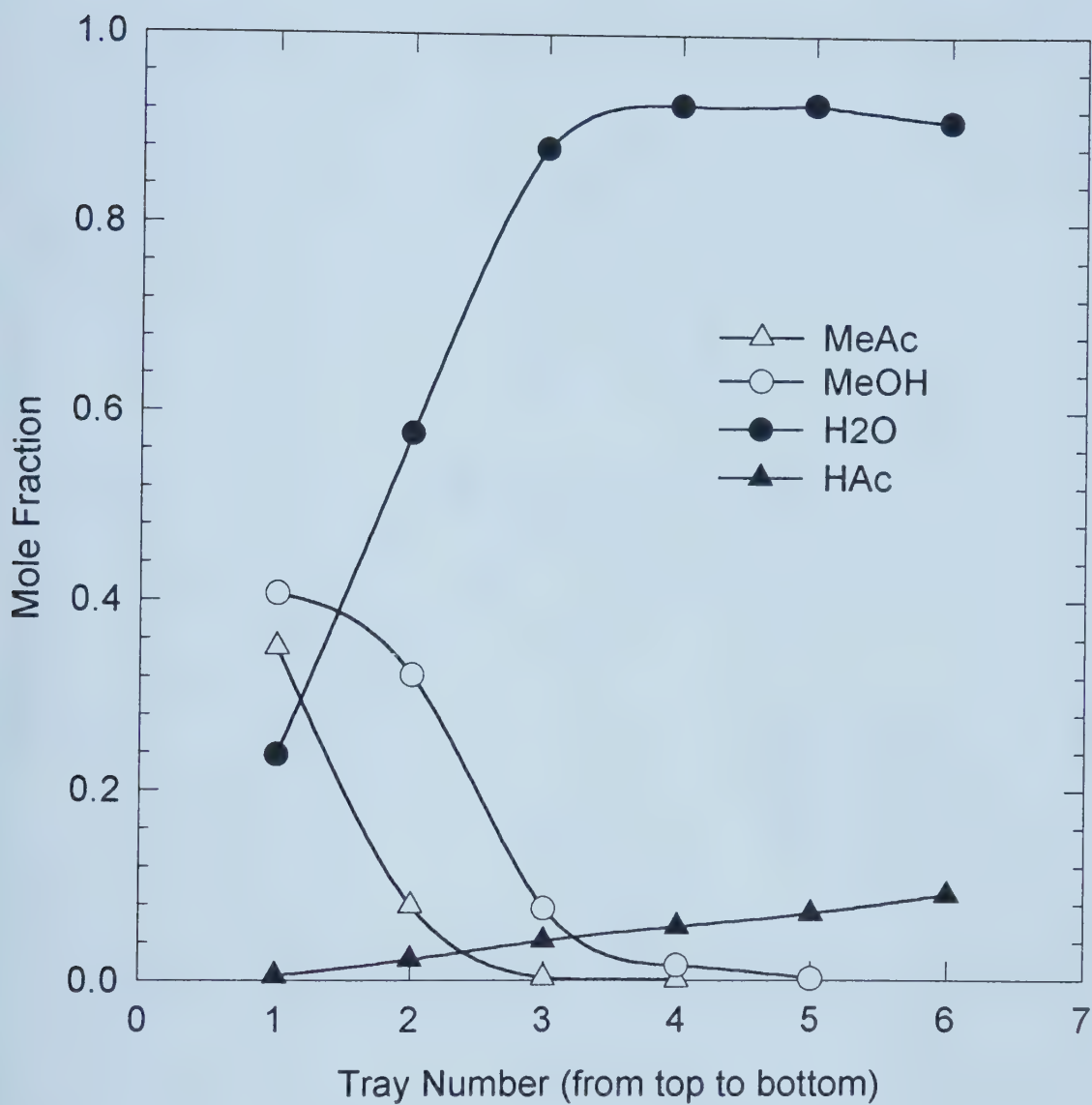


Figure 6-12. Measured Component Composition Profiles.



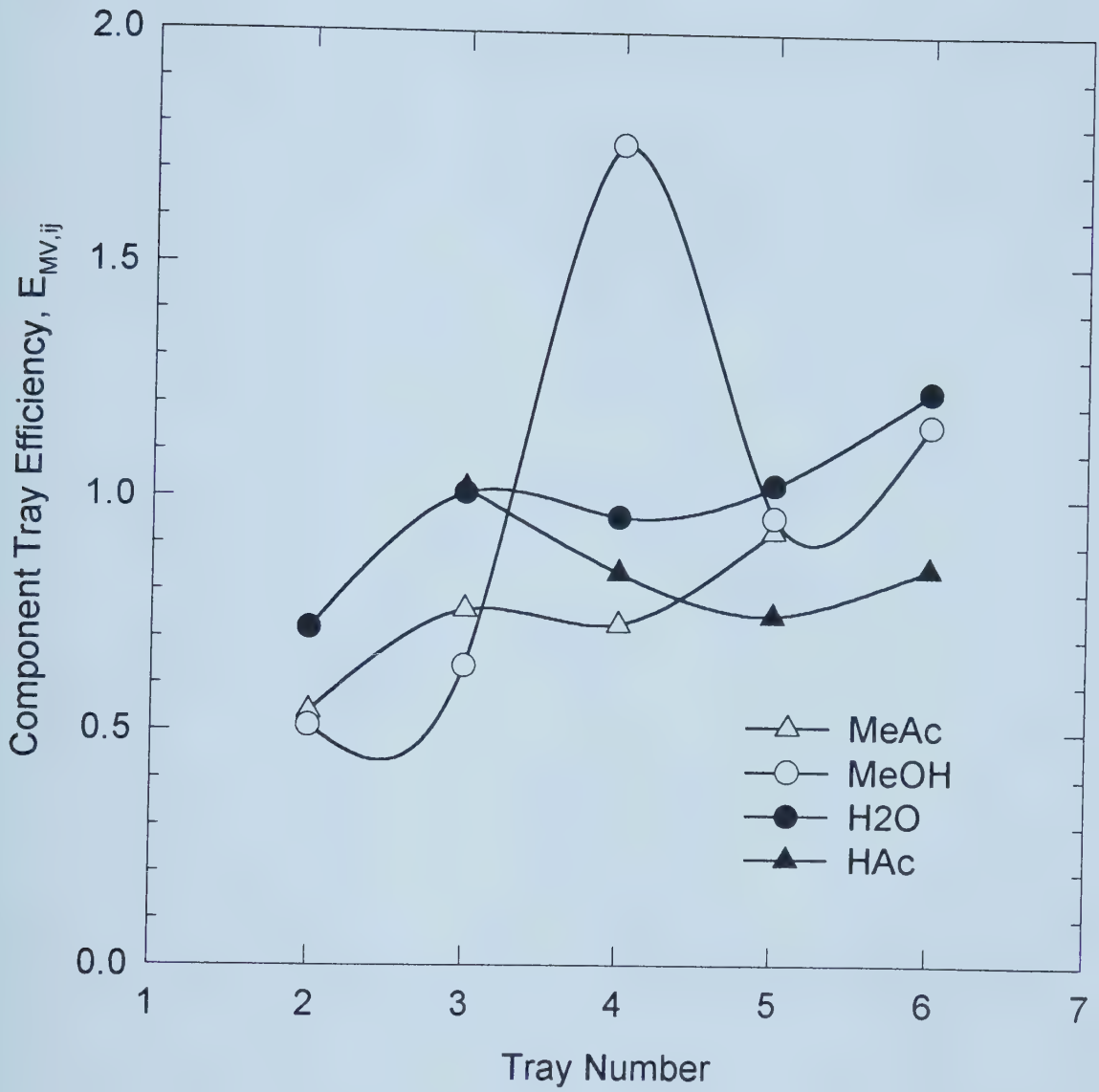


Figure 6-13. Measured Component Tray Efficiencies.





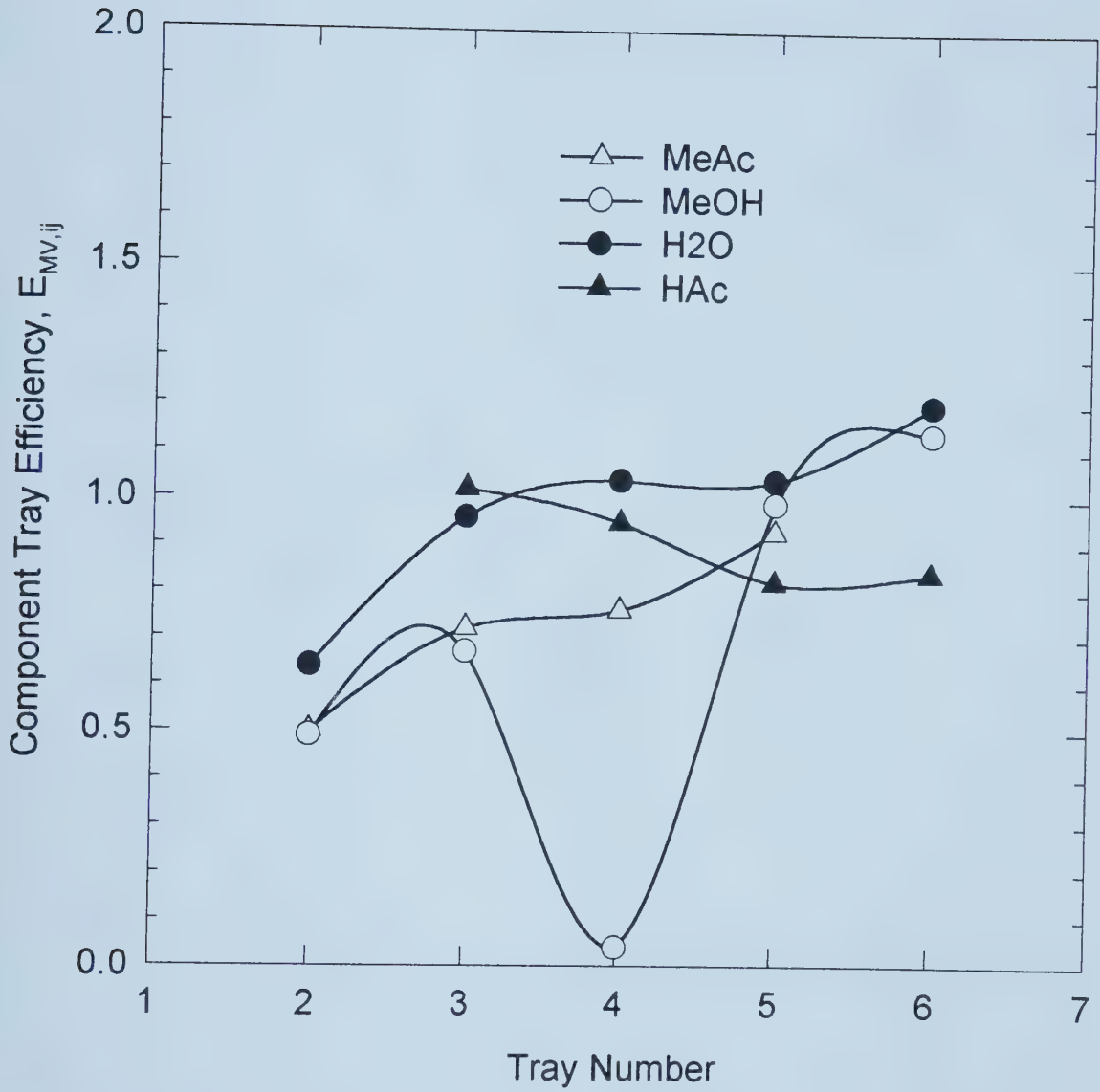


Figure 6-14. Measured Component Tray Efficiencies.



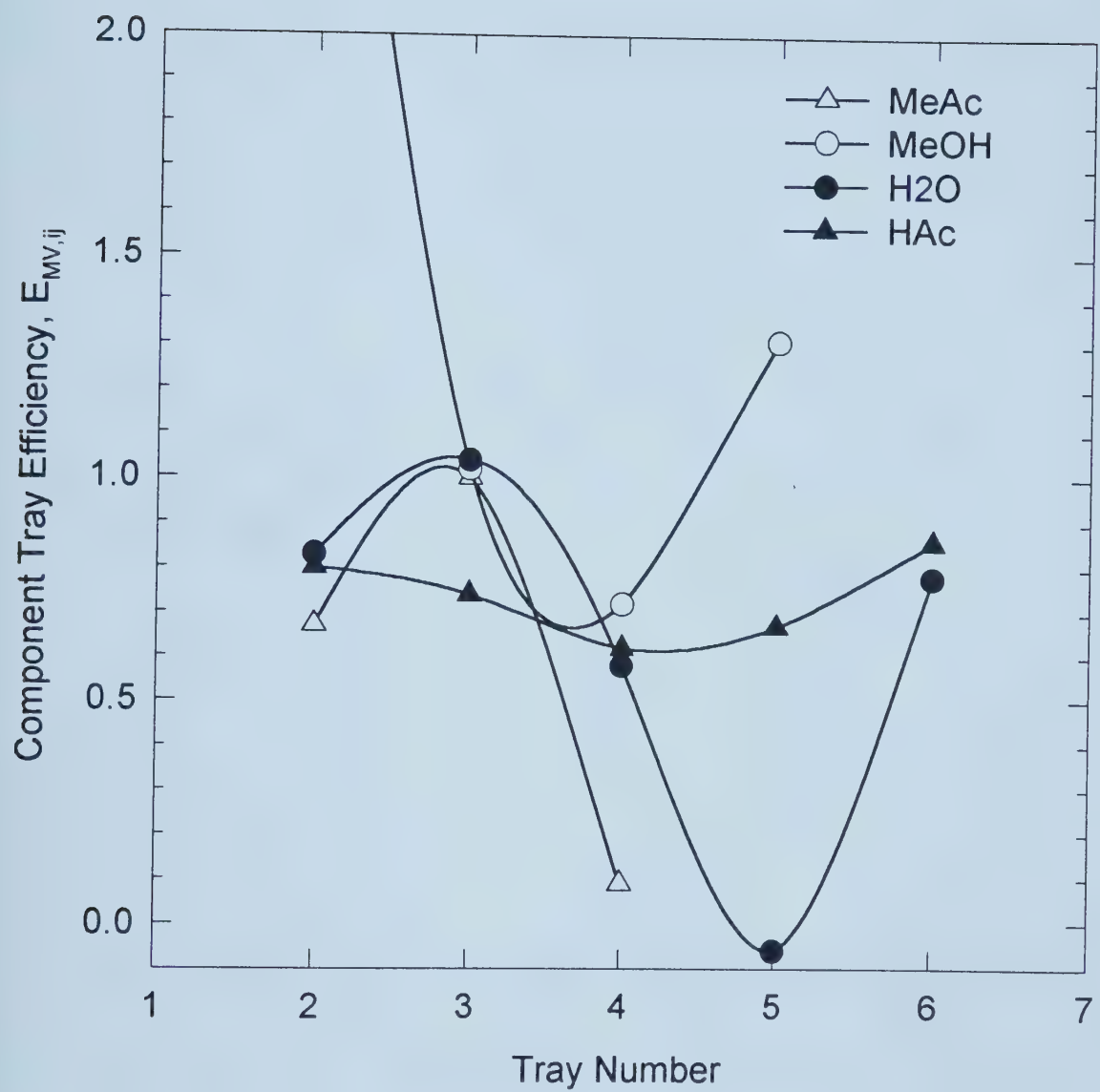


Figure 6-15. Measured Component Tray Efficiencies.



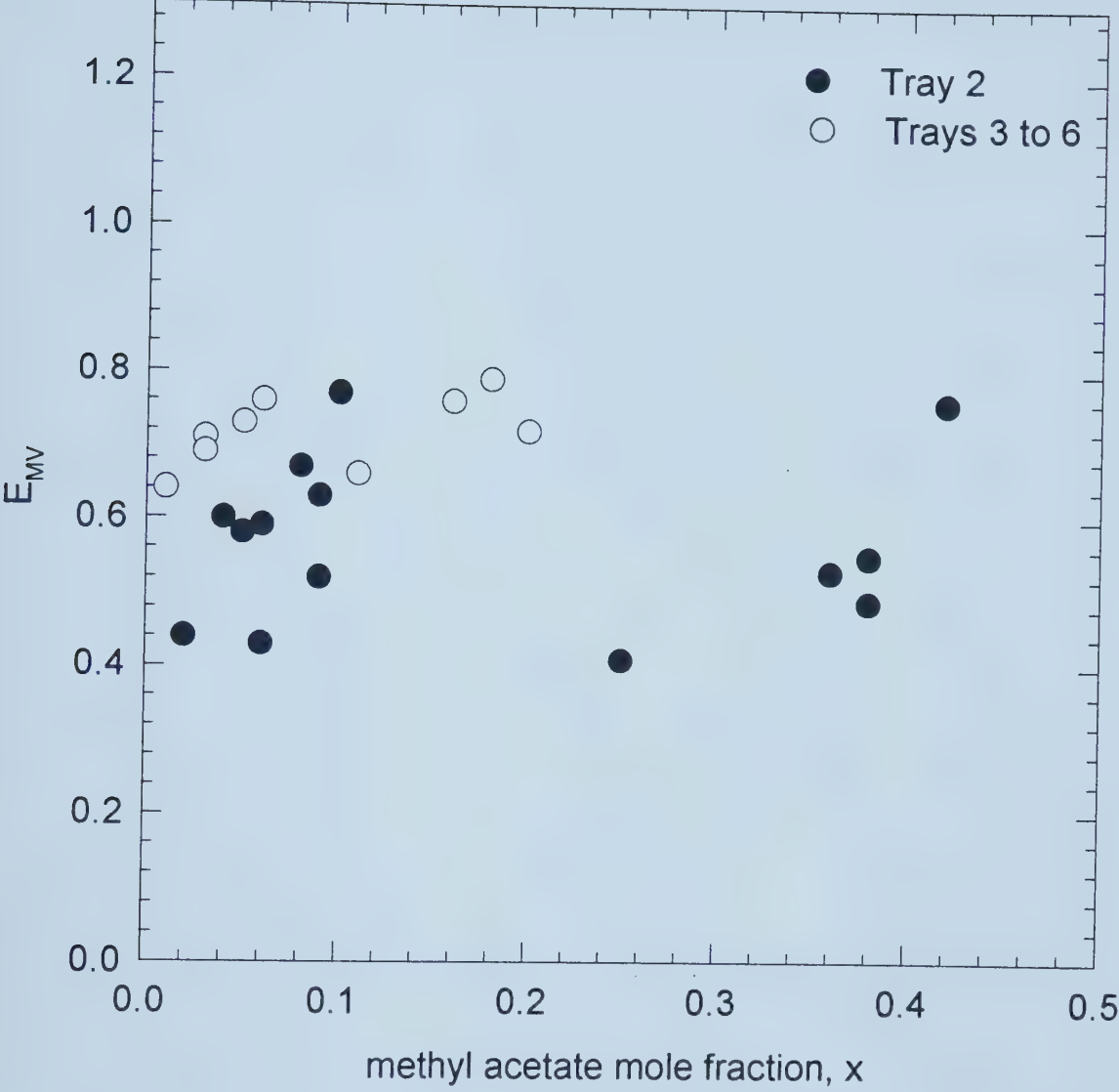


Figure 6-16. Measured Tray Efficiencies for Methyl Acetate.



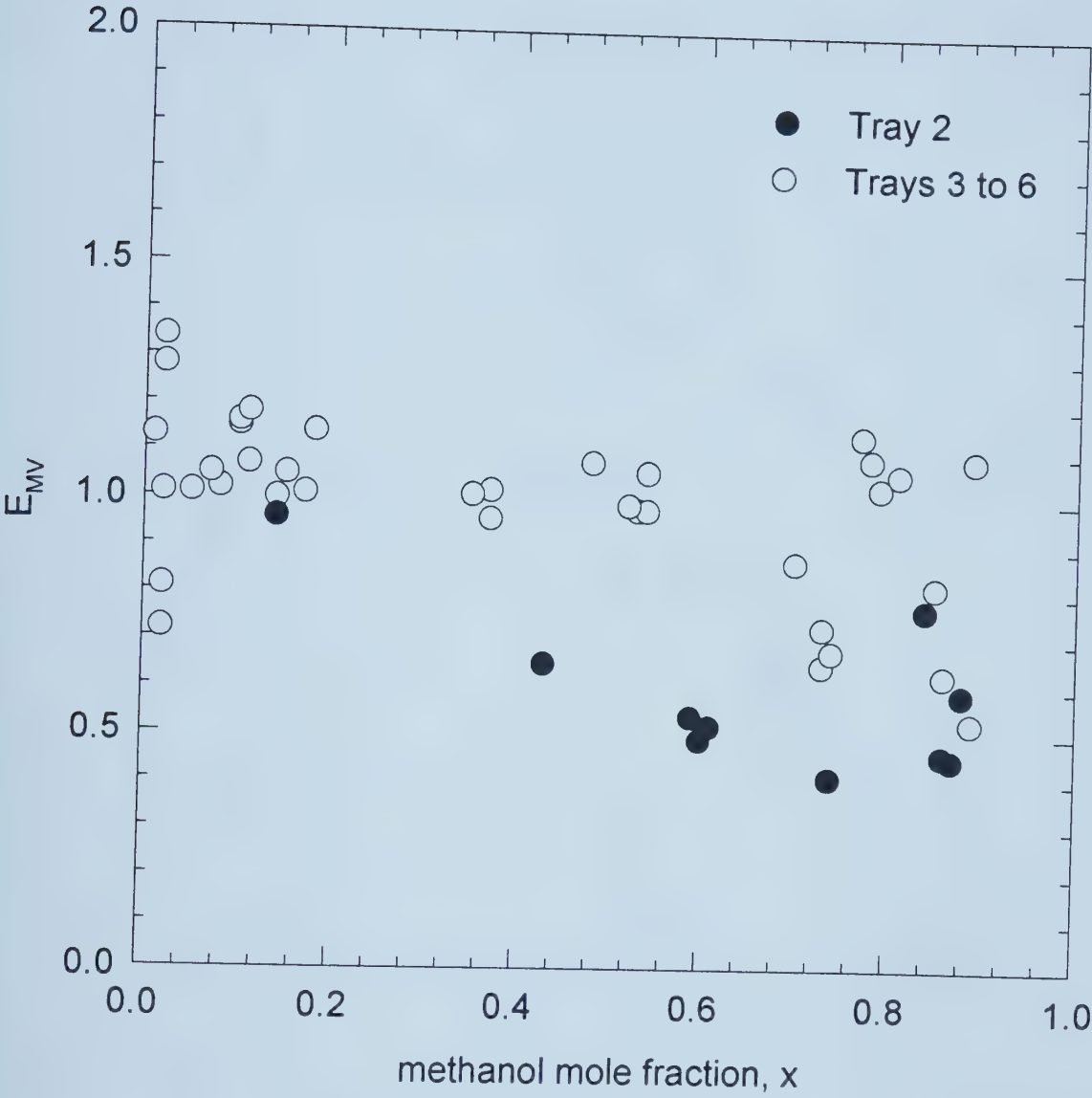


Figure 6-17. Measured Tray Efficiencies for Methanol.





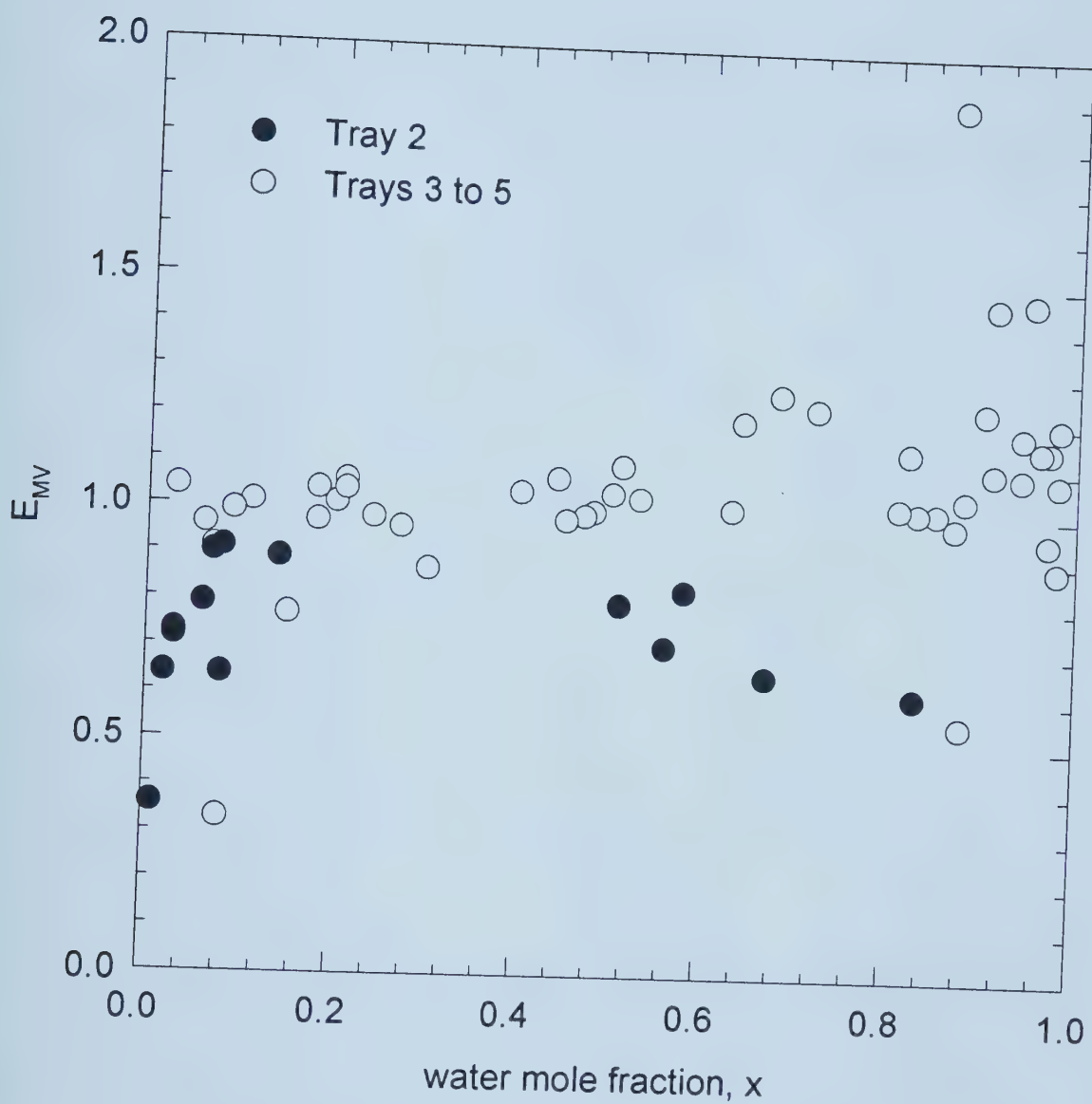


Figure 6-18. Measured Tray Efficiencies for Water.



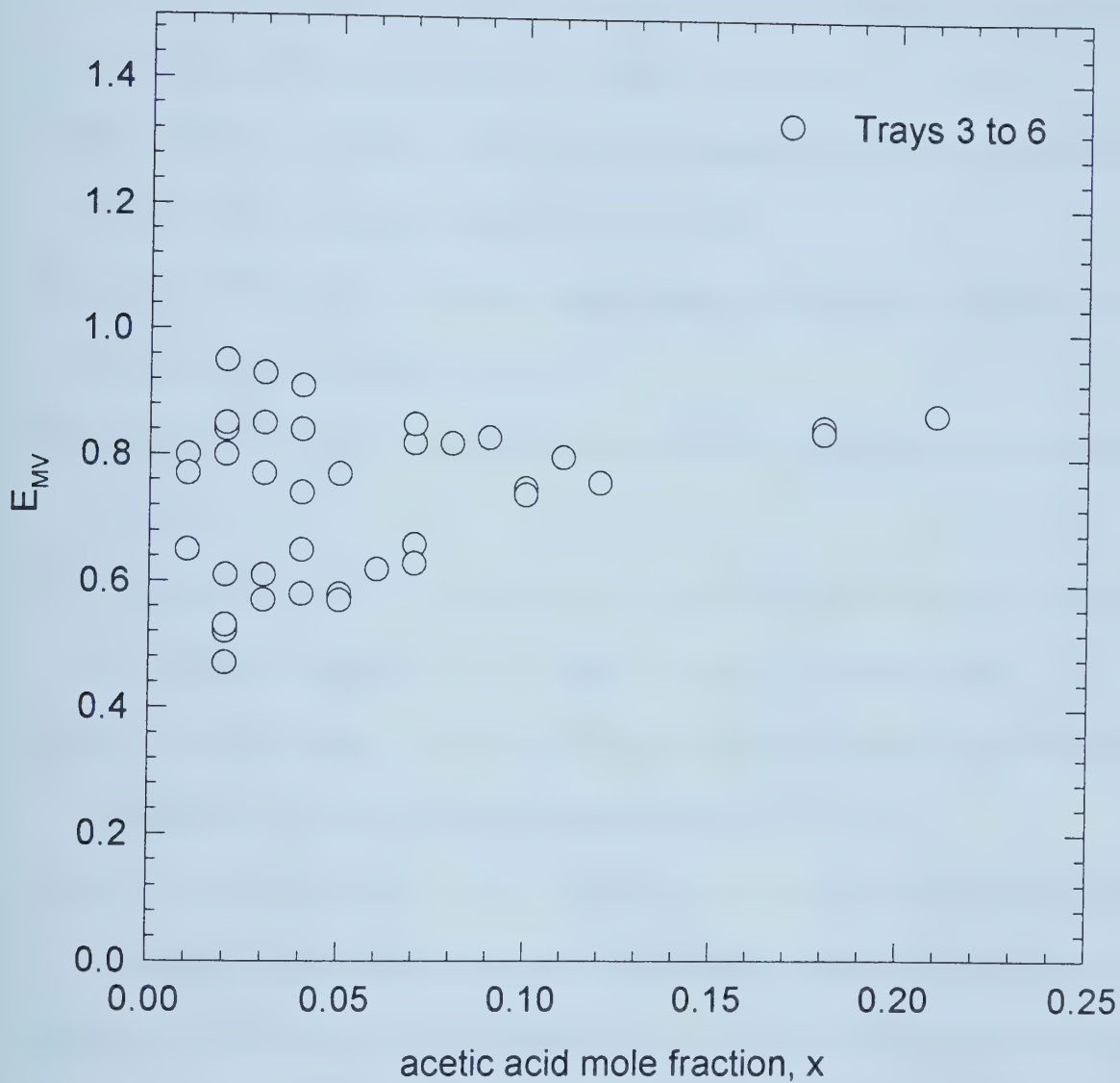


Figure 6-19. Measured Tray Efficiencies for Acetic Acid.



## 6.6 Literature Cited

- Biddulph, M.W., Kalbassi, M.A. and Dribika, M.M. (1988) Multicomponent Efficiencies in Two Types of Distillation Column. *AIChE J.* **34**, 618-625.
- Biddulph, M.W. and Kalbassi, M.A. (1988) Distillation Efficiencies for Methanol/1-Propanol/Water. *Ind. Eng. Chem. Res.* **27**, 2127-2135.
- Biddulph, M.W. (1977a) Deducing Multicomponent Distillation Efficiencies from Industrial Data. *Chem. Eng. J.* **14**, 7-15.
- Biddulph, M.W. (1977b) Tray Efficiency Is Not Constant. *Hydrocarbon Proc.* **56**(10), 145-148.
- Chan, H. and Fair, J.R. (1984) Prediction of Point Efficiencies on Sieve Trays. 2. Multicomponent Systems. *Ind. Eng. Chem. Process Des. Dev.* **23**, 820-827.
- Diener, D.A. and Gerster, J.A. (1968) Point Efficiencies in Distillation of Acetone-Methanol-Water. *Ind. Eng. Chem. Process Des. Dev.* **7**, 339-345.
- Dribika, M.M. and Biddulph, M.W. (1987) Surface Tension Effects on a Large Rectangular Tray with Small Diameter Holes. *Ind. Eng. Chem. Res.* **26**, 1489-1494
- Krishna, R. (1981) An Alternative Linearized Theory of Multicomponent Mass Transfer. *Chem. Eng. Sci.* **36**, 219-222.
- Krishna, R. (1977) A Film Model Analysis of Non-Equimolar Distillation of Multicomponent Mixtures. *Chem. Eng. Sci.* **32**, 1197-1203.
- Krishna, R., Martinez, H.F., Sreedhar, R. and Standart, G.L. (1977) Murphree Point Efficiencies in Multicomponent Systems. *Trans IChemE* **55**, 178-183.



- Krishna, R. and Standart, G.L. (1976) A Multicomponent Film Model Incorporating a General Matrix Method of Solution to the Maxwell-Stefan Equations. *AIChE J.* **22**, 383-389.
- Lockett, M.J. (1986) Distillation Tray Fundamentals. Cambridge University Press.
- Lockett, M.J. and Ahmed, I.S. (1983) Tray and Point Efficiencies from a 0.6 Metre Diameter Distillation Column. *Chem. Eng. Res. Des.* **61**, 110-118.
- Mahendru, H.L. and Hackl, A. (1979) Contribution to the Design of Sieve Trays without Downcomers. *Inst. Chem. Eng. Symp. Ser.* **56**, 3.2/35-47.
- Medina, A.G., McDermott, C. and Ashton, N. (1979) Prediction of Multicomponent Distillation Efficiencies. *Chem. Eng. Sci.* **34**, 861-866.
- Ognisty, T.P. and Sakata, M. (1987) Multicomponent Diffusion: Theory vs. Industrial Data. *Chem. Eng. Prog.* **83**(3), 60-65.
- Rao, D.P., Prem Kumar, R.S., Pandit, P. and Das, T.C.T. (1995) Multicomponent Tray Efficiencies Accounting for Entrainment. *Chem. Eng. J.* **57**, 237-246.
- Simth, L.W. and Taylor, R. (1983) Film Models for Multicomponent Mass Transfer: A Statistical Comparison. *Ind. Eng. Chem. Fundam.* **22**, 97-104.
- Taylor, R. and Smith, L.W. (1982) On Some Explicit Approximate Solutions of the Maxwell-Stefan Equations for the Multicomponent Film Model. *Chem. Eng. Commun.* **14**, 361-370.
- Toor, H.L. (1964a) Prediction of Efficiencies and Mass Transfer on a Stage with Multicomponent Systems. *AIChE J.* **10**, 545-548.
- Toor, H.L. (1957) Diffusion in Three-component Gas Mixtures. *AIChE J.* **3**, 198-207.





- Toor, H.L. (1964b) Solution of the Linearized Equations of Multicomponent Mass Transfer: II. Matrix Methods. *AIChE J.* **10**, 460-465.
- Toor, H.L. (1964c) Solution of the Linearized Equations of Multicomponent Mass Transfer: I. *AIChE J.* **10**, 448-455.
- Vogelpohl, A. (1979) Murphree Efficiencies in Multicomponent Systems. *I. Chem. E. Symposium Series* No. **56**, 2.1/25-2.1/31, Institution of Chemical Engineers, London.
- Xu, Z.P., Afacan, A., and Chuang, K.T. (1994) Efficiency of Dualflow Trays in Distillation. *Can. J. Chem. Eng.* **72**, 607-613.
- Young, G.C. and Weber, J.H. (1972) Murphree Point Efficiencies in Multicomponent Systems. *Ind. Eng. Chem. Process Des. Dev.* **11**, 440-446.
- Zuiderweg, F.J. (1983) Marangoni Effect in Distillation of Alcohol-Water Mixtures. *Chem. Eng. Res. Des.* **61**, 388-390.



## CHAPTER 7. CATALYTIC DISTILLATION —

### EXPERIMENTAL RESULTS

#### 7.1 Introduction

Catalytic distillation is a very complicated process involving almost all the unit operations in chemical engineering, such as catalytic reaction, fluid flow, thermodynamics, mass transfer and staged separations. In the previous chapters fundamental models have been established for the catalytic reaction and vapor-liquid equilibrium. Multicomponent separation efficiencies have been measured under conditions similar to those used in the catalytic distillation. With these fundamental models and efficiency data, and available process simulation software, the catalytic distillation process for removing acetic acid from water can be simulated. However, the simulated results may still need to be verified by experimental results because the process is complex and some assumptions had to be made in the modeling and simulation.

Although catalytic distillation has been a hot topic in the last two decades, published experimental results are very scarce. There are two reasons for this: 1) the experiments are difficult and expensive to carry out so that many people in the academic area are only interested in modeling and computer simulation; 2) the experimental results may have commercial value and so, are kept secret. The latter could be the reason that there are more awarded patents than published journal papers.

Of the published results, most are about etherification and esterification using ion exchange resins as catalysts.



For etherification, the most important process is the production of oxygenates, which are used as a blending stock for the production of high octane and unleaded gasoline. Bravo et al. (1993) presented experimental data regarding production of *tert*-amyl methyl ether (TAME) from a catalytic distillation pilot plant. The experiments were carried out in a 0.15 m diameter column, 11 m high. Ion exchange resin Amberlite XAD was used as a catalyst. The detailed column internals were not reported. They found that the amount of methanol in the feed was the most significant variable with respect to operation, conversion and recovery. Flato and Hoffmann (1992) reported test results from a 53 mm diameter fixed bed reaction column for manufacturing methyl *tert*-butyl ether (MTBE). The packing elements were Raschig rings (6×6 mm) manufactured from strongly acidic macroreticular ion exchange resins. The swelling behavior is a great disadvantage of the sulphonated rings; they should never be stored under dry conditions because the first contact with liquid may cause them to break (Flato and Hoffmann, 1992). Hao et al. (1995) also studied the MTBE process in a 100 mm pilot catalytic distillation column with specially designed column internals. Over 90% conversion of isobutene can be obtained in the column.

The esterification processes mostly relate to carboxylic acid and alcohol or olefins. Saha and Sharma (1996) carried out the esterification of formic acid with cyclohexene in a 25.4 mm diameter column packed with an acidic ion exchange resin. The effect of variables such as feed flow rate, molar ratio of reactants, concentration of formic acid, and feed location, was studied. Stevanovic et al. (1992) studied batch distillation with esterification of acetic acid and ethanol in a 33 mm column packed with ion exchanger



Amberlite-120. They noted high column pressure drop because of the low void fraction of the packed bed.

Some other catalytic distillation processes are shown in Table 1-1.

No experimental studies have been reported on the removal of dilute acetic acid from water by catalytic distillation. In this chapter, experimental results will be reported for the catalytic distillation process of acetic acid esterification with methanol over an ion exchange catalyst – Amberlyst 15. The effect of feed rate, feed ratio of methanol to acetic acid, feed location, top product rate, boil-up rate, reflux ratio, etc., will be discussed.

## 7.2 Experimental

The catalytic distillation experiments were carried out in the same column as for tray efficiency measurements. The test flowsheet is similar to that shown in Figure 6-1 with two feed and two product lines opened for continuous operation. Same dualflow trays were used with the dimensions shown in Table 6-1. The column contained seven identical dualflow trays spaced 216 mm apart. Catalyst units as shown in Figure 5-4 were placed above trays 3 to 7 (counting from top to bottom) in the column. In some runs, tray 2 was also installed with a catalyst unit to study its effect on the catalytic distillation process. The catalyst baskets were filled with the same catalyst, Amberlyst 15, used in the kinetics measurement. Average loading of the catalyst for each catalyst basket was about 270 grams (wet). The column was insulated with 60 mm thick fiberglass to minimize heat loss. The insulation could be removed for the observation of column operation and the measurement of froth height.





Each tray was equipped with the same thermocouple and liquid sampler as used in the tray efficiency measurement (see Figure 6-2). A 3 mL syringe was used to withdraw the liquid sample through the tubing. The tray pressure drop was measured with a U-type manometer with water as an indicator.

The column was operated continuously with one feed of pure methanol, one feed of acetic acid-water mixture to the column and two products withdrawn from the column top and bottom.

An Opto-22 system interfaced with a personal computer was used for the process control and data acquisition. There are seven automatic control loops: two for feed pumps, one for the top product pump, two for liquid levels/pumping rates (column bottom/bottom product rate and condenser bottom/reflux rate), one for the steam rate, and one for the cooling water rate (column pressure). The liquid mixtures in the two feeds and the reflux were heated and controlled with three temperature controllers. The temperatures for the steam inlet and outlet, the cooling water inlet and outlet, the column bottom, the condenser bottom and each tray were displayed and recorded by the computer.

The column was started with total reflux operation. When steam, reflux and cooling water rates reached the set points, two feed and two product pumps were started. The operation set points were reached usually within 30 minutes. Steady-state column operation (constant temperature profile and flow rates) could usually be achieved in two to five hours depending on the feed and reflux rates. Then, nine liquid samples (seven from each tray, one from the condenser bottom and one from the column bottom) were taken



and analyzed by a gas chromatograph. Other hydraulic data were recorded, including tray pressure drop and visual froth heights.

In the column, liquid and vapor pass countercurrently through the tray and the catalyst unit alternately. Separation occurs mainly on the dualflow trays by the direct contact of up flow vapor and down flow liquid and the formation of froth for mass transfer. Reaction can be neglected because there was no catalyst present on the trays. The catalytic liquid phase reaction takes place in the catalyst unit placed between two trays, by the liquid mixture from the top tray directly contacting the solid catalyst in the catalyst basket. After passing through the fixed catalyst bed, the reaction effluent drops from the bottom of the catalyst unit to the next tray for separation.

The water from a reverse osmosis (RO) system was used for preparing the acetic acid-water mixture. With the RO system, about 99% dissolved solids were removed from city tap water. Industrial grade acetic acid (99.5 % glacial, supplied by Vanwater&Rogers, B.C.) and methanol (99.7 methanol assay, also supplied by Vanwater&Rogers, B.C.) were used for the preparation of the acetic acid-water feed and methanol feed. The catalyst, Amberlyst 15 (wet), was supplied by Rohm and Haas and its characteristic data are listed in Table 2-1.

### **7.3 Results And Discussion**

In the experiments, a total of 33 runs were carried out to investigate the effect of various parameters on the removal of acetic acid from water. The ranges of the various parameters are summarized as follows:



- catalyst units placed: above trays 3 to 7, or above trays 2 to 7
- feed rate of methanol (pure): 5.0 to 30.6 g/min
- feed rate of acetic acid-water mixture: 140 to 220 g/min
- acetic acid concentration in the feed: 2.6 to 9.9 wt%
- mole ratio of methanol to acetic acid in feeds: 1.0 to 8.3
- top product rate: 5.3 to 50.1 g/min
- reflux ratio: 3.5 to 78.1
- vapor F-factor (column top): 0.44 to 0.87
- acetic acid conversion: 20 to 60%

Table 7-1 summarizes the experimental results from the 33 runs. Most runs were conducted with 140 g/min feed of the acetic acid-water mixture containing 5 wt% of the acid. The methanol feed rate was usually in excess. With the feed of the acetic acid-water mixture above tray 2, no acid was detected from the top vapor condensate. The top product contains mostly methanol and methyl acetate as well as a small amount of water. The bottom stream is water and unreacted acetic acid. The overall mass balance is within 2%. For most runs, over 50% of acetic acid was removed in the 1.5 metre high column. All the parameters listed above have an effect on the removal of acetic acid. Some important effects of the operating parameters on the column performance are discussed as follows.



### 7.3.1 *Effect of the Catalyst*

Figure 7-1 shows concentration profiles of the four components (methyl acetate, methanol, water and acetic acid) from two runs with and without catalyst (Runs #9 and #33). For Run #9, catalyst baskets filled with Amberlyst 15 were placed above trays 3 to 7. In Run #33 the catalyst, Amberlyst 15, was replaced with inert glass beads as used in Chapter 6. The other operating conditions for the two runs were all the same as was listed in the figure. The feed acetic acid concentrations were 5 wt% for both runs.

It should be noted that the middle data points in the concentration profiles are important for analyzing and understanding the catalytic distillation process while the end data points show the outcome of the operations. The data points for acetic acid at the right end (corresponding to the column bottom) are especially important because they show the concentration of acetic acid in the bottom stream. By comparing it with the concentration of acetic acid in the feed mixture, one may find how much acetic acid was removed.

From Figure 7-1 it can be seen that under similar operating conditions, the concentration of reaction product, methyl acetate, at the column top is 19.5 wt% for Run #9 with catalyst applied while only 0.46 wt% for Run #33 without catalyst used. It is not surprising that the conversion rate of acetic acid is low without the catalyst. As shown in Chapter 2, the esterification of acetic acid with methanol is very slow without the presence of a catalyst. The concentration profiles of methanol and water are similar for the two runs because their concentrations are much higher than methyl acetate and acetic acid, and changes in concentration due to the reaction are not significant. For Run #33, the





concentration of acetic acid increases down the column because it is the least volatile component. At the column bottom, the acetic acid concentration is close to that in the feed of the acetic acid-water mixture (5 wt%) due to the fact that only 1.2 wt% of acetic acid was converted to methyl acetate and the bottom product rate is close to the feed rate of the acetic acid-water mixture. However, for Run #9 the concentration of acetic acid decreases significantly from tray 2 to 6 due to the fact that with the catalyst applied, the conversion rate of acetic acid is higher than the separation rate in this region. From tray 6 to the column bottom, the acetic acid concentration bounces back because of the sharp decrease in methanol concentration resulting in a low reaction rate. The average acetic acid concentration in the column for Run #9 is significantly lower than Run #33, with only 1.97 wt% of acetic acid left in the column bottoms.

Figure 7-1 also shows that the concentration profiles change significantly at the two feed locations. The acetic acid-water mixture was fed above tray 2 and the methanol above tray 6. Once the acid-water mixture was fed onto tray 2 and mixed with the liquid on that tray, the acetic acid concentration decreases immediately from 5 wt% to about 2 wt%. No acetic acid was detected above tray 2 because all the other three components are more volatile than acetic acid. Methanol concentration decreases and water concentration increases quite significantly at tray 2 because of the introduction of the acetic acid-water mixture. At tray 6, it can be seen that both methanol and acetic acid concentrations change greatly. Methanol is more volatile than acetic acid and water and tends to flow upward. Therefore, the methanol concentration on tray 7 (below tray 6) is significantly lower than



tray 6. On the contrary, the acetic acid concentration starts to bounce back at tray 7 because of the low methanol concentration and low reaction rate.

Conversion of acetic acid to methyl acetate occurs mainly between the two feed trays due to the relatively high concentration of both reactants, methanol and acetic acid.

### ***7.3.2 Effect of the Catalyst Zone***

Because the acetic acid esterification is reversible, it is not sensible to place the catalyst units on the trays where the concentrations of the reaction products in the liquid phase are relatively high compared with the reactant concentrations. There exists an optimum reaction zone for each specific column design under certain operating conditions. In our case, the concentration of methyl acetate in the liquid phase below tray 1 is usually low compared with those of the reactants due to: 1) the low concentration of the reactant, acetic acid, therefore a low reaction rate; 2) the high volatility of methyl acetate so that once it is produced in the liquid phase it tends to pass to the vapor phase. On the first tray, the methyl acetate concentration is usually high but the acetic acid concentration is very low as discussed in Section 7.1. Therefore, the reverse reaction in the liquid mixture may dominate on this tray and the catalyst unit should not be placed under tray 1 (above tray 2). The reflux liquid mixture from the condenser to tray 1 contains an even higher concentration of methyl acetate and a lower concentration of acetic acid, and therefore the catalyst unit should not be placed above tray 1. For the rest of the trays, forward reaction dominates and the catalyst should be applied.



From Figure 7-1 it can be seen that the methanol concentration drops greatly below the methanol feed tray. Therefore, the reaction rate on these trays could be much lower than the main reaction zone between the two feeds. However, the net reaction will always be in the right direction and catalyst should be used for those trays to maximize the reaction zone. In an industrial column, the reboiler may have a large liquid hold-up and the conversion rate can be greatly increased by putting catalyst there.

Based on the above analysis, the catalyst units were placed on trays 3 to 7 but not on the top two trays in most of the tests.

### ***7.3.3 Effect of the Boil-up Rate***

With the same feed, same top product rates and the same column configurations, an increase in boil-up rate results in an increase in reflux rate and vapor/liquid loading in the column. As shown by Xu et al. (1994), dualflow tray efficiency increases with an increase in vapor/liquid loading due to the significant effect of the loading on froth height. This is one of the characteristics of dualflow trays which is different from the conventional downcomer trays. Better separation of the liquid mixture can be achieved with the increase in reflux rate at the expense of higher energy consumption. Hence, it can be concluded that an increase in boil-up rate will facilitate the separation of liquid mixtures. This is desirable from a separation point of view.

In a catalytic distillation column, the overall column performance is determined not only by separation efficiency but also by reaction rate. High separation efficiency does not mean better column performance for catalytic distillation. The best performance is



achieved by matching separation efficiency with reaction rate. As shown in Chapter 2, the reaction rate of acetic acid esterification is quite low even with the use of a catalyst. The separation of reaction products may not be a controlling factor because of the high volatility of methyl acetate.

In the existing catalytic distillation column, the reaction rate is determined by the reactant concentrations. Figures 7-2 and 7-3 show the effect of boil-up rates (reflux rate) on the component concentration profiles in the column. For these three runs, reaction occurs mainly on trays 3 to 6 with catalyst present and relatively high concentrations of both reactants, methanol and acetic acid. On tray 7, the reaction rate is low because of the low concentration of methanol. From the figures it can be seen that in the reaction/separation zone (trays 3 to 6), both methanol and acetic acid concentrations, therefore the reaction rate, decrease with the increase in boil-up (reflux) rate. Figure 7-3 clearly shows that higher boil-up (reflux) rate results in a higher concentration of acetic acid at the column bottom with less acetic acid removed.

The above results indicate that the catalytic distillation process is not a simple combination of a catalytic reaction and separation. In the design of column internals and choosing the operating conditions one has to consider both reaction and separation as well as their interaction.

#### ***7.3.4 Effect of the Top Product Rate***

With the same feed and boil-up rates, a change in the top product rate changes the reflux rate (reflux ratio). The effect of the top product rate on the reflux rate and bottom







product rate is insignificant because they are much higher than the top rate. The most important effect of changing the top product rate is on the methanol distribution in the column, which in turn affects the reaction rate.

When the top product rate is reduced the reflux ratio increases. Therefore, the concentration of the more volatile component, methyl acetate, at the column top increases and methanol concentration decreases. This indicates that more methanol may stay in the column. Also, more unreacted methanol will return to the column through reflux when the top product rate is reduced. Therefore, the concentration of methanol in the column may increase with the decrease in top product rate, resulting in a higher reaction rate.

Figures 7-4 and 7-5 show two pairs of operations with different feed ratios of methanol to acetic acid. With a low ratio of methanol to acetic acid (1:1, mole) in the feeds as shown in Figure 7-4, the effect of the top product rate on methanol concentration and acid removal is significant. When the top product rate is reduced from 7.7 to 5.8 g/min, the methanol concentration in the column increases dramatically and the acetic acid conversion rate increases from 19.8% to 38%. Although methyl acetate concentration also increases in the column, it has little effect on the acid removal because its concentration is still much lower than methanol and acetic acid in the main reaction zone (trays 3 to 6). As discussed above, at the column top the methyl acetate concentration increases and methanol concentration decreases when the top product rate is reduced. When the ratio of methanol to acetic acid is high (8:1 by mole) as shown in Figure 7-5, the effect of the top product rate on acid removal is very small because there is a large amount of excess methanol and its concentration profile remains fairly constant in the main reaction zone.



### ***7.3.5 Effect of the Feed Ratio of Methanol to Acetic Acid***

It is obvious that the higher the ratio of methanol to acetic acid, the more acetic acid will be removed due to the higher reaction rate. As shown in Figure 7-6, the acid removal increases from 19.8 to 52.1% when the methanol/acetic acid ratio is increased from 1 to 3.7 due to the significant increase in methanol concentration in the main reaction zone from trays 3 to 6. However, as shown in Figure 7-7, when the ratio increases from 3.7 to 8.3, there is little effect on acid removal. Although the methanol concentration is lower when the methanol/acid ratio is equal to 3.7, there is still a large amount of excess and is still much higher than the acetic acid concentration. Also, the acetic acid concentration in the column is higher for this run. Therefore, the reaction rate in the column may be similar for these two runs.

### ***7.3.6 Effect of the Feed Location***

As with conventional distillation columns, feed location is a very important parameter affecting the performance of catalytic distillation columns. Determination of feed locations is dependent on many factors such as product specifications, volatility of components and vapor-liquid equilibrium behavior.

For the acetic acid esterification, the acetic acid-water mixture has a higher boiling point than methanol. The acid should be fed at the upper portion of the column and methanol at the lower portion so that methanol can contact acetic acid countercurrently. The feed location of the acetic acid-water mixture is determined by the top product specifications. If low water content is desired, the feed location should move down the



column to increase the rectifying section. Similarly, if low methanol concentration is desired for the bottom product, the feed location of methanol should move up to increase the stripping section. Because of the short column used in our tests, feed locations cannot be moved up or down very much.

Figure 7-8 shows the effect of feed locations on component concentration profiles and the removal of acetic acid. The first test was conducted with the feed of the acetic acid-water mixture to tray 2 and methanol to tray 6. Next, the feed of the acetic acid-water mixture was moved down to tray 3 while the methanol feed remained at tray 6. Last, the feed of the acid-water mixture was moved back to tray 2 but the methanol feed was moved up to tray 5. From the figure it can be seen that the change of methanol feed location has little effect on the acid removal and all the component concentration profiles are similar to the first test. However, when the feed position of the acid-water mixture was moved down one tray, the component concentration profiles change significantly and acid removal is reduced from 52.5 to 40.1%.

The reason for this dramatic effect is that when the acid feed was moved down from tray 2 to tray 3, one very effective catalytic reaction section (the catalyst unit between tray 2 and tray 3) with a high concentration of the reactant, methanol, was lost. This catalyst unit collects the reaction mixture from tray 2 but no acetic acid was detected on that tray as shown in Figure 7-8. In fact, a reverse reaction may occur in that catalyst unit because of the very low acetic acid concentration.



## 7.4 Conclusions

Catalytic distillation experiments were conducted in a 100 mm diameter column installed with seven dualflow trays and five catalyst units for the removal of dilute acetic acid from water. Methanol was introduced to the column to react with acetic acid. An ion exchange catalyst (Amberlyst 15) was used to accelerate the reaction.

The acid esterification was the rate-controlling step in the process due to the low concentration of acetic acid. It was found that the main reaction zone between the two feed trays has a relatively high concentration of both reactants, methanol and acetic acid, and the reaction takes place mostly in that part of the column. The effects of various parameters such as feed composition, reflux rate, top product rate, and feed location, on the acid removal were investigated. It was found that the reflux rate, the top product rate and the acid-water feed location are important operating variables.

When the feed contains 2.5 to 9.9 wt% of acetic acid in water, more than 50 wt% of acetic acid can be converted to methyl acetate in the 1.5 metre high column.





Table 7-1. Summary of Catalytic Distillation Data

Run#	MeOH Feed g/min	HAc Feed g/min	HAc Conc. wt%	M/H <sup>a</sup> mole Ratio	Catal. /Feed <sup>b</sup>	Top g/min	Bottom g/min	Reflux g/min	Top Product Composition, wt%				Mass Balanc %	HAc Conv. %
									H <sub>2</sub> O	MeOH	MeAc	HAc, T/B		
1	30	140	4.91	8.2	2-7/2-6	36	133	398.2	10.9	77	10.5	0//2.89 <sup>c</sup>	-0.59	44.1
2	30	140	4.91	8.2	2-7/2-6	35.9	133	310	9.81	77.5	11.5	0//2.67	-0.68	48
3	30	140	5.01	8.0	2-7/2-6	36.4	133	223.3	10.6	76.9	11.1	0//2.64	-0.34	50
4	30	140	5.01	8.0	2-7/2-6	50.1	120	176.2	39.1	51	5.3	0.6//3.81		30.9
5	30	140	4.82	8.3	3-7/2-6	36.1	134.2	304.7	10.1	77.2	11.3	0//2.42	0.18	51.9
6	30	140	4.82	8.3	3-7/2-6	36.3	133	225.4	10.5	76.2	12.2	0//2.30	-0.41	54.6
7	30	140	4.82	8.3	3-7/2-6	36.3	133	182.5	11.5	75.1	12.2	0//2.32	-0.41	54.2
8	30	140	4.82	8.3	3-7/2-6	27.58	139.7	263.5	7.9	75.6	16.6	0//2.03	-1.6	57.9
9	30	140	5.01	8.0	3-7/2-6	23.3	145.6	281.6	7.04	73.9	19.5	0//1.97	-0.65	59.2
10	30	140	5.07	7.9	3-7/2-6	16.9	151.5	323.9	6.4	69.2	25.4	0//1.99	-0.92	57.6
11	30	140	5.07	7.9	3-7/2-6	23.3	145.6	238.8	8.2	72.2	19.9	0//2.05	-0.65	57.9
12	30	140	5.07	7.9	3-7/2-6	23	144	340	6.2	74.6	19.9	0//2.13	-1.75	56.7
13	23.2	140	4.93	6.3	3-7/2-6	16.68	146	313.6	6.5	67.6	27.1	0//1.89		60.1
14	13.5	140	4.93	3.7	3-7/2-6	16.9	136	301	7.2	67.5	26.3	0//2.10		58.7
15	5	180	5.01	1.0	3-7/2-6	7.72	175.8	238.3	20.6	51.4	27.3	0//4.12	-0.8	19.8
16	23.2	180	4.87	5.0	3-7/2-6	16.67	184.2	325.4	7.43	61.9	32.1	0//2.25	-1.1	52.8
17	23	220	4.87	4.0	3-7/2-6	16.67	227.2	327.9	7.91	56.4	37.5	0//2.47	0.36	47.5
18	5	180	4.96	1.1	3-7/2-6	5.78	175.3	451.6	6.36	34.8	62.5	0//3.15	-2.1	38
19	30.6	140	5.02	8.2	3-7/2-6	16.72	155.7	322.9	6.31	68.2	26.6	0//2.58	1.067	54.4
20	23	140	5.02	6.1	3-7/2-6	16.62	146.7	319.2	6.29	67.6	27.3	0//2.27	0.196	52.7
21	13.3	140	5.02	3.5	3-7/2-6	11.62	140.7	355.6	6.04	57.6	38.5	0//2.30	-0.639	54
22	30.6	140	5.01	8.2	3-7/3-6	16.55	156.3	335.4	2.83	74.7	23.9	0//2.37	1.32	47.1
23	13.5	140	5.01	3.6	3-7/3-6	16.52	136.3	291.7	5.05	75	20.8	0//3.08	-0.44	40.1
24	30.5	140	4.92	8.3	3-7/2-5	16.84	153.4	313.8	6.74	67.3	27	0//2.14	-0.15	52.3
25	13.5	140	4.92	3.7	3-7/2-5	16.82	135.5	291.2	7.28	67.6	26	0//2.44	-0.77	52.1
26	30.4	140	4.94	8.2	3-7/2-6	22.89	145.1	331.9	6.53	74.3	20.8	0//2.09	-1.4	56.1
27	30.4	140	4.94	8.2	3-7/2-6	22.94	144.7	282.6	7.27	73	20.2	0//2.09	-1.63	56.2
28	30.4	140	4.94	8.2	3-7/2-6	23.15	144.3	225	8.08	72.2	20.1	0//2.13	-1.74	55.5
29	27.5	140	9.92	3.7	3-7/2-6	34.4	135.8	278.9	8.07	65.6	27.3	0//4.85	1.59	52.6
30	27.5	140	9.92	3.7	3-7/2-6	17.54	153.5	351.1	5.35	46.5	50.5	0//4.64	2.11	48.7
31	7	140	2.55	3.7	3-7/2-6	8.48	136.2	283.1	8.12	69.9	22.5	0//1.34	-1.58	48.9
32	7	140	2.55	3.7	3-7/2-6	5.26	139.5	339.3	6.39	61.1	34.3	0//1.25	-1.54	51.3
33	30.5	140	5.11	8.0	No/2-6	23.3	145.6	268.8	8.41	89.9	0.46	0//4.85	-0.94	1.21

<sup>a</sup> M/H - methanol/acetic acid<sup>b</sup> Catal/Feed - catalyst units, tray no. - tray no./feed location, tray no. - tray no.<sup>c</sup> top acetic acid concentration//bottom acetic acid concentration



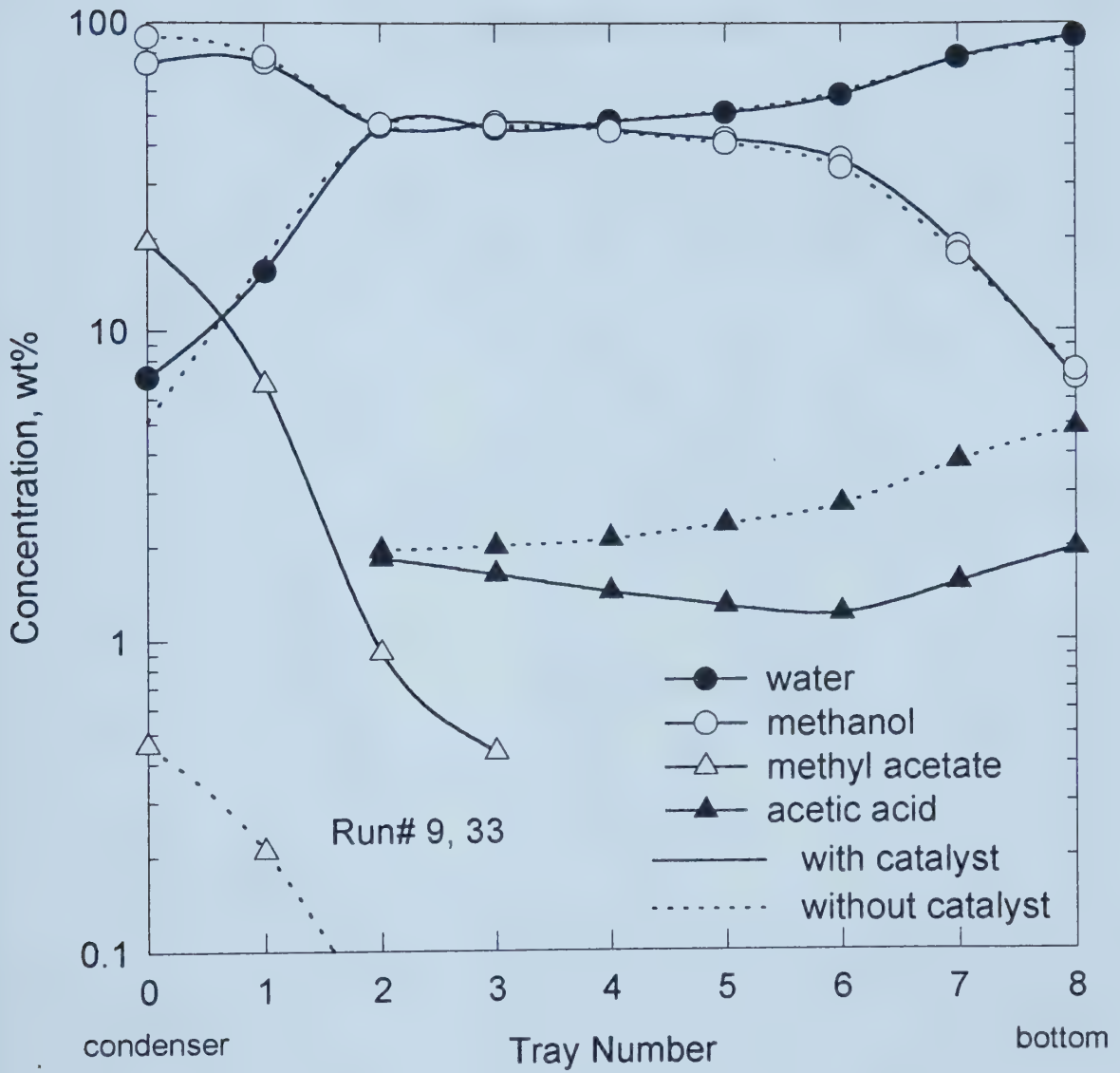


Figure 7-1. Effect of Catalyst. Feed: MeOH, 30 g/min; HAc-Water, 140 g/min, 5

wt% of HAc Top product rate: 23.3 g/min



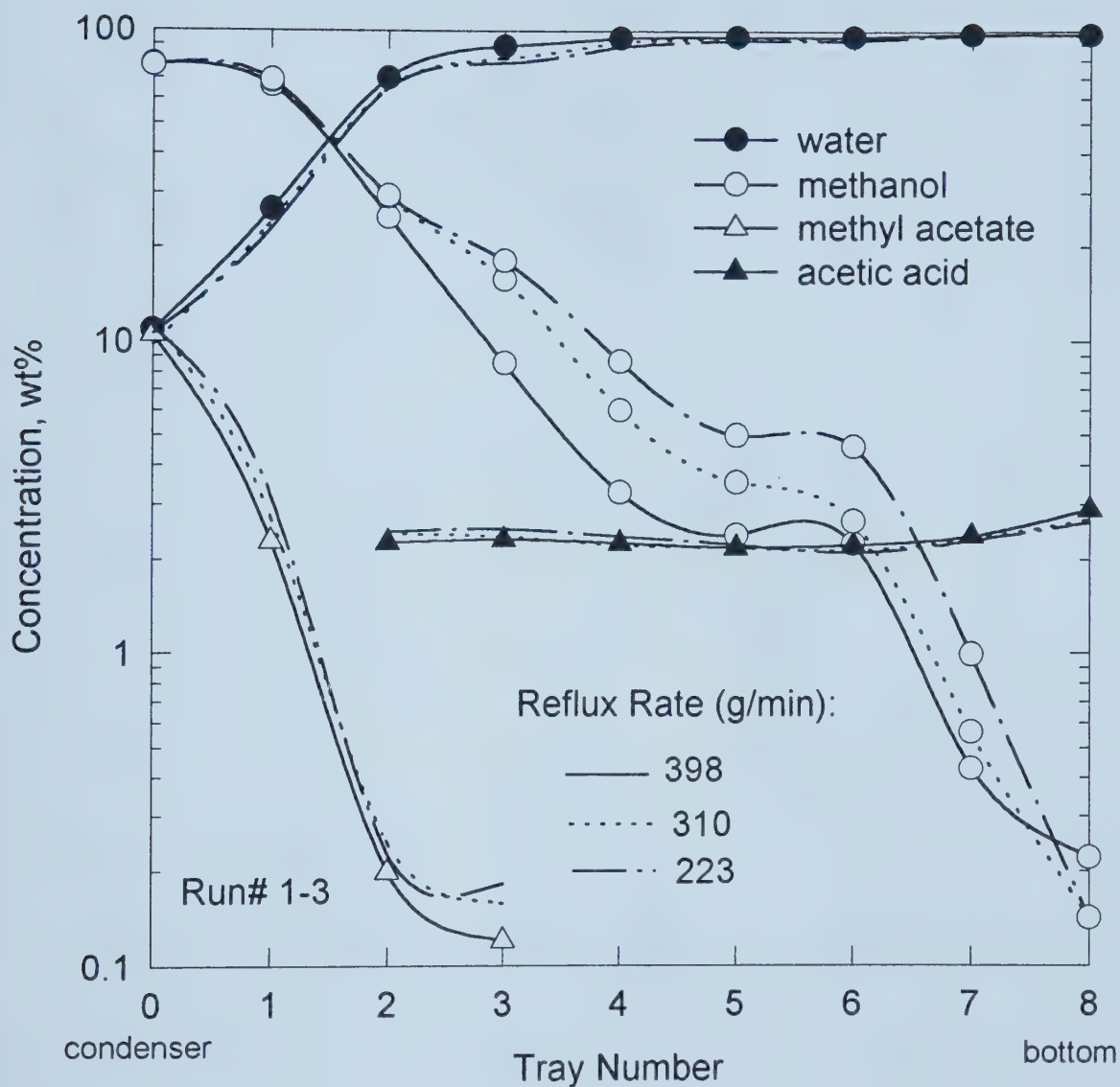


Figure 7-2. Effect of Boil-up Rate (Reflux Rate). Feed: MeOH, 30 g/min; HAc-Water, 140 g/min, 5 wt% of HAc Top product rate: 36 g/min



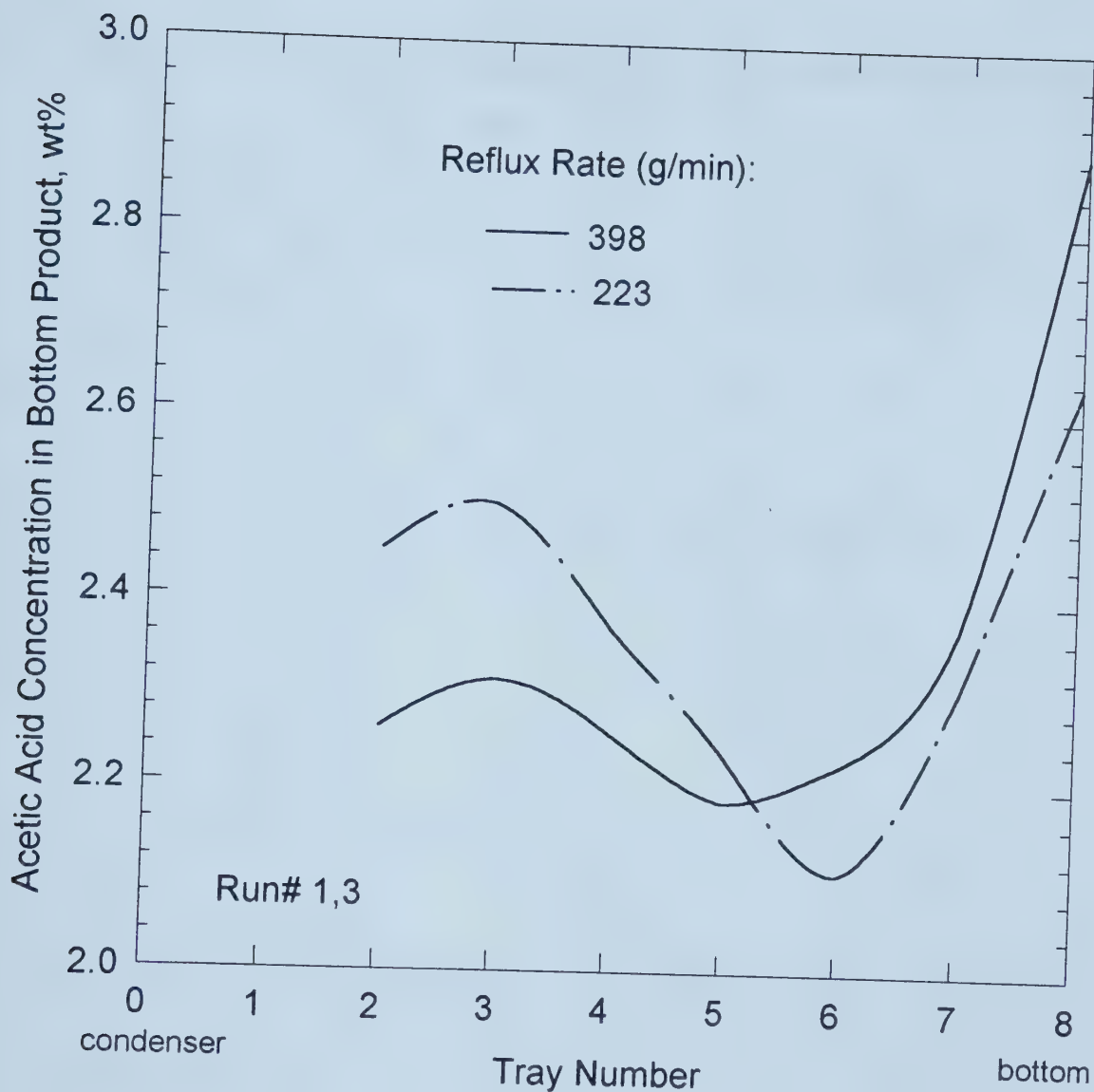


Figure 7-3. Effect of Boil-up Rate (Reflux Rate). Feed: MeOH, 30 g/min; HAc-Water, 140 g/min, 5 wt% of HAc Top product rate: 36 g/min





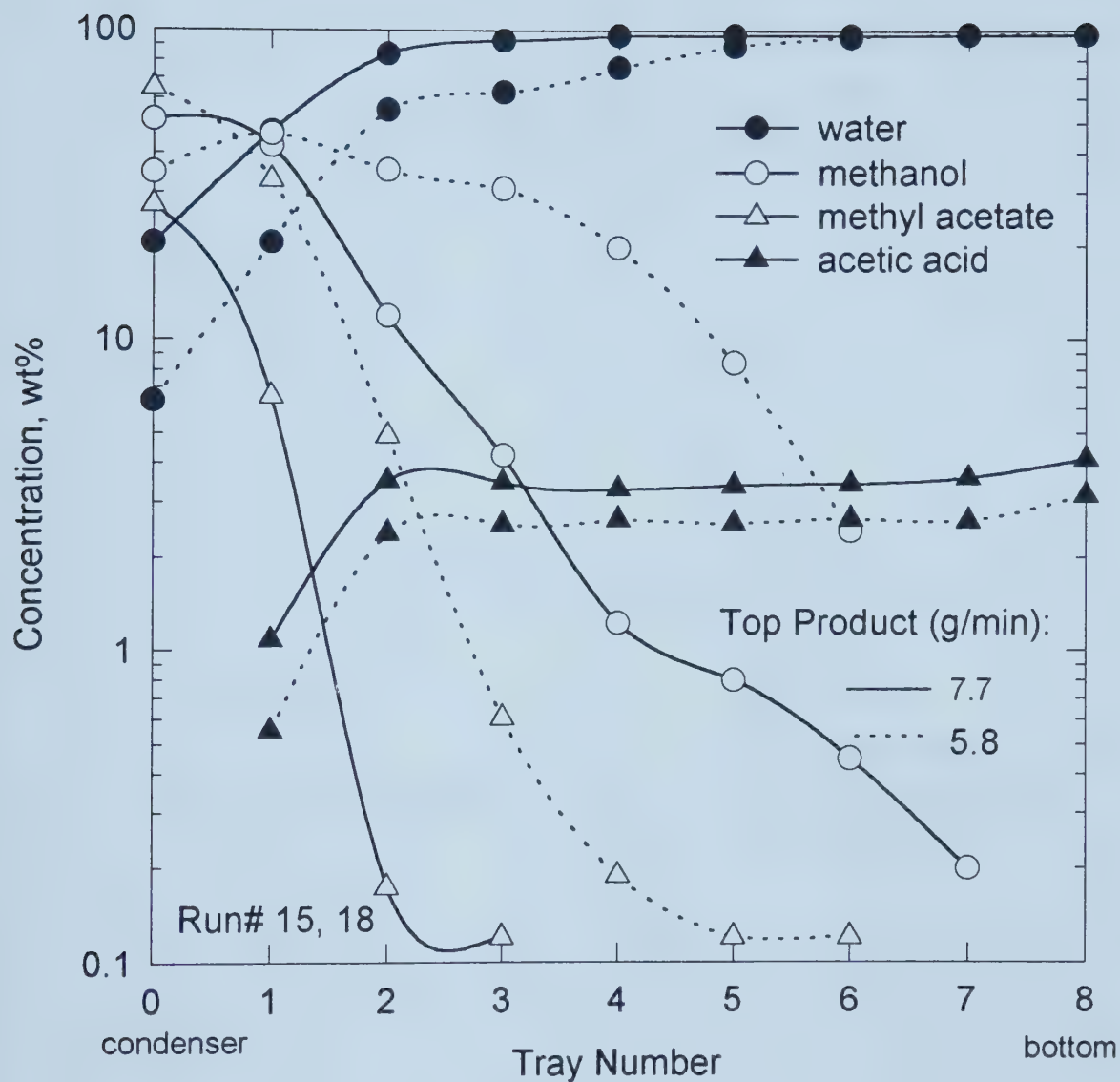


Figure 7-4. Effect of Top Product Rate. Feed: MeOH, 5 g/min; HAc-water, 180 g/min, 5 wt% of HAc



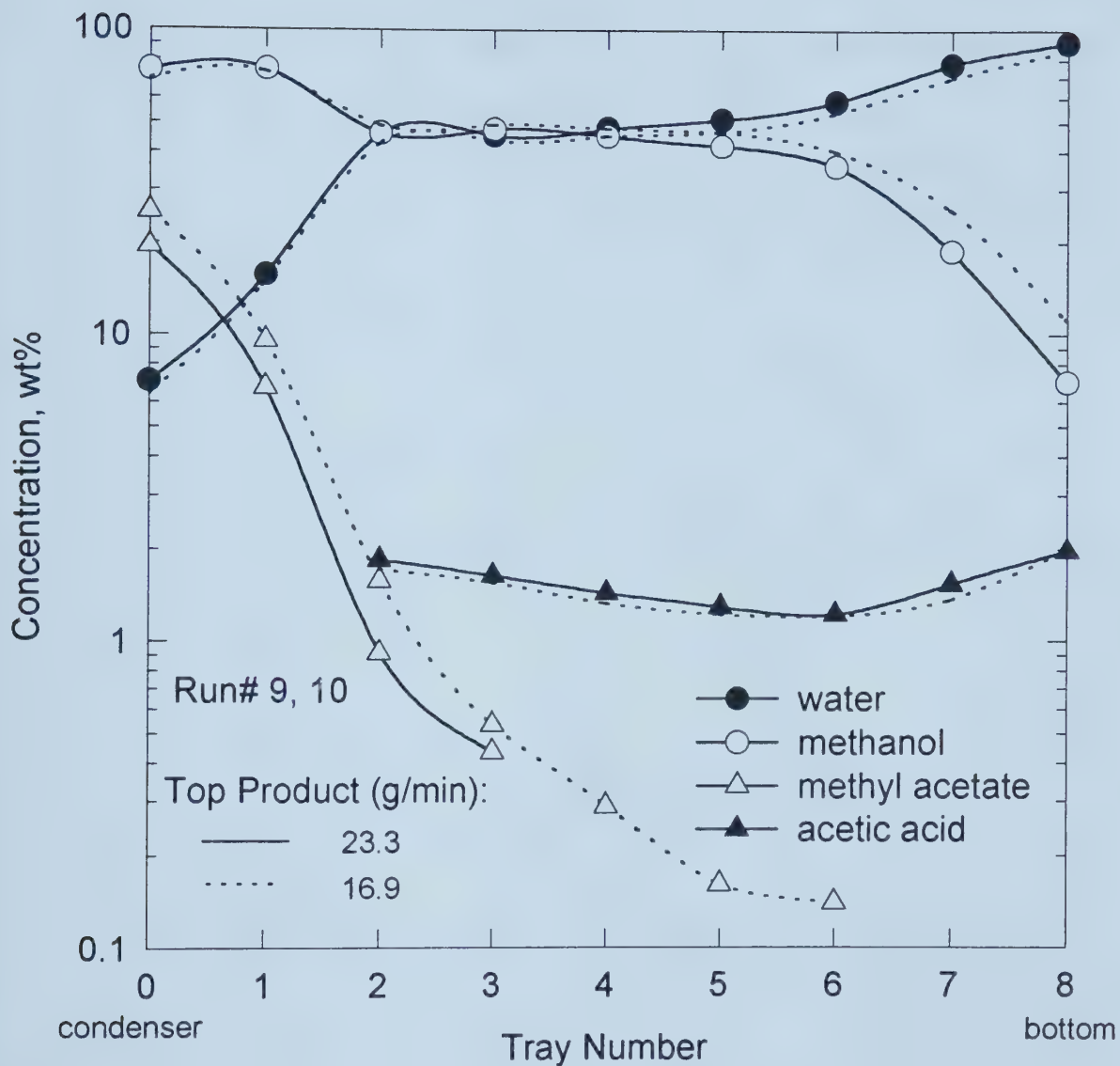


Figure 7-5. Effect of Top Product Rate. Feed: MeOH, 30 g/min; HAc-water, 140 g/min, 5 wt% of HAc



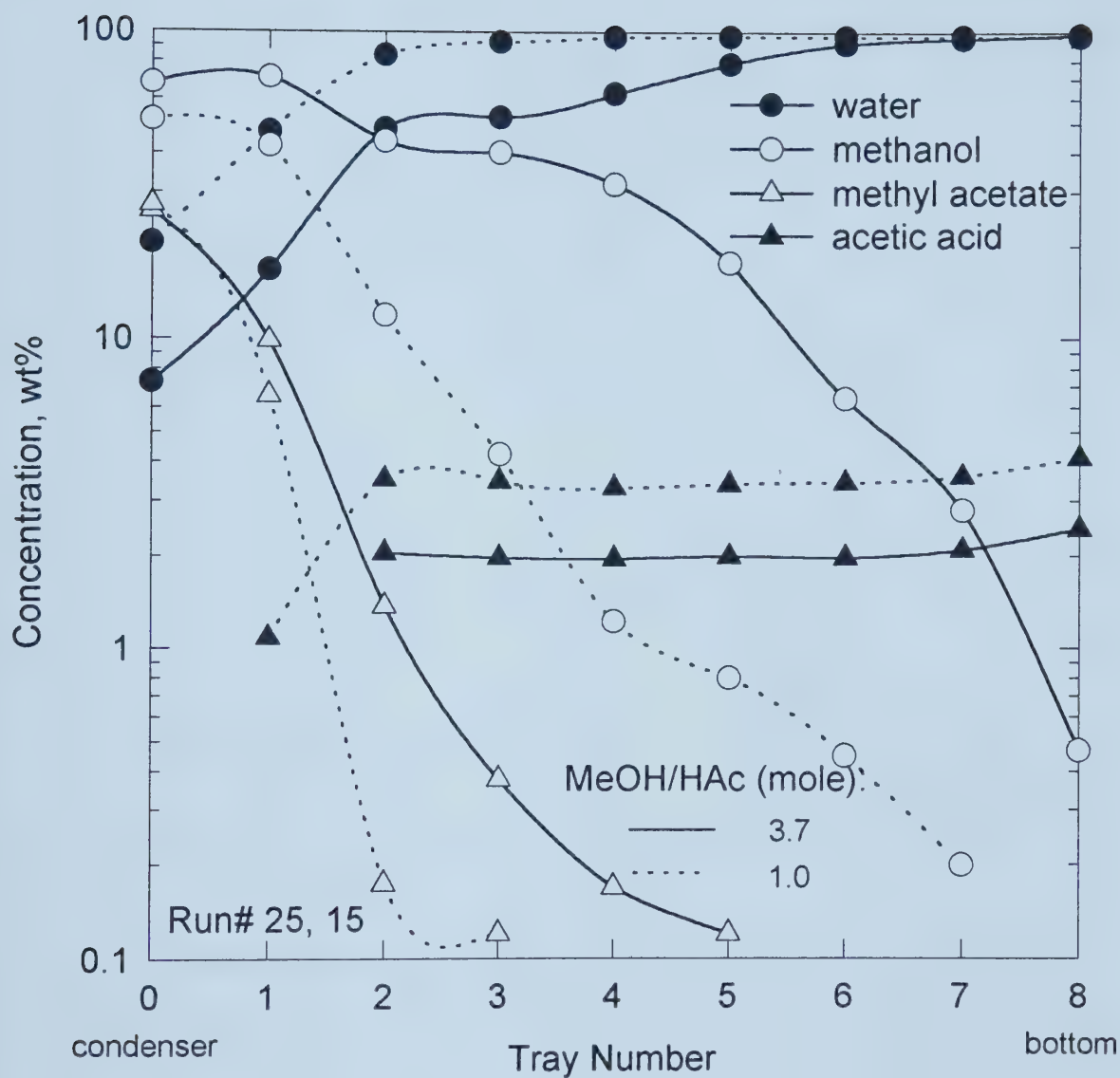


Figure 7-6. Effect of Feed Ratio of Methanol to Acetic Acid.



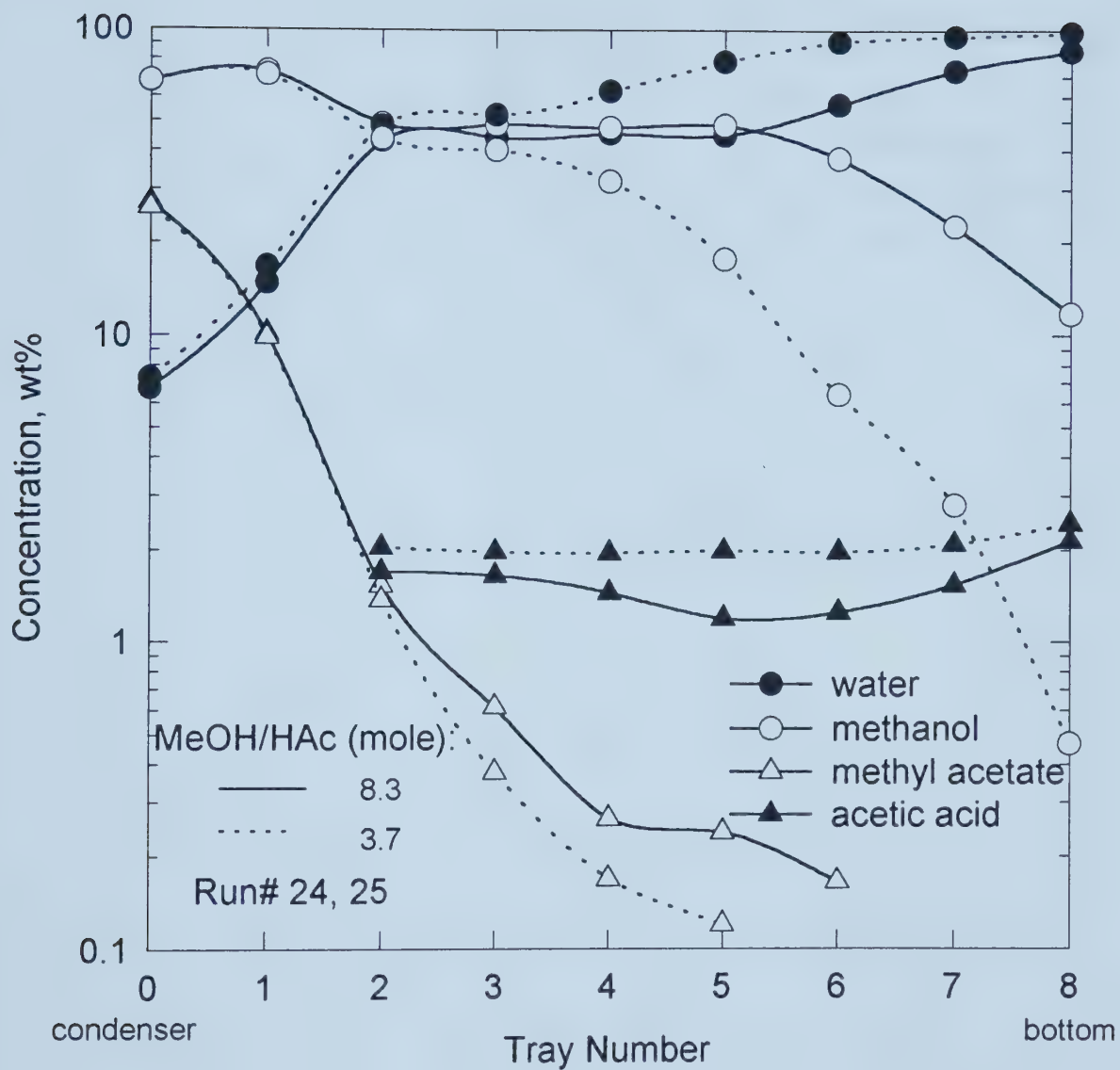


Figure 7-7. Effect of Feed Ratio of Methanol to Acetic Acid.





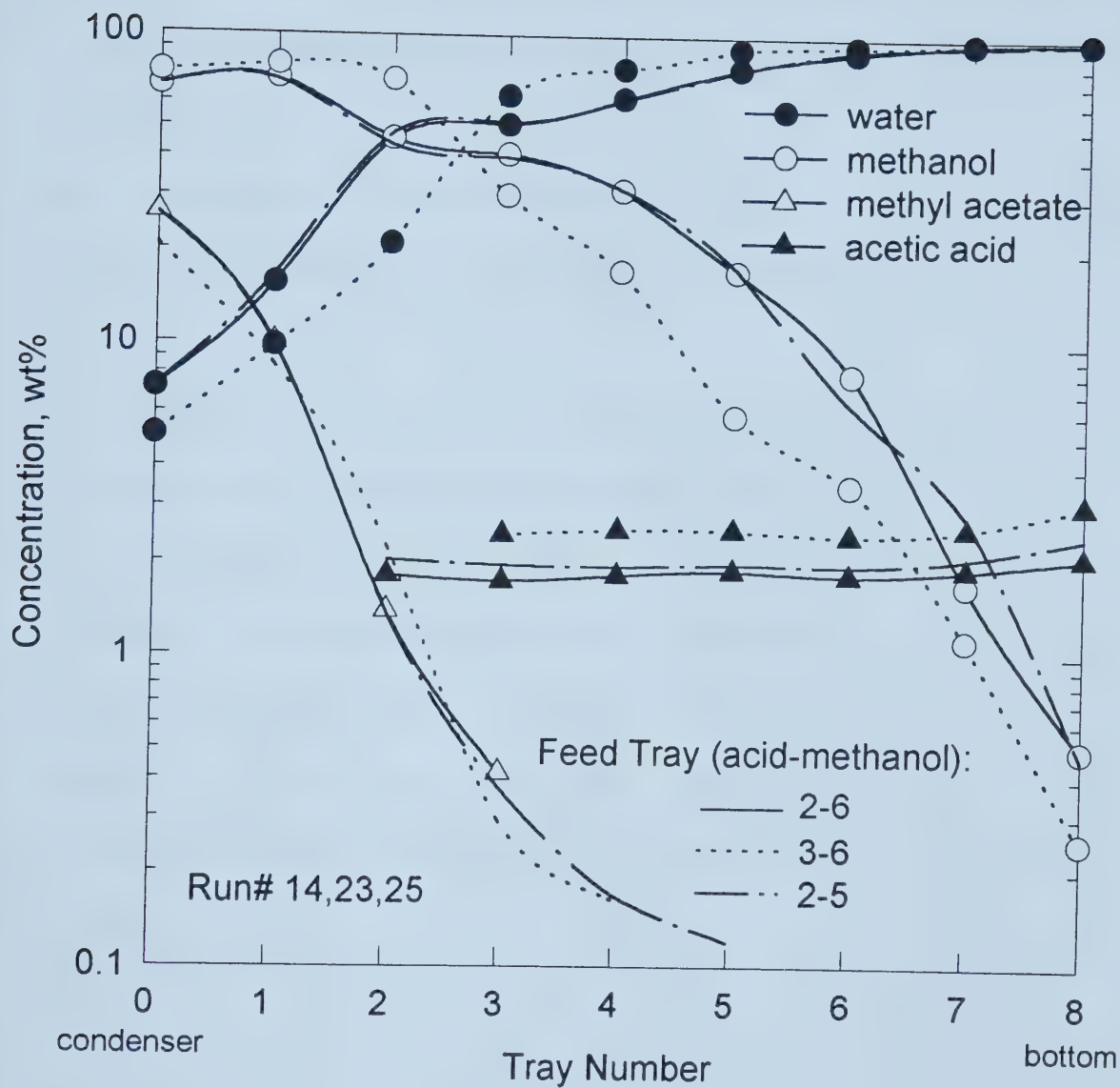


Figure 7-8. Effect of Feed Location. Feed: MeOH, 13.5 g/min; HAc-water, 140 g/min, 5 wt% of HAc Top product rate: 16.8 g/min



## 7.5 Literature Cited

- Bravo, J.L. and Pyhalahti, A. (1993) Investigations in a Catalytic Distillation Pilot Plant: Vapor/Liquid Equilibrium, Kinetics, and Mass-Transfer Issues. *Ind. Eng. Chem. Res.* **32**, 2220-2225.
- Flato, J. and Hoffmann, U. (1992) Development and Start-up of a Fixed Bed Reaction Column for Manufacturing Antiknock Enhancer MTBE. *Chem. Eng. Technol.* **15**, 193-201.
- Hao, X.R., Wang, J.S., Yang, Z.R. and Bao, J. (1995) Novel Catafractionation Technology for the Production of Methyl *tert*-Butyl Ether. *Chem. Eng. J.* **56**, 11-18.
- Saha, B. and Sharma, M.M. (1996) Esterification of Formic Acid, Acrylic Acid and Methacrylic Acid with Cyclohexene in Batch and Distillation Column Reactors: Ion-Exchange Resins as Catalysts. *Reactive & Functional Polymers* **28**, 263-278.
- Stevanovic, J.S, Vukovic, M.M., Caricic, B.B., Trisovic, B., and Jezdic, S. (1992) Reaction Distillation with Ion Exchangers. *Separation Science and Technology* **27**, 613-630.



## CHAPTER 8. CATALYTIC DISTILLATION — MODELING AND SIMULATION

### 8.1 Introduction

In developing a new process the experimental data obtained from a laboratory may not be used directly in the design of an industrial process and equipment because of the limited data points and the small scale of the equipment used in the tests. However, they are essential in the understanding and modeling of the process. When valid models are built based on experimental data, industrial processes and equipment can be simulated for new designs as well as for the analysis and optimization of the existing process operation.

To simulate a catalytic distillation process basic models such as kinetics and vapor-liquid equilibrium are needed for the specific process and for the specific column internals used. Based on the models and mass and energy balance, a group of nonlinear equations and/or partial differential equations are developed. Then the equations are solved with a proper method. There exist several commercial simulation packages for solving these equations. Therefore, our focus is on the establishment of basic models for the process.

### 8.2 Basic Models

The basic models for a catalytic distillation process involve reaction kinetics, vapor-liquid equilibrium, mass transfer and column internals. For the quaternary system, methyl acetate-methanol-water-acetic acid, reaction kinetics, vapor-liquid equilibrium and mass transfer have been studied in Chapters 2, 4 and 6 respectively. They are now applied



in the simulation of the catalytic distillation process for removing dilute acetic acid from water.

### 8.2.1 Reaction Kinetics

In Chapter 2, the reaction kinetics for dilute acetic acid esterification with methanol was studied in a one litre batch reactor. The kinetics equation was expressed as:

$$r_{MeAc} = k_0 W \exp(-E / RT) (C_{MeOH} C_{HAc} - C_{MeAc} C_{H_2O} / K) \quad (8.1)$$

To apply Equation (8.1) to the catalytic distillation process, the following assumptions are made:

1. Each catalyst unit placed between two dualflow trays in the catalytic distillation column is modeled as a continuous stirred tank reactor (CSTR).
2. External diffusion resistance is negligible.

Each catalyst unit can be simulated as a series of CSTRs, which is supported by the simulation package, Aspen Plus (Aspen Technology, Inc., 1996). Because of the short catalyst bed used, so the low reaction conversion, and possible axial dispersion, each unit is modeled as one CSTR.

For the catalyst unit with the CSTR model the model parameter, effective liquid hold-up, needs to be found. The actual liquid hold-up in the catalyst unit can be estimated from the pressure drop for the liquid flow through the catalyst unit as expressed in Equation (5.1):

$$h_L = -\frac{\Delta p}{\rho_L g} \quad (8.2)$$





where

$$-\Delta p = 65.4H \frac{\mu_f (1 - \varepsilon)^2 V_f}{d_s^2 \varepsilon^{11/3}} \quad (5.1)$$

Because of the complicated liquid flow pattern in the column the model parameter for the catalyst units, effective liquid hold-up, is different from the actual liquid hold-up in the catalyst units and will be found by fitting the measured acetic acid concentration at the column bottom with the simulated values.

### 8.2.2 Vapor-Liquid Equilibrium

As shown in Chapter 4, the best correlation for the vapor-liquid equilibrium of the methyl acetate-methanol-water-acetic acid system was obtained with the NRTL model in combination with Marek's method (Marek and Standart, 1954; Marek, 1955). The model parameters are listed in Table 4-1 with the third model parameter  $\alpha_{12}=0.37$  for all six binary mixtures. This model can be used for the catalytic distillation process without any modifications.

### 8.2.3 Mass Transfer

The mass transfer in distillation columns at steady state can be simulated using either an equilibrium stage model or a rate-based (i.e. non-equilibrium stage) model. Most of the published literature and commercial simulation packages utilize the equilibrium stage models. However, the rate-based models (Krishanmurthy and Taylor, 1985a,b; Taylor et al., 1987) are attracting the interest of an increasing number of people.



Transport processes (mass transfer, heat transfer) between vapor and liquid in distillation are very complicated. They are dependent on various factors, such as the physical properties, column internals, and operating conditions. The ideal equilibrium situation can rarely be achieved on a real stage due to the limitations of the vapor-liquid contact time and contact area. It is here that the equilibrium stage models and the rate-based models use different strategies to simulate the transport processes across one real stage.

As shown in Figure 8-1, the mass balance of component  $i$  around stage  $j$  (no feed, no reaction) can be written as:

$$l_{i,j-1} - l_{i,j} + v_{i,j+1} - v_{i,j} = 0 \quad (8.3)$$

In simulation, the changes in the flow rates of the components in both the vapor and liquid phase across one real stage are due to the mass transfer between the vapor and liquid phases and need to be evaluated. With the equilibrium stage models, stage (or component) efficiencies are used to account for the departure from the equilibrium situation on each stage. If Murphree tray efficiency is used, then

$$E_{MV}|_{i,j} = \frac{y_{i,j} - y_{i,j+1}}{y_{i,j}^* - y_{i,j+1}} \quad (8.4)$$

where

$$y_{i,j}^* = K_{i,j} x_{i,j} \quad (8.5)$$

The relationships between component flow rates and overall flow rates can be expressed as:

$$v_{i,j} = y_{i,j} V_j \quad (8.6)$$



$$l_{i,j} = x_{i,j} L_j \quad (8.7)$$

Combining Equations (8.4) to (8.7) yields

$$l_{i,j} = \left( \frac{v_{i,j} - v_{i,j+1}}{E_{MV}|_{i,j}} + v_{i,j+1} \right) A_{i,j} \quad (8.8)$$

where

$$A_{i,j} = \frac{L_j}{V_j K_{i,j}} \quad (8.9)$$

Substituting Equation (8.8) into Equation (8.3) and rearranging it, a tridiagonal matrix form can be written with the component vapor flow rates on trays as variables. The equation can then be solved by the Thomas method to obtain the component vapor flow rates on each stage. The change of component flow rates in the vapor phase due to interface mass transfer across one real stage can then be found. The change of component flow rates in the liquid phase can be obtained by Equation (8.8).

For the rate-based models, the material balance for a stage is split into two parts, one for each phase (see Figure 8-2). The overall mass balance for component  $i$  on stage  $j$  is still the same as shown in Equation (8.3)

For the vapor phase,

$$v_{i,j+1} - v_{i,j} + N_{i,j}^V = 0 \quad (8.10)$$

and for the liquid phase,

$$l_{i,j-1} - l_{i,j} + N_{i,j}^L = 0 \quad (8.11)$$

Combining Equations (8.3), (8.10) and (8.11) yields

$$N_{i,j}^{I'} = -N_{i,j}^L \quad (8.12)$$



Instead of using stage efficiencies to find the change in component flow rates in both vapor and liquid phases, the rate-based models use the following rate equations to directly evaluate the component mass transfer rates between vapor and liquid phases,

$$N_{i,j}^V = f(k_{i,k}^V a_j, y_{k,j}^I, \bar{y}_{k,j}^V, \bar{T}_j^V, T_j^I, N_{k,j}^V, k = 1, 2, \dots, m) \quad (8.13)$$

Substituting Equation (8.13) into Equations (8.10) and (8.11), the changes in both vapor and liquid phases across one real stage can be found.

The advantages in using the equilibrium stage models are:

1. The models and solution methods for distillation processes are well developed, and commercial simulation packages are available.
2. Stage efficiencies in distillation are well documented and many correlations are available for predicting stage efficiency, especially for trayed columns.
3. The range of stage efficiency is usually between 0.4 to 1.0 and can be easily estimated based on the data from existing similar distillation columns and rules-of-thumb.

The main problem with the equilibrium stage model, as shown in Chapter 6, is that for multicomponent systems, component tray efficiencies may be different from each other. This may cause difficulties in the determination and application of the component tray efficiencies. It is a common practice to use a single tray efficiency for all components if no component tray efficiency data are available.

The rate-based model mechanistically describes the mass transfer process in distillation and directly calculates the mass transfer rates between vapor and liquid phases. The problems with this model are quite clear.





1. The difficulties in determination and prediction of component mass transfer coefficients are more or less the same as for stage efficiency. Effects of physical properties, column internals and operating conditions have to be considered.
2. Very few experimental data on mass transfer coefficients are available for various column internals under distillation conditions.
3. The simple equations derived from equipment such as wetted-wall columns or from such a process as absorption may not be suitable for the prediction of mass transfer coefficients for trays and packings in distillation.
4. The range of mass transfer coefficients can be very wide and they are not easily estimated by the available operating data and rules-of-thumb.

The rate-based models are a recent development compared with the equilibrium stage models. More fundamental studies are required on the mass transfer coefficients and the interfacial area under distillation conditions both theoretically and experimentally. At this stage, equilibrium stage models are the more reliable choice for trayed columns because the tray efficiency data are more readily available than the mass transfer coefficients and interfacial area. For packed columns, both rate-based and equilibrium stage models are similar in terms of reliability.

In this study, the equilibrium stage model is used because the dualflow tray was used as a separation device and tray efficiency can be more reliably measured than the mass transfer coefficients and effective interfacial area under distillation conditions. The



Murphree component tray efficiency is used for calculating the mass transfer process on dualflow trays.

As shown in Chapter 7, the ranges of component concentration variations in the catalytic distillation tests are much narrower than in the tray efficiency measurements. For example, in catalytic distillation, acetic acid concentration in the column is very low, usually less than 2 wt% with no appreciable amount on the top two trays. The methyl acetate is mainly present on the top two trays and the concentrations on the other trays are less than 1 wt%.

Based on the measured component tray efficiencies in Chapter 6, the efficiency data are estimated for the catalytic distillation tests and are listed in Table 8-1. It will be shown later that the catalytic distillation process is reaction controlled and the effect of component efficiencies on the removal of acetic acid is not significant.

#### ***8.2.4 Column Internals***

In our catalytic distillation column, column internals are composed of dualflow trays and catalyst units for separation and reaction respectively. In simulation, each tray (including the reboiler and condenser) or catalyst unit is treated as a stage as shown in Figure 8-3. Mass transfer, but not reaction, mainly occurs on the dualflow trays. Therefore, a certain value of component tray efficiency is assigned to each component for each tray while the reaction rate on the dualflow trays is set at zero. On the other hand, reaction occurs mainly in the catalyst units and mass transfer in the units can be neglected. The reaction rate expressed as Equation (8.1) is assigned to each catalyst unit. Although



the catalyst units may contribute to some extent to mass transfer as shown in Chapter 6, here their contribution is confined to the dualflow trays. Therefore, separation efficiency for catalyst units is assigned as zero. In calculation, a small efficiency value, e.g.  $1.0 \times 10^{-4}$ , was set for each unit to avoid calculation overflow as shown in Equation (8.8).

## 8.3 Model Equations And Solution Methods

### 8.3.1 Model Equations

A catalytic distillation column at steady state is represented by a set of nonlinear equations. The model equations are: material balances, equilibrium equations, summation equations, heat (energy) balances and reaction equations, that is, "MESH+Reaction".

The set of equations for stage  $j$  in the catalytic distillation column is as follows:

Material balance on components ( $i=1, m$ ),

$$l_{i,j-1} - l_{i,j} + v_{i,j+1} - v_{i,j} + f_{i,j} - w_{i,j} + r_{i,j} = 0 \quad (8.14)$$

where

$$r_{i,j} - \text{reaction rate,} = \alpha_i (r_{MeAc} V_L)_j \text{ mol/s} \quad (8.15)$$

As shown in Equations (8.3) to (8.12), component tray efficiencies are needed to solve the mass balance equation (8.14).

From Equations (4-1) and (4-5), the equilibrium equations can be expressed in a simple format:

$$y^*_{i,j} - K_{i,j} x_{i,j} = 0 \quad (8.16)$$



where  $K_{i,j}$ =equilibrium constant, which is a very complicated function of the vapor-liquid composition, temperature and pressure and can be evaluated from equations developed in Chapter 4.

Summation equations,

$$\sum_{i=1}^m x_{i,j} - 1 = 0 \quad (8.17)$$

$$\sum_{i=1}^m y_{i,j} - 1 = 0 \quad (8.18)$$

Energy balance,

$$L_{j-1}h_{j-1}^L + V_{j+1}h_{j+1}^V - (L_j + W_j^L)h_j^L - (V_j + W_j^V)h_j^V + F_jh_j^F + Q_j = 0 \quad (8.19)$$

Reaction equations are expressed in Equations (8.15) and (8.1).

Compared with conventional distillation columns, the model equations for catalytic distillation columns are similar except for the additional reaction equations. Therefore, most of the simulation methods used for catalytic distillation columns are an extension of those used for conventional distillation.

### 8.3.2 Solution Methods

Since most of these equations are highly nonlinear, with strong coupling both within each set, and from one set to another, all of the rigorous methods for solving them are based on successively approximating the exact solution. The commonly used solution methods can be classified into three categories: simultaneous correction (or global Newton) methods; relaxation methods; and tearing (or equation decoupling or partitioning) methods. Table 8-2 summarizes the publications in the area of simulating





steady-state multi-stage equilibrium or rate-based distillation towers with and without chemical reactions. Of these, the simultaneous correction methods and tearing methods are the methods usually used in solving reactive distillation problems.

## TEARING (EQUATION DECOUPLING OR PARTITIONING) METHODS

In the tearing methods, the equations are derived and grouped, or partitioned and paired with variables to be solved in a series of steps. Although different couplings of equations and variables must be used for mixtures with different boiling ranges, the tearing method does not require computing of derivatives and the tridiagonal matrix algorithm can be implemented to decrease computer storage space and increase computation efficiency. However, when the difference in boiling point between components is too large, the kinetics are complex, or the liquid solution is highly nonideal, the tearing method is difficult to converge (Chang and Seader, 1988). The reason for this is composition lag in the calculation. In the tearing methods, K-values and enthalpies are generated using the compositions from the previous trial. This is the major disadvantage of the methods for highly nonideal systems, where K-values (especially activity coefficients) and enthalpies are highly composition dependent. Tearing methods are recommended in the simulation of distillation with ideal or mildly nonideal systems (Kister, 1992).

The most important group of the tearing methods is the so-called "Inside-Out" method. What sets the inside-out algorithm apart from all the other approaches is the introduction of two levels of computation. An outside loop retains the lengthy rigorous enthalpy and equilibrium calculations while the inside loop uses simple local models for the



calculation of these quantities. Since up to 80% of the time in a simulation program can be spent evaluating thermodynamic quantities, this leads to a significant acceleration in reaching solutions. The base for this method is the choice of the primary solution variables. An important attribute of these variables is that they are very weak functions of variables for which initial estimates may be very poor, such as stage temperature, interstage phase rates, and liquid and vapor mole fractions (Boston and Sullivan, 1974). This approach was first developed by Boston and his coworkers (1970, 1972, 1974, 1978, 1980) for conventional distillation simulation. Russell (1983) explored the application of the inside-out algorithm to a wide range of tower configurations. Chimowitz and his coworkers (Simandl, 1988) devoted much attention to the improvement of the local models used in the inner loop. They added explicit composition dependence to models where Boston had used temperature dependence only. This improved the area of validity of the local models.

Simandl and Svrcek (1991) extended the inside-out algorithm to distillation with chemical reactions. By using the production of ethyl acetate as a test case, they found that both simultaneous correction and inside-out algorithms can be used to solve the systems of equations describing distillation with chemical reactions. The algorithms were of equal robustness but the inside-out algorithm was approximately three times faster.

The inside-out methods are now the methods of choice for mainstream commercial column simulation programs. They have displaced some of the traditional tearing methods and their application should continue to grow (Kister, 1992). The inside-out approach is the basis of all the rigorous distillation models including reactive distillation in Aspen Plus



(Venkataraman et al., 1990). It is also the first choice of PRO/II (Simulation Sciences, Inc., 1994) and Hysim (Hyprotech, 1992) for simulation of conventional distillation processes.

## SIMULTANEOUS CORRECTION (GLOBAL NEWTON) METHODS

In simultaneous correction methods, the equations are first linearized and then solved simultaneously using a single level iterative procedure such as the Newton-Raphson algorithm. The methods may vary in their choice of variables and equations for the Newton-Raphson calculation, but none of the equations is solved in any separate step outside of the Newton-Raphson calculation. When the initial estimates are enough for the solution, this algorithm converges very quickly due to its quadratic convergence rate. Since the generally applicable Newton-Raphson method is employed for solving the equations, the algorithm is equally robust for all types of chemical systems and physical arrangements of the column (Murthy, 1984). The greatest drawbacks of these methods are the time spent in evaluating and inverting a Jacobian matrix at every iteration and the need for a starting value close enough to the solution. They also need a large amount of storage and involve complicated derivative operations. Various attempts have been made to improve the efficiency of the Newton-Raphson method by approximating the Jacobian matrix rather than evaluating it rigorously (Simandl, 1988).

Naphtali and Sandholm (1971) were perhaps the first to propose the use of the simultaneous correction method for multicomponent separation calculations. Murthy (1984) extended the Naphtali and Sandholm approach to columns in which chemical



reactions are present. Zhang (1989) used a modified Newton-Raphson algorithm to simulate a tray-type reactive distillation column. The commercial simulation packages, Process and PRO/II, developed by Simulation Science Inc., also use the simultaneous correction method for solving both conventional and reactive distillation columns.

## RELAXATION METHODS

Relaxation methods find a steady-state solution of a column as if it was an operating column changing with time (Komatsu, 1977). The column is initialized using some realistic condition such as startup, with the liquid on every stage having the feed composition at its bubble point. The column is carried to the steady-state condition by successive approximations of the unsteady-state distillation equations. These unsteady-state equations are modifications to the equations to include changes in the variables with respect to time. The relaxation methods make stable, stepwise movements toward the steady-state values. They offer great stability and convergence over a wide range of column conditions and configurations irrespective of column complexity, dependence of equilibrium ratios on composition, or even the deviation of the starting values from the solution. The main disadvantage is the deceleration in convergence rate as the solution is approached.

## CHOICE OF SOLUTION METHODS

In the established basic models of the catalytic distillation process, the MESH+Reaction model equations can be solved using a commercial process simulation





package. To date, both PRO/II and Aspen Plus can be used for catalytic (reactive) distillation simulation. PRO/II (Simulation Sciences Inc., 1994) uses a simultaneous correction method to solve the catalytic distillation equations. We found that it was extremely difficult to obtain converged results using PRO/II when the user subroutine for reaction kinetics was implemented. Aspen Plus applies the inside-out method to the simulation of catalytic distillation processes and convergence behavior was found to be excellent for all cases we studied. Because Aspen Plus can be successfully used to solve the model equations for our catalytic distillation process, it was not necessary to write the solution program ourselves. In subsequent sections, all the simulation results were obtained using Aspen Plus. An example of input and output files for the simulation of the catalytic distillation process using Aspen Plus is shown in the Appendix.

## 8.4 Results And Discussion

### 8.4.1 *Effective Liquid Hold-up in Catalyst Units*

The model parameter for the catalyst unit, the effective liquid hold-up, was found to be  $2.7 \times 10^{-5} \text{ m}^3$  by fitting the measured acetic acid concentrations at the column bottom with the simulated values. The liquid hold-ups calculated using Equation (8.2) are 1.3 to  $2.5 \times 10^{-5} \text{ m}^3$ . The difference between the effective and the calculated liquid hold-ups can be explained by: (1) the calculated liquid hold-up accounts only for the liquid in the liquid-full portion of the catalyst bed. In the operation, liquid flowed through the whole catalyst bed from top to bottom and the catalyst particle surface may have been covered with liquid even though the intraparticle channels were not full of liquid; (2) the liquid in the catalyst



bed was not totally mixed as the CSTR model assumed; (3) random and uneven liquid distribution was observed from dualflow trays to the catalyst units.

#### ***8.4.2 Simulation of the Experimental Results***

As shown in Chapter 7, a total of 32 runs were conducted for the catalytic distillation tests in the 100 mm diameter column. Various parameters such as feed composition and location, top product rate, and reflux ratio were changed to investigate their effect on the removal of acetic acid from water. The main purpose of obtaining a variety of experimental data is to verify the developed models and simulation results for the catalytic distillation process. With the verified models, simulation can be conducted to investigate the effect of various parameters independently and to design industrial columns for the process.

With the established models and equations in Sections 8.2 and 8.3, the simulation package, Aspen Plus, was used to solve the MESH+Reaction equations. Convergent results were obtained for all the 32 runs. UNIX version (9.3-1) and PC version (9.3) gave similar results.

It should be noted that in the following figures showing a comparison of measured and simulated concentration profiles, the tray number is counted from the condenser to the reboiler, i.e., the compositions measured from the condenser bottom are shown in the figures as the compositions on tray 1 and those from the reboiler as tray 9.

Figures 8-4 to 8-7 show the measured and simulated concentration profiles under similar feed rates and feed compositions but different top product rates. With the top



product rates reduced from Figures 8-4 to 8-7, the methanol concentration in the column increases, more acetic acid was converted and its content in the column bottom is reduced. From the figures it can be seen that the simulated values track the measured compositions quite well for the variations in top product rates.

Figures 8-8 and 8-9 show the simulated composition profiles for two runs with similar operating conditions but different boil-up rates and thus different reflux ratios (10.2 and 14.8 respectively). Again, the experimental values and simulation results are consistent for both runs.

Figures 8-10 and 8-11 show the simulated composition profiles for the two runs with similar operating conditions but different feed rates of methanol (13.5 and 23.0 g/min respectively). With a lower methanol feed rate as shown in Figure 8-10, the methanol concentration in the column is much lower. The simulation profiles agree well with the measured values.

Figures 8-12 and 8-13 show the simulated composition profiles for the two runs with similar operating conditions but different feed rates of the acetic acid-water mixture (180 and 220 g/min respectively). It should be noted from these figures that the concentrations of acetic acid on tray 2 (actually tray 1) are now high enough to be detected by GC and the simulated values follow the trend very well.

Figures 8-14 to 8-17 show the measured and simulated composition profiles for the four runs with various feed locations and methanol rates. In the previous runs, the methanol feed was at tray 7 and the acetic acid-water feed at tray 3. In Figures 8-14 and 8-15 the acetic acid-water feed was moved down to tray 4 while in Figures 8-16 and 8-17



the methanol feed was moved up to tray 6. It can be seen from these figures that the simulation results agree well with the measured values for the different feed locations. The effect of feed location on the removal of acetic acid from water has been discussed in Chapter 7.

The above results were mostly obtained with the feed concentration of acetic acid in water about 5 wt%. Figures 8-18 and 8-19 show the simulation results for the two runs with 9.92 and 2.25 wt% of acetic acid in water respectively. Again, the simulation profiles follow the measured values closely.

From the above results it can be concluded that the established simulation program can successfully simulate various experimental cases.

#### ***8.4.3 Other Simulation Case Studies***

In Chapter 7 experimental results were obtained for the effect of various parameters on the catalytic distillation process. However, the results are by no means thorough for two reasons: 1) too much experimental work would be involved; 2) some parameters cannot be studied independently. With the verified models and the simulation scheme it is possible to study the effect of some important parameters by computer simulation. The simulation results may provide more detailed information for the column design.

Figure 8-20 shows the effect of component tray efficiencies on the concentration profiles. The solid lines express the simulation results for run #10 with component tray efficiencies varying from 0.75 to 1.05 while the other two types of lines show the results





with the same component tray efficiencies equal to 0.5 and 1.5 respectively. It can be seen that the difference between component concentration profiles is minimal and slightly more acid was removed with higher component tray efficiencies. This indicates that for the reaction-controlled process it is more important to improve the reaction rate rather than the tray efficiency.

Figure 8-21 shows that the effect of effective liquid hold-up in the catalyst units on the removal of acetic acid is very significant. By increasing the liquid hold-up four times from  $2.7 \times 10^{-5}$  to  $1.08 \times 10^{-4} \text{ m}^3$ , the acid concentration at the column bottom drops 3.3 times from 1.75 wt% to 0.53 wt%. The increase in liquid hold-up can be achieved by increasing the catalyst amount (i.e. height of the catalyst bed) placed between the two trays. However, it should be kept in mind that because of the reaction equilibrium, the catalyst bed may not be as effective when the reaction is close to equilibrium. Figure 8-22 shows the simulation results for run #10 with the changing bed height of each catalyst unit in the column. It can be seen that when the bed height is increased beyond one metre, the increase in acid removal becomes insignificant.

The optimum bed height per catalyst unit is dependent on the reaction rate and separation efficiency. Figure 8-23 shows the effect of the catalyst bed height on acid removal with a fixed column height. The simulation is based on run #10. In the original run, seven dualflow trays and five catalyst units were installed in the column. The catalyst units were placed above trays 3 to 7 and the bed height for each catalyst unit is 0.09 m. If two trays (tray 3 and tray 5) in the reaction/separation zone are taken out and the space left is filled with catalyst, we have now five separation trays and three catalyst units



located between tray 2 and 4, tray 4 and 6, and tray 6 and 7. The total catalyst bed height increases from 0.45 to 0.69 and the average bed height increases from 0.09 to 0.23 m. From Figure 8-23 it can be seen that the acetic acid concentration decreases from 1.75 to 1.65 wt%. If one more tray (tray 6) is taken out, four separation trays (trays 1, 2, 4 and 7) are left with two catalyst units located between tray 2 and 4, and tray 4 and 7. The total height of the catalyst bed increases now to 0.82 m and the average bed height increases to 0.41 m. From the figure it can be seen that the acid concentration decreases further to 1.6 wt%. If the last tray in the reaction zone (tray 4) is taken out, three trays (trays 1, 2 and 7) are left with only one catalyst unit between trays 2 and 7. The total catalyst bed height as well as the average bed height increases to 0.95 m. In this case, the acid concentration at the column bottom increases sharply. This indicates that the catalyst bed is too high and the reaction is close to equilibrium so the extra catalyst bed is not efficient. Figure 8-23 clearly shows that the optimum catalyst bed height is about 0.3 m. It should be noted that optimum combinations of reaction trays and catalyst units are dependent on many factors and are different from case to case.

Figure 8-24 shows the effect of the reaction zone on the removal of acetic acid from water. For the original run #10 the catalyst units were placed above trays 3 to 7. Simulation results show that net reaction rates in all the catalyst units are positive with a total value of 4.39 mol/h. The acetic acid concentration at the column bottom is 1.75 wt%. If a similar catalyst unit is added above tray 2 the simulation results as shown in Figure 8-24 indicate an increase in the acid concentration at the column bottom from 1.75 to 1.84 wt%. The reason is the net negative reaction rate (-0.42 mol/h) on this added



catalyst unit because of the high concentration of reaction products (methyl acetate and water) and very low concentration of acetic acid. The net reaction rates in the other five catalyst units are positive with a total rate of 4.68 mol/h. Therefore, the net reaction rate for the whole column is 4.26 mol/h and less than 4.39 mol/h for the original run without the catalyst unit above tray 2. Because the change in the overall reaction rate is insignificant, it may be difficult to detect this difference from experiments.

#### ***8.4.4 Simulation for an Industrial Column***

Computer simulation is the first step, and an essential step, in the design of industrial catalytic distillation columns. Accurate simulation results are the key to a successful design. The simulation results depend mostly on the validity of the vapor-liquid equilibrium and the reaction kinetics models.

Using the above established simulation program, an industrial column with 25 separation stages and 19 catalyst units was simulated. The catalyst units were placed above trays 6 to 24. The column internals and column configurations were similar to the test column except that the height of the catalyst unit was increased from 0.09 m to 0.2 m. It is assumed that the effective liquid hold-up in the catalyst unit is proportional to the height of the catalyst bed. Component tray efficiencies similar to those listed in Table 8-1 were used. The simulation results are summarized in Table 8-3. For comparison, Table 8-3 also lists the simulation results for a simple distillation process for the separation of a similar acetic acid-water mixture. A typical tray efficiency of 0.7 was applied for all trays for the binary mixture. For the simple distillation process, water is withdrawn from the



column top and the acetic acid content in the water is similar to that in the bottom of the catalytic distillation process. It can be seen from the table that with a similar amount of acetic acid removal from water, the catalytic distillation process needs fewer separation stages and consumes only 14.8% of the energy of the simple distillation process. The vapor and liquid loadings for the catalytic distillation process are only 20% and 30%, respectively, of that for the simple distillation process. The fewer separation stages and lower vapor/liquid loadings indicate that the column size required for the catalytic distillation process could be much smaller than that for the simple distillation process. The concentration of acetic acid in the catalytic distillation column is lower than 3.5 wt% and stainless steel 304 can be used for the construction of the column and internals. On the other hand, a very expensive material such as titanium is needed for the simple distillation column and reboiler because of the high concentration of the acetic acid mixture.

## 8.5 Conclusions

A simulation program was established by incorporating the models developed in this study for reaction kinetics, vapor-liquid equilibrium, column internals and the measured component tray efficiencies into a commercial simulation package, Aspen Plus. A catalytic distillation process was simulated for the removal of acetic acid from water. Various experimental cases are available to verify the simulation results. It was found that the simulation results agree well with the measured composition profiles for the reaction and separation system of methyl acetate-methanol-water-acetic acid.







By using the simulation program, various parameters such as the reaction zone, effective liquid hold-up and component tray efficiencies were studied for their effects on the performance of the catalytic distillation process. The results from the simulation are essential for the design of industrial columns, such as for the optimum design of the internals with the optimum combination of catalyst bed and separation trays for reaction and separation.

With the established simulation program an industrial column with 25 separation stages and 19 catalyst units was simulated for the removal of acetic acid from water by catalytic distillation. Another process by the simple distillation method was also simulated for comparison. The simulation results show that the catalytic distillation needs only half of the separation stages and 14.8% of the energy as used by simple distillation. By using the catalytic distillation process, the column size may be reduced and the corrosion problem avoided.



## 8.6 Nomenclature

$a_i$	stoichiometric coefficient of component $i$
$a_j$	effective mass transfer area on tray $j$ , $m^2$
$A_i$	absorption factor defined in Equation (8.9)
$C_i$	mole fraction of component $i$ in mixture
$r_{MeAc}$	reaction rate, $mol/s \cdot L_{liq}$
$d_s$	medium diameter of particles, mm
$E$	activation energy, $=58500 \text{ J/mol}$
$E_{MV}$	Murphree tray efficiency
$f$	component feed rate, $mol/s$
$F$	total feed rate, $mol/s$
$h$	mixture enthalpy, $J/mol$
$H$	height of catalyst bed, m
$h_L$	clear liquid height, m
$l$	liquid component flow rate, $mol/s$
$L$	total liquid flow rate, $mol/s$
$m$	number of components in the mixture
$N$	mass transfer rate between vapor and liquid, $mol/s$
$k$	mass transfer constant, $mol/m^2s$
$K$	equilibrium constant for reaction or vapor-liquid equilibrium
$k_o$	reaction constant, $=1.76 \times 10^6$



$\Delta p$	pressure drop for liquid flowing through fixed porous media, Pa
$Q$	energy input plus heat of reaction, J/s
$r$	component reaction rate, mole/s
$R$	gas constant, =8.314 J/(mol.K)
$T$	temperature, K
$v$	component vapor flow rate, mol/s
$V$	total vapor rate, mol/s
$V_f$	liquid superficial velocity in the packed bed, m/s
$V_L$	effective liquid hold-up in a catalyst unit, L
$w$	component side-withdrawn rate, mol/s
$W$	catalyst loading, g.cat/L <sub>liq</sub>
$W_j$	total withdraw rate, mol/s
$x$	component mole fraction in liquid
$y$	component mole fraction in vapor
$y^*$	equilibrium component mole fraction in vapor with liquid
$\rho_L$	liquid density, kg/m <sup>3</sup>
$\mu_f$	liquid viscosity, Pa·s
$\varepsilon$	void fraction of catalyst packed bed

superscript

F	feed
I	interface



L            liquid

V            vapor

subscript

i            component number

j            tray number





Table 8-1. Component Tray Efficiencies

Component	Trays 1 to 2	Trays 3 to 7
methyl acetate	0.4-0.8	0.6-0.9
methanol	0.4-0.8	0.9-1.2
water	0.5-0.9	0.9-1.2
acetic acid	not present	0.6-0.9



Table 8-2. Rigorous Methods for Simulation of Catalytic Distillation

Reference for Reactive Distillation	Extension from Standard Distillation	Calculation Methods
Suzuki et al. (1971)	Wang-Henke (1966)	Tearing (Bubble-Point), Iteration
Nelson (1971)	Tierney et al. (1967, 1969)	Tearing, Newton-Raphson, Damping
Komatsu-Holland (1977)	Holland (1981)	Tearing, Newton-Raphson, $\theta - \eta$
Kaibel et al. (1979)		Tearing, Newton-Raphson
Tierney-Riquelme (1982)		Tearing
Venkataraman et al. (1990)		Tearing (Inside-Out)
Kinoshita et al. (1983)		Tearing
Holland (1981)	Holland (1981)	Tearing
Izarraraz et al. (1980)	Holland (1981)	Tearing, $\theta$ -method
Jelinek-Hlavacek (1976)		Relaxation, Relaxation Factor
Komatsu (1977)		Relaxation, Relaxation Factor
Mori et al. (1989)		Relaxation
Simandl-Svrcek (1991)	Naphtali-Sandholm (1971), Boston (1970, 1980), Russell (1983)	Global Newton and Tearing (Inside-Out)
Murthy (1984)	Naphtali-Sandholm (1971)	Global Newton
Simandl (1988)	Naphtali-Sandholm (1971), Boston (1970, 1980), Russell (1983)	Global Newton and Tearing (Inside-Out)
Xu-Chen (1988)	Naphtali-Sandholm (1971)	Global Newton
Zheng-Xu (1992)	Taylor et al. (1985a, 1985b, 1987)	Global Newton, Rate-based Model
Simulation Packages:		
Aspen Technology, Inc., Aspen Plus (1996)		Tearing (Inside-Out)
Simulation Sciences, Inc., PRO/II (1994)		Newton-Raphson



Table 8-3. Simulation Results for Removal of Acetic Acid from Water by Catalytic Distillation and Simple Distillation

	Simple Distillation	Catalytic Distillation
Feed:		
HAc/Water	10,000 kg/h, 5 % HAc	10,000 kg/h, 5 % HAc
MeOH	no	500 kg/h, pure
Product:		
Top	9,500 kg/h, 0.32 % HAc, 99.68% H <sub>2</sub> O	600 kg/h, 95.99% MeAc, 1.04 MeOH, 2.96% H <sub>2</sub> O, 0.0024% HAc
Bottom	500 kg/h, 93.87 HAc, 6.13% H <sub>2</sub> O	9,900 kg/h, 0.0025% MeAc, 2.47% MeOH, 97.20% H <sub>2</sub> O, 0.33% HAc
Stages	distillation - 50 ( $E_{MV}=0.7$ )	distillation - 25 ( $E_{MVij}=0.7-1.1$ ) catalyst units - 19
Reflux Ratio	1.65	24
Liquid Loading (kg/h)	48,000 to 170,000	14,240 to 24,420
Vapor Loading (kg/h)	15,670 to 83,920	4,354 to 16,400
Reboiler Duty (MMKCal/h)	14.2	2.1
Condenser Duty (MMKCal/h)	13.8	1.9





Figure 8-1 Equilibrium Stage Model





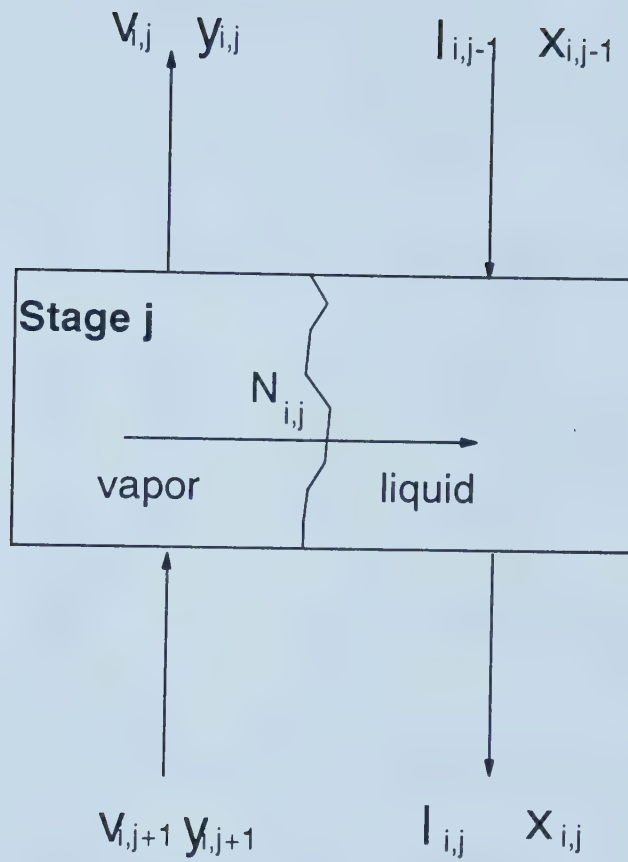


Figure 8-2 Non-Equilibrium Stage Model



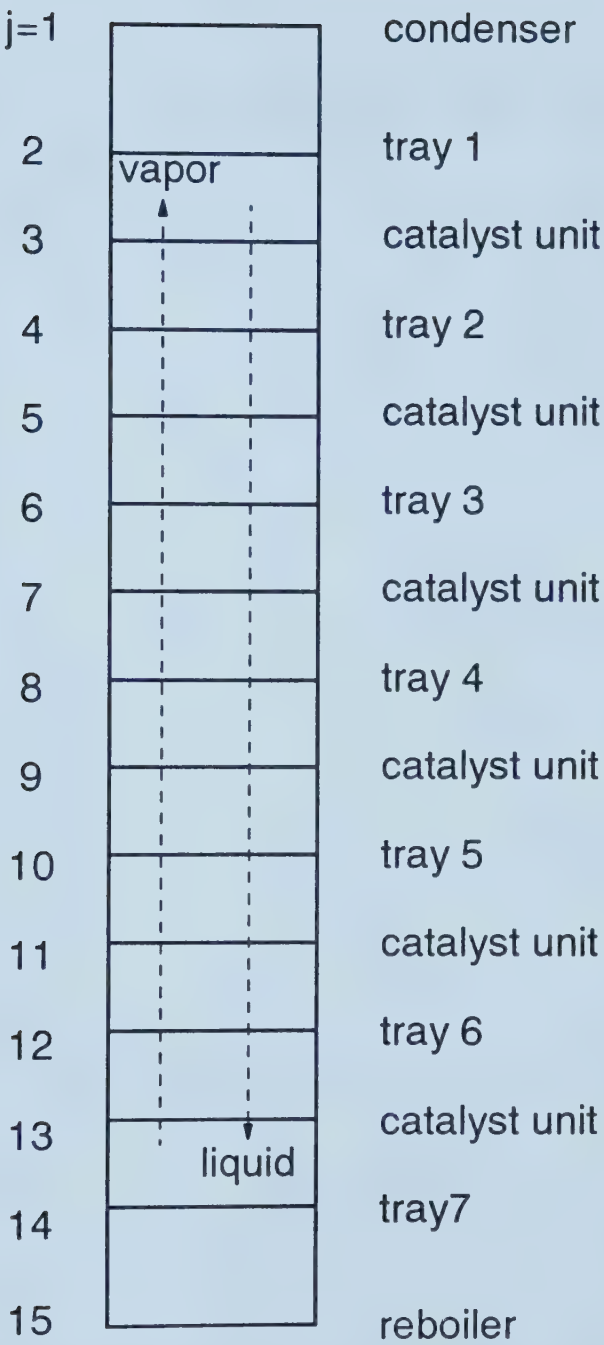


Figure 8-3 Column Model



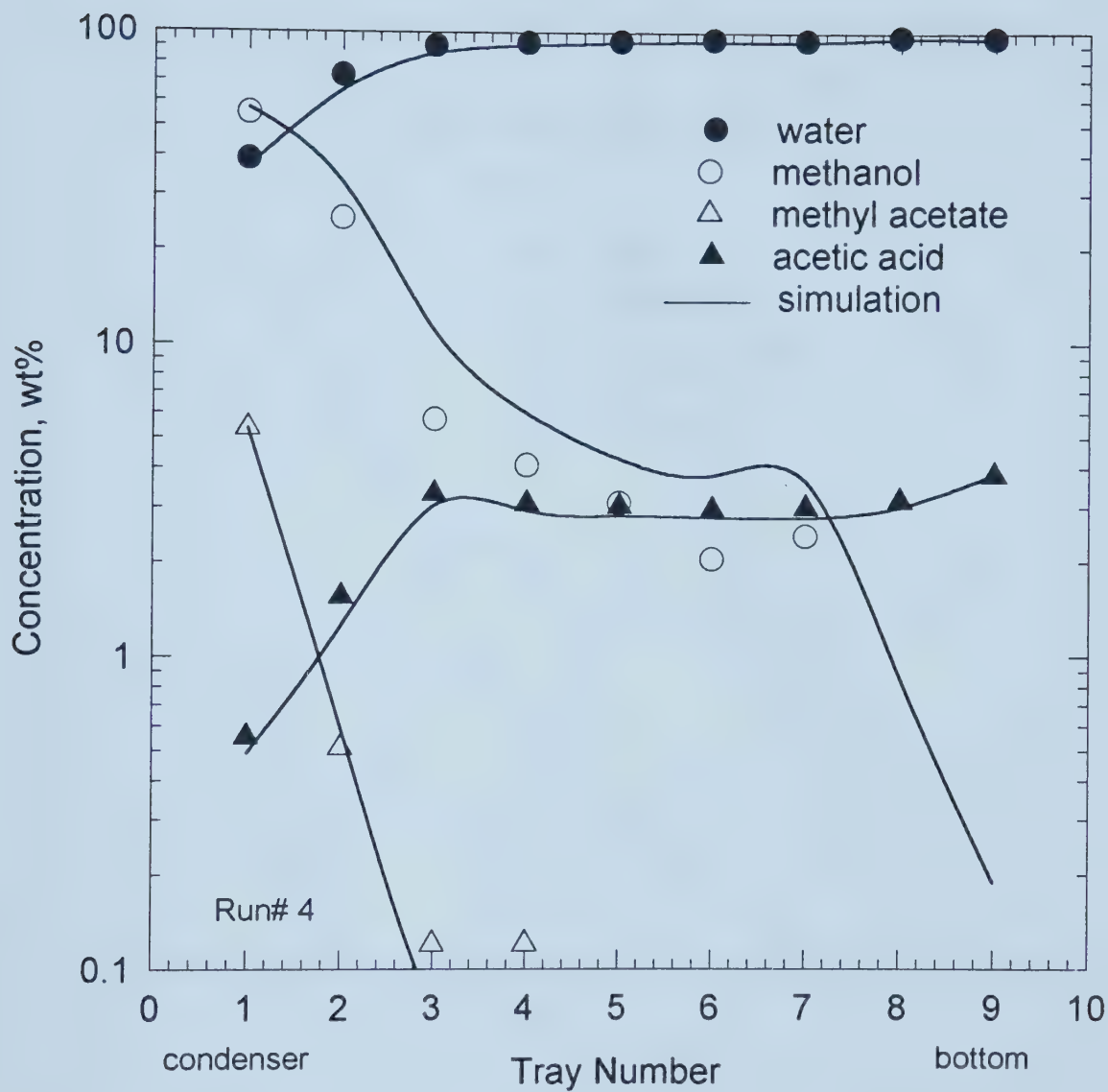


Figure 8-4. Simulation of Run #4 with Top Product Rate of 50.1 g/min.



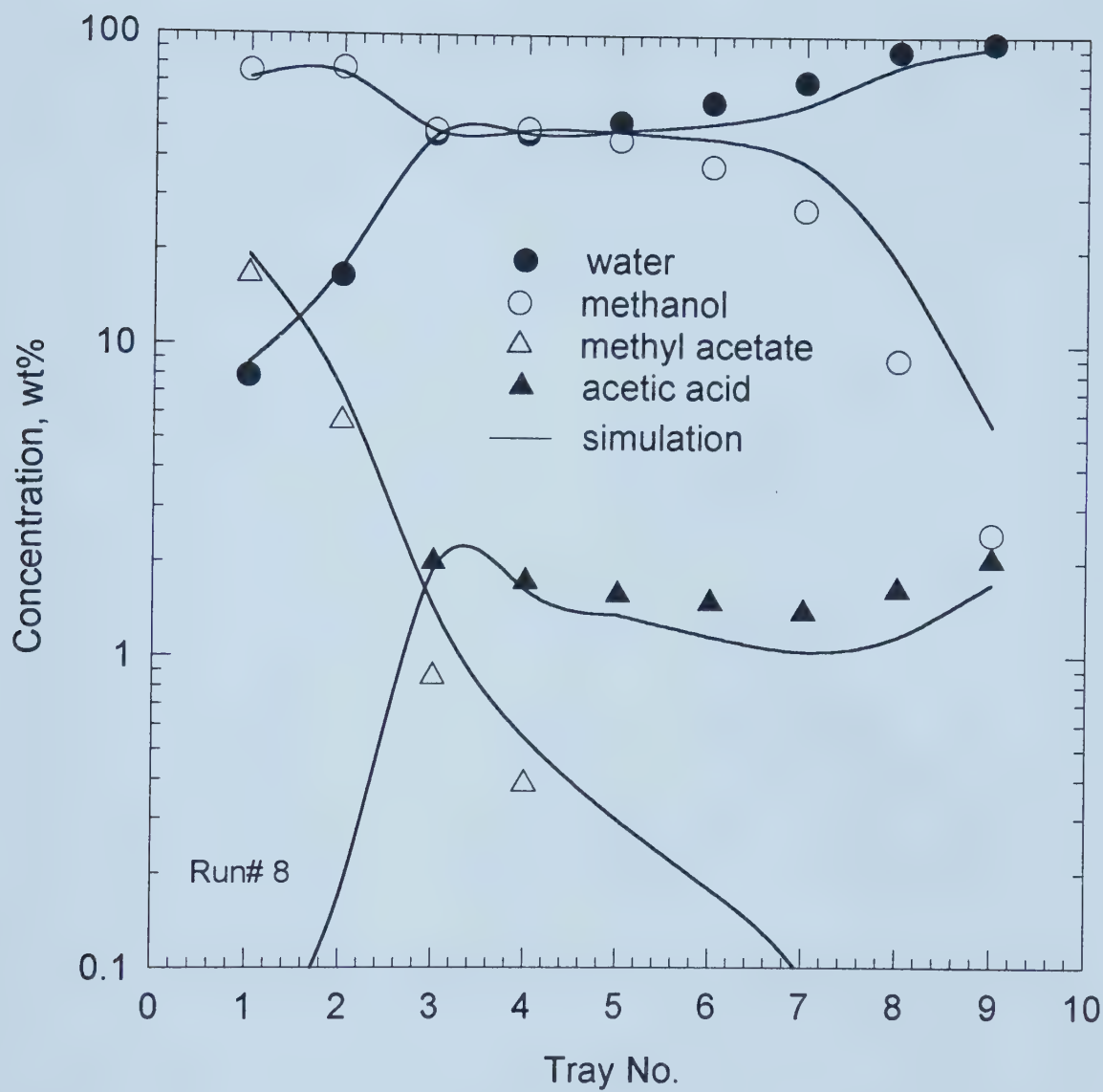


Figure 8-5. Simulation of Run #8 with Top Product Rate of 27.6 g/min.





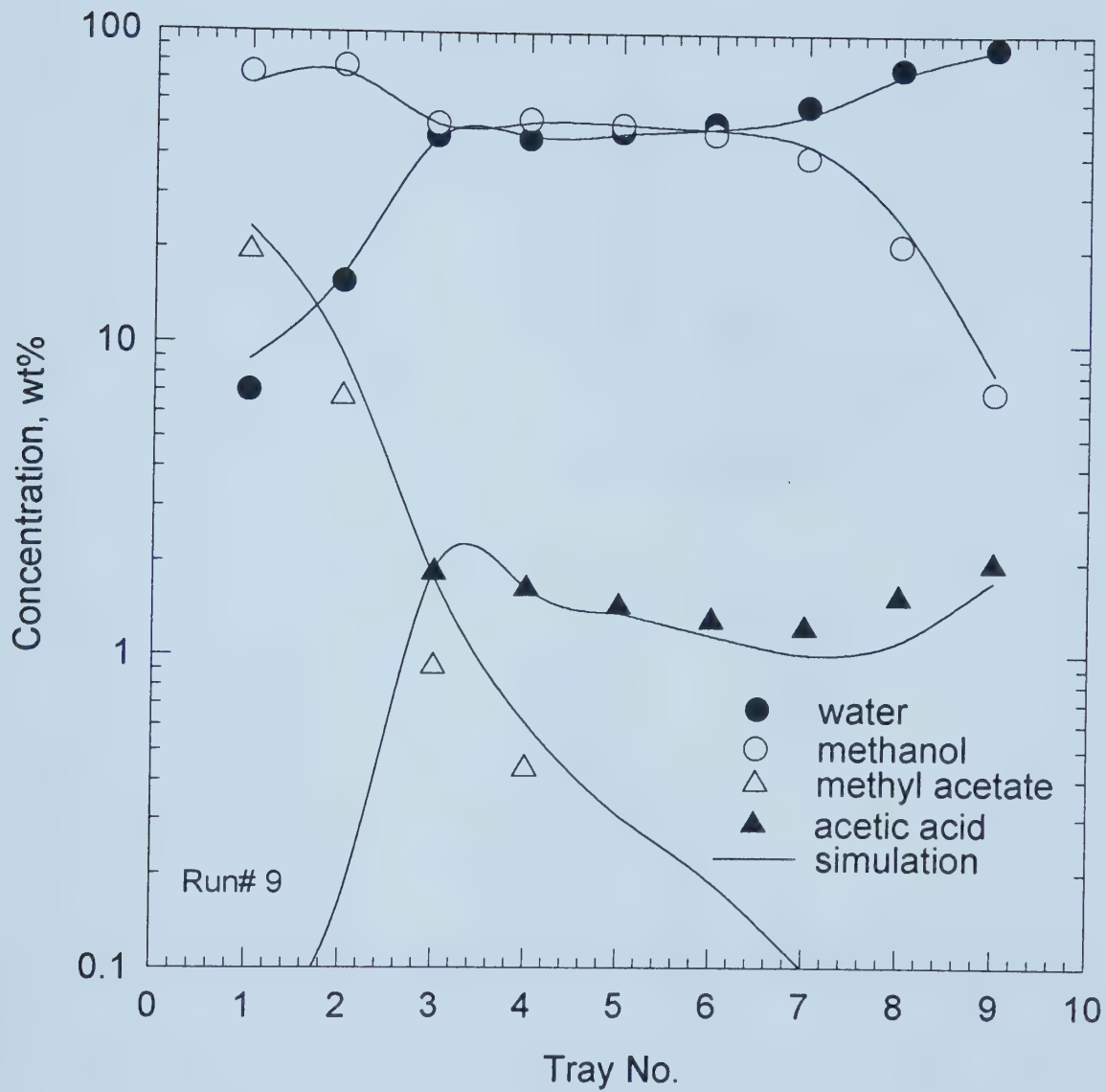


Figure 8-6. Simulation of Run #9 with Top Product Rate of 23.3 g/min.



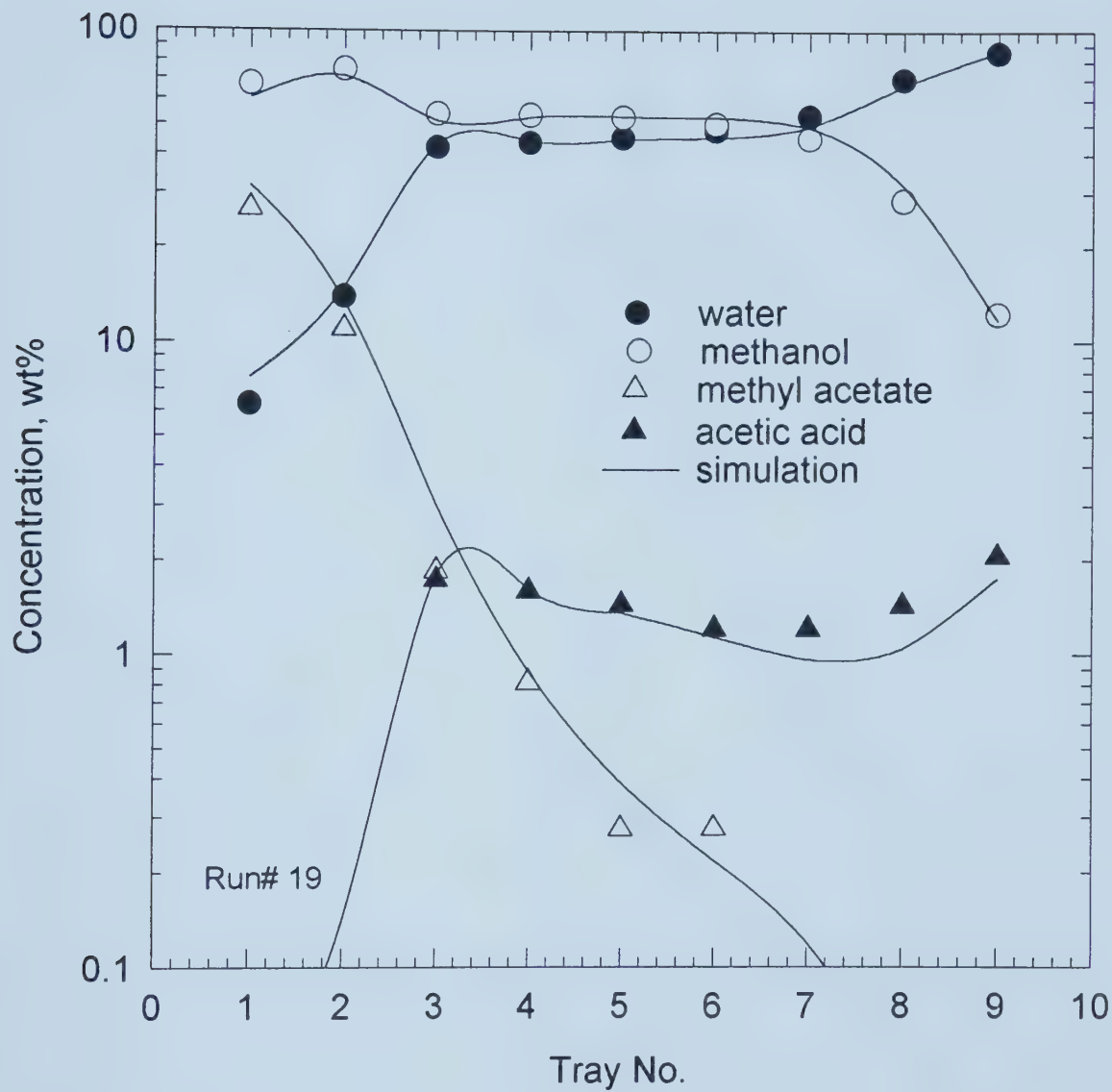


Figure 8-7. Simulation of Run #19 with Top Product Rate of 16.7 g/min.



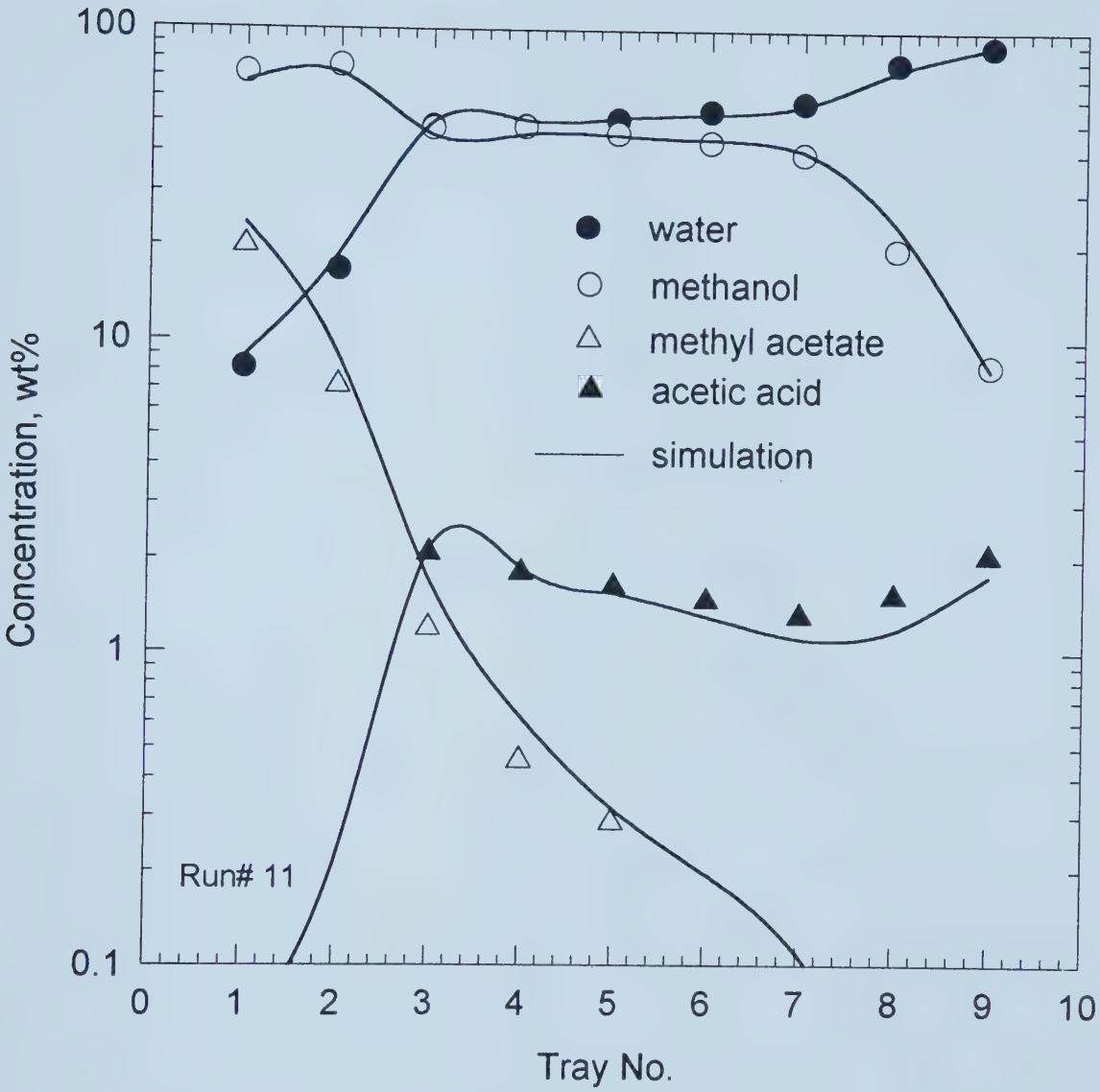


Figure 8-8. Simulation of Run #11 with Reflux Ratio of 10.2.



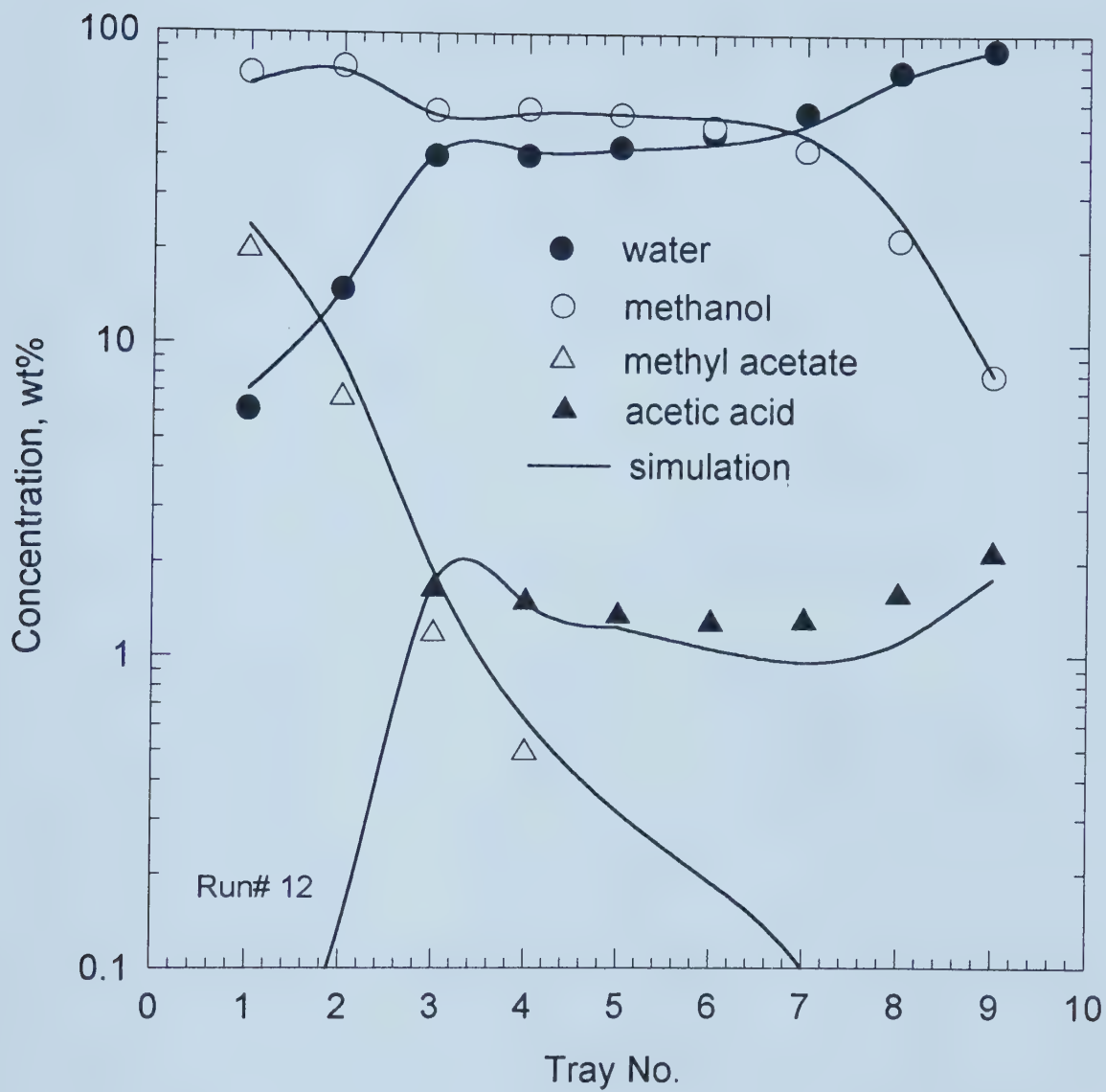


Figure 8-9. Simulation of Run #12 with Reflux Ratio of 14.8.





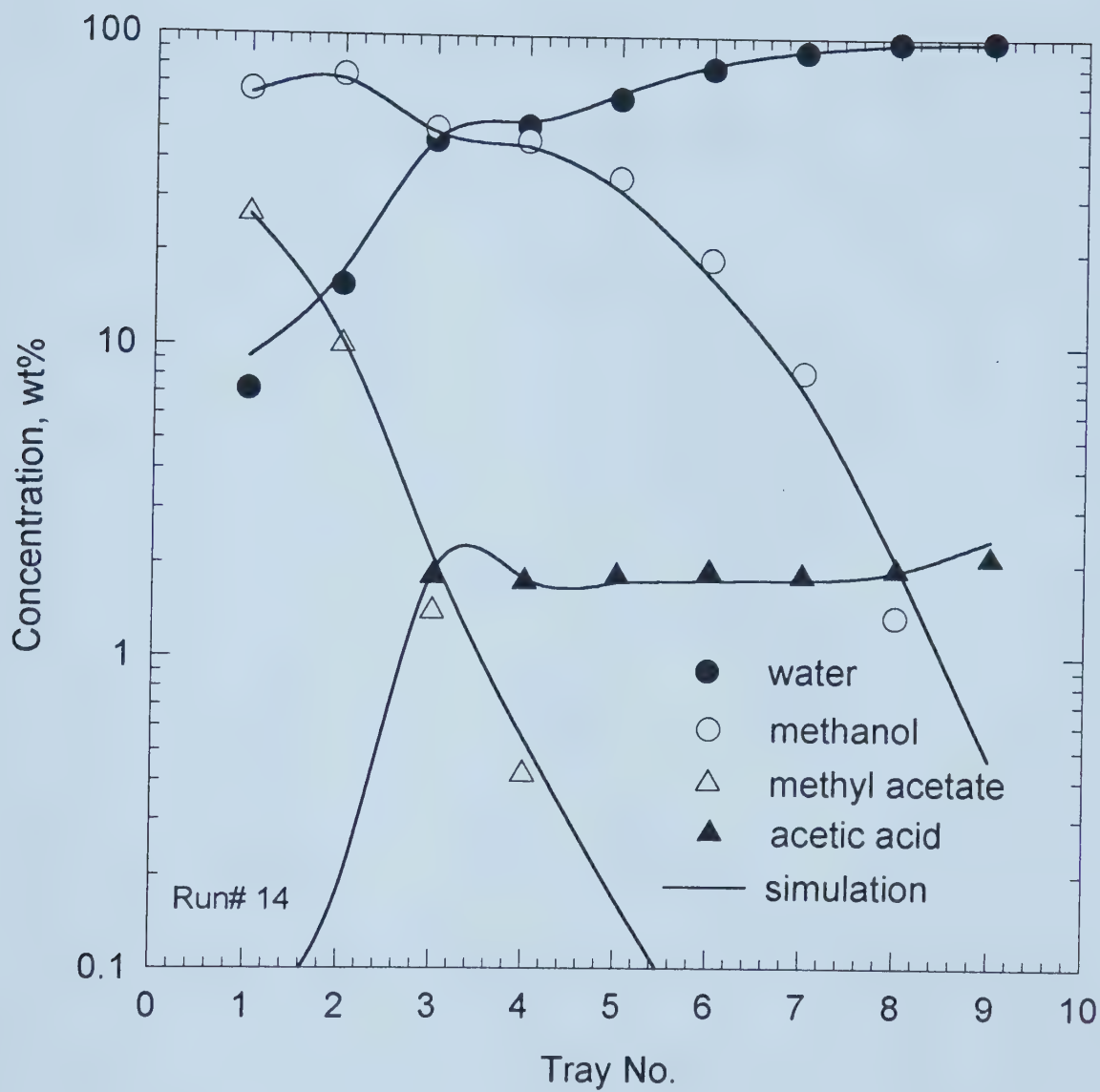


Figure 8-10. Simulation of Run #14 with a Methanol to Acetic Acid Feed Ratio of

3.7.



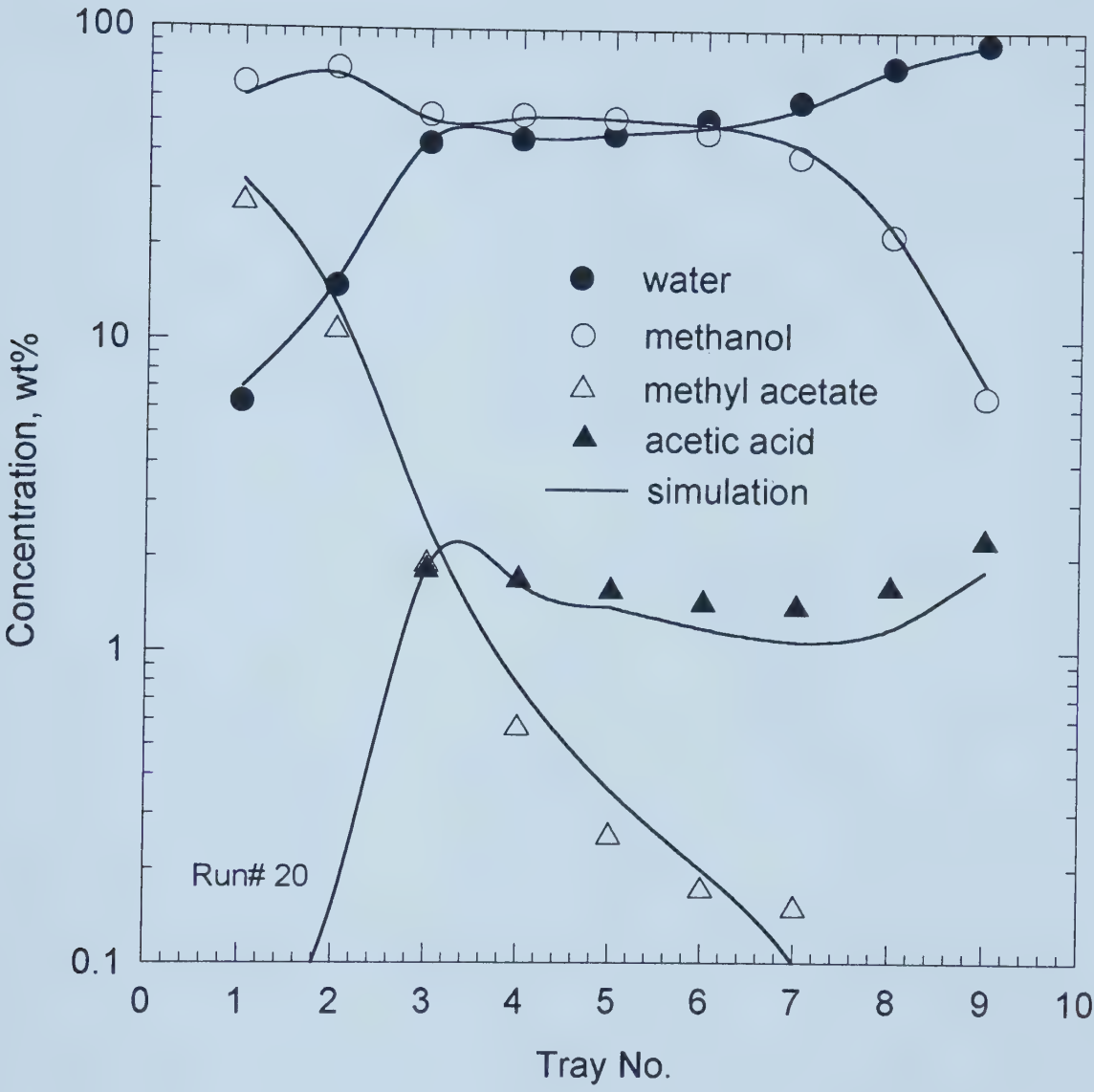


Figure 8-11. Simulation of Run #20 with a Methanol to Acetic Acid Feed Ratio of 6.1.



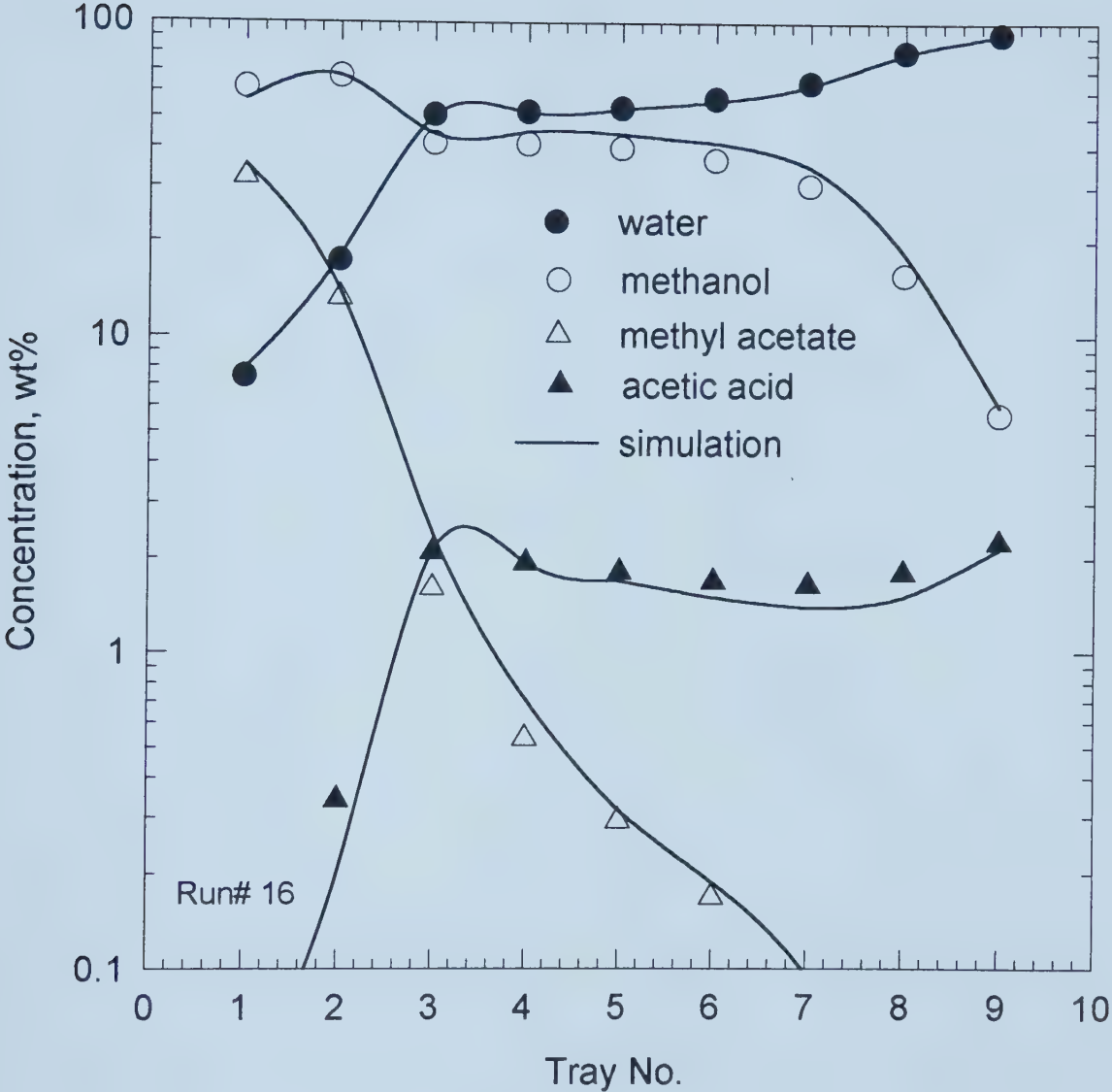


Figure 8-12. Simulation of Run #16 with a Acetic Acid-Water Feed Rate of 180 g/min.



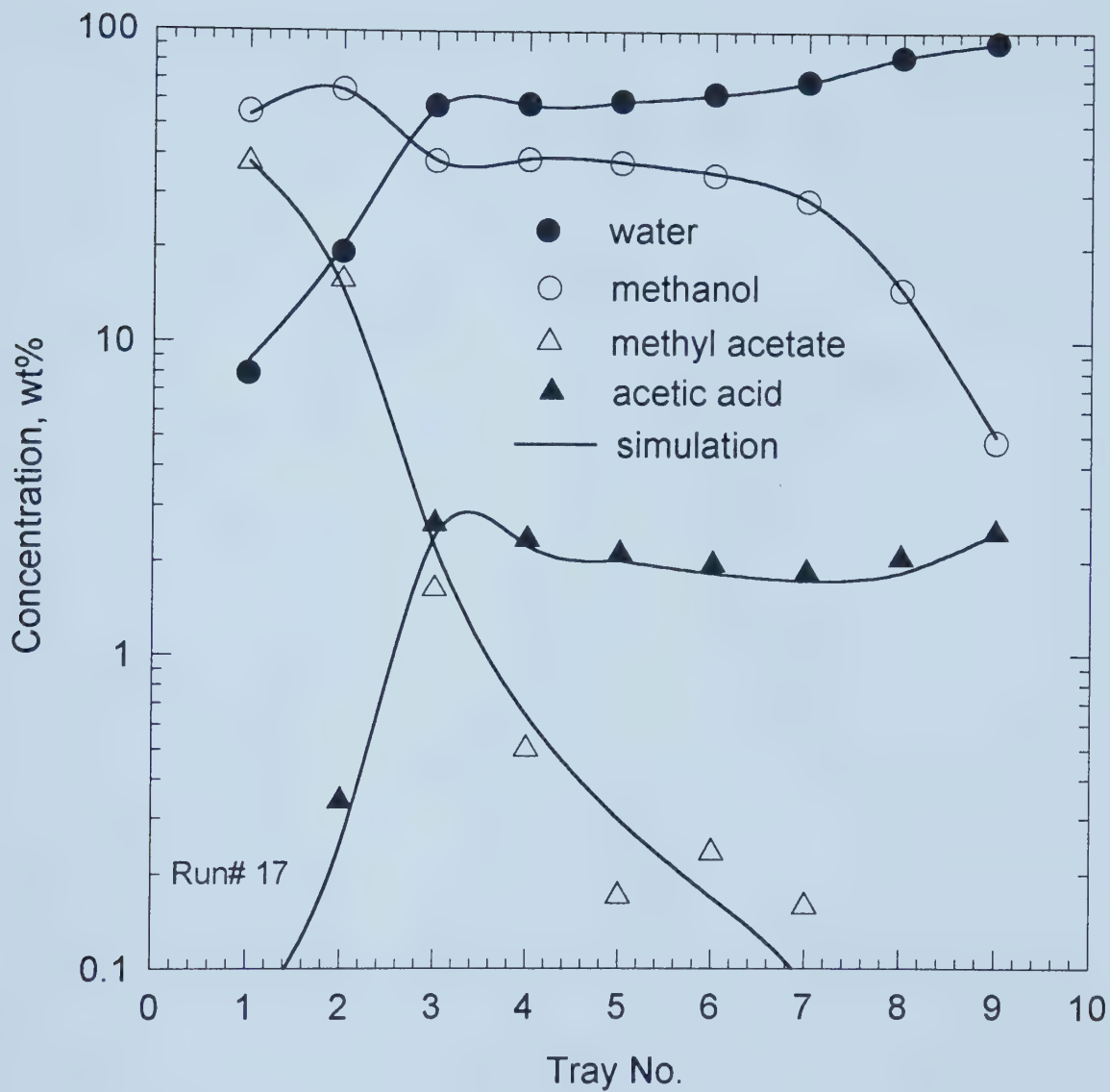


Figure 8-13. Simulation of Run #17 with a Acetic Acid-Water Feed Rate of 220 g/min.





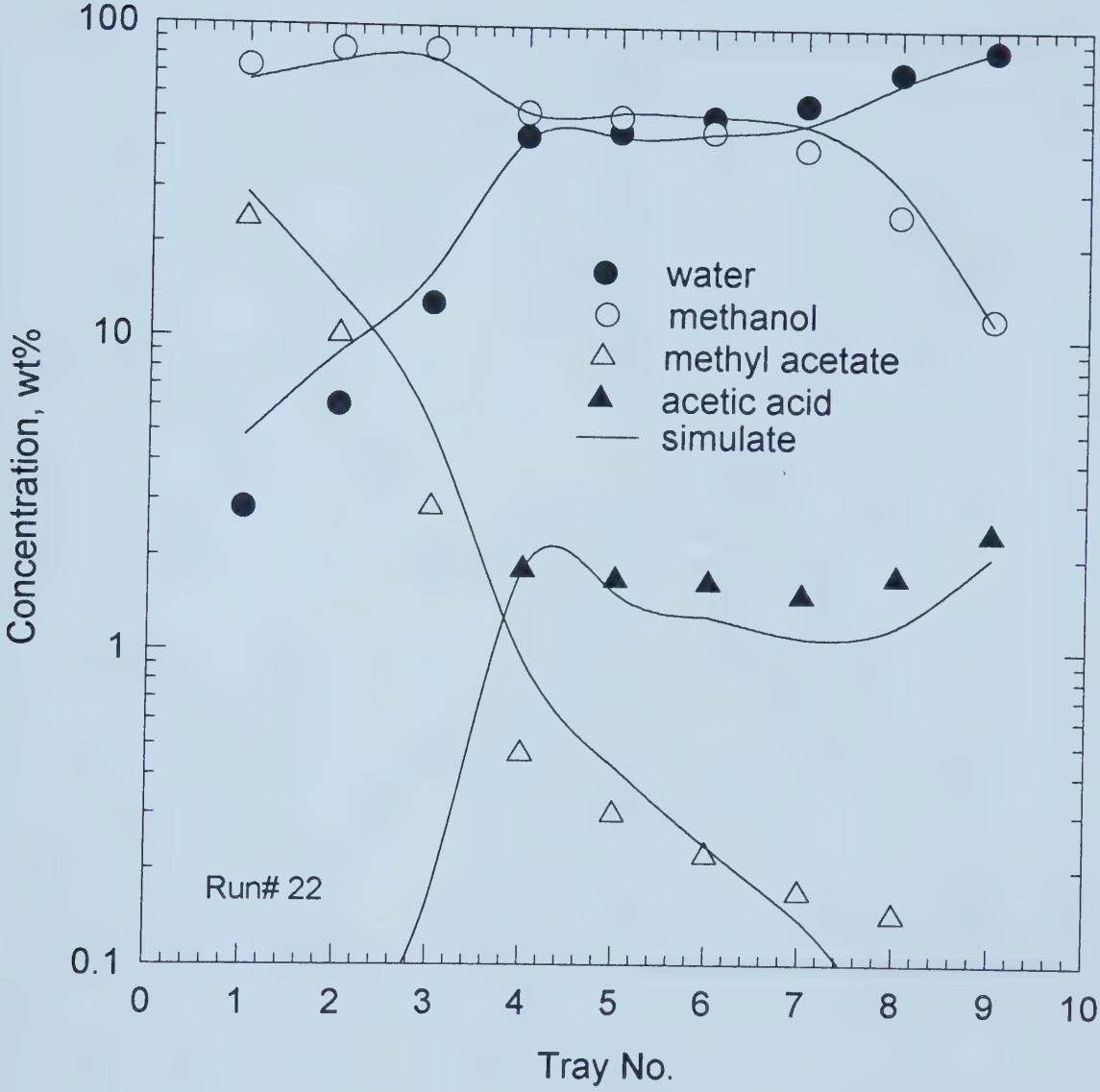


Figure 8-14. Simulation of Run #22 with Acetic Acid-Water Feed Moved down.



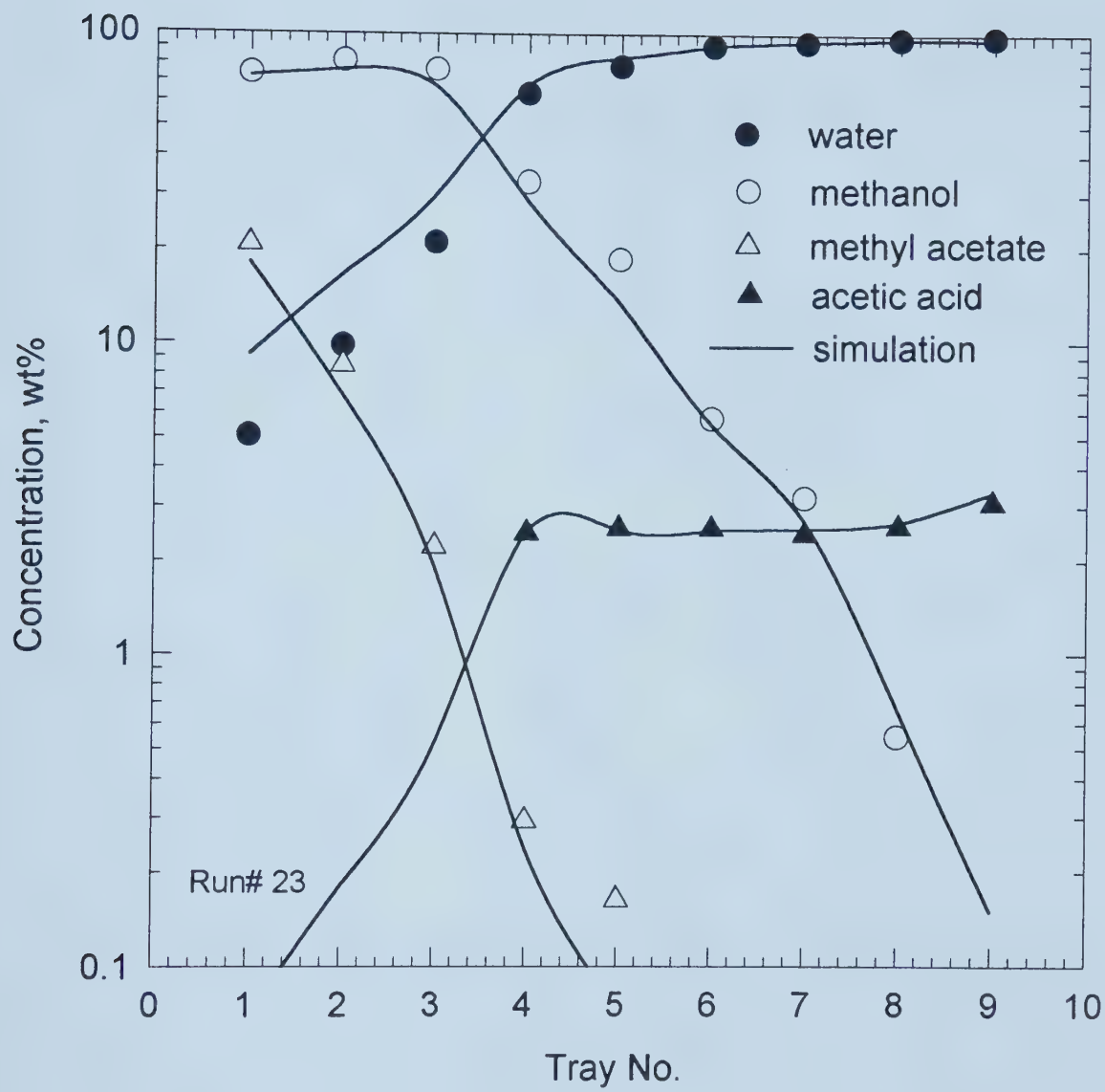


Figure 8-15. Simulation of Run #23 with Acetic Acid-Water Feed Moved down.



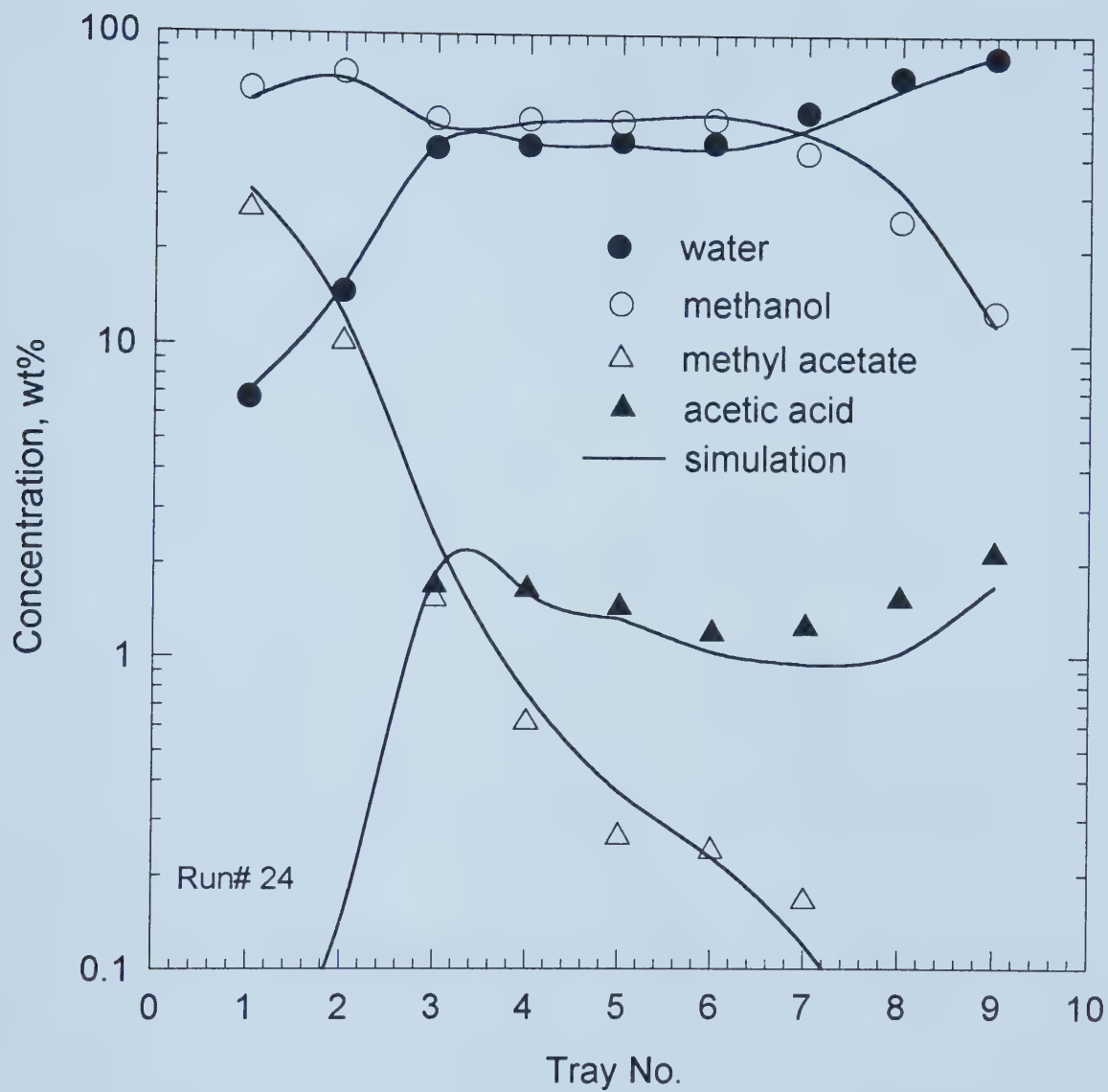


Figure 8-16. Simulation of Run #24 with Methanol Feed Moved up.



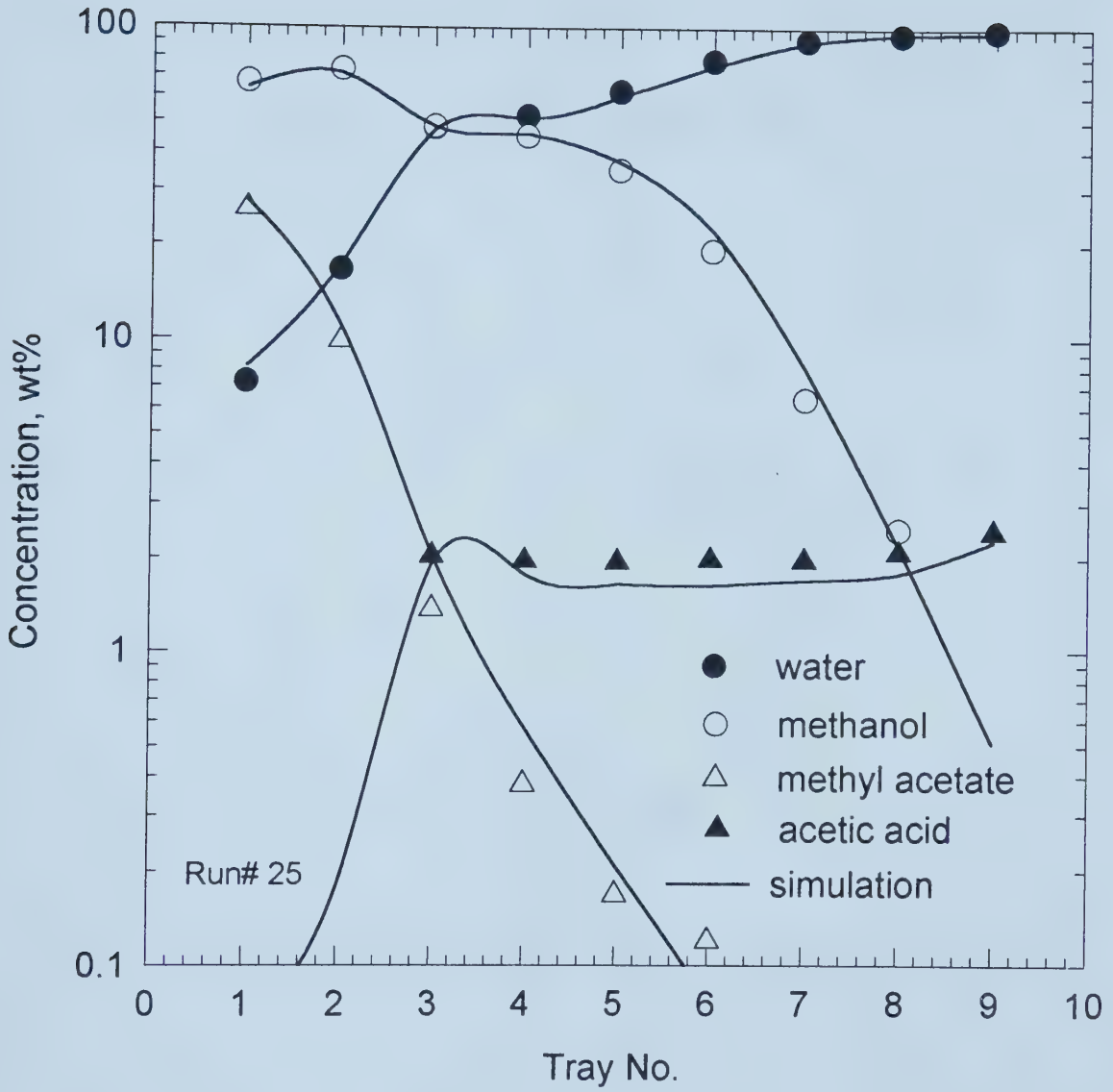


Figure 8-17. Simulation of Run #25 with Methanol Feed Moved up.





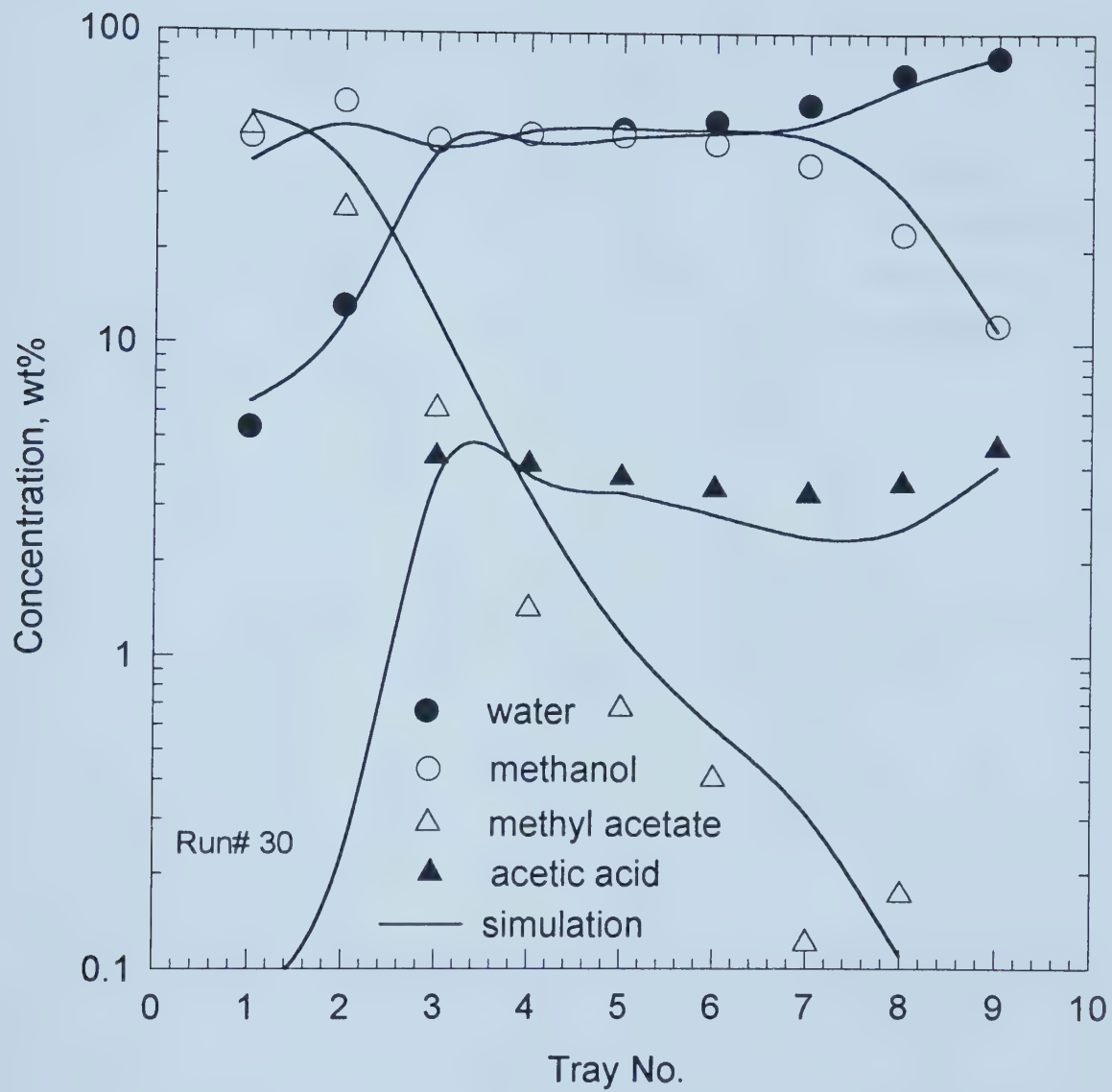


Figure 8-18. Simulation of Run #30 with Acetic Acid Feed Containing 9.9 wt% of Acetic Acid.



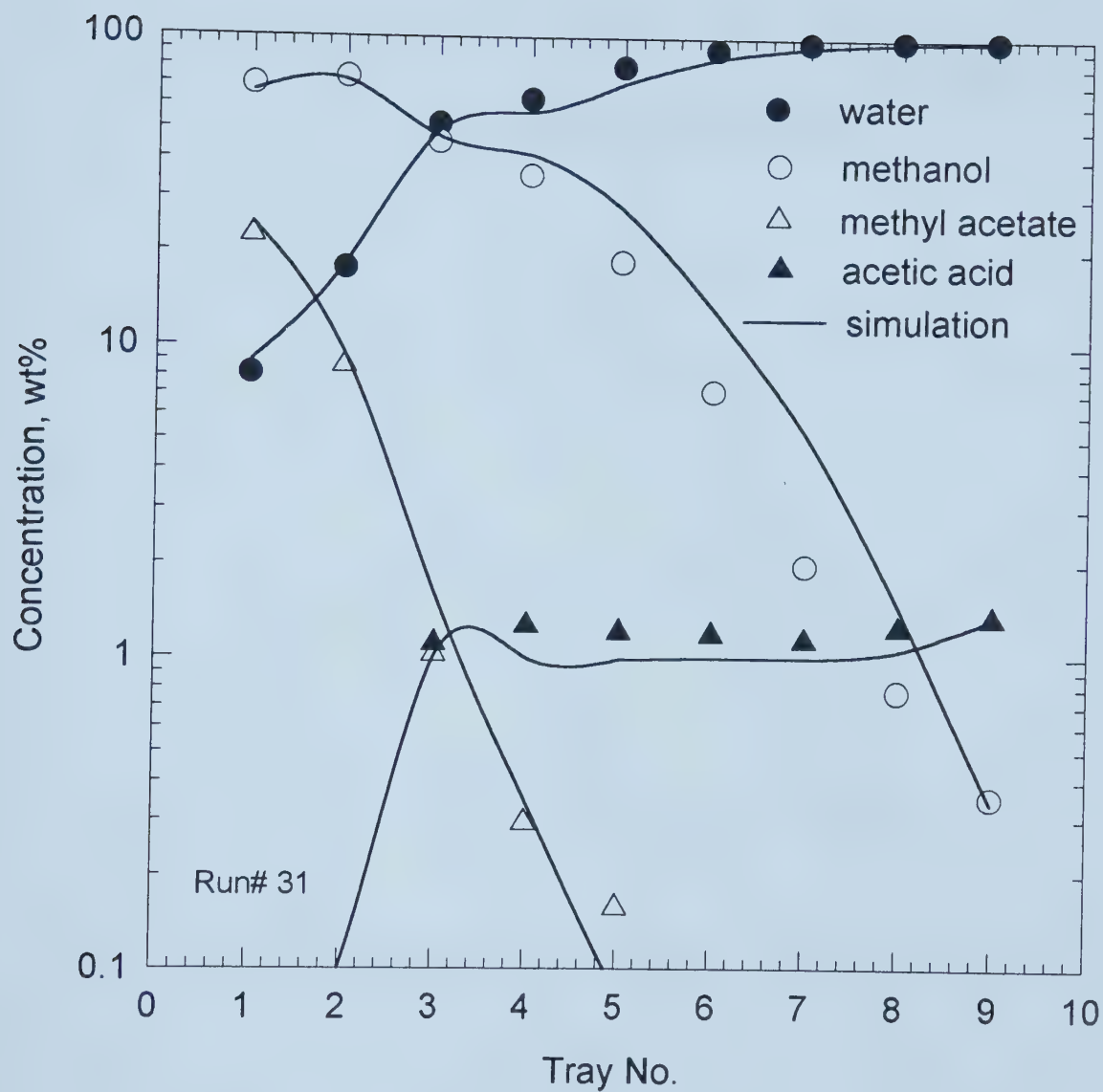


Figure 8-19. Simulation of Run #31 with Acetic Acid Feed Containing 2.55 wt% of Acetic Acid.



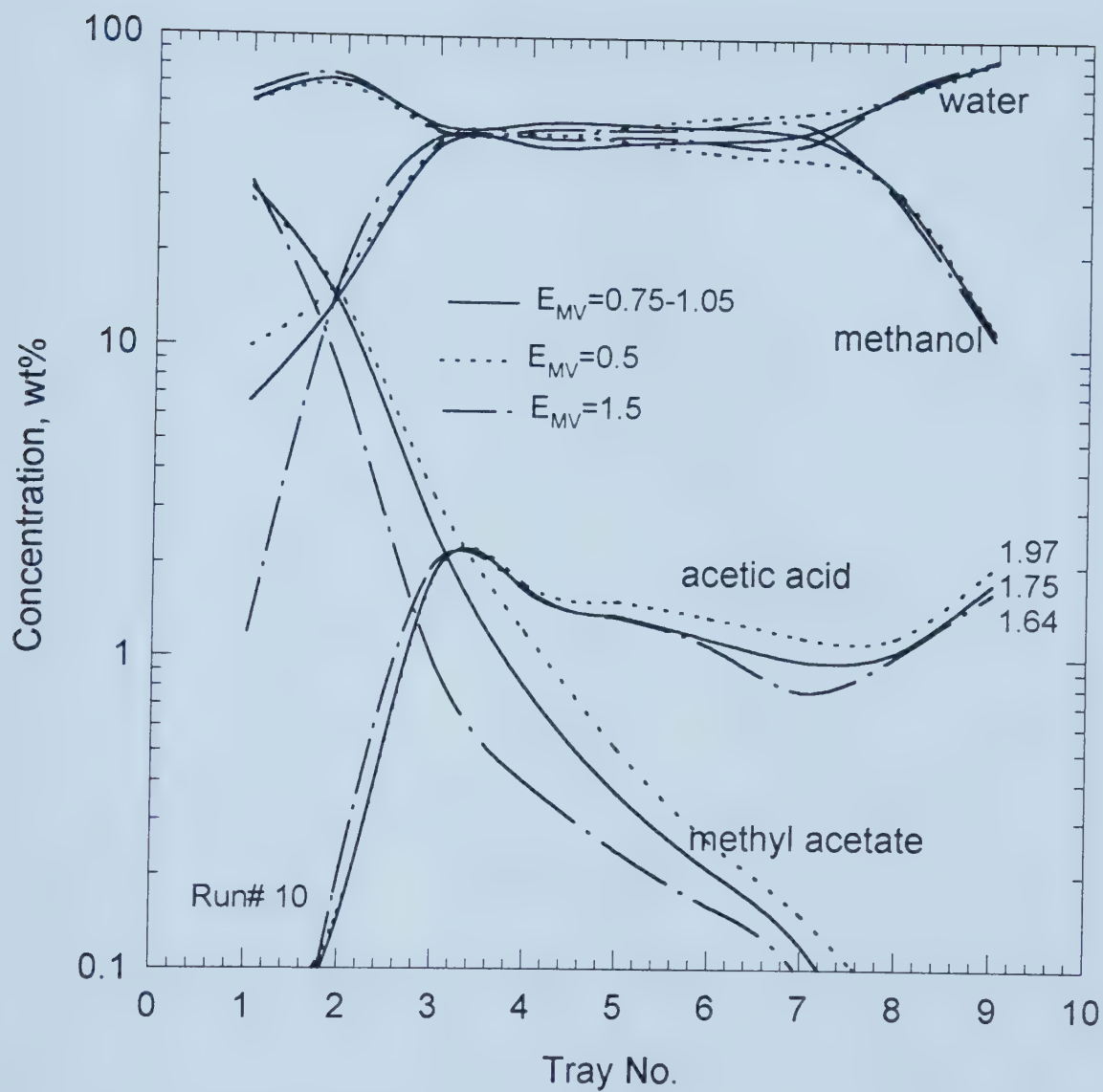


Figure 8-20. Simulation for the Effect of Tray Efficiency.



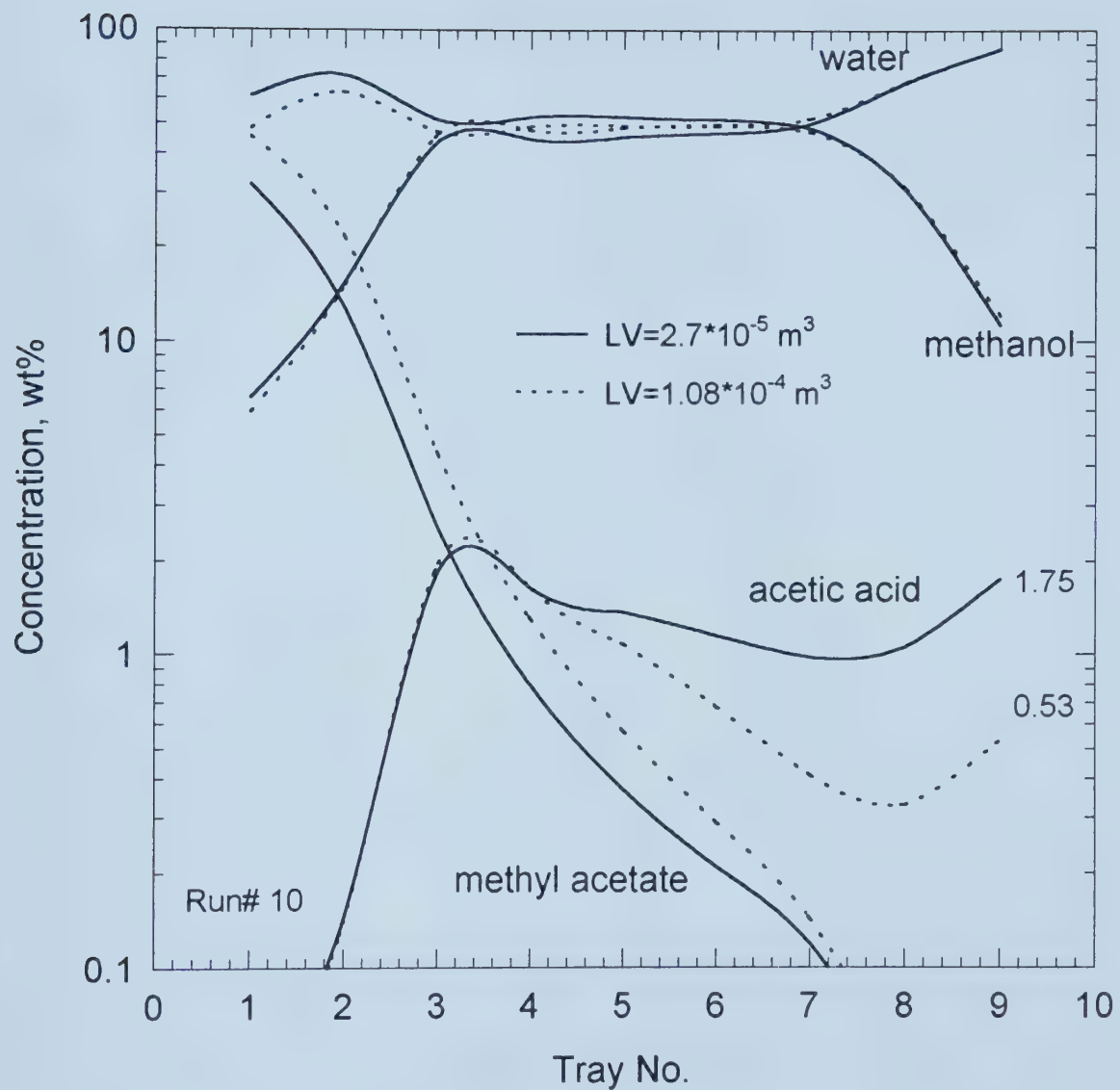


Figure 8-21. Simulation for the Effect of Liquid Hold-up.





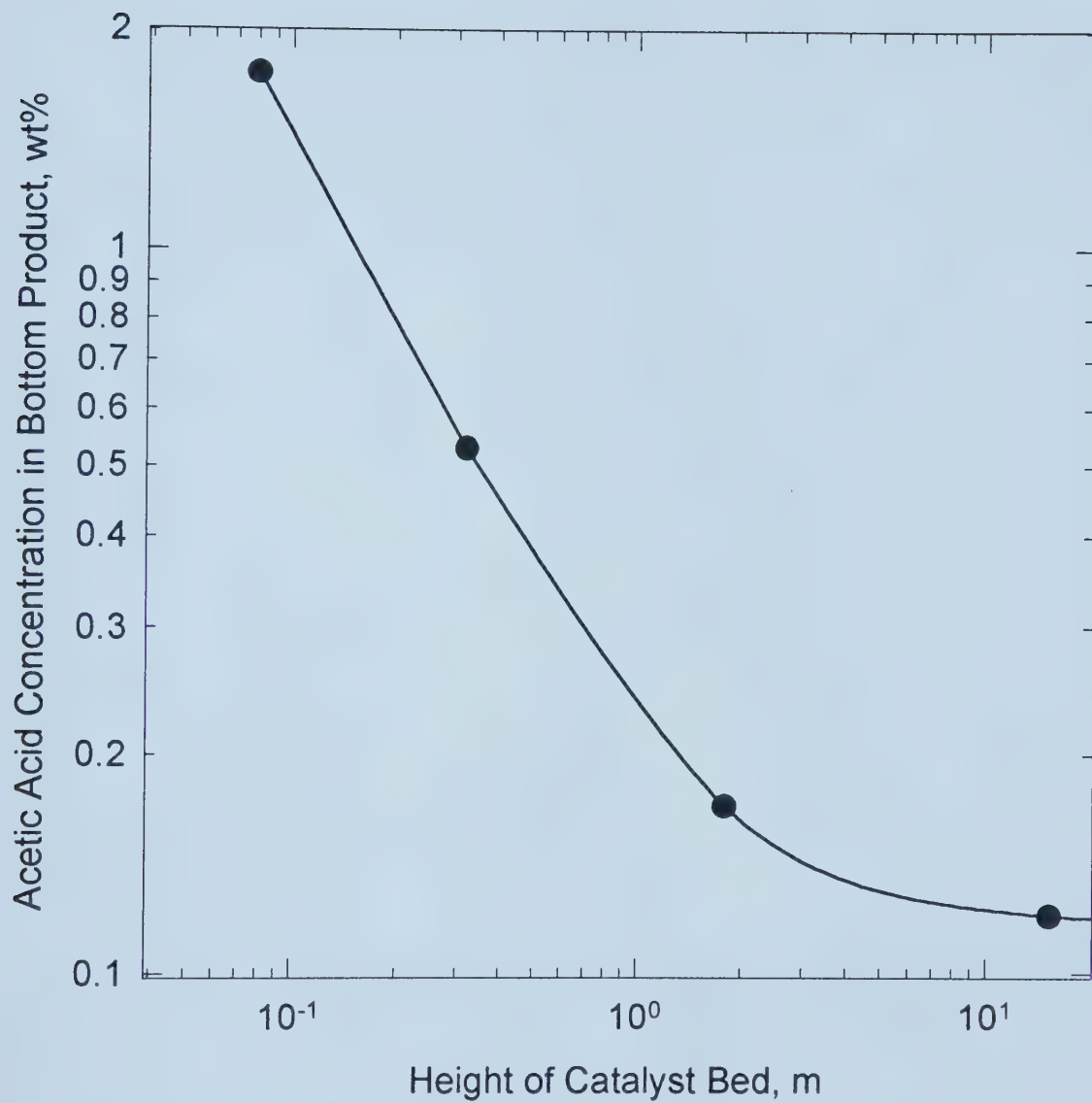


Figure 8-22. Simulation for the Effect of Catalyst Bed Height on Acid Removal.



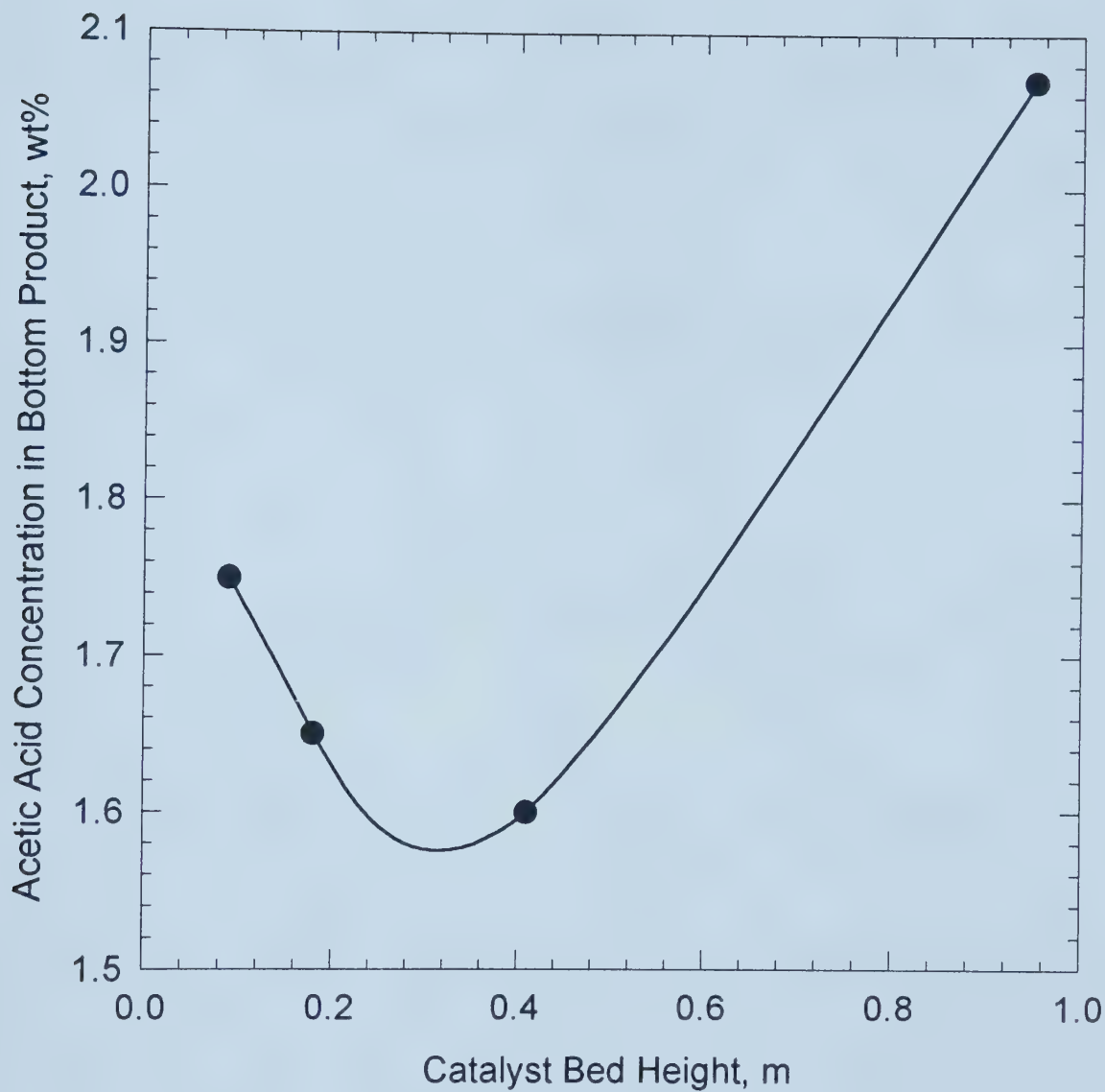


Figure 8-23. Simulation for Optimum Height of the Catalyst Bed.



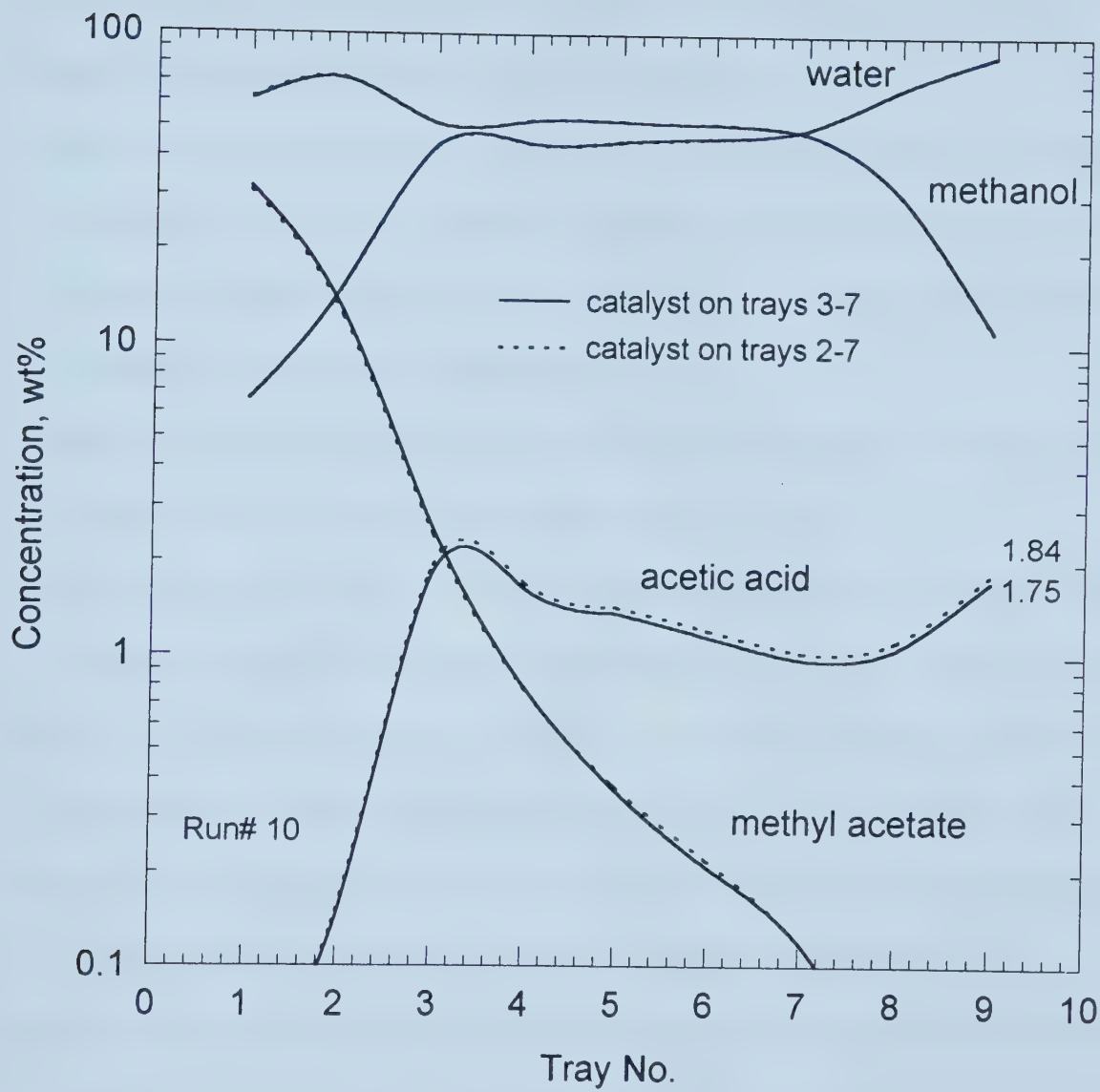


Figure 8-24. Simulation for the Effect of Catalyst Zone.



## 8.7 Literature Cited

- Aspen Technology, Inc. (1996) *Aspen Plus*, version **9.3**, Cambridge, Massachusetts.
- Boston, J.F. (1970) Ph.D. Thesis, Tulane University, New Orleans.
- Boston, J.F. (1980) Inside-Out Algorithms for multicomponent Separation Process Calculations. In *Computer Applications to Chemical Engineering-Process Design and Simulation: based on a symposium*, ACS Symposium Series. 124, pp.135-151, American Chemical Society, Washington, D.C.
- Boston, J.F. and Britt, H.I. (1978) A. Radically Different Formulation and Solution of the Single-Stage Flash Problem. *Comput. Chem. Eng.* **2**, 109-122.
- Boston, J.F. and Sullivan, S.L. (1972) An Improved Algorithm for Solving the Mass Balance Equations in Multistage Separation Process. *Can. J. Chem. Eng.* **50**, 663-669.
- Boston, J.F. and Sullivan, S.L. (1974) A New Class of Solution Methods for Multicomponent, Multistage Separation processes. *Can. J. Chem. Eng.* **52**, 52-63.
- Chang, Y.A. and Seader, J.D. (1988) Simulation of Continuous Reactive Distillation by a Homotopy-Continuation Method. *Comput. Chem. Eng.* **12**, 1243-1255.
- Holland, C.D. (1981) *Fundamentals of Multicomponent Distillation*, McGraw-Hill, New York.
- Hyprotech, Ltd. (1992) *HYSIM User's Guide*, Version 2.0, Hyprotech, Ltd., Calgary.
- Izarraraz, A., Bentzen, G.W., Bentzen, G.W., Antony, R.G. and Holland, C.D. (1980) Solve More Distillation Problems Part 9-When Chemical Reactions Occur. *Hydrocarbon Processing* **59**(4), 195-203.





- Jelinek, J. and Hlavacek, V. (1976) Steady State Countercurrent Equilibrium Stage Separation with Chemical Reaction by Relaxation Method. *Chem. Eng. Commun* **2**, 79-85.
- Kaibel, G., Mayer, H.H. and Seid, B. (1979) Reaction in Distillation Columns. *Ger. Chem. Eng.* **2**, 180-187.
- Kinoshita, M., Hashimoto, I. and Takamatsu, T (1983) A New Simulation Procedure for Multicomponent Distillation Column Processing Nonideal Solutions or Reactive Solutions. *J. Chem. Eng. Jpn* **16**, 370-377.
- Kister, H.Z. (1992) *Distillation Design*, McGraw-Hill, Inc., New York.
- Komatsu, H. (1977) Application of the Relaxation Method for Solving Reacting Distillation Problems. *J. Chem. Eng. Jpn* **10**, 200-205.
- Komatsu, H. and Holland, C.D. (1977) A New Method of Convergence for Solving Reactive Distillation Problems. *J. Chem. Eng. Jpn* **10**, 292-297.
- Krishanmurthy R. and Taylor, R. (1985a) A Nonequilibrium Stage Model of Multicomponent Separation Processes Part 1 Model Description and Method of Solution. *AIChE J.* **31**, 449-455.
- Krishanmurthy R. and Taylor, R. (1985b) Simulation of Packed Distillation and Absorption Columns. *Ind. Eng. Chem. Process Des. Dev.* **24**, 513-524.
- Marek, J. (1955) Vapor-Liquid Equilibrium in Mixtures Containing an Associating Substance. II. Binary Mixtures of Acetic Acid at Atmospheric Pressure. *Collection Czechoslov. Chem. Commun.* **20**, 1490-1502.



- Marek, J. and Standart, G. (1954) Vapor-Liquid Equilibrium in Mixtures Containing an Associating Substance. I. Equilibrium Relationships for Systems with an Associating Component. *Collection Czechoslov. Chem. Commun.* **19**, 1074-1084.
- Mori, H., Yamada, I., Hiraoka, S., Tsuiki, T. and Moriya, A. (1989) A Relaxation Algorithm for Solving Operation-type Distillation Problems with a Chemical Reaction. *International Chem. Eng.* **29**, 328-335.
- Murthy, A.K.S. (1984) Simulation of Distillation Column Reactors. In *Proc. Summer Computer Simulation Conference*, 630-635.
- Naphtali L. and Sandholm, D.P. (1971) Multicomponent Separation Calculations by Linearization. *AIChE J.* **17**, 148-153.
- Nelson, P.A. (1971) Countercurrent Equilibrium Stage Separation with Reaction. *AIChE J.* **17**, 1043-1049.
- Russell, R.A. (1983) A Flexible and Reliable Method Solves Single-Tower and Crude-Distillation-Column Problems. *Chem. Eng.* **90**(21), 53-59.
- Simandl, J. (1988) *Simulation of Distillation Towers with Chemical Reactions*, Ph.D. Thesis, University of Calgary.
- Simandl, J. and Svrcek, W.Y. (1991) Extension of the Simultaneous-Solution and Inside-Outside Algorithms to Distillation with Chemical Reactions. *Computer Chem. Eng.* **15**, 337-348.
- Simulation Sciences, Inc. (1994) *PROvision (version 1.0, PRO/II 4.0)*, Simulation Sciences, Inc., California.



- Suzuki, I., Yagi, H., Komatsu, H. and Hirata, M. (1971) Calculation of Multicomponent Distillation Accompanied by a Chemical Reaction. *J. Chem. Eng. Jpn* **4**, 26-33.
- Taylor, R., Powers, M.F., Lao, M. and Arehole, A. (1987) The Development of a Nonequilibrium Model for Computer Simulation of Multicomponent Distillation and Absorption Operations. *I. Chem. E. Symposium Series* No. 104, B321-335, Institution of Chemical Engineers, London.
- Tierney, J.W. and Bruno, J.A. (1967) Equilibrium Stage Calculations. *AIChE J.* **13**, 556-563.
- Tierney, J.W. and Riquelme, G.D. (1982) Calculation Methods for Distillation Systems with Reaction. *Chem. Eng. Commun.* **16**, 91-108.
- Tierney, J.W. and Yanosik, J.L. (1969) Simultaneous Flow and Temperature Correction in the Equilibrium Stage Problem. *AIChE J.* **15**, 897-901.
- Venkataraman S., Chan, W.K. and Boston, J.F. (1990) Reactive Distillation Using ASPEN PLUS. *Chem. Eng. Prog.* **86**(8), 45-54.
- Wang, J.C. and Henke, G.E. (1966) Tridiagonal Matrix for Distillation. *Hydrocarbon Processing* **45**(8), 155-163.
- Xu, X. and Chen, H. (1988) Simulation of Distillation Processes with Reactions in Series. *J. of Chem. Industry and Engineering (China)* **3**(1), 57-69.
- Zhang, R. (1989) Simulation of Tray-type Reactive Distillation Columns. *J. of East China Institute of Chemical Technology* **15**(1), 25-31.



Zheng, Y. and Xu, X. (1992) Study on Catalytic Distillation Processes Part II Simulation of Catalytic Distillation Processes-Quasi-Homogeneous and Rate-Based Model. *Trans. IChemE Part A* **70**, 465-470.





## CHAPTER 9. CONCLUSIONS AND RECOMMENDATIONS

A catalytic distillation process for the removal of dilute acetic acid from water was studied in a 100 mm diameter column installed with a novel column internal composed of dualflow trays and catalyst units. The performance of the catalytic distillation column is dependent on many factors such as reaction rate, separation efficiency, flowsheet, column internals and operating conditions. Detailed studies were conducted on the reaction kinetics, vapor-liquid equilibrium and component tray efficiencies for the modeling and simulation of the catalytic distillation process, the design of the test column and the analysis of the experimental data.

Kinetic measurements were conducted in a one litre batch reactor (Xu and Chuang, 1996). Methanol was added to the dilute acetic acid solution and reacted with the acid in water to form methyl acetate and water. The reaction can be accelerated by solid acid catalysts. It was found that Amberlyst 15 (supplied by Rohm and Haas, USA) was an effective catalyst for this reaction. The effects of stirrer speed, reaction temperature, reactant concentration and catalyst loading on the reaction rate were investigated. The external resistance to the reaction process was insignificant in the test range of stirrer speeds from 160 to 760 rpm. The effect of temperature on the reaction rate was found to be significant and a relatively high activation energy (58.5 kJ/mol) was obtained for the reaction. The reaction rate is proportional to the catalyst loading. Based on the experimental results, a complete kinetic equation for describing the reaction catalyzed by



Amberlyst 15 was developed. This equation was used in the simulation and design of the catalytic distillation column for removing acetic acid from wastewater.

A theoretical analysis was performed to determine the effect of internal diffusion on the second-order reversible esterification of acetic acid with methanol catalyzed by the solid acid catalyst, Amberlyst 15 (Xu and Chuang, 1997a). The results of the analysis show that the catalyst effectiveness factors are greater than 0.94 for beads smaller than 0.6 mm diameter at a reaction temperature lower than 80 °C. However, the effectiveness factors were less than 0.77 for beads larger than 1.0 mm diameter at reaction temperatures higher than 94 °C. For Amberlyst 15 with an average particle size of 0.7 mm diameter, an overall effectiveness factor of 0.87 was predicted for a reaction temperature of 94 °C. The predicted effectiveness factors agree with those obtained from the kinetic measurements.

The vapor-liquid equilibrium of the methyl acetate-methanol-water-acetic acid system has been measured and correlated using third order Margules equations (Marek, 1954) by Sawistowski and Pilavakis (1982). In this study, a new correlation for the prediction of the system vapor-liquid equilibrium was developed (Xu and Chuang, 1997b). It is based on the NRTL model for predicting liquid activity coefficients and Marek's method (Marek and Standart, 1954; Marek, 1955) for predicting the vapor-liquid equilibrium of the system containing associating components. When compared with the model developed by Sawistowski and Pilavakis (1982), the new correlation has few parameters, is easier to incorporate into computer simulation programs and shows a better agreement with the experimental data (Sawistowski and Pilavakis, 1982).



The component tray efficiencies were measured in a 100 mm diameter column. The column and column internals are similar to those used in the catalytic distillation tests. The column was composed of seven dualflow trays and five catalyst units which are located between the bottom six trays. However, the catalyst baskets were packed with inert glass beads instead of solid acid catalyst to prevent a catalyzed reaction. The middle five trays (trays 2 to 6) were the test trays.

The component tray efficiencies were found to be different from one another. Two components, methanol and water, with middle boiling points have higher but more scattered efficiencies than the other two. The component efficiencies for the trays with catalyst units on them (trays 3 to 6) are mostly between 0.6 to 0.8, 0.9 to 1.2, 0.9 to 1.2, 0.6 to 0.9 for methyl acetate, methanol, water and acetic acid respectively. The efficiencies of tray 2 without the catalyst unit are usually lower because of the lower froth height due to the negative surface tension gradient of the test mixtures at the column top and the absence of mass transfer from the catalyst unit.

Catalytic distillation experiments were conducted with a methanol stream introduced to the lower part of the column and the acetic acid-water mixture to the upper part. An ion exchange resin (Amberlyst 15) was installed in the catalyst units to accelerate the reaction.

Various parameters such as feed composition, feed rate, feed location, top product rate and boil-up rate were investigated for their effect on the removal of acetic acid from water and on product composition. It was found that the feed methanol rate, top product rate and feed location are the most important factors affecting the column performance



(acid removal). In general, an increase in the methanol feed rate and the distance between the two feed locations, and a decrease in the top product rate will improve the column performance because of the resulting higher concentration of methanol in the main reaction zone located between the two feed trays.

When the feed contains 2.5 to 9.9 wt% of acetic acid in water more than 50 wt% of acetic acid can be converted to methyl acetate in the 1.5 metre high test column.

Based on the fundamental studies of reaction kinetics, vapor-liquid equilibrium and component tray efficiencies, a computer program has been set up by incorporating the basic models for kinetics, vapor-liquid equilibrium and column internals into a commercial simulation package, Aspen Plus (Aspen Technology, Inc., 1996). The models and simulation program were verified by comparing the simulation results with a variety of experimental data. It was found that the simulation results agree well with the measured composition profiles for the reaction and separation system at various operating conditions including changes in feed rate, feed composition, feed location, top product rate, and reflux rate.

By using the simulation program, various parameters such as the location of the catalyst units, the height of a catalyst bed between two trays and component tray efficiencies were studied. It was found the effect of component tray efficiencies is insignificant because the process is reaction-controlled. There exists an optimum height of the catalyst bed for a specific case and the optimum value can be obtained from the computer simulation.





With the established simulation program, an industrial column with 25 separation stages and 19 catalyst units was simulated for the removal of acetic acid from water by catalytic distillation. Another process by simple distillation method was also simulated for comparison. The simulation results show that the catalytic distillation needs only half of the separation stages and consumes 14.8% of the energy as simple distillation. By using the catalytic distillation process, the column size is reduced and corrosion problems are avoided.

Further study on this subject should be focused on laboratory experiments and applications to industrial processes.

More laboratory experiments may be conducted using a higher column, for example, three times higher than the existing column. In this case, the height of the catalyst units and feed locations may be changed broadly to further verify the simulation results.

The problem for catalytic distillation internals using dualflow trays is that the operation of dualflow trays is sensitive to the tray level and vapor/liquid loading. They are only suitable for small columns. Novel column internals for large industrial catalytic distillation columns have been designed (Chuang and Xu, 1996a). It is believed that these internals can be used not only for this process but also for many other catalytic distillation applications using solid catalyzed liquid reaction, such as the production of methyl *tert*-butyl ether (MTBE) and *tert*-amyl methyl ether (TAME).

It should be noted that the process studied for the removal of dilute acetic acid from water can be applied to the removal of other carboxylic acids such as formic acid and



acrylic acid as well as the acid mixtures from water (Chuang and Xu, 1996b). Other alcohols such as ethanol and propanol as well as the alcohol mixtures can replace methanol depending on the utility of the reaction products. This process may have many other applications in the future removing dilute heavy chemicals from mixtures.



## 9.1 Literature Cited

- Aspen Technology, Inc. (1996) *Aspen Plus*, version **9.3**, Aspen Technology, Inc., Massachusetts.
- Marek, J. (1955) Vapor-Liquid Equilibrium in Mixtures Containing an Associating Substance. II. Binary Mixtures of Acetic Acid at Atmospheric Pressure. *Collection Czechoslov. Chem. Commun.* **20**, 1490-1502.
- Marek, J. (1954) Quaternary Four-Suffix Margules Equation. *Collection Czechoslov. Chem. Commun.* **19**, 1-3.
- Marek, J. and Standart, G. (1954) Vapor-Liquid Equilibrium in Mixtures Containing an Associating Substance. I. Equilibrium Relationships for Systems with an Associating Component. *Collection Czechoslov. Chem. Commun.* **19**, 1074-1084.
- Sawistowski, H. and Pilavakis, P.A. (1982) Vapor-Liquid Equilibrium with Association in Both Phases. Multicomponent Systems Containing Acetic Acid. *J. Chem. Eng. Data* **27**, 64-71.
- Xu, Z.P. and Chuang, K.T. (1996) Kinetics of Acetic Acid Esterification over Ion Exchange Catalysts. *Can J Chem. Eng.* **74**, 493-500.
- Xu, Z.P. and Chuang, K.T. (1997a) Effect of Internal Diffusion on Heterogeneous Catalytic Esterification of Acetic Acid. *Chem. Eng. Sci.*, in press.
- Xu, Z.P. and Chuang, K.T. (1997b) Correlation of Vapor-Liquid Equilibrium Data for Methyl Acetate-Methanol-Water-Acetic Acid Mixtures. *Ind. Eng. Chem. Res.* **36**, 2866-2870.



Chuang, K.T. and Xu, Z.P. (1996a) Apparatus for Catalytic Distillation. Applying for US patent.

Chuang, K.T. and Xu, Z.P. (1996b) Distillation Process. Applying for US patent.





## **APPENDIX. Input And Output Files For The Simulation Of Catalytic Distillation Using Aspen Plus**

Input File: pp. 251-253

Output File: pp. 254-260

Case: Run #10 for removal of acetic acid from water

Operating Conditions:

methanol feed: 30 g/min, 50 °C, tray 2

acid-water feed: 140 g/min, 70 °C, tray 6, 5 wt% acid

reflux: 323.9 g/min, 29 °C

top product: 16.9 g/min

catalyst units: on trays 3 to 7



TITLE 'CATALYTIC DISTILLATION'

IN-UNITS MET VOLUME-FLOW='CUM/HR' ENTHALPY-FLO='MMKCAL/HR' &  
 HEAT-TRANS-C='KCAL/HR-SQM-K' PRESSURE=BAR TEMPERATURE=C &  
 VOLUME=CUM DELTA-T=C HEAD=METER MOLE-DENSITY='KMOL/CUM' &  
 MASS-DENSITY='KG/CUM' MOLE-ENTHALP='KCAL/MOL' &  
 MASS-ENTHALP='KCAL/KG' HEAT=MMKCAL MOLE-CONC='MOL/L' &  
 PDROP=BAR

DEF-STREAMS CONVEN ALL

DATABANKS PURECOMP / AQUEOUS / SOLIDS / INORGANIC / &  
 NOASPENPCD

PROP-SOURCES PURECOMP / AQUEOUS / SOLIDS / INORGANIC

COMPONENTS

MEAC C3H6O2-3 MEAC /  
 MEOH CH4O MEOH /  
 WATER H2O WATER /  
 HAC C2H4O2-1 HAC

FLWSHEET

BLOCK B1 IN=F1 F2 OUT=TP BP

PROPERTIES NRTL-HOC

PROP-DATA NRTL-1

IN-UNITS SI

PROP-LIST NRTL

BPVAL MEAC MEOH 0.0 284.9 .37 0.0 0.0 0.0 0.0 &  
 1000.0

BPVAL MEOH MEAC 0.0 230.0 .37 0.0 0.0 0.0 0.0 &  
 1000.0

BPVAL MEAC WATER 0.0 442.4 .37 0.0 0.0 0.0 0.0 &  
 1000.0

BPVAL WATER MEAC 0.0 860.3 .37 0.0 0.0 0.0 0.0 &  
 1000.0

BPVAL MEAC HAC 0.0 613.4 .37 0.0 0.0 0.0 0.0 1000.0

BPVAL HAC MEAC 0.0 -320.0 .37 0.0 0.0 0.0 0.0 1000.0

BPVAL MEOH WATER 0.0 -123.80 .37 0.0 0.0 0.0 0.0 &  
 1000.0

BPVAL WATER MEOH 0.0 463.7 .37 0.0 0.0 0.0 0.0 &  
 1000.0

BPVAL MEOH HAC 0.0 -19.90 .37 0.0 0.0 0.0 0.0 &  
 1000.0

BPVAL HAC MEOH 0.0 .29 .37 0.0 0.0 0.0 0.0 1000.0

BPVAL WATER HAC 0.0 493.8 .37 0.0 0.0 0.0 0.0 &  
 1000.0

BPVAL HAC WATER 0.0 -94.5 .37 0.0 0.0 0.0 0.0 &  
 1000.0

PROP-SET TRANSPOT RHOMX KINVIS MUMX SIGMAMX UNITS='KG/CUM' &  
 'SQM/SEC' 'CP' 'DYNE/CM' SUBSTREAM=MIXED PHASE=L V

STREAM F1

SUBSTREAM MIXED TEMP=70.0 PRES=0.95

MASS-FLOW MEAC 0.0 / MEOH 0.0 / WATER 7974.5 / HAC &  
 425.5



## STREAM F2

SUBSTREAM MIXED TEMP=50.0 PRES=0.95  
 MASS-FLOW MEAC 0.0 / MEOH 1800.0 / WATER 0.0 / HAC &  
 0.0

## BLOCK B1 RADFRAC

PARAM NSTAGE=15 EFF=MURPHREE  
 FEEDS F1 4 / F2 12  
 PRODUCTS TP 1 L / BP 15 L  
 P-SPEC 1 0.935  
 COL-SPECS DP-COL=.0120 MOLE-RDV=0.0 MASS-D=1016.4 &  
 MASS-RR=19.12  
 SC-REFLUX TEMP=29.0 OPTION=0  
 COMP-EFF 1 MEAC 0.0001 / 1 MEOH 0.0001 / 1 WATER &  
 0.0001 / 1 HAC 0.0001 / 2 MEAC 0.7 / 2 MEOH 0.75 &  
 / 2 WATER 0.75 / 2 HAC 0.7 / 3 MEAC 0.0001 / 3 &  
 MEOH 0.0001 / 3 WATER 0.0001 / 3 HAC 0.0001 / 4 &  
 MEAC 0.7 / 4 MEOH 0.8 / 4 WATER 0.75 / 4 HAC 0.75 &  
 / 5 MEAC 0.0001 / 5 MEOH 0.0001 / 5 WATER 0.0001 &  
 / 5 HAC 0.0001 / 6 MEAC 0.9 / 6 MEOH 1.05 / 6 &  
 WATER 1.05 / 6 HAC 0.75 / 7 MEAC 0.0001 / 7 MEOH &  
 0.0001 / 7 WATER 0.0001 / 7 HAC 0.0001 / 8 MEAC &  
 0.9 / 8 MEOH 1.05 / 8 WATER 1.05 / 8 HAC 0.74 / 9 &  
 MEAC 0.0001 / 9 MEOH 0.0001 / 9 WATER 0.0001 / 9 &  
 HAC 0.0001 / 10 MEAC 0.9 / 10 MEOH 1.05 / 10 &  
 WATER 1.05 / 10 HAC 0.75 / 11 MEAC 0.0001 / 11 &  
 MEOH 0.0001 / 11 WATER 0.0001 / 11 HAC 0.0001 / &  
 12 MEAC 0.9 / 12 MEOH 1.05 / 12 WATER 1.05 / 12 &  
 HAC 0.72 / 13 MEAC 0.0001 / 13 MEOH 0.0001 / 13 &  
 WATER 0.0001 / 13 HAC 0.0001 / 14 MEAC 0.9 / 14 &  
 MEOH 1.05 / 14 WATER 1.05 / 14 HAC 0.75 / 15 MEAC &  
 0.0001 / 15 MEOH 0.0001 / 15 WATER 0.0001 / 15 &  
 HAC 0.0001  
 REAC-STAGES 5 5 R1 / 7 7 R1 / 9 9 R1 / &  
 11 11 R1 / 13 13 R1  
 HOLD-UP 5 5 VOL-LHLDP=.0270 / 7 7 &  
 VOL-LHLDP=.0270 / 9 9 VOL-LHLDP=.0270 / 11 11 &  
 VOL-LHLDP=.0270 / 13 13 VOL-LHLDP=.0270  
 TRAY-REPORT TRAY-OPTION=ALL-TRAYS FORMAT=PROFILE &  
 PROPERTIES=TRANSPOT

## CONV-OPTIONS

PARAM CHECKSEQ=NO

## REPORT INPUT

PROPERTY-REP NOPARAMS NOPCES NOPROP-DATA NODFMS NOPROJECT

## REACTIONS R1 REAC-DIST

DESCRIPTION "ESTERIFICATION"  
 PARAM SUBROUTINE=RN2  
 REAC-DATA 1 KINETIC  
 STOIC 1 MEOH -1 / HAC -1 / MEAC 1 / WATER 1



```

SUBROUTINE RN2 (      N,      NC,      NRK,      NRKV,      NRKL,
1      T,      DUM1,      DUM2,      P,      VF,
2      F,      X,      Y,      IDX, NBOPST,
3      KDIAG,      STOIC, IHLBAS, HLDLIQ, TIMLIQ,
4      IHVBAS, HLDVAP, TIMVAP,      NINT,      INT,
5      NREAL,      REAL,      CRATE)

IMPLICIT REAL*8 (A-H,O-Z)

DIMENSION X(NC), Y(NC), IDX(NC), NBOPST(6), STOIC(NC,NRK),
2      INT(NINT), REAL(NREAL), CRATE(NC)

X1=X(1)
X2=X(2)
X3=X(3)
X4=X(4)

RATE = HLDLIQ*4.2*10**9*
& EXP(-58500.0/(8.314*T))*
& (X2*X4-X3*X1/(6.39-0.012*(T-273.15)))

CRATE(1) = RATE

CRATE(2) = -RATE

CRATE(3) = RATE

CRATE(4) = -RATE

RETURN
END

```





SPEN PLUS VER: PC-DOS REL: 9.3-1 INST: UALB-PC 06/11/97

# ----- FLowsheet Connectivity by Streams -----

STREAM	SOURCE	DEST	STREAM	SOURCE	DEST
F2	----	B1	F1	----	B1
TP	B1	----	BP	B1	----

# ----- FLowsheet Connectivity by Blocks -----

BLOCK	INLETS	OUTLETS
B1	F1 F2	TP BP

# ----- COMPUTATIONAL SEQUENCE -----

SEQUENCE USED WAS:

B1

# ----- OVERALL FLOWSHEET BALANCE -----

	***	MASS AND ENERGY BALANCE	***	
	IN	OUT	GENERATION	RELATIVE DIFF.
CONVENTIONAL COMPONENTS				
(KMOL/HR )				
MEAC	0.000000E+00	4.54496	4.54496	-0.147004E-08
MEOH	56.1760	51.6310	-4.54496	0.118935E-09
WATER	442.652	447.197	4.54496	-0.149402E-10
HAC	7.08546	2.54050	-4.54496	0.942953E-09
TOTAL BALANCE				
MOLE (KMOL/HR )	505.913	505.913	0.000000E+00	0.000000E+00
MASS (KG/HR )	10200.0	10200.0		-0.178332E-15
ENTHALPY (MMKCAL/H)	-33.8590	-33.6900		-0.499036E-02

# ----- COMPONENTS -----

ID	TYPE	FORMULA	NAME OR ALIAS	REPORT NAME
MEAC	C	C3H6O2-3	C3H6O2-3	MEAC
MEOH	C	CH4O	CH4O	MEOH
WATER	C	H2O	H2O	WATER
HAC	C	C2H4O2-1	C2H4O2-1	HAC

	***	MASS AND ENERGY BALANCE	***	
	IN	OUT	GENERATION	RELATIVE DIFF.
TOTAL BALANCE				
MOLE (KMOL/HR )	505.913	505.913	0.000000E+00	0.000000E+00
MASS (KG/HR )	10200.0	10200.0		-0.178332E-15
ENTHALPY (MMKCAL/H)	-33.8590	-33.6900		-0.499036E-02

\*\*\*\*\*

\*\*\*\* INPUT DATA \*\*\*\*

\*\*\*\*\*

\*\*\*\* INPUT PARAMETERS \*\*\*\*



NUMBER OF STAGES	15
ALGORITHM OPTION	STANDARD
INITIALIZATION OPTION	STANDARD
HYDRAULIC PARAMETER CALCULATIONS	NO
INSIDE LOOP CONVERGENCE METHOD	NEWTON
DESIGN SPECIFICATION METHOD	NESTED
MAXIMUM NO. OF OUTSIDE LOOP ITERATIONS	25
MAXIMUM NO. OF INSIDE LOOP ITERATIONS	10
MAXIMUM NUMBER OF FLASH ITERATIONS	50
FLASH TOLERANCE	0.000100000
OUTSIDE LOOP CONVERGENCE TOLERANCE	0.000100000

\*\*\*\* COL-SPECS \*\*\*\*

MOLAR VAPOR DIST / TOTAL DIST	0.0
MASS REFLUX RATIO	19.1200
MASS DISTILLATE RATE	1,016.40
DIST + REFLUX SUBCOOLED TEMP	29.0000

\*\*\*\* REAC-STAGES SPECIFICATIONS \*\*\*\*

STAGE	TO	STAGE	REACTIONS/CHEMISTRY ID
5		5	R1
7		7	R1
9		9	R1
11		11	R1
13		13	R1

\*\*\*\* HOLD-UP SPECIFICATIONS \*\*\*\*

STAGE	TO	STAGE	LIQUID HOLDUP	VAPOR HOLDUP
5		5	2.7000-02 CUM	MISSING
7		7	2.7000-02 CUM	MISSING
9		9	2.7000-02 CUM	MISSING
11		11	2.7000-02 CUM	MISSING
13		13	2.7000-02 CUM	MISSING

\*\* STOICHIOMETRIC COEFFICIENTS \*\*

RXN NO.	MEAC	MEOH	WATER	HAC
1	1.000	-1.000	1.000	-1.000

\*\*\*\* COMPONENT MURPHREE EFFICIENCY \*\*\*\*

STAGE	MEAC	MEOH	WATER	HAC
1	1.0000-04	1.0000-04	1.0000-04	1.0000-04
2	0.7000	0.7500	0.7500	0.7000
3	1.0000-04	1.0000-04	1.0000-04	1.0000-04
4	0.7000	0.8000	0.7500	0.7500
5	1.0000-04	1.0000-04	1.0000-04	1.0000-04
6	0.9000	1.0500	1.0500	0.7500
7	1.0000-04	1.0000-04	1.0000-04	1.0000-04
8	0.9000	1.0500	1.0500	0.7400
9	1.0000-04	1.0000-04	1.0000-04	1.0000-04
10	0.9000	1.0500	1.0500	0.7500
11	1.0000-04	1.0000-04	1.0000-04	1.0000-04
12	0.9000	1.0500	1.0500	0.7200
13	1.0000-04	1.0000-04	1.0000-04	1.0000-04
14	0.9000	1.0500	1.0500	0.7500
15	1.0000-04	1.0000-04	1.0000-04	1.0000-04

\*\*\*\*\*  
 \*\*\*\* RESULTS \*\*\*\*  
 \*\*\*\*\*



## \*\*\* COMPONENT SPLIT FRACTIONS \*\*\*

COMPONENT:	OUTLET STREAMS	
	TP	BP
MEAC	.99971	.29140E-03
MEOH	.36859	.63141
WATER	.86446E-02	.99136
HAC	.24515E-02	.99755

## \*\*\* SUMMARY OF KEY RESULTS \*\*\*

TOP STAGE TEMPERATURE	C	54.3581
BOTTOM STAGE TEMPERATURE	C	88.8493
TOP STAGE LIQUID FLOW	KMOL/HR	552.226
BOTTOM STAGE LIQUID FLOW	KMOL/HR	478.467
TOP STAGE VAPOR FLOW	KMOL/HR	0.0
BOTTOM STAGE VAPOR FLOW	KMOL/HR	553.406
MOLAR REFLUX RATIO		19.1200
MOLAR BOILUP RATIO		1.15662
CONDENSER DUTY (W/O SUBCOOL)	MMKCAL/H	-4.75073
REBOILER DUTY	MMKCAL/H	5.27178
DIST + REFLUX SUBCOOLED TEMP	C	29.0000
SUBCOOLED REFLUX DUTY	MMKCAL/H	-0.35208

## \*\*\*\* PROFILES \*\*\*\*

\*\*NOTE\*\* REPORTED VALUES FOR STAGE LIQUID AND VAPOR RATES ARE THE FLOWS FROM THE STAGE INCLUDING ANY SIDE PRODUCT.

STAGE	TEMPERATURE C	PRESSURE BAR	ENTHALPY KCAL/MOL		HEAT DUTY MMKCAL/H
			LIQUID	VAPOR	
1	54.358	0.93500	-66.015	-57.543	-4.7507
SUBC	29.000	0.93500	-66.653		-0.3520
2	62.683	0.93586	-61.304	-57.413	
3	62.424	0.93671	-61.306	-52.722	
4	72.952	0.93757	-63.404	-52.579	
5	72.533	0.93843	-63.422	-51.168	
6	73.905	0.93929	-63.196	-51.150	
7	73.551	0.94014	-63.209	-50.805	
8	74.170	0.94100	-63.144	-50.797	
9	73.882	0.94186	-63.156	-50.701	
10	74.456	0.94271	-63.177	-50.694	
11	74.218	0.94357	-63.188	-50.729	
12	75.221	0.94443	-63.432	-50.716	
13	75.045	0.94529	-63.447	-51.710	
14	79.902	0.94614	-64.998	-51.651	
15	88.849	0.94700	-66.588	-54.098	5.2717

STAGE	FLOW RATE KMOL/HR		FEED RATE KMOL/HR			PRODUCT RATE KMOL/HR	
	LIQUID	VAPOR	LIQUID	VAPOR	MIXED	LIQUID	VAPOR
1	552.2	0.0000E+00					
SUBC	552.2					27.4466	
2	550.0	552.2					
3	540.4	577.5					
4	1009.	567.9	449.7374				
5	1007.	586.7					
6	1009.	584.4					
7	1007.	586.5					
8	1008.	585.0					



9	1007.	585.8	
10	1007.	584.6	
11	1005.	584.5	
12	1057.	583.0	56.1759
13	1053.	578.6	
14	1032.	574.3	
15	478.5	553.4	478.4668

\*\*\*\* MASS FLOW PROFILES \*\*\*\*

STAGE	FLOW RATE KG/HR		FEED RATE KG/HR			PRODUCT RATE KG/HR	
	LIQUID	VAPOR	LIQUID	VAPOR	MIXED	LIQUID	VAPOR
1	0.2045E+05	0.0000E+00					
SUBC0.	0.2045E+05					1016.4000	
2	0.1642E+05	0.2045E+05					
3	0.1613E+05	0.1744E+05					
4	0.2429E+05	0.1715E+05	8400.0000				
5	0.2423E+05	0.1691E+05					
6	0.2407E+05	0.1684E+05					
7	0.2403E+05	0.1668E+05					
8	0.2393E+05	0.1664E+05					
9	0.2390E+05	0.1655E+05					
10	0.2374E+05	0.1651E+05					
11	0.2370E+05	0.1636E+05					
12	0.2448E+05	0.1632E+05	1800.0000				
13	0.2437E+05	0.1530E+05					
14	0.2179E+05	0.1518E+05					
15	9184.	0.1261E+05				9183.6000	

\*\*\*\* MOLE-X-PROFILE

STAGE	MEAC	MEOH	WATER	HAC
1	0.16554	0.69338	0.14085	0.22691E-03
2	0.39644E-01	0.68341	0.27624	0.70816E-03
3	0.39520E-01	0.68340	0.27637	0.70864E-03
4	0.46172E-02	0.39164	0.59638	0.73688E-02
5	0.56689E-02	0.38984	0.59819	0.63039E-02
6	0.12437E-02	0.39286	0.59965	0.62388E-02
7	0.23280E-02	0.39130	0.60122	0.51517E-02
8	0.61588E-03	0.39032	0.60394	0.51232E-02
9	0.15384E-02	0.38899	0.60527	0.42001E-02
10	0.37959E-03	0.38261	0.61277	0.42429E-02
11	0.11499E-02	0.38137	0.61401	0.34733E-02
12	0.21548E-03	0.35534	0.64093	0.35105E-02
13	0.81682E-03	0.35377	0.64250	0.29139E-02
14	0.68648E-04	0.21043	0.78603	0.34705E-02
15	0.27680E-05	0.68135E-01	0.92657	0.52966E-02

\*\*\*\* MOLE-Y-PROFILE

STAGE	MEAC	MEOH	WATER	HAC
1	0.16557	0.69336	0.14084	0.22689E-03
2	0.16554	0.69338	0.14085	0.22691E-03
3	0.45628E-01	0.68388	0.26980	0.68529E-03
4	0.45611E-01	0.68388	0.26982	0.68536E-03
5	0.15684E-01	0.70595	0.27776	0.60665E-03
6	0.15679E-01	0.70595	0.27776	0.60665E-03
7	0.80315E-02	0.71002	0.28144	0.51530E-03
8	0.80292E-02	0.71002	0.28144	0.51530E-03
9	0.50754E-02	0.70790	0.28655	0.47249E-03
10	0.50738E-02	0.70790	0.28655	0.47249E-03
11	0.30781E-02	0.69695	0.29943	0.54591E-03
12	0.30768E-02	0.69695	0.29943	0.54593E-03
13	0.14961E-02	0.59175	0.40583	0.92875E-03
14	0.14950E-02	0.59174	0.40584	0.92881E-03
15	0.12561E-03	0.33345	0.66453	0.18917E-02





STAGE	MEAC	**** K-VALUES		****
		MEOH	WATER	HAC
1	2.6784	0.74351	0.29154	0.21115E-01
2	5.4721	1.0192	0.35428	0.43018E-01
3	5.4222	1.0079	0.35048	0.44338E-01
4	12.657	1.7321	0.44799	0.96569E-01
5	12.545	1.7067	0.43962	0.94277E-01
6	13.290	1.7975	0.46348	0.10212
7	13.193	1.7749	0.45616	0.99790E-01
8	13.570	1.8189	0.46640	0.10352
9	13.490	1.8001	0.46033	0.10169
10	13.951	1.8488	0.46864	0.10559
11	13.884	1.8330	0.46354	0.10454
12	15.094	1.9472	0.47508	0.11310
13	15.054	1.9349	0.47141	0.11371
14	23.995	2.7536	0.53198	0.17515
15	45.378	4.8940	0.71720	0.35715

		****	RATES OF GENERATION		****
		KMOL/HR			
STAGE	MEAC	MEOH	WATER	HAC	
1	0.0000E+00	0.0000E+00	0.0000E+00	0.0000E+00	
2	0.0000E+00	0.0000E+00	0.0000E+00	0.0000E+00	
3	0.0000E+00	0.0000E+00	0.0000E+00	0.0000E+00	
4	0.0000E+00	0.0000E+00	0.0000E+00	0.0000E+00	
5	1.088	-1.088	1.088	-1.088	
6	0.0000E+00	0.0000E+00	0.0000E+00	0.0000E+00	
7	1.104	-1.104	1.104	-1.104	
8	0.0000E+00	0.0000E+00	0.0000E+00	0.0000E+00	
9	0.9354	-.9354	0.9354	-.9354	
10	0.0000E+00	0.0000E+00	0.0000E+00	0.0000E+00	
11	0.7791	-.7791	0.7791	-.7791	
12	0.0000E+00	0.0000E+00	0.0000E+00	0.0000E+00	
13	0.6392	-.6392	0.6392	-.6392	
14	0.0000E+00	0.0000E+00	0.0000E+00	0.0000E+00	
15	0.0000E+00	0.0000E+00	0.0000E+00	0.0000E+00	

STAGE	MEAC	**** MASS-X-PROFILE		****
		MEOH	WATER	HAC
1	0.33116	0.59995	0.68521E-01	0.36797E-03
2	0.98373E-01	0.73351	0.16670	0.14245E-02
3	0.98089E-01	0.73367	0.16682	0.14258E-02
4	0.14206E-01	0.52119	0.44623	0.18379E-01
5	0.17450E-01	0.51903	0.44779	0.15730E-01
6	0.38618E-02	0.52763	0.45280	0.15704E-01
7	0.72304E-02	0.52568	0.45412	0.12971E-01
8	0.19218E-02	0.52681	0.45831	0.12960E-01
9	0.48016E-02	0.52514	0.45943	0.10627E-01
10	0.11925E-02	0.51988	0.46812	0.10805E-01
11	0.36133E-02	0.51834	0.46920	0.88475E-02
12	0.68927E-03	0.49164	0.49857	0.91029E-02
13	0.26143E-02	0.48974	0.50008	0.75603E-02
14	0.24082E-03	0.31930	0.67059	0.98697E-02
15	0.10683E-04	0.11374	0.86967	0.16572E-01

STAGE	MEAC	**** MASS-Y-PROFILE		****
		MEOH	WATER	HAC
1	0.33120	0.59992	0.68514E-01	0.36792E-03
2	0.33116	0.59995	0.68521E-01	0.36797E-03
3	0.11194	0.72572	0.16097	0.13629E-02
4	0.11190	0.72574	0.16099	0.13631E-02
5	0.40312E-01	0.78481	0.17361	0.12640E-02
6	0.40298E-01	0.78482	0.17361	0.12640E-02
7	0.20915E-01	0.79976	0.17824	0.10878E-02
8	0.20909E-01	0.79977	0.17824	0.10878E-02
9	0.13309E-01	0.80295	0.18274	0.10044E-02



10	0.13305E-01	0.80295	0.18274	0.10044E-02
11	0.81476E-02	0.79794	0.19274	0.11714E-02
12	0.81443E-02	0.79794	0.19274	0.11714E-02
13	0.41920E-02	0.71717	0.27653	0.21096E-02
14	0.41890E-02	0.71716	0.27654	0.21097E-02
15	0.40848E-03	0.46905	0.52555	0.49871E-02

STAGE	RHOMX LIQUID	RHOMX VAPOR	KINVISC LIQUID	KINVISC VAPOR	MUMX LIQUID
-------	-----------------	----------------	-------------------	------------------	----------------

	KG/CUM	KG/CUM	SQM/SEC	SQM/SEC	CP
--	--------	--------	---------	---------	----

1	822.3669	MISSING	4.5845-07	MISSING	0.3770
2	790.9114	1.2841	4.7071-07	8.3994-06	0.3722
3	791.2181	1.0480	4.7194-07	1.0620-05	0.3734
4	818.9840	1.0110	4.4109-07	1.1380-05	0.3612
5	819.8569	0.9674	4.4256-07	1.1943-05	0.3628
6	816.9242	0.9638	4.3763-07	1.2039-05	0.3575
7	817.6742	0.9532	4.3876-07	1.2177-05	0.3587
8	816.8871	0.9521	4.3642-07	1.2215-05	0.3565
9	817.5120	0.9473	4.3731-07	1.2276-05	0.3575
10	818.0256	0.9464	4.3487-07	1.2311-05	0.3557
11	818.5761	0.9391	4.3560-07	1.2411-05	0.3565
12	823.0167	0.9368	4.3046-07	1.2480-05	0.3542
13	823.5859	0.8854	4.3096-07	1.3278-05	0.3549
14	855.8712	0.8722	4.0162-07	1.3682-05	0.3437
15	897.1475	0.7300	3.5192-07	1.6890-05	0.3157

STAGE	MUMX VAPOR	SIGMAMX LIQUID
-------	---------------	-------------------

	CP	DYNE/CM
--	----	---------

1	MISSING	26.6282
2	1.0786-02	31.8988
3	1.1130-02	31.9357
4	1.1506-02	45.1854
5	1.1555-02	45.3274
6	1.1604-02	45.1820
7	1.1609-02	45.3029
8	1.1631-02	45.3306
9	1.1630-02	45.4313
10	1.1651-02	45.6815
11	1.1655-02	45.7711
12	1.1692-02	46.8303
13	1.1756-02	46.9266
14	1.1933-02	52.5692
15	1.2330-02	57.1833

STREAM ID	BP	F1	F2	TP
FROM :	B1	----	----	B1
TO :	----	B1	B1	----

SUBSTREAM: MIXED

PHASE:	LIQUID	LIQUID	LIQUID	LIQUID
--------	--------	--------	--------	--------

COMPONENTS: KMOL/HR

MEAC	1.3244-03	0.0	0.0	4.5436
MEOH	32.6001	0.0	56.1759	19.0309
WATER	443.3311	442.6520	0.0	3.8658
HAC	2.5342	7.0854	0.0	6.2280-03



TOTAL FLOW:					
KMOL/HR	478.4668	449.7374	56.1759	27.4466	
KG/HR	9183.6000	8400.0000	1800.0000	1016.4000	
CUM/HR	10.2364	8.8822	2.3422	1.1876	
STATE VARIABLES:					
TEMP C	88.8493	70.0000	50.0000	29.0000	
PRES BAR	0.9470	0.9500	0.9500	0.9350	
VFRAC	0.0	0.0	0.0	0.0	
LFRAC	1.0000	1.0000	1.0000	1.0000	
SFRAC	0.0	0.0	0.0	0.0	
ENTHALPY:					
KCAL/MOL	-66.5880	-68.2203	-56.5589	-66.6529	
KCAL/KG	-3469.2438	-3652.5306	-1765.1423	-1799.8812	
MMKCAL/HR	-31.8606	-30.6817	-3.1773	-1.8294	
ENTROPY:					
CAL/MOL-K	-36.4551	-36.9469	-56.1555	-59.5569	
CAL/GM-K	-1.8993	-1.9781	-1.7525	-1.6082	
DENSITY:					
KMOL/CUM	46.7415	50.6332	23.9837	23.1110	
KG/CUM	897.1475	945.7064	768.4915	855.8433	
AVG MW	19.1938	18.6775	32.0421	37.0318	

\*\*\*\*\*  
\*  
\* CALCULATIONS WERE COMPLETED NORMALLY \*  
\*  
\* ALL UNIT OPERATION BLOCKS WERE COMPLETED NORMALLY \*  
\*  
\* ALL STREAMS WERE FLASHED NORMALLY \*  
\*  
\*\*\*\*\*

















**B52411**